CHARACTERISATION AND THERMAL DECOMPOSITION PATTERNS OF SOME IRON (III) CHROMATES

Patrick Joseph Mineely, B.Sc. (Hons.), M.Sc. (LaTrobe)

A thesis submitted for the degree of Doctor of Philosophy of the Australian National University

Department of Chemistry
Faculty of Science
Australian National University

July 1991

CORRECTION

Throughout the thesis the quadrupole coupling energy Eq has been incorrectly substituted for the quadrupole splitting ΔE, except on p22 where Eq is defined as the quadrupole coupling energy in equation 3.1.3. The relationship between the two parameters is

$$\Delta E = 2Eq.$$

Therefore to convert the experimental values for quadrupole splittings given in the thesis to the correct values a factor of 2 needs to be applied. For example $Eq=0.15mms^{-1}$ should be read as $0.30mms^{-1}$ when comparing with literature values. The linewidths and peak areas quoted in the thesis are unaffected by this change.

CONTENTS

ABSTRACT

A study of the thermal decomposition reactions of the chromates $MFe(CrO_4)_2.2H_2O$, M = NH_4, Na or K; $MFe(CrO_4)_2$, M = Rb, Cs or Tl; $Fe_2(CrO_4)_3.nH_2O$, n = 1 or 3; $FeOHCrO_4$, $2Fe_2O_3.4CrO_3.H_2O$, and $KFe_3(CrO_4)_2(OH)_6$ was undertaken. The room-temperature Mössbauer spectra of the chromates and their pyrolysis intermediates are also reported. A study of the use of low-melting hydrated iron(III) salts for the synthesis of iron(III) chromates was also made.

Decomposition of the chromates $MFe(CrO_4)_2.nH_2O$ (M = Na, K, Rb, Cs or Tl, n = 0 or 2) yielded, as the final products, the dichromate $M_2Cr_2O_7$ (M = K, Rb or Cs) or chromate (M = Na or Tl), and iron(III) and chromium(III) oxides. The formation of Cr(IV) oxide during the pyrolysis of $NH_4Fe(CrO_4)_2$ is discussed. Pyrolyses of the normal chromates $Fe_2(CrO_4)_3.nH_2O$ (n = 1 and 3) and basic chromates $FeOHCrO_4$, $2Fe_2O_3.4CrO_3.H_2O$ and $KFe_3(CrO_4)_2(OH)_6$ were observed to involve the intermediate phase $Fe_2O(CrO_4)_2$.

Mössbauer isomer shifts, quadrupole splittings and linewidths have been measured for a number of chromates. These parameters have been correlated with available structural information and the correlations applied to chromates of unknown structure. The results indicate that Mössbauer spectroscopy offers some scope as a diagnostic tool.

Synthetic routes to iron(III) chromates were examined using iron(III) nitrate 9-water as a solvent with incorporation of alkali metal dichromates. From these systems, novel chromates of the type $M_2Fe_3(OH)_5(CrO_4)_3.3H_2O$ (M = Li or Na), in addition to the chromates $MFe(CrO_4)_2.nH_2O$ (n = 0 or 2, M = K, Rb, Cs or NH_4), were isolated and characterised chemically and spectroscopically.

DECLARATION

I hereby declare that the contents in this thesis are my own work except where due reference to the work of others has been made.

Sign .....

ACKNOWLEDGEMENTS

I would like to extend my appreciation to the following for their helpful discussions, Drs. Dereham Scott, Naida Gill and Meta Sterns. Thanks also to Drs. Geoff Whittle and Andrew Stewart for their time and help during the Mössbauer investigations. I would also like to acknowledge the help of my colleagues within the Department. Thanks is also extended to Dr. J. O. Hill and Mr. Denis Bogsanyi for making available, respectively, differential thermal analysis and infrared spectroscopy facilities.

I would also like to thank Dr. Meta Sterms for the conversion of 2θ data for XRD traces in Chapter 4 to plot form and for assistance with the Rietveld program computations.

I also acknowledge the award of a Commonwealth Post-graduate research award during the latter half of my candidature. I also thank Prof. Ron Warrener for his initial offer of a fractional tutorship within the Department.

Finally I would like to extend my appreciation to Anita and Jessica for their friendship and support during the course of this work.

PUBLICATIONS

The following papers have been published from the results of this work: (See Appendix III)

1. Mineely, P.J. and Scott D.L.,"The Characterisation of Some Iron Chromates", Aust. J. Chem., 1987,40,387.

2. Mineely, P.J.,"Thermal Decomposition of Some Iron(III) Chromates", Aust. J. Chem., 1988,41, 263.

3. Mineely, P.J.,"Characterisation of Some New Chromates $M_2Fe_3(OH)_5(CrO_4)_3.3H_2O$ (M = Li, Na)", Thermochimica Acta, 1989,137,197.

CHAPTER ONE

INTRODUCTION

Iron chromates are used as components in heat resistant paints[1] and as catalysts[2] for the production of hydrocarbons from carbon monoxide gas.Fundamental studies into their chemical and physical behaviour could therefore be of interest. The present work utilizes the techniques of thermal analysis, X-ray powder diffraction and ^{57}Fe-Mössbauer spectroscopy to examine the decomposition pathway(s) of several iron chromates.

Most studies to date on the chemistry of iron(III) chromates have focused on aspects of preparation and structure determination. Early reports[3,4] describe the precipitation of compounds containing oxochromato phases e.g. $Fe_2O_2CrO_4$[4], from aqueous solutions of potassium chromate and iron(III) chloride. Hensgen[5] has reported the preparation of the double salts $M_2CrO_4.Fe_2(CrO_4)_3.4H_2O$, where M = NH_4, K, from mixtures of dichromate and iron(III) chloride in aqueous solution. Weinland and Mergenthaler[6] prepared the chromate $K_2CrO_4.Fe_2(CrO_4)_3.4H_2O$, reported previously[5], by heating to 70°C aqueous solutions of $Fe(NO_3)_3.9H_2O$ (175 g/L) and $K_2Cr_2O_7$ (454 g/L). Metallic chromates prepared by the heating of mixtures containing MCl_3, where M = Al(III) or Fe(III), Na_2CrO_4, CrO_3 and H_2O in sealed tubes at 200°C for 4 h were reported by Briggs[7] to be basic in nature and the product, when M = Fe(III), was analysed as $Fe_2O(CrO_4)_2.H_2O$. Husain and Partington[8] reported the precipitation of

iron(III) dichromate $Fe_2(Cr_2O_7)_3$ from the reaction of chromium trioxide in aqueous solution with an excess of iron(III) hydroxide at 80-90°C for several days. In a recent review, Bonnin[9] discussed the ternary phase system Fe_2O_3-CrO_3-H_2O.

A number of iron(III) chromates can be isolated:

(a) the chromates $MFe(CrO_4)_2.nH_2O$ where M = NH_4,Na,K,Rb,Cs or Tl and n = 2,1,or 0,

(b) the basic chromates $FeOHCrO_4$ and $MFe_3(CrO_4)_2(OH)_6$ where M = NH_4, Na or K,

(c) the normal chromate hydrates $Fe_2(CrO_4)_3.nH_2O$ where n = 1 or 3.

Under the conditions used, Bonnin[9] failed to observe the formation of anhydrous iron(III) chromate, iron(III) dichromate or oxochromato phases from aqueous solutions as reported by earlier workers[3,4,7]. The crystal structures of the iron(III) chromates prepared by Bonnin[9] have since been reported[10-21]. The structures may be visualised as consisting of FeO_6 octahedra linked by CrO_4 tetrahedra to give chains, sheets or three dimensional frameworks. Oxygen atoms from H_2O, OH^- or CrO_4^{2-} groups make up the co-ordination octahedra around iron(III) and dehydration results

in further crosslinking as chromate oxygens fill the vacated sites[17].

Popel and Boldog[22] have isolated from aqueous solutions of iron(III) nitrate and alkali metal chromates several new types of iron(III) chromates. For reactions where the mole ratio of nitrate to chromate (0.007 - 0.025 M) was in the range 0.15 to 0.30, sparingly soluble iron(III) hydroxy chromates of variable composition were formed. On increasing the mole ratio to between 0.5 and 1.0, the formation of the double salts $M_2CrO_4.Fe_2(CrO_4)_3.nH_2O$, where M = NH_4, K and n = 0,4, occurred. The hydroxy chromates were poorly crystalline and this prevented elucidation of their structures. Chemical analysis indicated the following formulae for these products:

(a) $Fe_2(OH)_4\ CrO_4.(3-4)H_2O$

(b) $Fe_3(OH)_7\ CrO_4.(1-2)H_2O$

(c) $M_3Fe_8(OH)_{15}(CrO_4)_6.4H_2O$ where M = NH_4, Na or K

The thermal decomposition of iron(III) chromates has not been extensively studied. Bonnin[9] reports that, in general, dehydration results in the formation of stable anhydrous iron(III) chromates. Popel[23] examined the thermal

decomposition of the chromates $MFe(CrO_4)_2.2H_2O$, M = Na or K, and $MFe(CrO_4)_2$, where M = Rb or Cs. Dehydration of the hydrates appeared to involve at least two stages, although no crystalline hydrate intermediate was isolated. On the basis of several weak lines in X-ray powder patterns of samples of $MFe(CrO_4)_2$, M = Na, K, it has been suggested[23] that the decomposition of the anhydrous chromates proceeded via an intermediate stage as the lines could not be assigned to any known phase. Popel[23] found the final decomposition products to be a mixture of $M_2Cr_2O_7$, where (M = K, Rb or Cs), Fe_2O_3 and Cr_2O_3 or, in the case of $NaFe(CrO_4)_2.2H_2O$, Na_2CrO_4, Fe_2O_3 and Cr_2O_3.

Physicochemical studies relating to the magnetic properties of iron(III) chromates have been reported by Powers et al[24], who examined $FeOHCrO_4$ and $KFe_3(CrO_4)_2(OH)_6$. The magnetic moments were very much lower than the spin only value of u_{eff} = 5.92, for isolated ferric ions, and were proposed to indicate extensive exchange interactions which were temperature dependent.

As can be seen from the available literature on iron(III) chromates[1-23], a variety of phases and methods of preparation for the chromates have been documented. The formation of intermediate phases during pyrolysis, may possibly be compared to observations reported in the literature for the analogous iron sulfates. Whilst the

final products from iron sulfates will differ, due to the formation of gaseous oxides of sulfur, the solid state intermediate types, e.g. oxosulfate species, formed on pyrolysis, may be relevant to the pyrolysis of chromates.

Margulis et al[25] have examined the thermal decomposition of iron(III) sulfate and iron(III) hydroxy sulfate and concluded that oxosulfato phases, e.g. $Fe_2O(SO_4)_2$, are not formed as intermediates during the pyrolysis process as shown in equations (1.1) and (1.2).

$$Fe_2(SO_4)_3 \longrightarrow Fe_2O_3 + 3SO_3 \qquad (1.1)$$

$$3FeOHSO_4 \longrightarrow Fe_2(SO_4)_3 + \tfrac{1}{2}Fe_2O_3 + \tfrac{3}{2}H_2O \qquad (1.2)$$

Warner and Ingraham[26] have reported results in agreement with those of Margulis et al[25], whilst Bristotti et al[27] have proposed, on the basis of combined Mössbauer-thermogravimetric experiments, the formation of oxosulfato compounds during the decomposition of iron(II) sulfate, reactions (1.3) and (1.4).

$$2FeSO_4.H_2O \longrightarrow FeOHSO_4 + \tfrac{1}{2}Fe_2O_3 + SO_2 + \tfrac{3}{2}H_2O \qquad (1.3)$$

$$FeOHSO_4 \longrightarrow \tfrac{1}{2}Fe_2O(SO_4)_2 + \tfrac{1}{2}H_2O \qquad (1.4)$$

Swamy et al[28-30] studied the oxidation-decomposition of ferrous sulfate hydrates and examined the effect of

experimental conditions on product formation. By using both isothermal and dynamic thermal analysis methods in combination with X-ray powder diffraction, Swami et al[28-30] were able to conclude that:

(a) under dynamic and isothermal heating, iron sulfate 4-water, 1-water and anhydrous, and hydroxy and oxosulfato compounds were formed,

(b) intermediate hydrate formation was accompanied by oxidation of iron (II), the extent of which increased with temperature,

(c) under isothermal heating the decomposition pathway was

$$FeSO_4.xH_2O \rightarrow FeSO_4.H_2O \rightarrow FeOHSO_4 \rightarrow Fe_2O(SO_4)_2$$

$$Fe_2O(SO_4)_2 \rightarrow Fe_2O_3 + SO_3$$

$$Fe_2O_3 + Fe_2(SO_4)_3$$

(d) under dynamic heating the decomposition pathway was

$$FeSO_4.xH_2O \rightarrow FeSO_4.H_2O \rightarrow FeSO_4 \rightarrow Fe_2O(SO_4)_2$$

$$Fe_2O(SO_4)_2 \rightarrow Fe_2O_3 + SO_3$$

$$Fe_2O_3 + Fe_2(SO_4)_3$$

Given the complexity of iron sulfate decomposition, the study of the chromates is relevant and could shed light on the thermal pathway for iron sulfates.

The aims of the work described in this thesis were threefold:

(a) To examine and define the thermal decomposition pathway(s) of iron(III) chromates by using a range of physical techniques, and to relate the decomposition processes to those of the analogous sulfates.

(b) To establish for the first time the Mössbauer parameters of iron(III) chromates. Because of the problems associated with poor crystallinity and variable composition of phases isolated from the reaction mixes used in the preparation of iron(III) chromates[9,22,31], techniques such as X-ray crystallography are not always applicable for structure elucidation. Mössbauer spectroscopy relies on the sensitivity of the nucleus of a given isotope to its electronic environment. Any correlations between structure and parameters such as quadrupole splittings, isomer shift and linewidth may provide useful information on structures yet unknown.

(c) To investigate the preparation of iron(III) chromates in media other than aqueous solutions e.g. by using fused salts. This may:

(i) facilitate preparation - previously used methods require equilibration times of 24 h to several months for the formation of chemically-identifiable products,

(ii) enable the synthesis of novel phases,

(iii) eliminate hydrolytic effects and make available high ion concentrations.

CHAPTER TWO

EXPERIMENTAL

2.1 INSTRUMENTATION

2.1.1 THERMOGRAVIMETRY (TG)

Thermogravimetry was performed on a Stanton Redcroft TG-750 thermal balance. Samples (5-7 mg) were powdered and heated in a platinum crucible (5 mm x 2 mm in depth) under a dynamic atmosphere of nitrogen. Calcium oxalate dihydrate was used periodically as a calibrant over the temperature range 20 - 600^{o}C. Calibration of the TG balance arm was undertaken prior to each run by zeroing the balance and recording the TG pen deflection when a standard weight was placed on the sample pan. Buoyancy effects were measured by heating the crucible alone up to 600^{o}C and correcting for the slight weight gain (0.1 mg) recorded by the balance arm. The TG traces could routinely be read to an accuracy of 0.02 mg in 10 mg on a setting of 10 mV. Analyses are reported as the average of 2 or 3 determinations.

All data were recorded in the manner prescribed by the International Confederation for Thermal Analysis (ICTA)[32].

2.1.2 **DIFFERENTIAL THERMAL ANALYSIS (DTA)**

Differential thermal analysis was carried out on a Rigaku-Denki modular thermoflex thermal analyser in platinum crucibles (5 mm x 2 mm) under a dynamic atmosphere of nitrogen. Alumina (Al_2O_3) powder was used as the reference material.

Traces showed a positive baseline drift which could not be corrected by use of slope control. Dr. J.O. Hill (LaTrobe University) is thanked for making available his instrument.

2.1.3 **ISOTHERMAL GRAVIMETRY**

Isothermal weight loss studies for the preparation of intermediate states, were performed in a RK - RB 01 heating unit. Samples were heated in pyrex glass crucibles (10 mm x 5 mm in diameter) under nitrogen. Temperature control to within $\pm$ 2^{o}C was achieved by the use of an AEI resistance thermometer controller.

2.1.4 **INFRARED SPECTROSCOPY (IR)**

Infrared spectra were measured on a Perkin-Elmer 1800 Fourier Transform infrared spectrophotometer using the KBr disk method. The spectra were obtained with the help of Mr. Denis Bogsanyi, Research School of Chemistry, Australian National University.

2.1.5 **MASS SPECTROMETRY**

Mass spectra were obtained on a Varian MAT CH7 mass spectrometer with the help of Mr. Geoff Gray of the Department of Chemistry, Australian National University.

2.1.6 **X-RAY POWDER DIFFRACTOMETRY (XRD)**

X-ray powder diffraction patterns were recorded with a Philips PW 1050 diffractometer, with a wide angle goniometer and CuKα radiation. Samples were mounted on a glass slide and placed in the beam path. Silicon (Si) was used as an external standard to calibrate the diffractometer and the average error in 2θ of the major peaks was $\pm$ 0.05^{o}. Powder patterns of the chromates were matched with patterns calculated from the available atomic coordinates of the respective chromates [10-21] by a Rietveld program[33] using the ANU UNIVAC 1100 computer system with the help of Dr M.Sterns or with those in the literature. For compounds other than iron chromates, the peaks were identified by comparing the `d' spacings with those listed in the ASTM diffraction data file[34].

2.1.7 **ATOMIC ABSORPTION SPECTROSCOPY (AAS)**

Atomic absorption spectroscopy was performed on a Varian Techtron 1200 spectrophotometer using an air-acetylene flame.

Compounds to be analysed were heated in warm aqueous mineral acid until dissolved (occasionally with difficulty). Standard solutions of Fe,Cr,Na and Li were prepared from iron wire dissolved in HCl,potassium dichromate,sodium chloride and lithium chloride, respectively. Errors in absorbance for the standard solutions were of the order of 2%. Results are the average of 2 or 3 readings.

2.1.8 **MÖSSBAUER SPECTROSCOPY**

Mössbauer spectra were obtained from a conventional constant-acceleration system[35] using a single line 50-60 mCi ^{57}Co source in a rhodium matrix. Samples containing about 2 mg cm^{-2} of iron were prepared by compressing powdered material with a benzophenone matrix, and, on the basis of line widths obtained, showed no significant broadening due to thickness effects.

The spectrometer was calibrated with natural α-iron foil and isomer shifts are reported relative to the centroid of this spectrum[36]; linewidths were of the order of 0.22mms^{-1}. Spectra were collected by a PDP 11/10 computer and fitted to pseudo-Lorenztian lineshapes using an iterative non-linear least squares method[37] on the ANU UNIVAC 1100 computer system. Goodness of fit was assumed on the basis of chi-square (χ^2) values, consistency of parameters and convergence of the fitting process. Estimates of variables introduced into the fitting process were not constrained. Figure 2.1

shows a schematic diagram of the instrumental arrangement. Measurements between 4.2 - 298K were achieved by the use of a variable temperature insert. The absorber material could be maintained at any temperature in the range 4.2 - 293K by use of a thermal leak leading to a liquid helium or nitrogen bath. Figure 2.2 shows a representative calibration spectrum indicating the inner doublet of alpha iron foil only; the line width is calculated as the full width of the peak at half peak height.

2.1.9 **MAGNETIC MEASUREMENTS**

Low temperature magnetic measurements were performed using a Newport 4 inch electromagnet fitted with appropriate pole pieces and a Cahn RG electrobalance. Measurements were made by Dr. Keith Murray, Department of Chemistry, Monash University, calibrant $HgCo(NCS)_4$. Room temperature measurements were performed (by the author) using the Gouy method.

2.2 **PREPARATIONS AND MATERIALS**

The following sections describe the handling and preparation of materials and reactants.

2.2.1 **MATERIALS**

B.D.H. (AnalaR) $(NH_4)_2Cr_2O_7$ (99.9%), CrO_3 (99%), $FeCl_3$ (99%), Rb_2CO_3 (98%); B.D.H. (L.R.) $(NH_4)_2CrO_4$ (95%), $Cs_2Cr_2O_7$ (99%), $Li_2Cr_2O_7.2H_2O$ (96%), $MgCrO_4.7H_2O$ (96%),

K_2CrO_4 (98%), $TlNO_3$ (98%); May and Baker (L.R.) $C_6H_5COC_6H_5$ (m.p. 48 - 50°C), Fe_2O_3 (98%), $K_2Cr_2O_7$ (99.5%), $Na_2Cr_2O_7.2H_2O$ (98%), Unilab (L.R.) Na_2CrO_4 (96%); and Ajax (A.R.) $Fe(NO_3)_3.9H_2O$ (98%) were all used as supplied.

The chromates were prepared as described in the literature, and characterised by elemental analysis and/or XRD methods to check purity. Appendix I details the preparative methods.

2.3 PROCEDURES

2.3.1 FUSED SALT - SOLUTE REACTIONS

Studies involving melts of iron(III) nitrate 9-water, were conducted in covered vitreosil or platinum crucibles. Weighed amounts (1 - 5 g) of iron(III) nitrate 9-water and reactant ($M_2Cr_2O_7$) were mixed thoroughly and heated in an oven at 65°C for 2 to 4 h. The cooled solidified melts were then placed in water and stirred, after which, the mixtures were filtered and the insoluble products characterised by chemical and physical methods.

2.3.2 ISOTHERMAL GRAVIMETRY

For the isolation of intermediates from pyrolysis processes and for the following of thermal decompositions under isothermal conditions, samples were weighed into pre-weighed

crucibles, and heated under nitrogen to the required temperature. Samples were periodically removed for analysis.

2.3.3 **GAS MEASUREMENTS**

The apparatus used is shown in Figure 2.3. The system was evacuated (tap B) prior to heating and lowered into a furnace which was then raised to the required temperature. At intervals of 0.5 h, tap A was opened and the pressure difference measured, moisture was collected in the P_2O_5 side arm so that only permanent gas was measured. After the pressure difference remained unchanged, the next temperature was set and measurement continued. The amount of gas formed was calculated from the temperature, volume of apparatus, mass of sample and pressure of gas.

Fig 2.1 Schematic diagram of Mössbauer Instrumentation

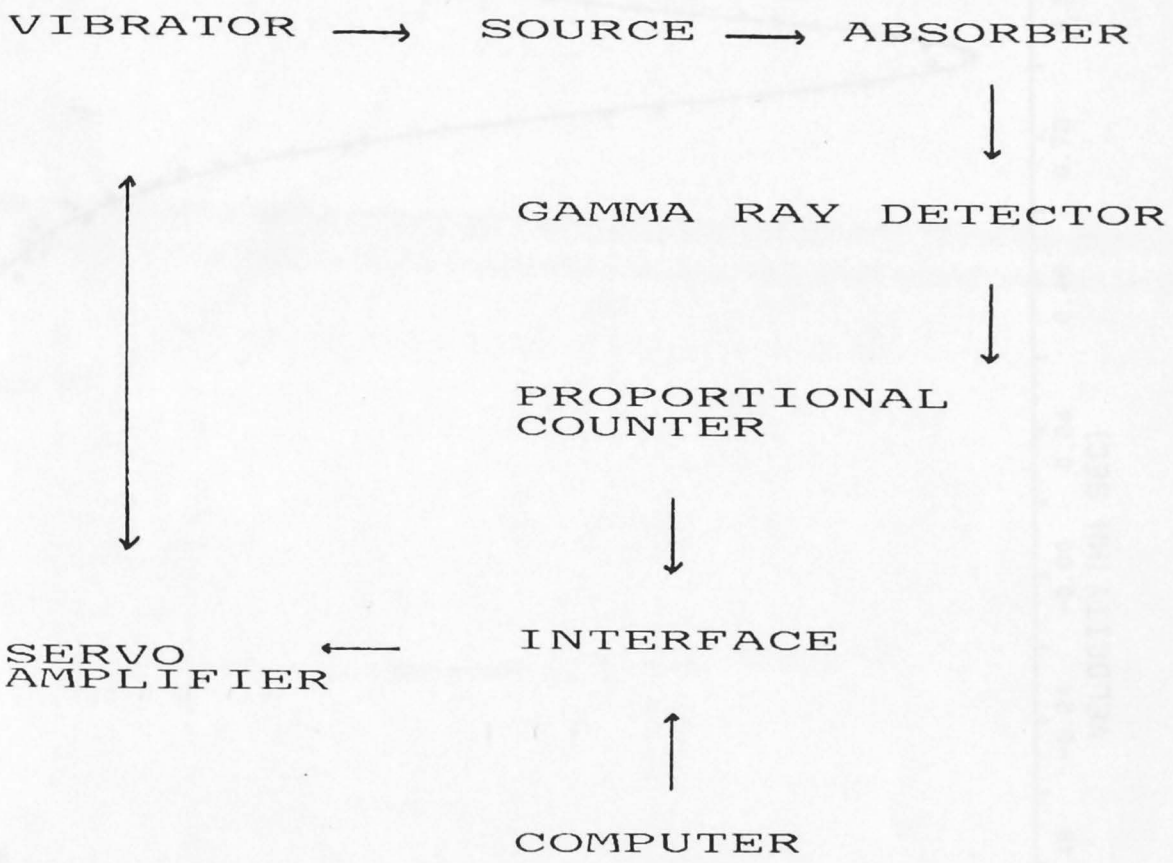

Fig 2.2 Calibration spectrum of α- iron

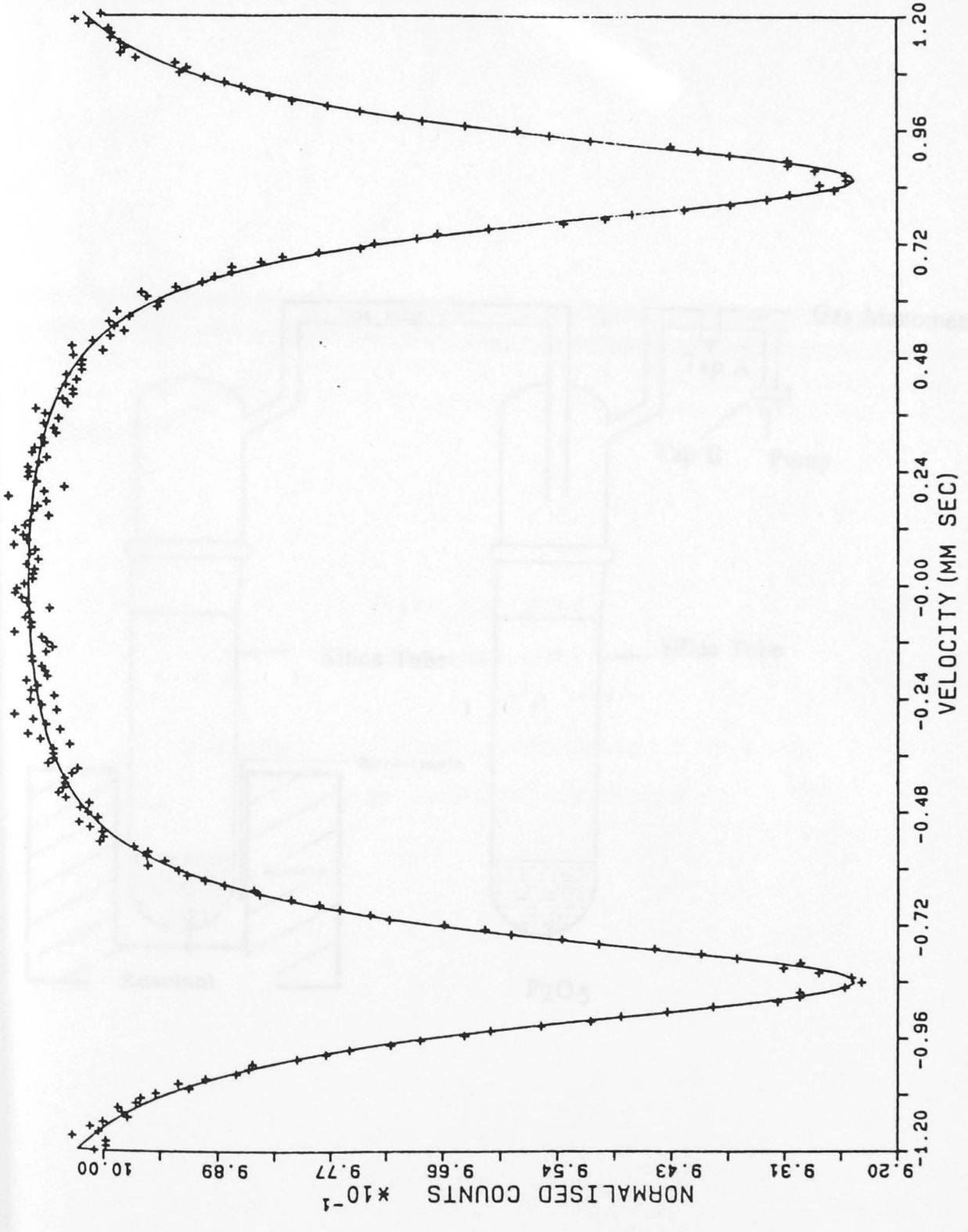

Fig 2.3 Schematic diagram of tensimetric apparatus

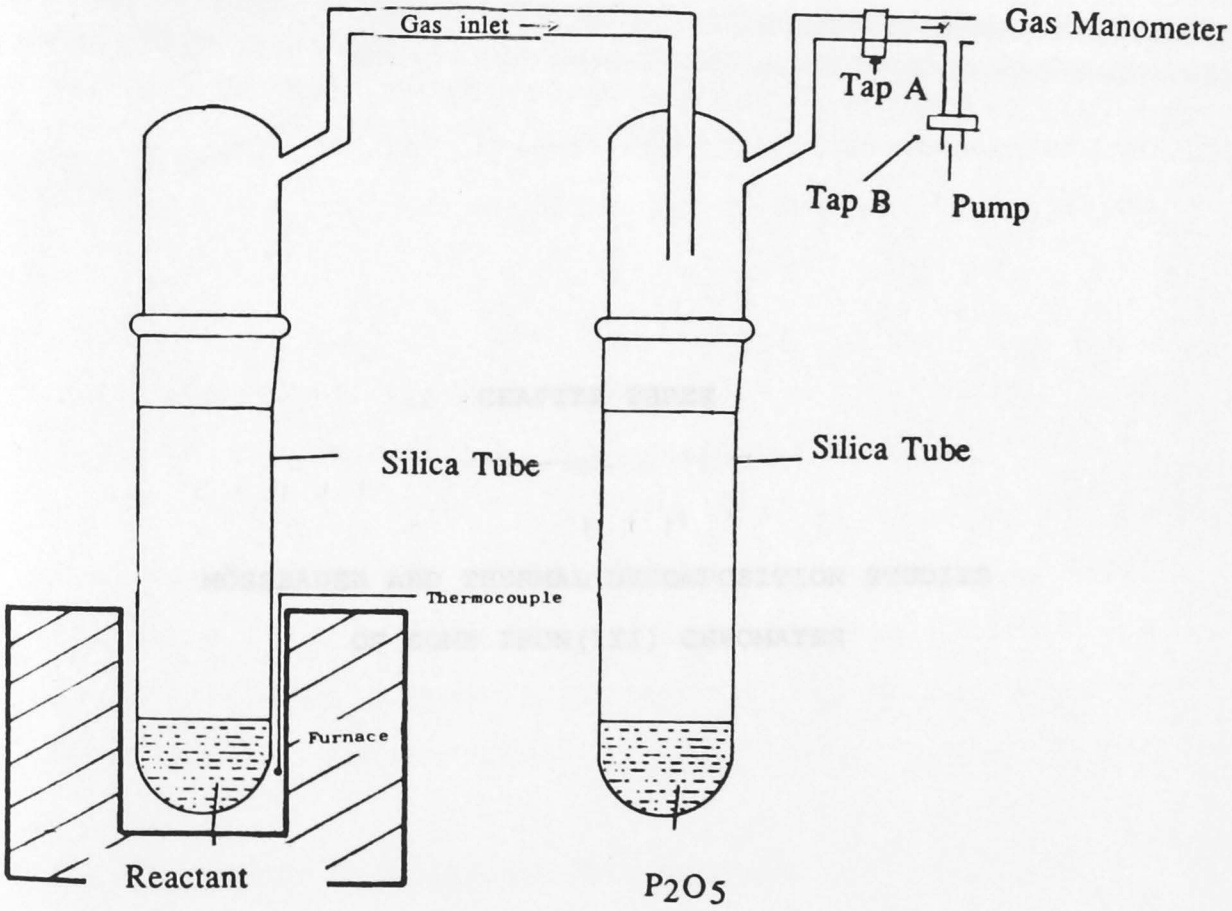

CHAPTER THREE

MÖSSBAUER AND THERMAL DECOMPOSITION STUDIES OF SOME IRON(III) CHROMATES

3.1 INTRODUCTION

In this chapter the results of thermal analysis and room temperature ^{57}Fe- Mössbauer studies of the chromates $MFe(CrO_4)_2.nH_2O$ (M = NH_4, Na, K, Rb, Cs, or Tl, n = 0, 1 or 2), $Fe_2(CrO_4)_3.nH_2O$ (n = 1, 3), $FeOHCrO_4$, $2Fe_2O_3.4CrO_3.H_2O$ and $KFe_3(CrO_4)_2(OH)_6$ are presented. Thermal analysis studies of iron chromates[9,23] were incomplete and contain features which have yet to be adequately explained. The observations on the thermal decomposition behaviour of ammonium and thallium chromates are potentially complicated by

(i) the volatility of ammonia,

(ii) the oxidisability of both cations.

The only reference to Mössbauer spectra of iron(III) chromates is a brief report by Takoshima and Ohaski[38] on technical grade iron(III) chromate - $Fe_2(CrO_4)_3$, with no discussion of the spectrum.

3.1.1 THEORY OF MÖSSBAUER SPECTROSCOPY

Mössbauer spectroscopy has been used for the characterisation of minerals and related compounds, including tourmalines[39], silicates[40] and sulfates[41], for which quadrupole and isomer shifts were related to site vacancy, ligand environment and identification of

crystalline phases. The ways in which Mössbauer spectroscopy has been utilised include:

(i) examination of the temperature dependence of the magnitude of quadrupole splittings (Eq) of Fe^{3+} ions in different environments,

(ii) studies of the Mössbauer spectra of a range of compounds with similar structures and the relating of the isomer shift (δ) and Eq values to crystallographic information.

Both of the above methods give information on the effects of nearest neighbour environments on site symmetries. The latter method was chosen in the present study of iron(III) chromates, owing to the availability of crystallographic data[10-21].

The mathematical treatment of the terms isomer shift, quadrupole splitting, line width and hyperfine field is dealt with extensively in the literature[42-44]. It is therefore sufficient to comment briefly on some aspects of these parameters.

The isomer shift (δ) is dependent on the electron density at the nucleus (equation 3.1.1). It can be, and often is, a useful parameter for the determination of electronic properties of the ion under investigation.

$$\delta = \frac{4\pi}{5} Ze^2 R_g^2 \left(\frac{\delta R}{R_g}\right)\left\{|\Psi_o|^2_a - |\Psi_o|^2_s\right\} \qquad 3.1.1$$

where $|\Psi_o|^2_a, |\Psi_o|^2_s$ = the electron density at the nucleus of absorber (a) and source (s)

Z = atomic number

e = charge of electron

$\frac{\delta R}{R_g}$ = the relative change in radius of the nucleus in excited and ground states.

The isomer shift can therefore be related to the formal oxidation state of the ion being measured.

The electric quadrupole splitting incorporates the nuclear quadrupole moment (Q), a measure of the deviation from spherical symmetry of the nuclear charge.

$$eQ = \int \rho r^2 (3\cos^2 - 1) d\tau \qquad 3.1.2$$

$+e$ = charge on the proton

ρ = nuclear charge density in the volume element $d\tau$ at a distance r from the centre of the nucleus at an angle θ to the axis of the nuclear spin

The nuclear quadrupole moment can interact with any electric field gradient that results from the spatial arrangement of the electron charges around the nucleus. Equation 3.1.3

describes this interaction for a nuclide with energy levels of nuclear spin quantum numbers 1/2 and 3/2.

$$Eq = \frac{e^2qQ}{4I(2I-1)} \left| 3m_I^2 - I(I+1) \right| \left(1 + \frac{\eta^2}{3}\right)^{\frac{1}{2}} \qquad 3.1.3$$

where Eq = quadrupole coupling energy

I = nuclear spin

m_I = magnetic quantum number of the nuclear level

η = asymmetry parameter related to the magnitude of the three components of the electrostatic field gradient V such that

$$0 \leq \eta \leqslant 1 \quad \text{and} \quad V_{zz} > V_{yy} \geqslant V_{xx}$$

where

$$\eta = \frac{|V_{xx} - V_{yy}|}{V_{zz}} \qquad 3.1.4$$

q is related to the maximum field gradient by the relationship $V_{zz} = eq$

The electric quadrupole splitting is zero for cubic symmetry and distortions from cubic symmetry lead to a quadrupole splitting. The coupling of Eq values can therefore yield qualitative information as regards physical distortion of the arrangement of ligands about iron which can be then compared to conclusions drawn from crystallographic and spectroscopic (e.g. IR) studies.

3.1.2 APPLICATIONS OF THERMAL ANALYSIS, MÖSSBAUER SPECTROSCOPY AND X-RAY DIFFRACTION METHODS FOR CHARACTERISATION OF MINERALS AND RELATED COMPOUNDS

The chemical phenomena occurring on heating of a sample, cannot always be detected by any one thermal analysis method. The complementary nature of DTA/TG, XRD and Mössbauer spectroscopy should therefore characterise more fully the processes occurring on heating of a material.

3.1.2.1 THERMAL ANALYSIS

Factors which can affect the shape of the thermal curve include:

(a) Reaction of the sample with the apparatus. For example, the decomposition temperature of sodium carbonate is lower in a quartz crucible than in a platinum one[45].

(b) Sublimation/condensation of the sample leads to irreproducible curves.

(c) Crucible size and shape. The size of the crucible and amount of substance play important roles in the determination of heating methods, diffusion rate of gases and surface area of sample. The use of symmetrical small crucibles, as in the present study, is recommended[46,47] to facilitate gas flow in the furnace.

The use of a closed crucible can alter appreciably the course of decomposition reaction due to the build up of gas pressure and resultant change in partial pressure of gas atmosphere in the furnace. The use therefore of an open crucible is preferable.

(d) Particle size. It is known that the more finely ground is a solid, the greater its reactivity. Vallet and Richer[48] have shown, through an extensive study of minerals, that the temperature of reaction (T_i) is lowered with decreasing particle size. In the present study all samples were ground and some variation in T_i may occur from run to run.

(e) Buoyancy. During heating of a crucible, an apparent weight increase is registered by the balance arm, caused in part by the furnace wall heating more rapidly than the atmosphere inside the furnace. Hot gas rises along the wall and displaces cooler air which impinges on the balance arm so that an apparent increase in weight is recorded. At the same time the density of air displaced by the sample and the crucible decreases on heating and also leads to an apparent increase in weight, which was observed experimentally to be about 0.1 mg over the temperature range 20 - 600°C. In the present study a small sample mass (5mg) and miniature furnace minimises much of the effect.

3.1.2.2 **DIFFERENTIAL THERMAL ANALYSIS**

Factors affecting the DTA curves have been studied in detail by Arens[49], and are similar to those discussed in section 3.1.2.1.

(a) Heating rate. High heating rates lead to a shift in the peak maxima (T_{max}) towards higher temperatures. The effect has been well studied in the dehydration of Kaolin[49,50]. Commonly recommended heating rates are 8 - 12^{o}C/min and are therefore routinely used.

(b) Gas atmosphere. Stone[51] has examined the effect of static and dynamic atmosphere on T_{max} for a range of mineral ores. T_{max} values for endothermic peaks are lowered in a dynamic atmosphere but the shape of the peak is unchanged. A further factor to be considered is whether the atmosphere, e.g. air may take part in the reaction. Metal oxalates decomposed in air show an exothermic peak in the DTA which is not present when the decomposition is carried out under N_2. The exotherm arises from the oxidation of CO to CO_2.

For the study of minerals and related compounds, differential thermal analysis provides a relatively quick and informative method of following reaction sequences. The following gives some indication of how exothermic and endothermic processes can be identified with a physical or chemical effect.

Endothermic reactions	-	dehydration
	-	dehydroxylation
	-	decomposition processes
	-	sintering, melting
	-	evaporation
Exothermic reaction	-	oxidation
	-	formation of crystalline material from amorphous phases

3.1.2.3 **MÖSSBAUER SPECTROSCOPY**

The criteria[52] for good fitting of a spectrum can be identified as,

(1) is χ^2 value statistically acceptable,

(2) are the number of iron sites found in the material consistent with other evidence e.g. crystallographic,

(3) are the parameters consistent with Mössbauer work on similar coordination sites?

A number of assumptions are made in the fitting process when using Mössbauer spectroscopy as a characterising tool. If the goodness of fit, as defined by χ^2, is poor an attempt is made to fit extra peaks to the spectrum. If χ^2 drops appreciably, and if the parameters become more reasonable compared to those from previous experiments, then the additional peak fitting is considered to be valid. Further

to this, complex spectra of a number of minerals of the same group will in general have comparable parameters - δ, Eq, Γ. In calculating peak areas in the present study, it is assumed that the Lorenztian line shape holds. Any deviation from Lorenztian will alter the estimate of peak area and may be due to absorber thickness, overlap of unresolved peaks or relaxation effects. Iron(III) compounds are particularly prone to relaxation effects[53], which can give rise to line broadening. However, in the majority of cases, the overlap of two or more Lorenztians is the most important cause of deviation[54].

Contributions to the electric field gradient (EFG) at the nucleus also need to be considered. These come from three sources:

(a) charges external to the atom, e.g. ionic charges in the lattice can produce a field gradient at a given atomic site;

(b) electrons belonging to the atom, e.g. electrons in unfilled d shells, can cause a field gradient at the nucleus;

(c) polarization of inner shells of the atom.

For ionic compounds factor (a) is dominant. However, it will be assumed that in a group of compounds of similar

structure the contributions to EFG may be expected to be constant.

The isomer shift is less sensitive to structural variance than the quadrupole splitting. In the present study of iron(III) chromates, δ may be expected to be the least informative parameter as the oxidation state of iron is not expected to change.

As it is possible that phases examined could be poorly crystalline, it is important to take into account the possibility of non-recoil-free events. The recoil-free fraction (f) is defined as that fraction of γ-rays for which emission or adsorption occurs without any energy loss. The mathematical description of f is well established[52] and will not be described here. In theory f should be equal to 0 for a totally free atom or 1 for a rigid lattice. Reality shows that f takes a value $0 \leqslant f \leqslant 1$ depending on factors such as,

(a) nuclear transition energy,

(b) mass of nucleus,

(c) rigidity of lattice,

(d) temperature.

The value of f can be determined by measuring the area under a peak corresponding to resonant absorption. The dependence of the recoil-free fraction on particle size

could therefore be a crucial factor in resolving broad spectra of poorly crystalline materials. Pollack et al[55] have addressed this problem experimentally by examining the diffusion of ^{57}Fe into fused quartz and pyrex glass. They[55] concluded that, in amorphous phases such as glass matrices, a large percentage of the emission processes still occurs without recoil, as the δ and Γ values for the diffused ^{57}Fe atoms were found to be independent of treatment, with Γ of spectra showing only a slight broadening.

The existence of α and β phases of iron chromates[10,13,19] could provide an interesting problem for peak identification. In general, the lowest concentration for distinguishing an active Mössbauer isotope in the presence of another is 5 - 10%[51]. Phase analysis has been applied to α-β separation in metals[56]. Housely et al[57,58] have examined synthetic ilmenite $FeTiO_3$ incorporating Fe^{3+} and Mg^{2+}. At low oxygen partial pressures (pO_2) a single phase exists, whilst at high pO_2 an additional phase is detected by Mössbauer spectroscopy - Fe_2TiO_5 - $(Fe,Mg)Ti_2O_5$ which is not observed in the X-ray powder diffraction profile of the material, because the amount is below the detection limit for this technique.

Fingerprinting of minerals by their Mössbauer spectra is a topic much discussed in the literature[52]. Gakiel and Malamund[59] have used Mössbauer spectroscopy to describe the metal oxidation states in the mineral ore $Fe_2Sb_2O_7$, whilst

investigations into the coordination number of the central atom of blue and yellow sapphirine[60] have been reported. The determination of the distribution of non-random cation sites in minerals is a difficult task, as the degree of ordering is dependent on both the differing sizes of lattice sites and of the cations occupying them. However, Mössbauer spectroscopy can aid in solving the problem owing to the sensitivity of the Mössbauer isotope to its environment. For example in silicate containing Fe^{2+} and Fe^{3+}, the differing magnitude of quadrupole splittings for each iron (Fe^{2+} 1-2 mms $^{-1}$, Fe^{3+} 0.3-0.6 mms^{-1}) permits resolution of the fine structure in spectra and peak identification.

Disadvantages of fingerprinting by Mössbauer spectroscopy are two-fold:

(1) the possible occurrence of strongly overlapping lines making resolution difficult. This may affect the identification of a mineral or phase by comparison of spectra with known standard spectra.

(2) the dependence of spectral resolution, in some instances, on particle size.

To standardise the fitting process in this work, the usual practice was to fit the minimum number of subspectra and to introduce more into the fit only as warranted; i.e. the number of variables was kept to the minimum necessary for

the physical interpretation of the spectrum. As for any technique, evaluation of the spectral feature(s) obtained requires correlation with other sources of information, e.g. chemical,analytical,spectral,thermal,crystallographic.

The relevant point which makes Mössbauer spectroscopy a useful tool is its sensitivity to sequences of thermal decomposition[61]. To illustrate this point, the dehydration of Fe-doped Kaolinite[62] ($Al_2O_3.2SiO_2.2H_2O$) to Mullite ($3Al_2O_3.2SiO_2$) and Cristobalite (SiO_2) at 1100°C will be summarized.

Duncan et al[62] utilized XRD, IR, DTA and Mössbauer spectroscopy to study the process. It was found that

(1) no change in the valence state of iron occurred,

(2) linewidth of Kaolin was narrow,

(3) linewidths of Kaolin heated to 650°C became diffuse,

(4) XRD patterns of residues quenched from 1100°C indicated the presence of Mullite. Accurate assignment by Mössbauer spectroscopy was prevented by line broadening,

(5) XRD patterns of residues obtained from quenching at 1200°C showed sufficiently sharp lines to show Fe^{3+} in more than one site.

Duncan et al[62] concluded that XRD and Mössbauer spectroscopy can be discordant, as indicated by the results for residues heated at 1200°C. The diffuse lines in Mössbauer spectra of residues from quenching at 1100°C, were thought to indicate that the iron in the samples had not reached immobility or uniform distribution, i.e. not being firmly bound in lattice sites.

In the fitting of Mössbauer spectra, it is assumed that the spectrum of the quenched material represents that of the specie(s) present at the elevated temperature.This assumption appears to hold for studies thus far where Mössbauer spectroscopy is used as a probe for thermal pathways.

3.1.2.4 **X-RAY POWDER DIFFRACTION**

A given crystalline substance always produces a characteristic diffraction pattern whether it is a component of a mixture or in the pure state. It is therefore often possible to identify an unknown solid phase by the relative intensity and position (as interplanar spacings, d, or diffraction angles 2θ , for a given wavelength λ , where $n\lambda = 2d\sin\theta$)of its X-ray reflection. A convenient method for polycrystalline powders is to use a counter diffractometer.

Factors which can affect the reliability of powder diffraction data are the precision with which the goniometer has been aligned and the care exercised during the preparation of the sample. Ideally, a sample for X-ray powder diffraction should consist of randomly orientated crystallites, in order to give a true representation of the relative intensities. The use of a flat `pressed' sample, a common method of sample preparation, may sometimes result in the crystallites showing some preferred orientation, which can affect the observed line intensities. Poor crystallinity in a sample is a prime source of line broadening and accurate determination of the true peak center may not be straightforward.

Referencing of an unknown was achieved by comparison with a known diffraction pattern e.g. those listed in the ASTM diffraction file [34], the pattern of authentic samples, or powder patterns calculated by a Rietveld type program[33] using unit cell dimensions and atomic coordinates of iron chromates reported in the literature [9-21].

For substances, which occur in the form of a powder, X-ray powder diffraction provides a useful tool for characterisation. Nevertheless, diffraction patterns should be regarded as one of a combination of techniques for the identification of a substance.

3.1.3 IRON CHROMATES

3.1.3.1 POTASSIUM IRON(III) CHROMATE HYDRATES, $KFe(CrO_4)_2.nH_2O$

Potassium iron(III) chromate 2-water[12] (Figure 3.1) crystallises in the space group C2/m; a = 10.857; b = 5.505; c = 10.334 Å and β= 137.87°. The structure consists of octahedral $FeO_4.2H_2O$ and tetrahedral CrO_4 units which are linked to form $[Fe(CrO_4)_2.2H_2O]^-_\infty$ chains with K^+ ions located between the chains. The environment of the iron atoms shows a slight deformation, with Fe-O and Fe-OH_2 bondlengths 1.94Å and 2.07Å, respectively. The oxygen atoms of the chromate tetrahedra can be termed as being either bonded or free; the former are part of the iron octahedra, whilst the latter form part of the co-ordination sphere of the K^+ ion. The Cr-O bond lengths vary between 1.59-1.73Å, whilst the O-Cr-O bond angles do not depart significantly from tetrahedral.

Bonnin[9] has reported that $KFe(CrO_4)_2.2H_2O$ dehydrates with the loss of two water molecules, in the range 180-270°C. The resulting anhydrous chromate was stable up to 370°C and underwent rapid loss of oxygen at 400°C. Popel[23] examined the decomposition of $KFe(CrO_4)_2.2H_2O$ over the range 190-300°C. Differential thermogravimetry (DTG) showed[23] that the dehydration process was complex, as indicated by

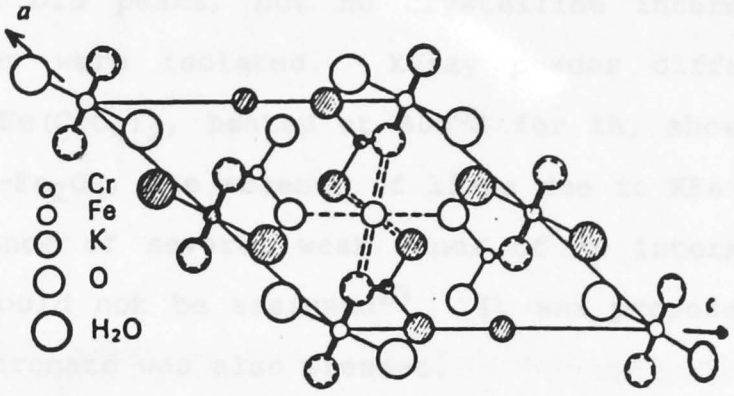

Fig 3.1a Crystal structure of $KFe(CrO_4)_2.2H_2O$ viewed along [010] axis (taken from reference 12)

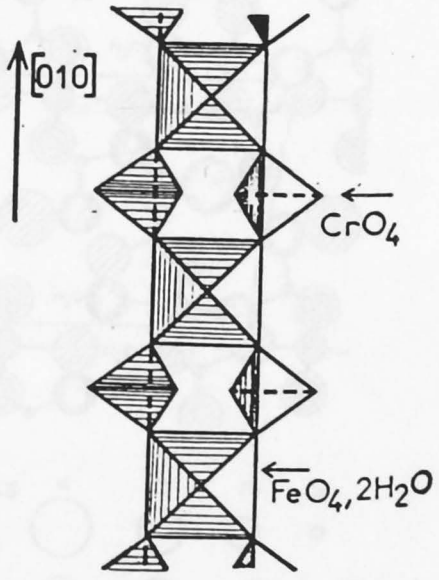

Fig3.1b Structure of $KFe(CrO_4)_2.2H_2O$ as chains of $[Fe(CrO_4)_2.2H_2O]^-$ along [010] axis (taken from reference 12)

splittings in DTG peaks, but no crystalline intermediate hydrate states were isolated. X-ray powder diffraction patterns of $KFe(CrO_4)_2$, heated at 400°C for 1h, showed the presence of α-Fe_2O_3, the absence of lines due to $KFe(CrO_4)_2$ and the presence of several weak lines of an intermediate phase which could not be assigned[23]. It was proposed that potassium dichromate was also present.

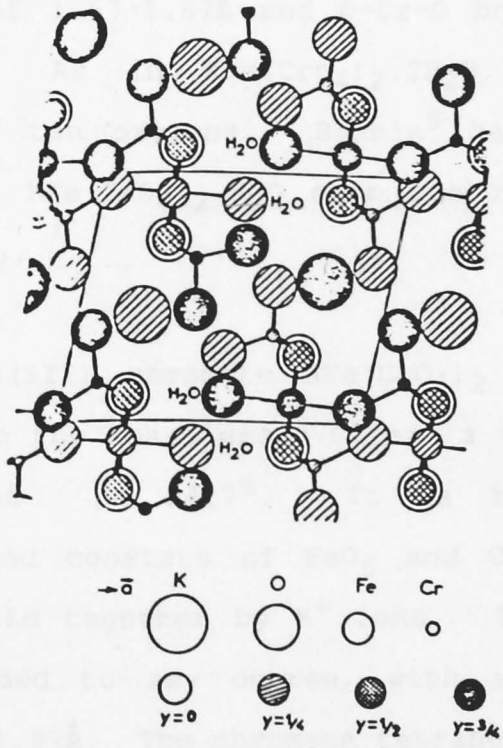

Fig. 3.2 Crystal Structure of $KFe(CrO_4)_2H_2O$ viewed along [010] axis (taken from reference 16)

Potassium iron(III) chromate 1-water[16] (Figure 3.2) crystallises in the space group $P2_1/m$; a = 9.363; b = 5.498; c = 7.667Å and β= 107.11°. $FeO_5.H_2O$ and CrO_4 units are arranged in $[Fe_2(CrO_4)_4.2H_2O]^{2-}_{\infty}$ chains along the b axis, which are linked by K^+ ions and hydrogen bonding. The iron octahedra are deformed slightly, with Fe-O and Fe-OH_2 bond lengths 2.01 and 2.07Å, respectively. The chromate tetrahedra contain both bonded and free oxygens with Cr-O bond lengths of 1.57-1.67Å and O-Cr-O bond angles between 107.8-111.1°. As in $KFe(CrO_4)_2.2H_2O$, the K^+ ion is coordinated by ten oxygens. Bonnin[9] has reported simple dehydration of $KFe(CrO_4)_2.H_2O$ over the range 230-290°C to form $KFe(CrO_4)_2$.

Potassium iron(III) chromate $KFe(CrO_4)_2$ [17], (Figure 3.3) crystallises in the space group C2/m; a = 8.64; b = 5.50; c = 7.64Å and β= 94.7°. It is isostructural with $KCr(CrO_4)_2$ [9] and consists of FeO_6 and CrO_4 units, linked into layers held together by K^+ ions. The iron octahedra are not deformed to any degree, with all the Fe-O bond lengths about 1.97Å. The chromate tetrahedra show Cr-O bond lengths and O-Cr-O bond angles in the ranges 1.56.-1.70Å and

108-112.8°, respectively. Popel[23] has reported the decomposition of $KFe(CrO_4)_2$ at 500°C to yield potassium dichromate, and iron(III) and chromium(III) oxides (equation 3.1).

$$KFe(CrO_4)_2 \rightarrow \tfrac{1}{2}K_2Cr_2O_7 + \tfrac{1}{2}Fe_2O_3 + \tfrac{1}{2}Cr_2O_3 + \tfrac{3}{4}O_2 \qquad (3.1)$$

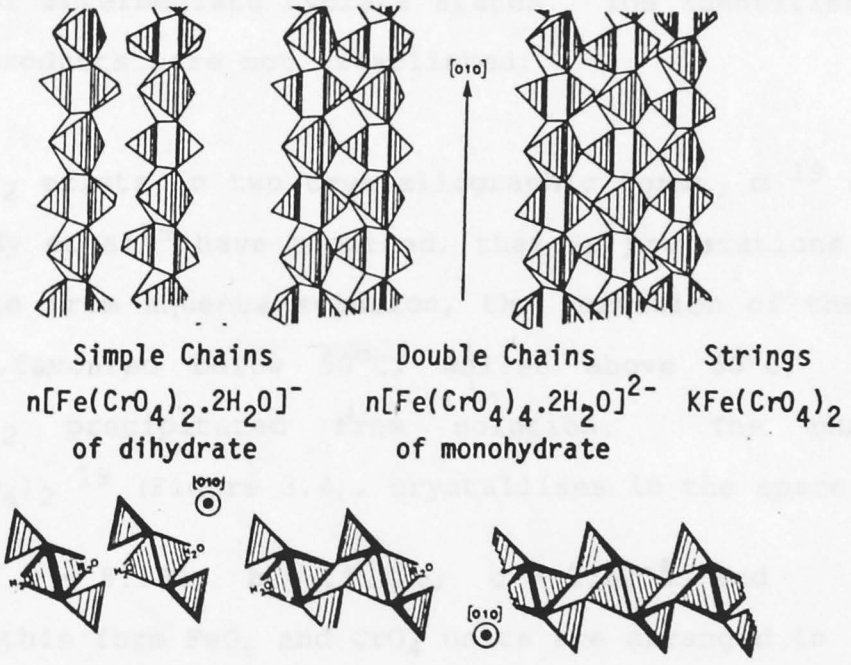

Fig. 3.3 Comparison of the crystal structures for the series $KFe(CrO_4)_2.nH_2O$, n = 0, 1 or 2 (taken from reference 17)

3.1.3.2 AMMONIUM IRON(III) CHROMATE HYDRATES, $NH_4Fe(CrO_4)_2.nH_2O$

The crystal structure of $NH_4Fe(CrO_4)_2.2H_2O$ has not been reported, but Mellier et al[38] and Bonnin[10], on the basis of infrared spectroscopy and X-ray powder diffraction methods, have proposed this compound to be isostructural with $KFe(CrO_4)_2.2H_2O$[12]. When heated, $NH_4Fe(CrO_4)_2.2H_2O$ is reported by Bonnin[9] to dehydrate by 130°C, without the formation of intermediate hydrate states. The identities of the final products were not established.

$NH_4Fe(CrO_4)_2$ exists in two crystallographic forms, α [19] and β [13]. Hardy et al[19] have reported, that in preparations of the chromate from aqueous solution, the formation of the α phase was favoured below 50°C, whilst above 50°C, β-$NH_4Fe(CrO_4)_2$ precipitated from solution. The phase α-$NH_4Fe(CrO_4)_2$ [19] (Figure 3.4), crystallises in the space group $P2_1$; a = 8.192; b = 15.136; c = 5.520Å and β= 90.59°. In this form FeO_6 and CrO_4 units are arranged in layers held together by NH_4^+ ions. The FeO_6 octahedra are slightly deformed, the average Fe-O bond distance being 1.97A, while the chromate tetrahedra have bond lengths (Cr-O) and bond angles (O-Cr-O) in the ranges 1.54-1.73Å and 100-111°, respectively.

Ammonium iron chromate (β-phase, Figure 3.5) crystallises in the orthorhombic space group Pnma; a = 14.508; b =

5.471 and c = 8.667Å. The structure[13] has a three dimensional framework of FeO_6 and CrO_4 units with NH_4+ ions located in interstices. The iron octahedra are more

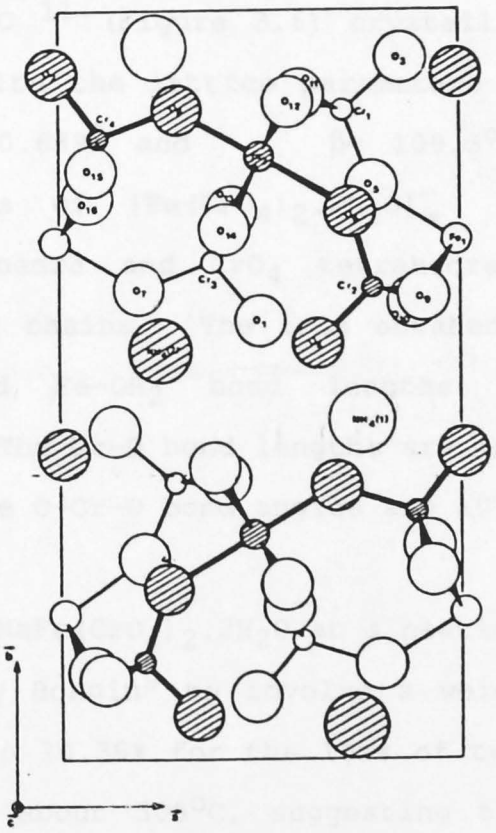

Fig. 3.4 Crystal structure of α-$NH_4Fe(CrO_4)_2$ viewed parallel to [001] axis (taken from reference 19)

symmetrical than those in the α-phase with the Fe-O bond length 1.96Å, while the chromate tetrahedra are distorted to a greater degree compared with those in the α-phase[19], with Cr-O bond lengths and O-Cr-O bond angles in the ranges 1.53 - 1.79Å and 100 - 114° respectively.

3.1.3.3 **SODIUM IRON(III) CHROMATE HYDRATES, $NaFe(CrO_4)_2.nH_2O$**

$NaFe(CrO_4)_2.2H_2O$ [11] (Figure 3.6) crystallises in the space group C2/c; with the lattice parameters a = 14.247; b = 5.425; c = 10.689Å and β= 109.3°. The structure contains chains of $[Fe(CrO_4)_2.2H_2O]^-_\infty$, consisting of $FeO_4.2H_2O$ octahedra and CrO_4 tetrahedra, with Na^+ ions located between chains. The iron octahedra are distorted, with Fe-O and $Fe-OH_2$ bond lengths 1.96 and 2.04Å, respectively. The Cr-O bond lengths are in the range 1.60 - 1.72Å whilst the O-Cr-O bond angles are 107.9 - 110.6°.

Dehydration of $NaFe(CrO_4)_2.2H_2O$ at a heating rate of 1°C/min was reported by Bonnin[9] to involve a weight loss of about 12%, compared to 10.38% for the loss of two water molecules, when heated to about 300°C, suggesting that the anhydrous chromate was not isolatable by heating of the dihydrate. Popel has shown however, that $NaFe(CrO_4)_2$ can be obtained by the isothermal heating of $NaFe(CrO_4)_2.2H_2O$ at 300°C in air[23]. The anhydrous chromate was stable to about 400°C, after which the loss of oxygen was detected.

The crystal structures of $NaFe(CrO_4)_2.H_2O$ and $NaFe(CrO_4)_2$ have not been reported but XRD studies[9] on $NaFe(CrO_4)_2.H_2O$ suggest that it is isostructural with $KFe(CrO_4)_2.H_2O$ [16] (Fig. 3.2), whilst, on the basis of XRD[9] and IR,[17] it has been proposed that $NaFe(CrO_4)_2$ is isostructural with $KFe(CrO_4)_2$.

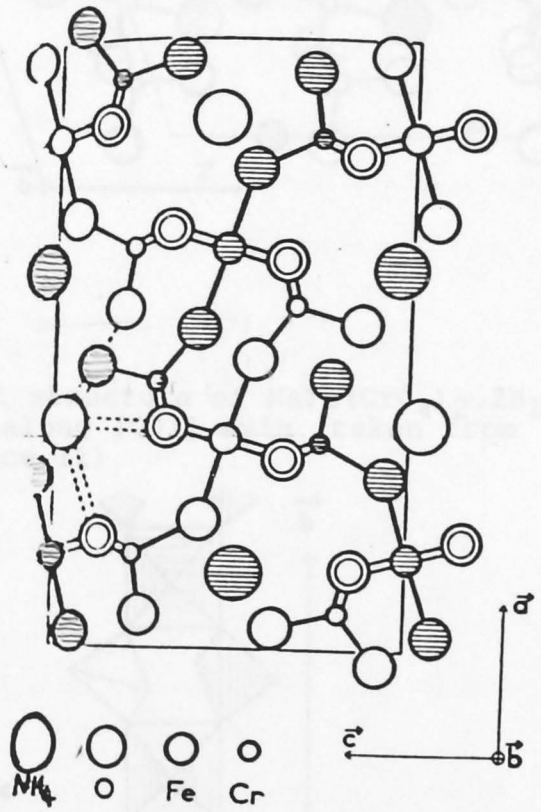

Fig. 3.5 Crystal structure of β-$NH_4Fe(CrO_4)_2$ viewed parallel to [010] axis (taken from reference 13)

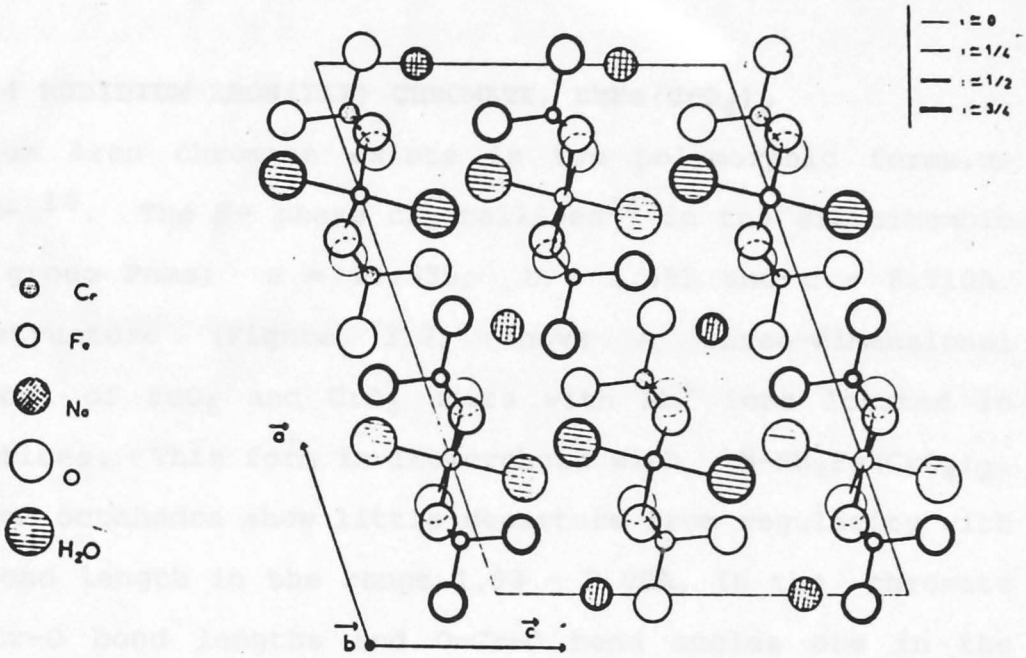

Fig. 3.6a Crystal structure of $NaFe(CrO_4)_2.2H_2O$ viewed along [001] axis (taken from reference 11)

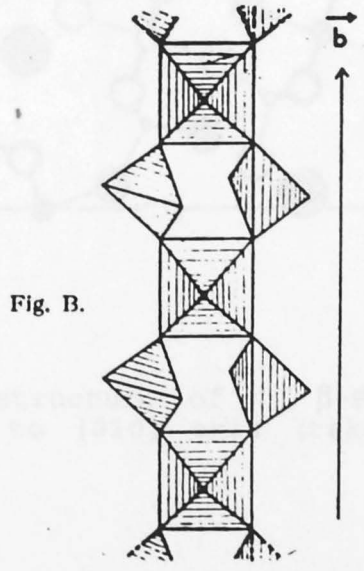

Fig. B.

Fig. 3.6b Structure of $NaFe(CrO_4)_2.2H_2O$ as chains of $[Fe(CrO_4)_2.2H_2O]^-$ along [001] axis

(taken from reference 11)

3.1.3.4 **RUBIDIUM IRON(III) CHROMATE, $RbFe(CrO_4)_2$**

Rubidium iron chromate exists in two polymorphic forms, α- and β- [14]. The β- phase crystallises[14] in the orthorhombic space group Pnma; a = 14.535; b = 5.483 and c = 8.710A. The structure (Figure 3.7) shows a three-dimensional framework of FeO_6 and CrO_4 units with Rb^+ ions located in interstices. This form is isomorphous with β-$NH_4Fe(CrO_4)_2$. The iron octahedra show little departure from regularity with Fe-O bond length in the range 1.98 - 2.00A. In the chromate ion, Cr-O bond lengths and O-Cr-O bond angles are in the ranges 1.58 - 1.66A and 107.9 - 112.2°, respectively.

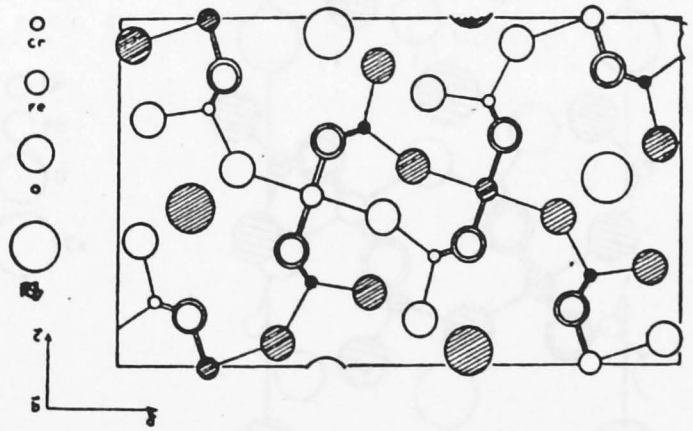

Fig. 3.7 Crystal structure of β-$RbFe(CrO_4)_2$ viewed parallel to [010] axis (taken from reference 14)

The structure of the α-phase has not been reported, but powder XRD studies[19] indicate this form to be isostructural with α-$NH_4Fe(CrO_4)_2$[19]. Hydrated forms of $RbFe(CrO_4)_2$ are unknown,[14] although Popel suggests that one quarter of a mole of water per mole of $RbFe(CrO_4)_2$ could be present as zeolite water,[23] on the basis of thermogravimetry. Decomposition of $RbFe(CrO_4)_2$ occurs endothermically in the range 400 - 500°C with the formation of rubidium dichromate, and iron(III) and chromium(III) oxides.

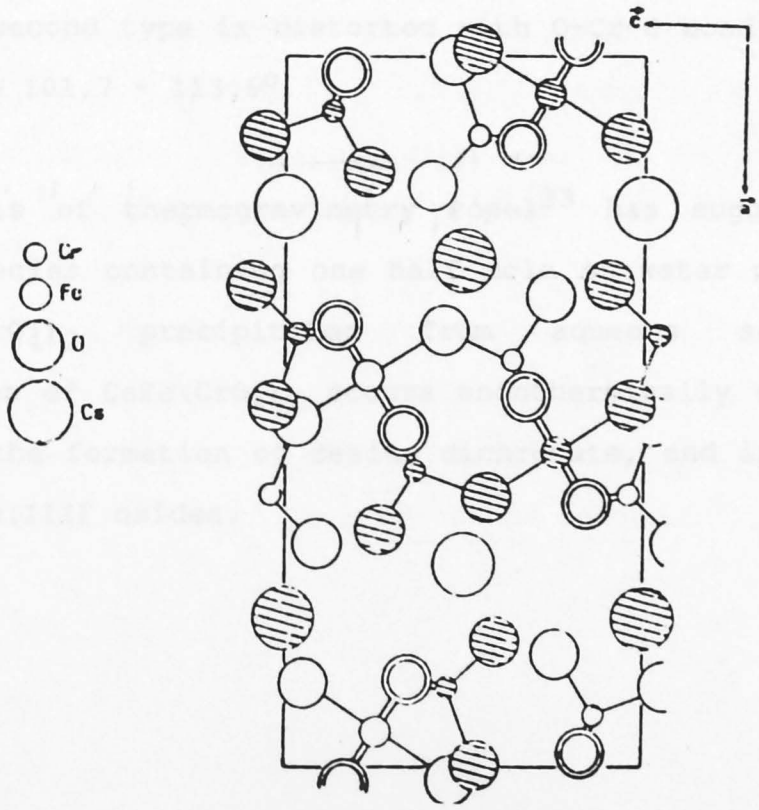

Fig. 3.8 Crystal structure of $CsFe(CrO_4)_2$ viewed along [010] axis(taken from reference 15)

3.1.3.5 **CESIUM IRON (III) CHROMATE, $CsFe(CrO_4)_2$**

$CsFe(CrO_4)_2$ [15] (Figure 3.8) crystallises in the space group Pnma; a = 15.590; b = 5.560 and c = 8.312Å. It is isostructural with $CsCr(CrO_4)_2$ [39] and contains chains of $[Fe(CrO_4)_2]^-$. The Fe-O bond lengths of 2.02Å in the octahedra are comparable to those reported for the series $MFe(CrO_4)_2.nH_2O$. The structure contains two crystallographically distinct chromate tetrahedra. Type one contains O-Cr-O bond angles in the range 108.6 - 110.5°, whilst the second type is distorted with O-Cr-O bond angles in the range 101.7 - 113.6°.

On the basis of thermogravimetry Popel[23] has suggested a hydrated species containing one half mole of water per mole of $CsFe(CrO_4)_2$ precipitated from aqueous solution. Decomposition of $CsFe(CrO_4)_2$ occurs endothermically at about 500°C with the formation of cesium dichromate, and iron(III) and chromium(III) oxides.

3.1.3.6 THALLIUM IRON(III) CHROMATE HYDRATES, $TlFe(CrO_4)_2.nH_2O$

The thallium salts exist with n = 0, 1 or 2. The structures have yet to be confirmed crystallographically, but powder XRD studies[9] have shown that for n = 1 or 2 the hydrates are isostructural with the potassium compounds. X-ray powder diffractometry has also shown[9] the anhydrous salt to be dimorphic, with α- and β- phases similar to those reported for $NH_4Fe(CrO_4)_2$[13,19]. Bonnin[9] has reported the dehydration of $TlFe(CrO_4)_2.2H_2O$ and $TlFe(CrO_4)_2.H_2O$ in the regions 180 - 250°C and 230 - 290°C, respectively, without intermediate hydrate formation. Bonnin[9] has also reported that the interconversion of α- to β- $TlFe(CrO_4)_2$ occurs at 330° in air. In contrast, interconversion of the $NH_4Fe(CrO_4)_2$ phases is not known to occur[9,19].

3.1.3.7 IRON(III) CHROMATE HYDRATES $Fe_2(CrO_4)_3.nH_2O$

Iron(III) chromate exists in the hydrated forms where n = 1 or 3. Suitable crystals for structure determination of iron(III) chromate 1-water have yet to be obtained[9].

Pyrolysis of this chromate indicates[9] that it does not form a stable anhydrous chromate, but undergoes simultaneous dehydration/decomposition at 250°C, with the weight loss becoming rapid above 300°C. $Fe_2(CrO_4)_3.3H_2O$ (Figure 3.9) crystallises[20] in the space group $P2_1/c$; a = 15.802; b = 5.436; c = 14.603Å and β= 108.13°. The structure consists of compact sheets $[Fe(CrO_4)_2]_\infty^{n-}$, connected by $[Fe(CrO_4).(H_2O)_3]_\infty^{n+}$ chains. The sheets are built of FeO_6 octahedra and CrO_4 tetrahedra, whereas the chains contain $FeO_3(H_2O)_3$ octahedra. The average bond lengths in the distorted octahedra are Fe-O 2.02Å and Fe-OH_2 2.00Å. The chromate tetrahedra contain Cr-O bond lengths and O-Cr-O bond angles in the ranges 1.57 - 1.75Å and 106.6° - 111.8°, respectively.

Bonnin[9] has reported dehydration of iron(III) chromate 3-water to take place between 30 - 270°C. Isothermal studies[9] at 220°C established on the basis of elemental analyses, that the product formed was $Fe_2(CrO_4)_3$. Its powder pattern was poor and different from those reported for the analogous $Cr_2(CrO_4)_3$ [63] and $Fe_2(SO_4)_3$[64].

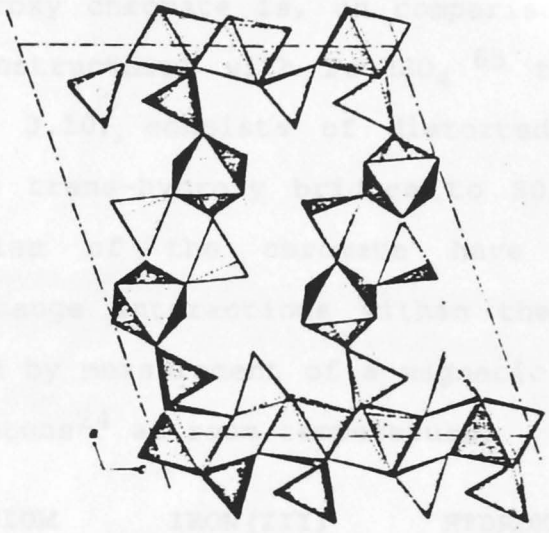

Fig. 3.9 Crystal structure of $Fe_2(CrO_4)_3.3H_2O$ along [010] axis, showing the linking of chains (taken from reference 20)

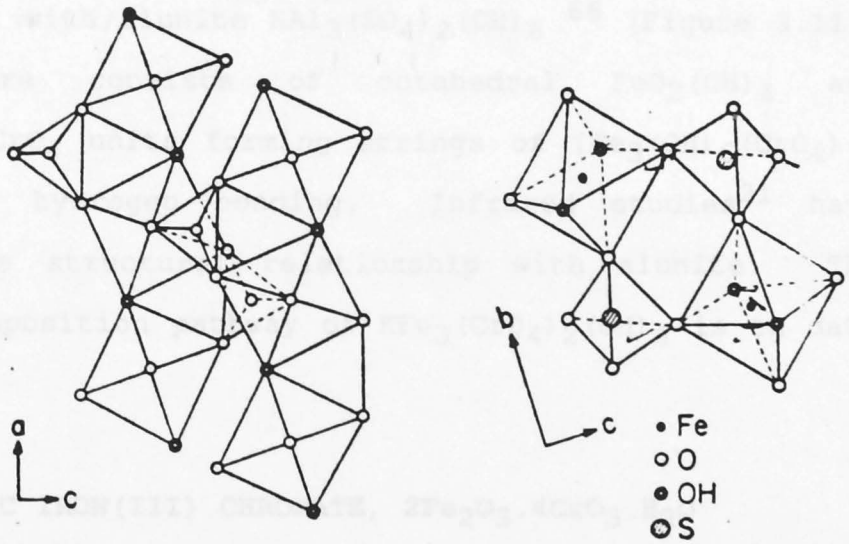

Fig. 3.10 Crystal structure of $FeOHSO_4$, viewed along the a and b axes (taken from reference 65)

3.1.3.8 **IRON(III) HYDROXY CHROMATE, $FeOHCrO_4$**

Iron(III) hydroxy chromate is, on comparison of XRD powder patterns[9], isostructural with $FeOHSO_4$ [65] the structure of which (Figure 3.10), consists of distorted Fe^{3+} octahedra linked by two trans-hydroxy bridges to SO_4^{2-} groups. No thermal studies of the chromate have been reported. Extensive exchange interactions within the structure have been confirmed by measurement of a magnetic moment, of about 3.4 Bohr magnetons[24] at room temperature.

3.1.3.9 **POTASSIUM IRON(III) HYDROXY CHROMATE, $KFe_3(CrO_4)_2(OH)_6$**

The basic chromate $KFe_3(CrO_4)_2(OH)_6$ [21] crystallises in the space group R3m; a_{hex} = 7.430 and c_{hex} = 17.440Å, isostructural with alunite $KAl_3(SO_4)_2(OH)_6$ [66] (Figure 3.11). The structure consists of octahedral $FeO_2(OH)_4$ and tetrahedral CrO_4 units forming strings of $[Fe_3(OH)_6(CrO_4)_3]$ connected by hydrogen bonding. Infrared studies[21] have confirmed the structural relationship with alunite. The thermal decomposition pathway of $KFe_3(CrO_4)_2(OH)_6$ is to date unknown.

3.1.3.10 **BASIC IRON(III) CHROMATE, $2Fe_2O_3.4CrO_3.H_2O$**

The basic chromate, $Fe_2O_3.4CrO_3.H_2O$, was reported by Briggs[7]. The structural or thermal properties of the compound are to date unknown.

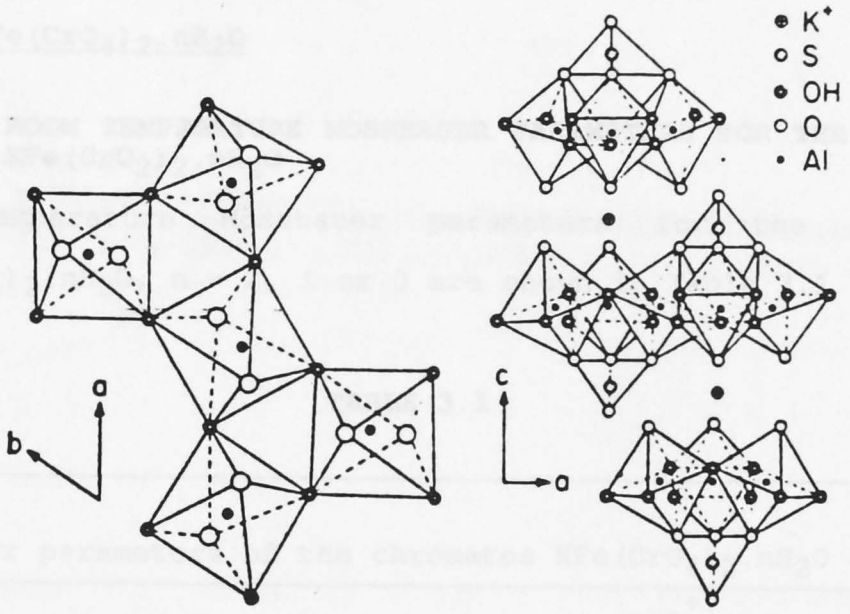

Fig. 3.11 Crystal structure of $KAl_3(SO_4)_2(OH)_6$, viewed along the c axis and b axis (taken from reference 24)

3.2 RESULTS AND DISCUSSION

3.2.1 $KFe(CrO_4)_2.nH_2O$

3.2.1.1 ROOM TEMPERATURE MÖSSBAUER PARAMETERS FOR THE SERIES $KFe(CrO_2)_2.nH_2O$

Room temperature Mössbauer parameters for the series $KFe(CrO_4)_2.nH_2O$, n = 2, 1 or 0 are shown in Table 3.1.

TABLE 3.1

Mössbauer parameters of the chromates $KFe(CrO_4)_2.nH_2O$ at 25°C

Compound	Mössbauer Parameters/mms^{-1} $^{+}$			Chi-squared
	δ	Eq	Γ	χ^2
$KFe(CrO_4)_2.2H_2O$	0.401(1)	0.341(3)	0.269(3)	1.08
$KFe(CrO_4)_2.H_2O$	0.410(2)	0.472(2)	0.263(5)	1.10
$KFe(CrO_4)_2$	0.412(7)	0.111(1)	0.227(1)	0.99

+ average error in parameters (given) in parenthesis

The Mössbauer spectra were resolved into simple quadrupole doublets with isomer shifts typical for Fe(III) ions. The difference in quadrupole splitting (Eq) between $KFe(CrO_4)_2.2H_2O$ and $KFe(Cro_4)_2.H_2O$ is surprising as, on the basis of Fe-O and Fe-OH_2 bond distances, the structure of the 1-water hydrate is the least distorted and would be

expected to show a smaller Eq. However, the quadrupole splitting for the anhydrous chromate is consistent with crystallographic studies[17], which show polyhedra in this compound to be closest to cubic symmetry.

3.2.1.2 **THERMAL DECOMPOSITION $KFe(CrO_4)_2.2H_2O$**

Figure 3.12 shows a representative curve for heating $KFe(CrO_4)_2.2H_2O$ at 10^oC/min. The proposed reaction stoichiometry is shown in Table 3.2, whilst differential thermal analysis (DTA), Figure 3.13, confirmed the two-step nature of the pyrolysis.

X-ray powder diffraction patterns of residues quenched from 320^oC and 500^oC confirmed the presence of products shown in reactions 3.2.1 and 3.2.2, with the exception of $K_2Cr_2O_7$. The absence of lines due to $K_2Cr_2O_7$ in XRD patterns was also reported by Popel[23]. The likely explanation is that the dichromate formed was finely divided. The presence of $K_2Cr_2O_7$ was confirmed when filtrates from the water extraction of samples, which had been heated to 500^oC, yielded orange crystals on slow evaporation. XRD patterns of the crystals completed the identification.

TABLE 3.2

Reaction stoichiometry for the thermal decomposition of $KFe(CrO_4)_2.2H_2O$ at heating rate 10^oC/min.

Decomposition steps	Wt loss % obs	calc	
$KFe(CrO_4)_2.2H_2O \rightarrow KFe(CrO_4)_2+2H_2O$	10.15±0.20	9.90	(3.2.1)
$KFe(CrO_4)_2 \rightarrow \frac{1}{2}K_2Cr_2O_7+\frac{1}{2}Fe_2O_3+\frac{1}{2}Cr_2O_3+\frac{3}{4}O_2$	6.89±0.35	7.34	(3.2.2)
$KFe(CrO_4)_2.2H_2O \rightarrow \frac{1}{2}K_2Cr_2O_7+\frac{1}{2}Fe_2O_3+\frac{1}{2}Cr_2O_3+\frac{3}{4}O_2+2H_2O$	16.10±0.25	16.53	(3.2.3)

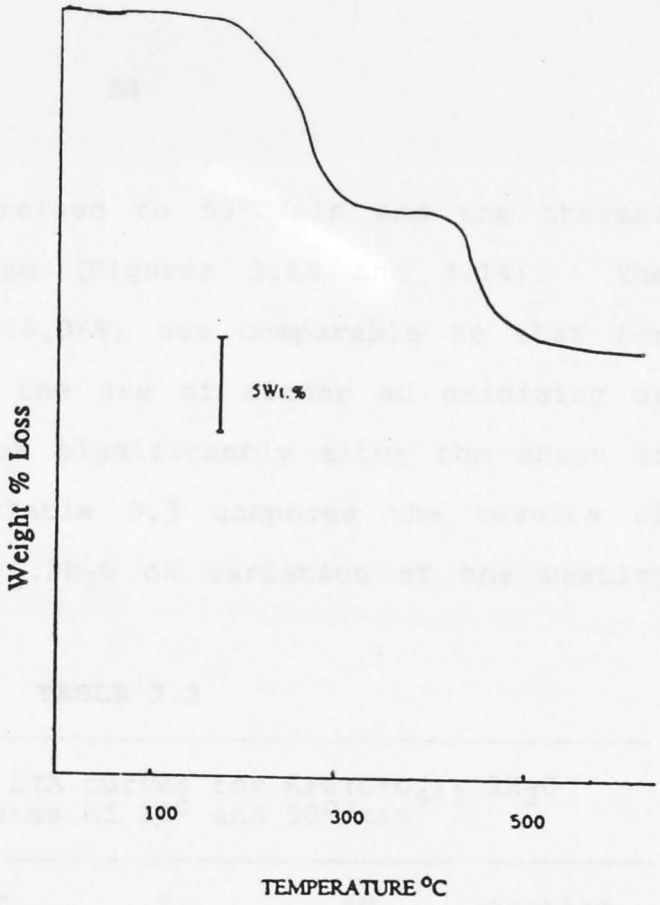

Fig 3.12 Representative thermogram for $KFe(CrO_4)_2.2H_2O$ heated at 10°C/min

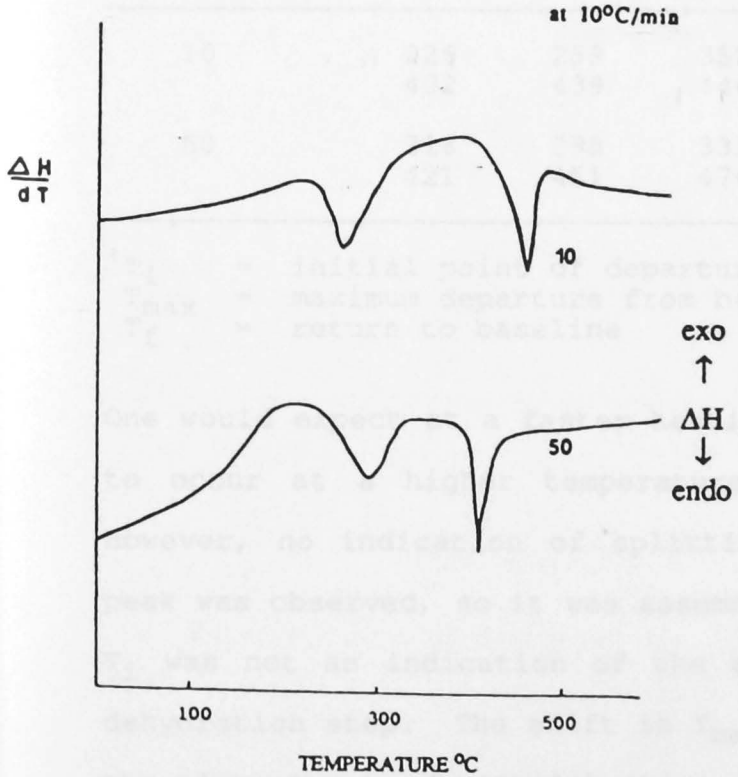

Fig 3.13 Representative differential thermal analysis curves for $KFe(CrO_4)_2.2H_2O$ heated at 10°C and 50°C/min

The heating rate was raised to 50°C/min and the thermal analysis curves examined (Figures 3.13 and 3.14). The observed weight loss (16.06%) was comparable to that for reaction 3.2.3, whilst the use of either an oxidising or inert atmosphere did not significantly alter the shape of the thermal curves. Table 3.3 compares the results of pyrolysis for $KFe(CrO_4)_2.2H_2O$ on variation of the heating rate.

TABLE 3.3

Comparison of the DTA curves for $KFe(CrO_4)_2.2H_2O$ at heating rates of 10° and 50°/min

Heating rate (°C/min)	$^{+}T_i$	T_{max}	T_f	ΔH	reaction
10	226	259	352	endo	$-H_2O$
	402	439	444	endo	$-O_2$
50	216	295	331	endo	$-H_2O$
	421	451	476	endo	$-O_2$

$^{+}T_i$ = initial point of departure from baseline
T_{max} = maximum departure from baseline
T_f = return to baseline

One would expect at a faster heating rate T_i for dehydration to occur at a higher temperature due to thermal lagging. However, no indication of splitting in the DTA dehydration peak was observed, so it was assumed that the lower value for T_i was not an indication of the existence of an additional dehydration step. The shift in T_{max} is to be expected due to the dependence of equilibration on heating rate; other

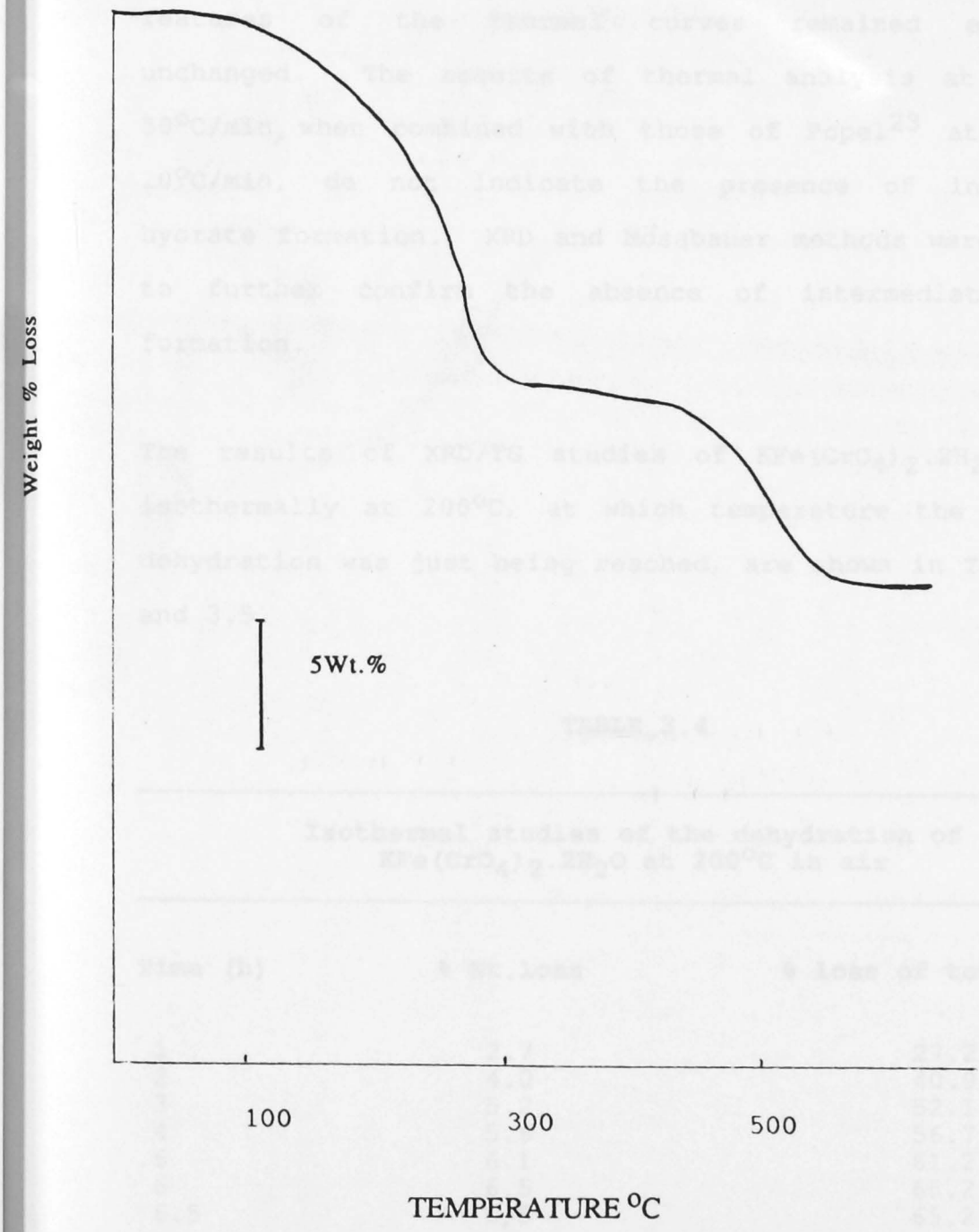

Fig 3.14 Representative thermogram for $KFe(CrO_4)_2.2H_2O$ heated at 50°C/min

features of the thermal curves remained essentially unchanged. The results of thermal analysis at 10°C and 50°C/min, when combined with those of Popel[23] at 2.5° and 10°C/min, do not indicate the presence of intermediate hydrate formation. XRD and Mössbauer methods were utilized to further confirm the absence of intermediate hydrate formation.

The results of XRD/TG studies of $KFe(CrO_4)_2.2H_2O$ heated isothermally at 200°C, at which temperature the onset of dehydration was just being reached, are shown in Tables 3.4 and 3.5.

TABLE 3.4

Isothermal studies of the dehydration of $KFe(CrO_4)_2.2H_2O$ at 200°C in air

Time (h)	% Wt.loss	% loss of total water
1	2.7	27.2
2	4.0	40.9
3	5.2	52.1
4	5.6	56.7
5	6.1	61.2
6	6.5	65.2
6.5	6.5	65.2

TABLE 3.5

X-ray powder diffraction data for $KFe(CrO_4)_2.2H_2O$ quenched after various periods of time at 200°C.

Time	d_{obs}(Å)	I_{rel}	Assignment	d_{cal}
1.5h	7.55	15	a + b	7.61 7.52
	5.09	60	b	5.16
	4.89	35	b	4.95
	4.25	15	a	4.30
	4.00	30	a	4.04
	3.83	25	a	3.80
	3.58	85	b	3.62
	3.38	20	b	3.41
	3.10	100	b	3.13
	2.97	50	a + b	3.01
	2.86	10	a	2.82
	2.80	25	b	2.82
	2.74	60	b + a	(2.75
	2.69	15	a	(
	2.55	25	b	2.56
	2.41	10	a	2.40
3h	7.60	70	a	7.61
	5.10	30	b	5.16
	4.92	20	b	4.95
	4.25	45	a	4.30
	4.10	65	a	4.04
	3.95	60	a	3.88
	3.60	70	b	3.62
	3.30	40	a + b	3.41
	3.10	100	b	3.13
	2.95	50	a + b	3.01
	2.80	60	b	2.82
	2.75	55	b	(2.75
	2.70	20	a	(
24h	7.60	65	a	7.61
	5.06	30	b	5.16
	4.87	20	b	4.95
	4.28	45	a	4.30
	4.00	85	a	4.04
	3.86	80	a	3.80
	3.61	75	b	3.62
	3.11	45	b	3.13
	2.99	100	a + b	3.01
	2.86	45	a	2.82
	2.73	70	a + b	2.75
	2.54	60	a	2.56

a = $KFe(CrO_4)_2$

b = $KFe(CrO_4)_2.2H_2O$

XRD patterns of residues from heating for 1.5 and 3h showed the absence of lines due to $KFe(CrO_4)_2.H_2O$,[16] indicating that the loss of about 50% of total water was due to dehydration of bulk $KFe(CrO_4)_2.2H_2O$ to $KFe(CrO_4)_2$ rather than monohydrate formation. XRD patterns of residues obtained after other heating periods showed only the presence of $KFe(CrO_4)_2.2H_2O$ and the anhydrous compound. Mössbauer spectra of samples removed at 1, 3, 24 and 28 h were measured (Table 3.6 and Figures 3.15 and 3.16).

The spectra were readily resolved into two overlapping quadrupole doublets (Figures 3.15 and 3.16). The quadrupole splitting (0.12 mms^{-1}) was assigned to the anhydrous chromate $KFe(CrO_4)_2$, whilst the outer doublet (0.4 mms^{-1}) was assigned to $KFe(CrO_4)_2.2H_2O$ rather than monohydrate on the basis of XRD studies (Table 3.3). The linewidth of the outer doublet was broad which, though not resolvable into a further quadrupole split doublet, could indicate the presence of a further intermediate, possibly the monohydrate. The absence in XRD patterns of d-spacings for the monohydrate could be due to poor crystallinity of the sample.

(a) 1h

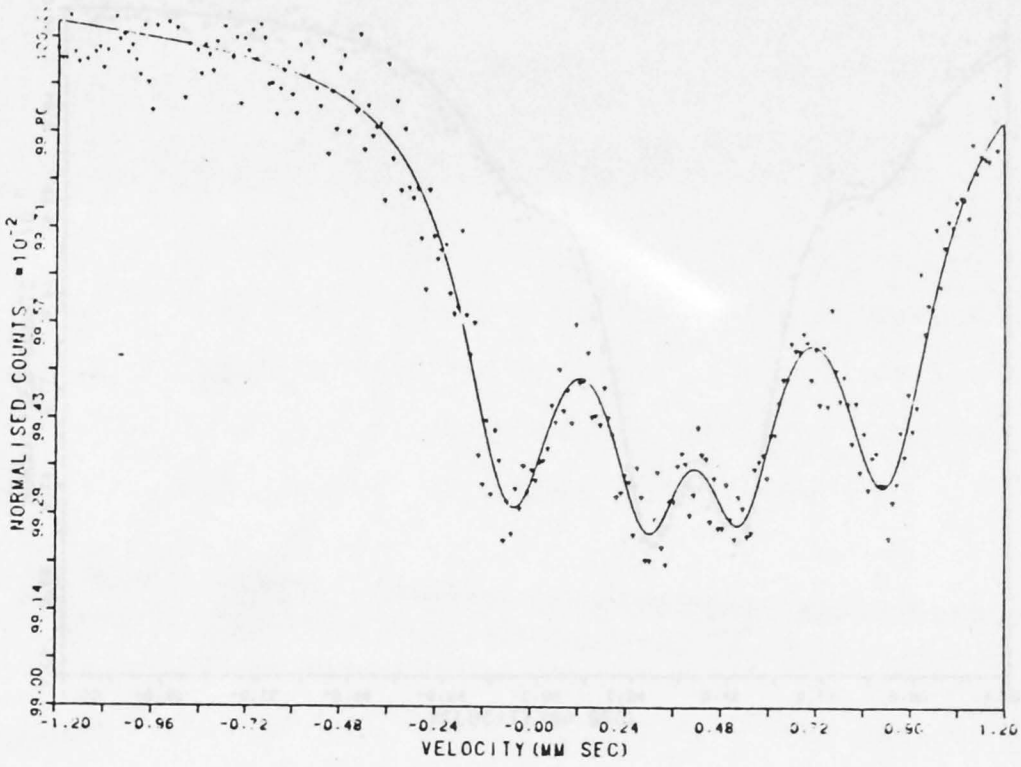

(b) 3h

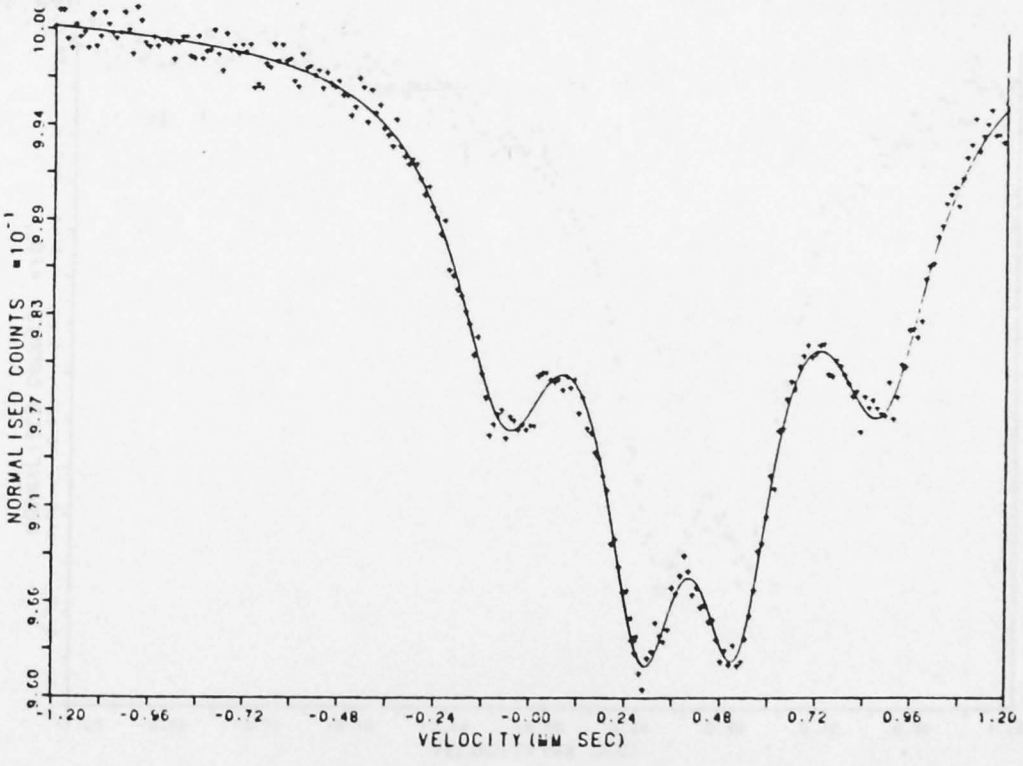

Fig 3.15 Mössbauer spectra of $KFe(CrO_4)_2.2H_2O$ quenched from 200°C after various periods of time

(a) 24h

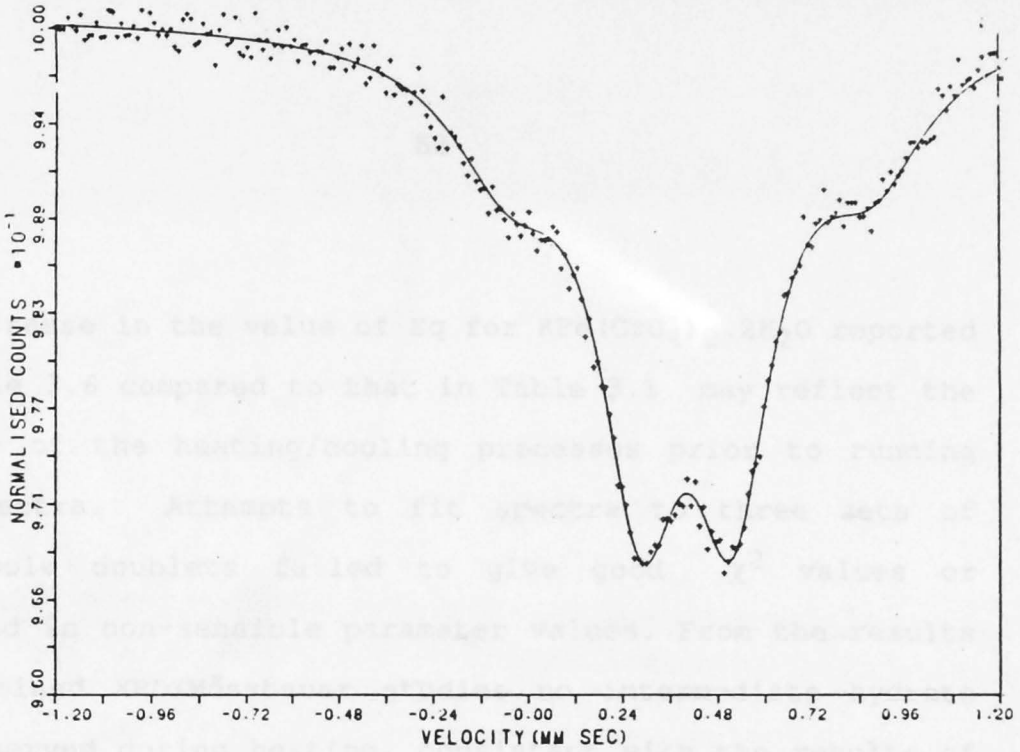

(b) 28h

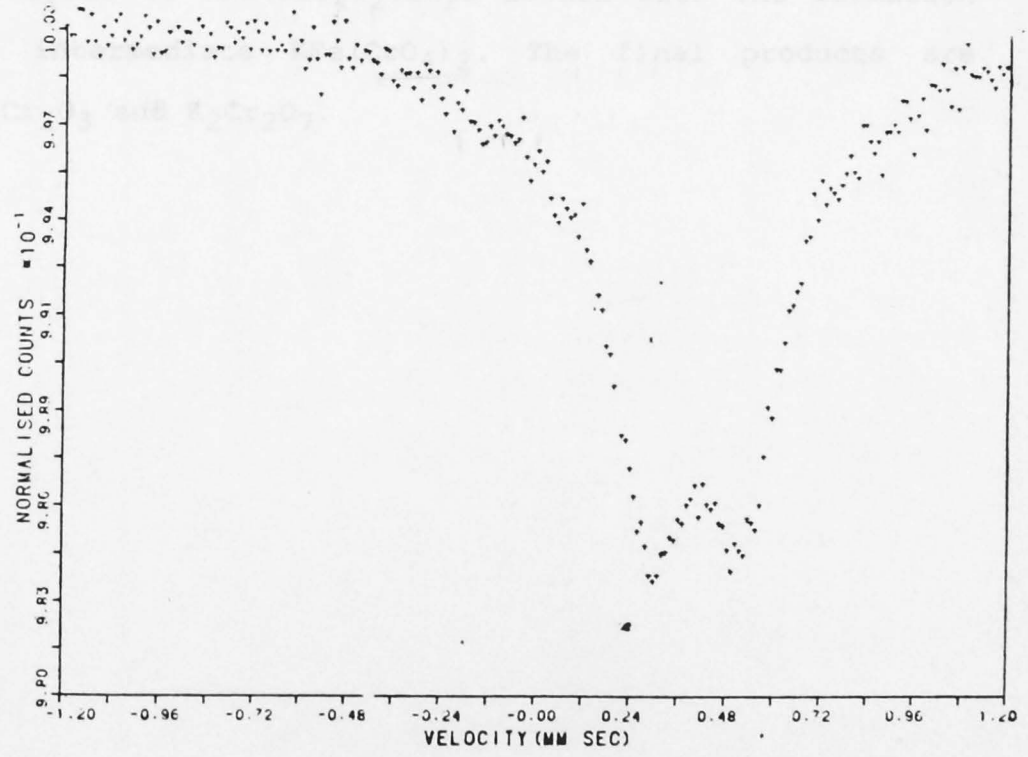

Fig 3.16 Mössbauer spectra of $KFe(CrO_4)_2.2H_2O$ quenched from 200°C after various periods of time

The increase in the value of Eq for $KFe(CrO_4)_2.2H_2O$ reported in Table 3.6 compared to that in Table 3.1 may reflect the effects of the heating/cooling processes prior to running the spectra. Attempts to fit spectra to three sets of quadrupole doublets failed to give good χ^2 values or resulted in non-sensible parameter values. From the results of combined XRD/Mössbauer studies no intermediate hydrate was observed during heating, consistent with the results of thermal analysis.

3.2.1.3 **CONCLUSION**

The pyrolysis of $KFe(CrO_4)_2.2H_2O$ occurs with the formation of the intermediate $KFe(CrO_4)_2$. The final products are Fe_2O_3, Cr_2O_3 and $K_2Cr_2O_7$.

TABLE 3.6

Mössbauer parameters of residues quenched after heating $KFe(CrO_4)_2.2H_2O$ at 200°C for various periods of time

Time (h)	Mössbauer parameters/mms^{-1}						Peak Area Ratio	
	δ_1	δ_2	Eq_1	Eq_2	Γ_1	Γ_2	A_1/A_2	X^2
1	0.416(1)	0.397(1)	0.119(1)	0.402(3)	0.299(1)	0.226(1)	1:8	0.92
3	0.389(1)	0.400(1)	0.117(1)	0.405(3)	0.248(2)	0.316(1)	1:1.1	1.350
24	0.387(7)	0.402(4)	0.116(1)	0.410(6)	0.250(2)	0.343(2)	5:1	1.15
28	0.399(1)	-	0.117(1)	-	0.282(3)	-	-	1.10

3.2.2 $NaFe(CrO_4)_2.nH_2O$

3.2.2.1 ROOM TEMPERATURE MÖSSBAUER PARAMETERS FOR THE SERIES $NaFe(CrO_4)_2.nH_2O$

Table 3.7 details the room temperature Mössbauer parameters for $NaFe(CrO_4)_2.nH_2O$, n = 0 and 2.

TABLE 3.7

Mössbauer parameters of the chromates $NaFe(CrO_4)_2.nH_2O$ at 25°C

	Mössbauer parameters /mms^{-1}			
Compound	δ	Eq	Γ	χ^2
$NaFe(CrO_4)_2.2H_2O$	0.411(2)	0.356(2)	0.309(7)	1.20
$NaFe(CrO_4)_2$	0.394(4)	0.156(1)	0.241(1)	1.41

The spectra consisted of simple quadrupole doublets at room temperature, and Eq parameters were consistent with the proposal by Gravereau and Hardy[17] that, for the series $MFe(CrO_4)_2.nH_2O$, dehydration results in a decrease in distortion within the iron octahedra. The Eq splittings were comparable to those reported in section 3.2.1.1 for the chromates $KFe(CrO_2)_2.nH_2O$, n = 0 and 2.

3.2.2.2 THERMAL DECOMPOSITION OF $NaFe(CrO_4)_2.2H_2O$

Thermal decomposition curves for sodium iron(III) chromate 2-water, heated at 10°C and 50°C/min are shown in Figures 3.17 and 3.18, and the corresponding differential thermal analysis curves are shown in Figure 3.19.

The thermogram at 10°C/min (Figure 3.17) indicates that dehydration proceeds by at least two stages, but no plateau separates the steps. The weight loss, 10.52%, up to 230°C, corresponded to the calculated loss of 10.31% for two water molecules (see Table 3.8), but there was a further slow weight loss to 320°C. The total weight loss to 320°C was 11.80 $\pm$ 0.15%, significantly greater than that for the loss of two moles of water. Differential thermal analysis showed the presence of endotherms at T_{max} 204, 222 and 265°C, the first two endotherms being attributable to dehydration processes.

X-ray powder diffraction patterns of residues quenched from 220°C showed good agreement with that of the anhydrous chromate, $NaFe(CrO_4)_2$ [10], whilst samples quenched from 320°C showed the presence of $NaFe(CrO_4)_2$[10] and $Na_2Cr_2O_7$[33]. XRD patterns of residues from heating to higher temperatures confirmed the presence of Fe_2O_3, Cr_2O_3, Na_2CrO_4 and $Na_2Cr_2O_7$ at 400 and 490°C by comparing with literature values[33]. The

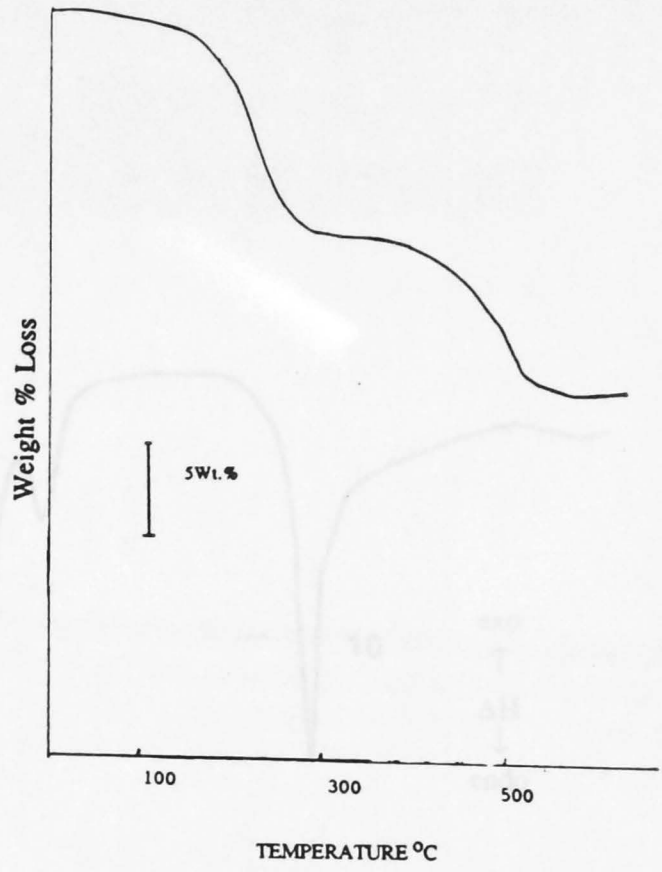

Fig 3.17 Representative thermogram for $NaFe(CrO_4)_2.2H_2O$ heated at 10°C/min

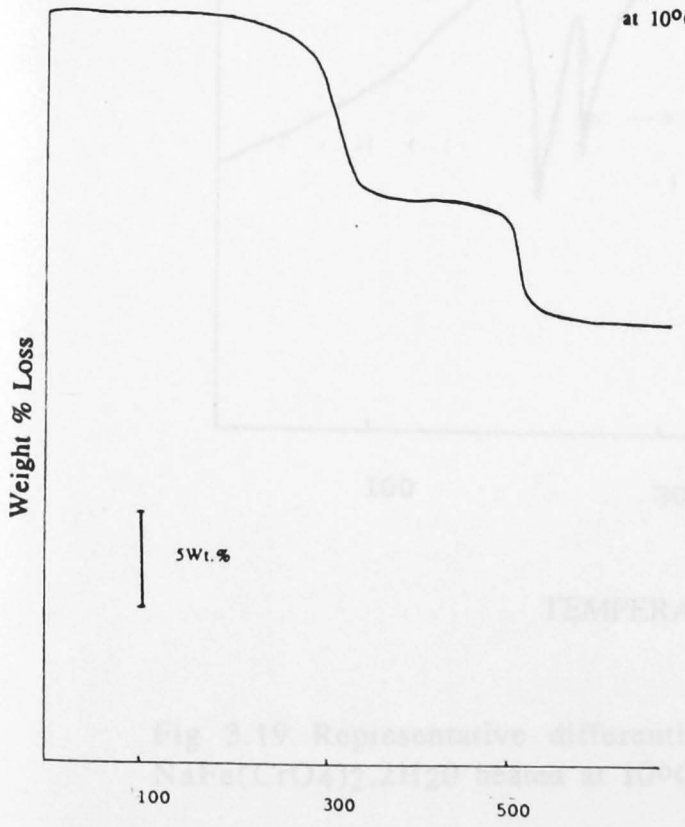

Fig 3.18 Representative thermogram for $NaFe(CrO_4)_2.2H_2O$ heated at 50°C/min

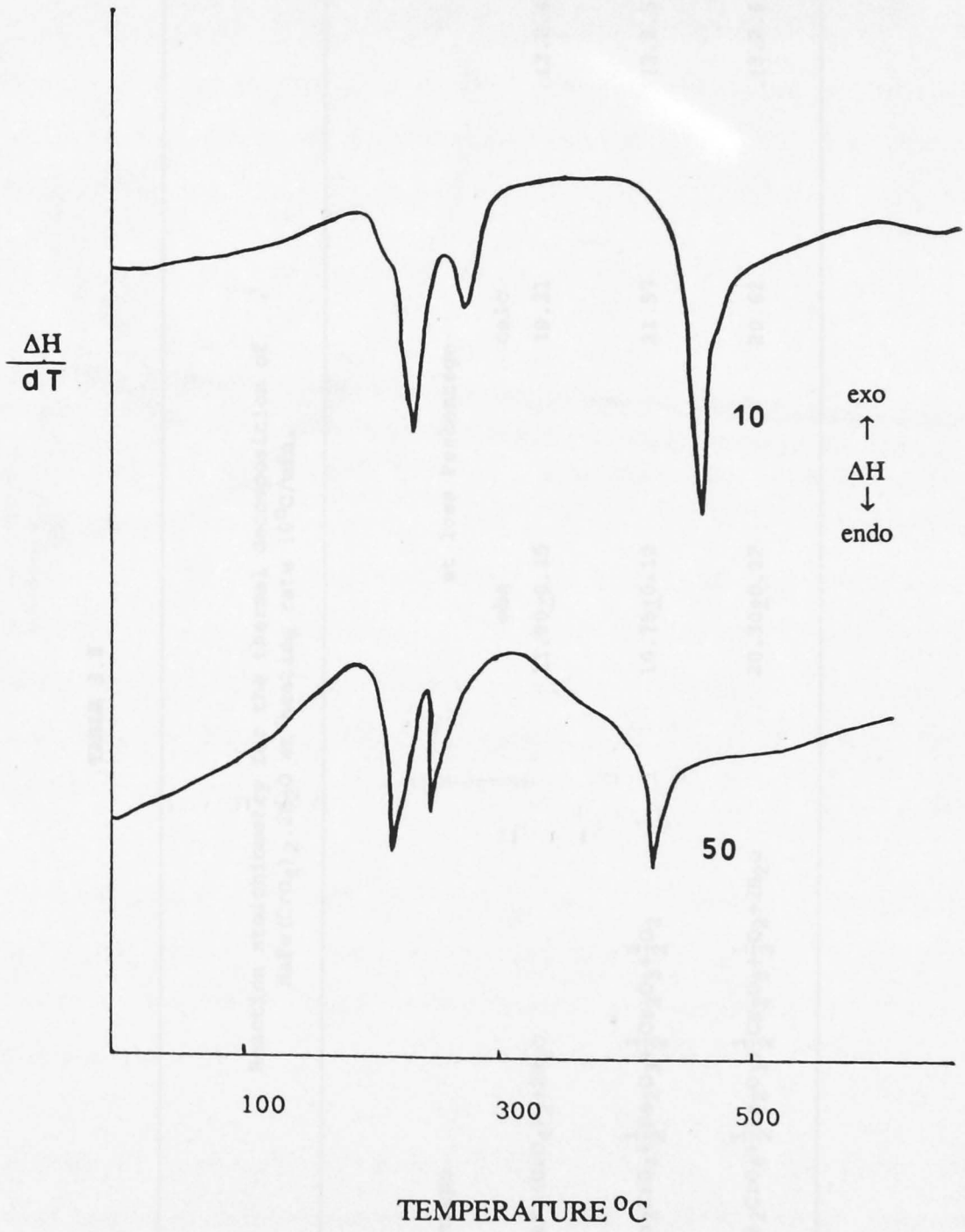

Fig 3.19 Representative differential thermal analysis curves for $NaFe(CrO_4)_2.2H_2O$ heated at 10°C and 50°C/min

TABLE 3.8

Reaction stoichiometry for the thermal decomposition of $NaFe(CrO_4)_2.2H_2O$ at heating rate 10^oC/min.

Decomposition steps	wt loss Percentage		
	obs	calc	
$NaFe(CrO_4)_2.2H_2O \rightarrow NaFe(CrO_4)_2+2H_2O$	11.80 ± 0.15	10.31	(3.2.4)
$NaFe(CrO_4)_2 \rightarrow Na_2CrO_4+\frac{1}{2}Fe_2O_3+\frac{1}{2}Cr_2O_3+\frac{1}{2}O_2$	10.75 ± 0.10	11.57	(3.2.5)
$NaFe(CrO_4)_2.2H_2O \rightarrow Na_2CrO_4+\frac{1}{2}Fe_2O_3+\frac{1}{2}Cr_2O_3+\frac{1}{2}O_2+2H_2O$	20.30 ± 0.12	20.62	(3.2.6)

occurrence of Na_2CrO_4 is due to the decomposition of $Na_2Cr_2O_7$, which takes place at temperatures above 400°C[88]. The observed weight loss of 11.80 ± 0.15% to 320°C was consistent with

$$NaFe(CrO_4)_2 \rightarrow \tfrac{1}{2}Na_2Cr_2O_7 + \tfrac{1}{2}Cr_2O_3 + \tfrac{1}{2}Fe_2O_3 + \tfrac{3}{4}O_2 \qquad 3.2.7$$

$$Na_2Cr_2O_7 \rightarrow Na_2CrO_4 + \tfrac{1}{2}Cr_2O_3 + \tfrac{3}{4}O_2 \qquad 3.2.8$$

the report by Bonnin[9] that attempts to prepare 'pure' $NaFe(CrO_4)_2$ by dehydration of $NaFe(CrO_4)_2.2H_2O$ results in a loss of 12%, indicating that dehydration/decomposition is occurring simultaneously. Popel[23], however, reported pure $NaFe(CrO_4)_2$ to be formed during thermal analysis of $NaFe(CrO_4)_2.2H_2O$ at heating rates 2.5°C and 10°C/min and by isothermal heating at 300°C in air.

In the present study, $NaFe(CrO_4)_2$ was formed on dehydration, but the shape of the thermogram and the calculated weight losses indicated that dehydration was accompanied by slow decomposition.

Mössbauer spectra (Figures 3.20 - 3.21) of residues from various quenching temperatures (100°, 320°C) were measured. Spectra of samples quenched from 110°C were simple quadrupole doublets assigned to $NaFe(CrO_4)_2.2H_2O$. Spectra of residues quenched from 320°C were fitted to two sets of quadrupole doublets:

(a) 25°

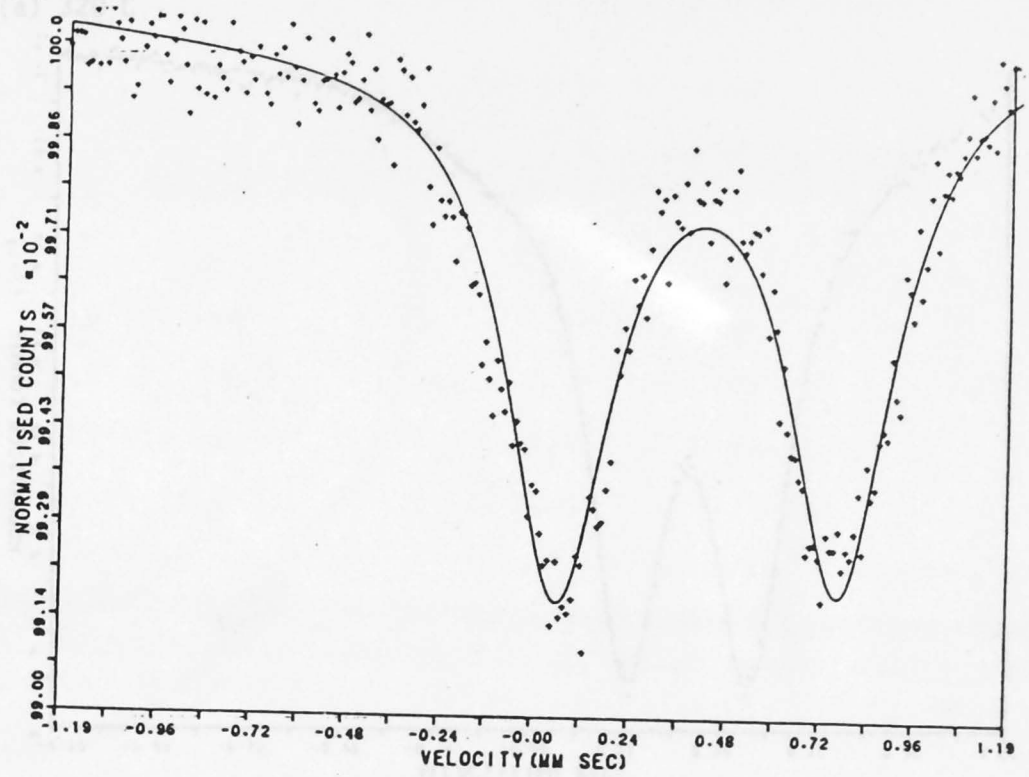

(b) 110°

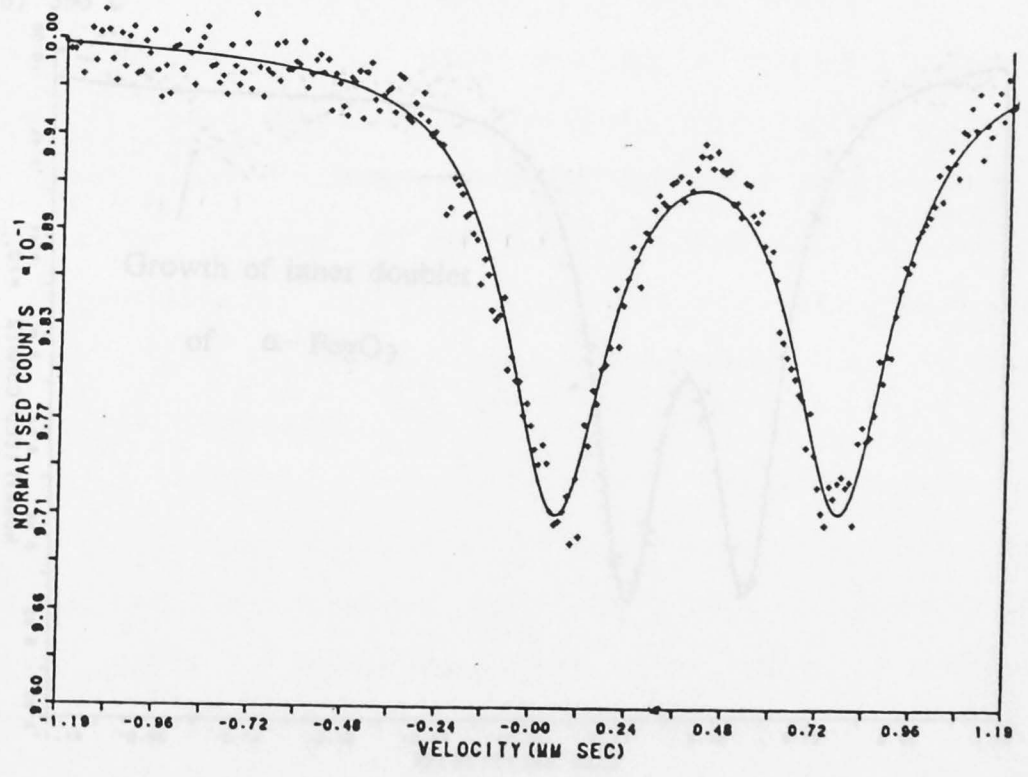

Fig 3.20 Mössbauer spectra of $NaFe(CrO_4)_2.2H_2O$ quenched from from various temperatures

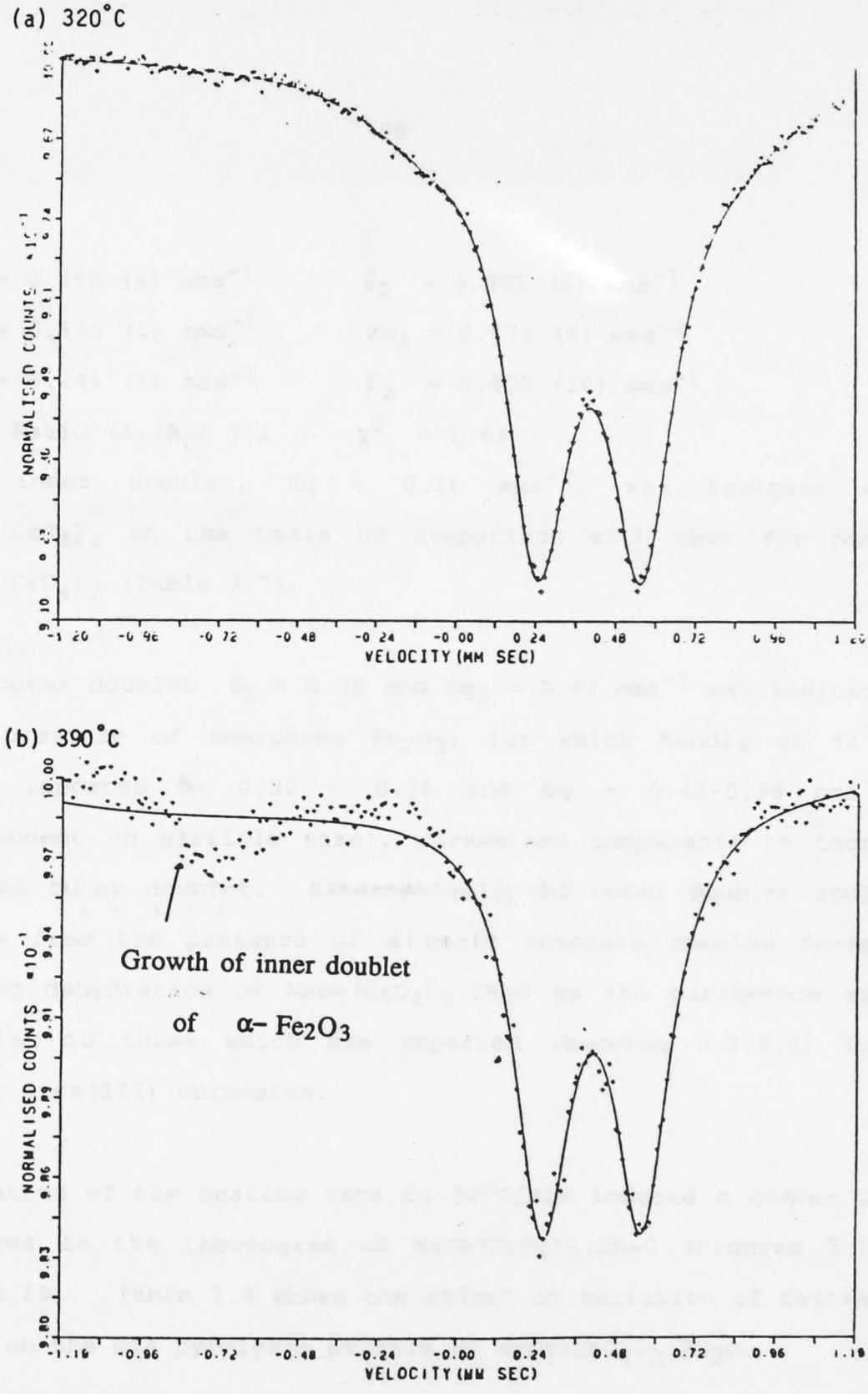

Fig 3.21 Mössbauer spectra of $NaFe(CrO_4)_2.2H_2O$ quenched from from various temperatures

δ_1 = 0.390 (4) mms^{-1} δ_2 = 0.361 (5) mms^{-1}

Eq_1 = 0.165 (1) mms^{-1} Eq_2 = 0.471 (4) mms^{-1}

Γ_1 = 0.241 (1) mms^{-1} Γ_2 = 0.478 (10) mms^{-1}

Area Ratio (A_1/A_2) 7:1 χ^2 = 1.41

The inner doublet, Eq = 0.16 mms^{-1}, was assigned to $NaFe(CrO_4)_2$ on the basis of comparison with that for pure $NaFe(CrO_4)_2$ (Table 3.7).

The outer doublet δ_2 = 0.36 and Eq_2 = 0.47 mms^{-1} may indicate the presence of amorphous Fe_2O_3, for which Kundig et al[78] have reported δ= 0.30 - 0.38 and Eq = 0.42-0.98 mms^{-1} (dependent on particle size), parameters comparable to those of the outer doublet. Alternatively, the outer doublet could arise from the presence of a basic chromate species formed during dehydration of $NaFe(CrO_4)_2.2H_2O$ as the parameters are similar to those which are reported (section 3.2.6.1) for basic iron(III) chromates.

Variation of the heating rate to 50°C/min induced a number of changes in the thermogram of $NaFe(CrO_4)_2.2H_2O$ (Figures 3.18 and 3.19). Table 3.9 shows the effect of variation of heating rate on the DTA pyrolysis profile of $NaFe(CrO_4)_2.2H_2O$.

TABLE 3.9

Comparison of the DTA curves for $NaFe(CrO_4)_2.2H_2O$ at various heating rates

Heating rate (^oC/min)	T_i	T_{max}	T_f	ΔH
10	187	204	210	endo
	210	221	248	endo
	248	269	280	endo
	420	446	458	endo
50	211	248	280	endo
	280	290	321	endo
	356	486	504	endo

At the heating rate of 50^oC/min, the endotherm with T_{max} at 248^oC was attributed to the formation of $NaFe(CrO_4)_2$, whilst that at 290^oC was attributed to a decomposition reaction. The weight loss to the plateau at 320^oC was 13.70%; greater than that for dehydration alone (10.31%) and higher than the 11.80% observed at 10^oC/min. This additional weight loss and observed changes in the DTA profile could indicate that the decomposition pathway of $NaFe(CrO_4)_2.2H_2O$ is dependent on heating rate. The final weight loss of 20.70% at 50^oC (calculated 20.63%) was consistent with that represented by reaction 3.2.6.

Mössbauer spectra of residues quenched from 320^oC were assigned to the presence of $NaFe(CrO_4)_2$ and superparamagnetic α-Fe_2O_3. The presence of α-Fe_2O_3 is consistent with a

decomposition process having occurred in addition to the loss of water for $NaFe(CrO_4)_2.2H_2O$.

3.2.2.3 **CONCLUSION**

The dehydration of $NaFe(CrO_4)_2.2H_2O$ involves a weight loss greater than that required for the stoichiometric loss of two molecules of water.It is postulated that dehydration is accompanied by decomposition to form an, as yet unidentified, intermediate, which decomposes above 320°C to a mixture of $Na_2Cr_2O_7$ and Fe_2O_3. It is also postulated that the intermediate is a basic chromate but its identity has yet to be established.

3.2.3 $NH_4Fe(CrO_4)_2.nH_2O$

3.2.3.1 ROOM TEMPERATURE MÖSSBAUER PARAMETERS FOR THE SERIES $NH_4Fe(CrO_4)_2.nH_2O$

Table 3.10 lists the room temperature Mössbauer parameters for the chromates $NH_4Fe(CrO_4)_2.nH_2O$. The spectra were all simple quadrupole doublets.

TABLE 3.10

Mössbauer parameters of the chromates $NH_4Fe(CrO_4)_2.nH_2O$ at 25°C

Compound	Mössbauer Parameters/mms^{-1}			Chi-squared
	δ	Eq	Γ	χ^2
$NH_4Fe(CrO_4)_2.2H_2O$	0.428(2)	0.510(2)	0.279(2)	1.10
$NH_4Fe(CrO_4)_2$ (α)	0.403(1)	0.104(1)	0.259(1)	1.12
$NH_4Fe(CrO_4)_2$ (β)+	0.400(2)	0.431(2)	0.391(7)	1.12

+ the value for this compound was obtained by a 'best' 1T2 fit of the spectrum of the residue from dehydration of the hydrate

The quadrupole splittings for the series were in general higher than those observed for the chromates $MFe(CrO_4)_2.nH_2O$ (M = Na, K) indicating that distortions of the iron octahedra are greater. The distortion may arise in part from the presence of hydrogen bonding[67], within and between the chains, due to the presence of NH_4^+ cation; further discussion on distortion effects can be found in Section 3.4.

3.2.3.2 THERMAL DECOMPOSITION OF $NH_4Fe(CrO_4)_2.2H_2O$

The thermal decomposition of $NH_4Fe(CrO_4)_2.2H_2O$ is potentially complicated by the oxidisability of NH_4^+ cation and is therefore of interest. Figure 3.22 shows a representative thermogram at a heating rate of 10°C/min. The proposed reaction stoichiometry is shown in Table 3.11.

The absence of intermediate hydrate formation and ease with which water was removed were consistent with the observations of Bonnin[9]. Diffraction patterns of residues quenched from 110°C were interpreted as being due to about 80% α-$NH_4Fe(CrO_4)_2$, the remainder being β-$NH_4Fe(CrO_4)_2$, (Table 3.12), on the basis of peak height and positions in experimental patterns compared to those in patterns for the respective chromates calculated from crystallographic data. Annealing of α-$NH_4Fe(CrO_4)_2$ at 135°C for 4 h failed to produce any evidence for the formation of the β-phase when examined by XRD and Mössbauer methods. Bonnin[9] reported that diffraction patterns of $NH_4Fe(CrO_4)_2.2H_2O$ heated at 130°C indicated the formation of β-$NH_4Fe(CrO_4)_2$ but did not conclusively establish the presence of α-$NH_4Fe(CrO_4)_2$ due to the poor quality of patterns obtained.

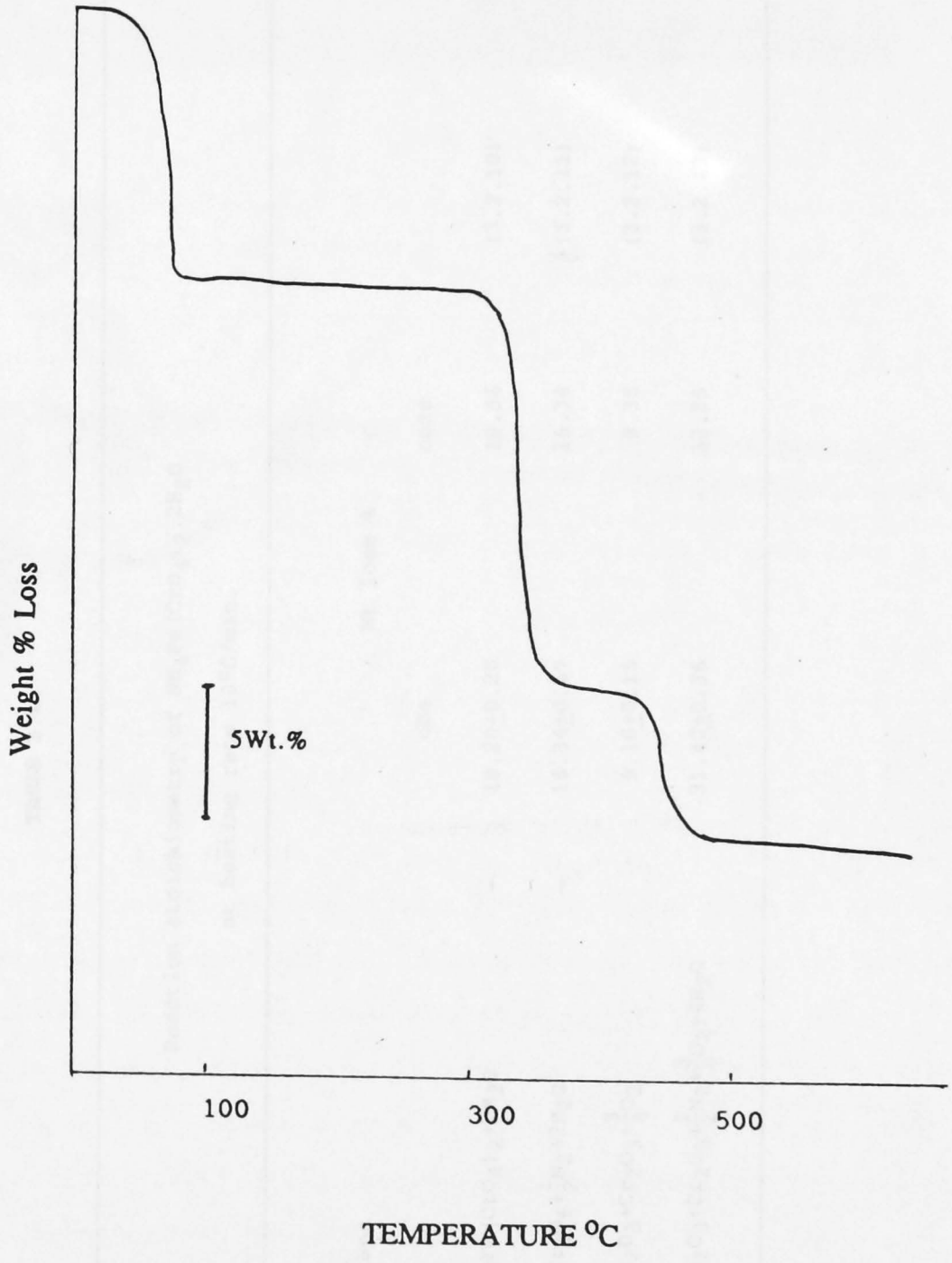

Fig 3.22 Representative thermogram for $NH_4Fe(CrO_4)_2.2H_2O$ heated at $10^oC/min$

TABLE 3.11

Reaction stoichiometry of $NH_4Fe(CrO_4)_2.2H_2O$

at heating rate 10^oC/min.

Decomposition steps	Wt loss % obs	Wt loss % calc	
$NH_4Fe(CrO_4)_2.2H_2O \rightarrow NH_4Fe(CrO_4)_2+2H_2O$	10.20±0.20	10.56	(3.2.10)
$NH_4Fe(CrO_4)_2 \rightarrow FeCr_2O_6+\frac{1}{2}N_2+2H_2O$	16.34±0.67	16.34	(3.2.11)
$FeCr_2O_6 \rightarrow \frac{1}{2}Fe_2O_3+Cr_2O_3+\frac{3}{4}O_2$	9.10±0.15	9.35	(3.2.12)
$NH_4Fe(CrO_4)_2.2H_2O \rightarrow \frac{1}{2}Fe_2O_3+Cr_2O_3+\frac{1}{2}N_2+\frac{3}{4}O_2+4H_2O$	31.40±0.36	32.25	(3.2.13)

TABLE 3.12

X-ray powder diffraction pattern in the range $10^{o} \leq 2\theta \leq 40^{o}$ of $NH_4Fe(CrO_4)_2.2H_2O$ cooled from 110°C

d_{obs}	d_{calc}[9]	I/I^{o}	phase[+]	d_{obs}	d_{calc}[9]	I/I^{o}	phase[+]
7.55	7.56	100	α	3.12	3.11	45	α β
5.23	5.21	16	β	3.00	3.01,3.02	33	α
4.39	4.37	30	α	2.88	2.91,2.85	10	α β
3.95	3.94,3.90	35	α β	2.76	2.76,2.73	20	α β
3.78	3.77	16	α	2.69	2.68	10	α β
3.66	3.71	20	β	2.50	2.52	15	α β
3.60	3.60,3.62	20	α	2.40	2.40,2.41	8	α β
3.38	3.38,3.33	50	α β				
3.11	3.17	50	α				

[+] α= α-$NH_4Fe(CrO_4)_2$

β= β-$NH_4Fe(CrO_4)_2$

Differential thermal analysis (Figure 3.23) showed that the loss of water proceeded in a single step as evidenced by the presence of a single endotherm at T_{max}, 90°C. The anhydrous chromate was stable to 270°C, at which point a slow decomposition began and a plateau was reached by 350°C (reaction 3.2.11). DTA showed the decomposition to involve two steps and to be exothermic.

The presence of an endotherm at 438°C in the DTA profile (Figure 3.23) was attributed to the decomposition of $FeCr_2O_6$ (reaction 3.2.12). XRD patterns of $NH_4Fe(CrO_4)_2.2H_2O$ residues quenched from 450°C showed lines at 3.65(m), 2.66(s), 2.42(m) and 1.83(m) which compared well with those

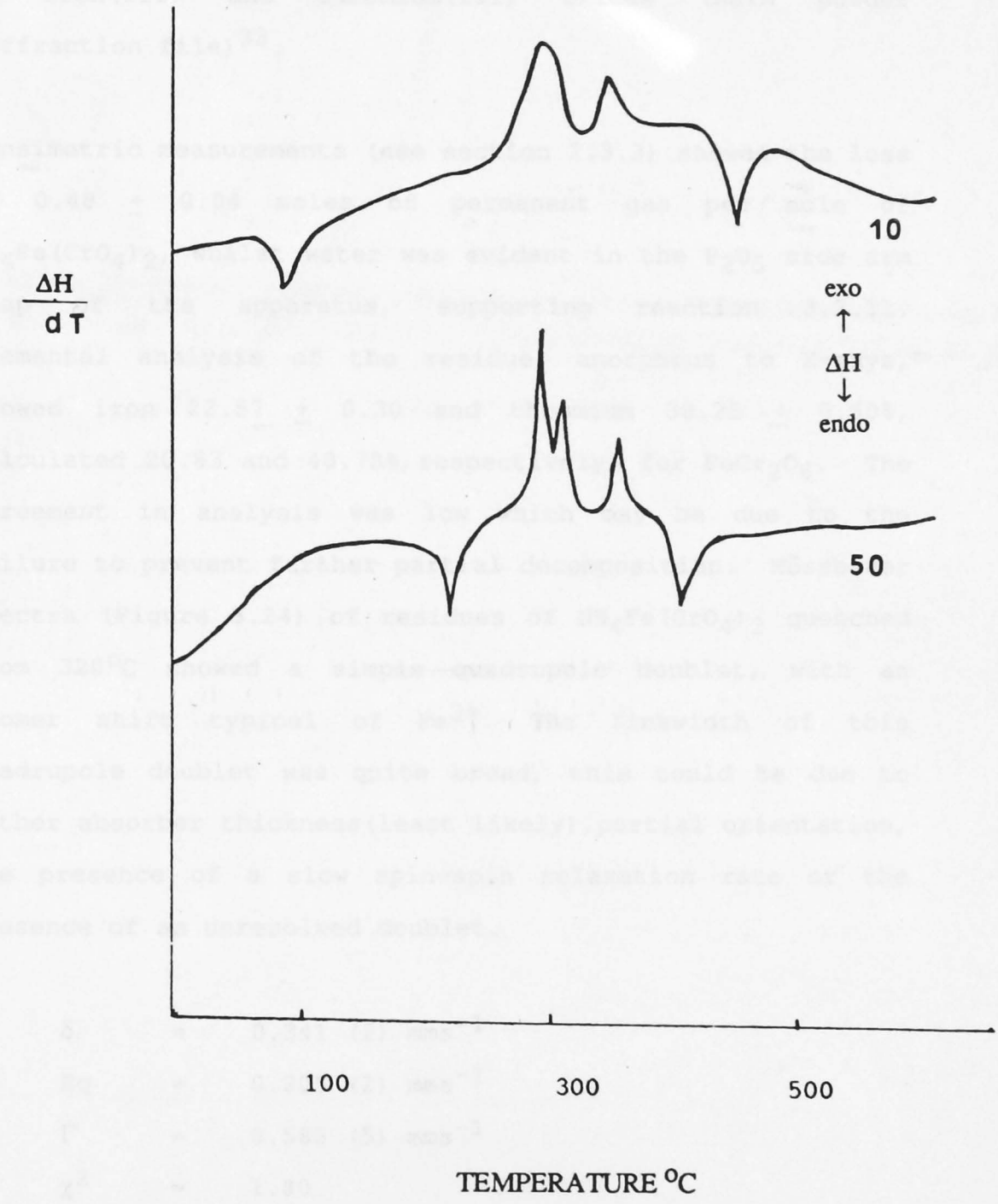

Fig 3.23 Representative differential thermal analysis curves for $NH_4Fe(CrO_4)_2.2H_2O$ heated at 10°C and 50°C/min

of iron(III) and chromium(III) oxides (ASTM powder diffraction file)[33].

Tensimetric measurements (see section 2.3.3) showed the loss of 0.48 ± 0.04 moles of permanent gas per mole of $NH_4Fe(CrO_4)_2$, whilst water was evident in the P_2O_5 side arm trap of the apparatus, supporting reaction 3.2.11. Elemental analysis of the residue, amorphous to X-rays, showed iron 22.57 ± 0.30 and chromium 38.25 ± 0.50%, calculated 20.83 and 40.75%, respectively, for $FeCr_2O_6$. The agreement in analysis was low which may be due to the failure to prevent further partial decomposition. Mössbauer spectra (Figure 3.24) of residues of $NH_4Fe(CrO_4)_2$ quenched from 320°C showed a simple quadrupole doublet, with an isomer shift typical of Fe^{3+}. The linewidth of this quadrupole doublet was quite broad, this could be due to either absorber thickness(least likely),partial orientation, the presence of a slow spin-spin relaxation rate or the presence of an unresolved doublet.

δ	=	0.341 (2) mms^{-1}
Eq	=	0.205 (2) mms^{-1}
Γ	=	0.585 (5) mms^{-1}
χ^2	=	1.80

Samples of $NH_4Fe(CrO_4)_2$ were placed in the heating chamber of a mass spectrometer in gold crucibles and evacuated to

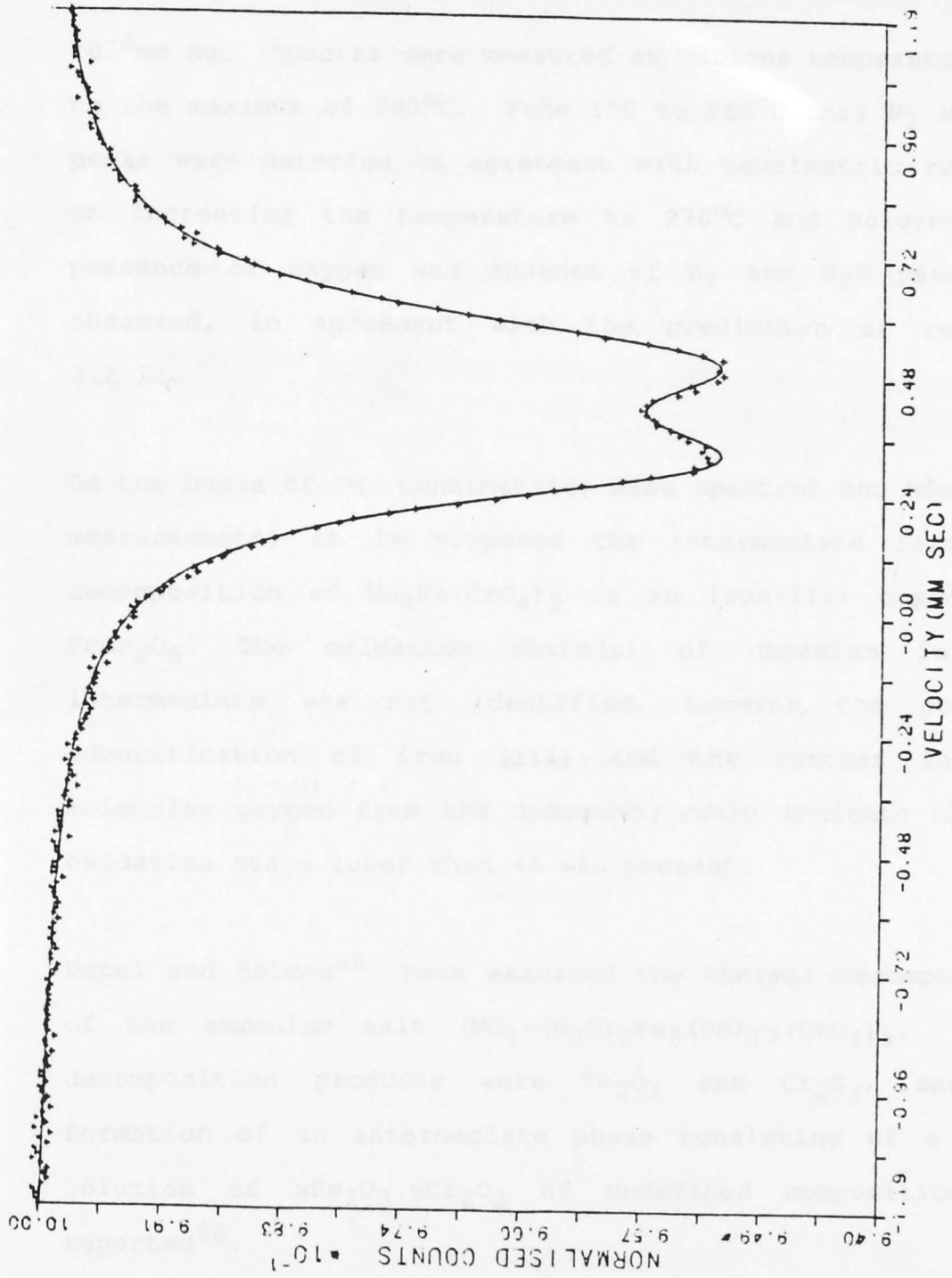

Fig 3.24 Mössbauer spectrum $NH_4Fe(CrO_4)_2$ quenched from 320°C

10^{-5}mm Hg. Spectra were measured at various temperatures up to the maximum of 280°C. From 150 to 260°C only N_2 and H_2O peaks were detected in agreement with tensimetric results. On increasing the temperature to 270°C and holding, the presence of oxygen and absence of N_2 and H_2O peaks was observed, in agreement with the prediction of reaction 3.2.12.

On the basis of TG, tensimetric, mass spectral and Mössbauer measurements, it is proposed the intermediate formed on decomposition of $NH_4Fe(CrO_4)_2$ is an iron(III) compound - $FeCr_2O_6$. The oxidation state(s) of chromium in this intermediate was not identified, however, the positive identification of iron (111) and the further loss of molecular oxygen from the compound would indicate that an oxidation state lower than +6 was present.

Popel and Boldog[68] have examined the thermal decomposition of the ammonium salt $(NH_4)(H_3O)_2Fe_8(OH)_{17}(CrO_4)_6$. Final decomposition products were Fe_2O_3 and Cr_2O_3, and the formation of an intermediate phase consisting of a solid solution of $xFe_2O_3.yCr_2O_3$ of undefined composition was reported[68].

Variation of the heating rate to 50°C/min in order to compare the results with those obtained for $MFe(CrO_4)_2.2H_2O$

(M = K, Na) induced a number of changes in the thermogram of $NH_4Fe(CrO_4)_2.2H_2O$, Table 3.13 and Figures 3.23 and 3.25. The total weight loss was 30.20 $\pm$ 0.06%.

Differential thermal analysis (Figure 3.23) of the ammonium chromate at a heating rate of 50°C/min indicated that the decomposition process was more complicated under fast heating rates, with the presence of additional endotherms. The literature on the decomposition of ammonium dichromate[69] and ammonium chromate[70] offers a number of alternate sequences. Mahieu et al[69] have examined, by evolved gas analysis (EGA) and thermogravimetry, the decomposition of $(NH_4)_2Cr_2O_7$, postulating the successive reduction of chromium from Cr(VI) - Cr(V) - Cr(IV) - Cr(III). The formation of chromates(V) is well documented[70,71],

TABLE 3.13

Variation in the DTA profile of $NH_4Fe(CrO_4)_2$ with temperature

Heating Rate (°C/min)	T_i	T_{max}	T_f	ΔH
10	215	282	311	exo
	321	336	382	exo
	419	438	447	endo
50	215	246	269	endo
	269	329	369	exo
	369	371	400	exo
	400	419	443	exo
	445	467	498	endo

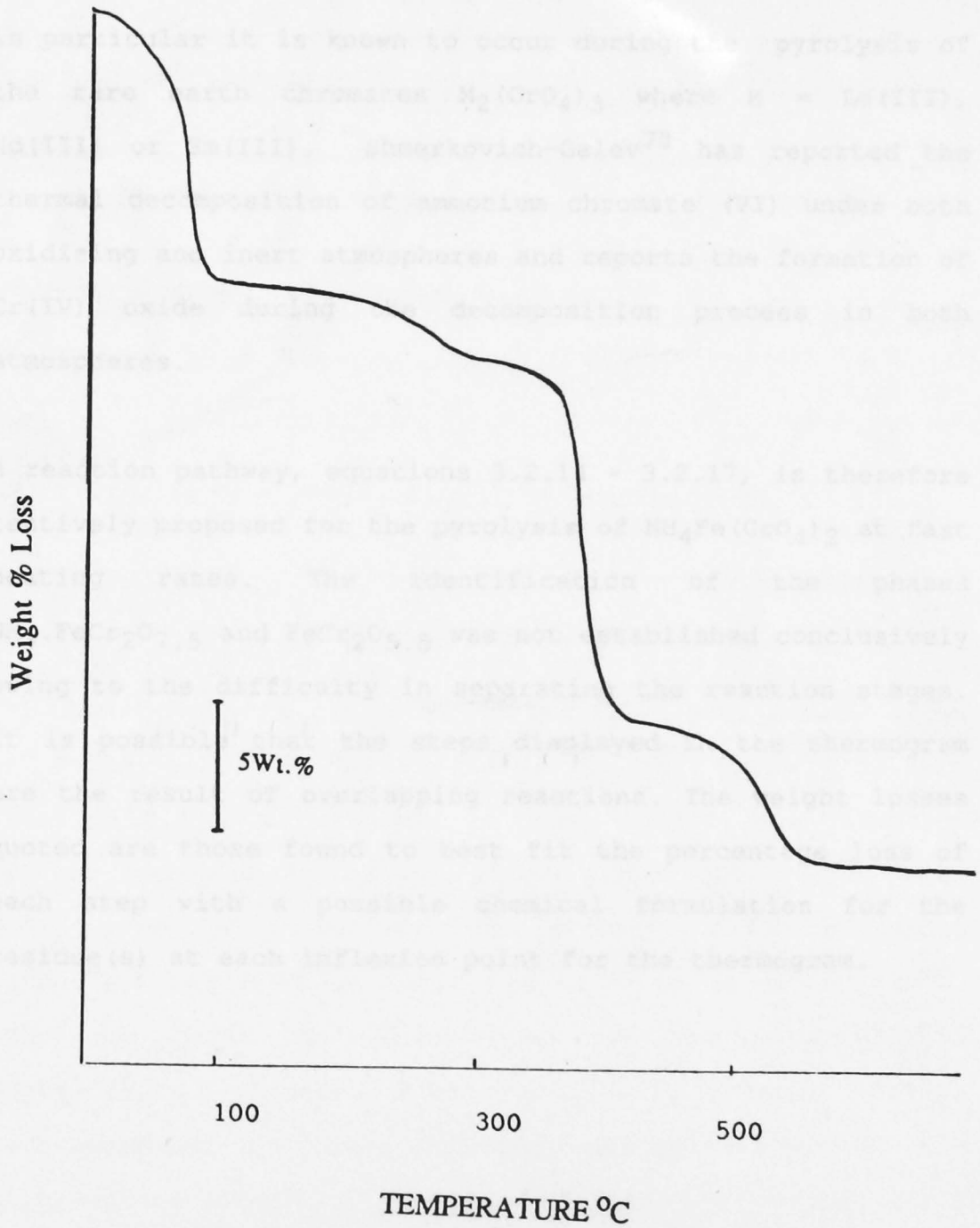

Fig 3.25 Representative thermogram for $NH_4Fe(CrO_4)_2.2H_2O$ heated at 50°C/min

in particular it is known to occur during the pyrolysis of the rare earth chromates $M_2(CrO_4)_3$ where M = La(III), Nd(III) or Sm(III). Shmerkovich-Galev[70] has reported the thermal decomposition of ammonium chromate (VI) under both oxidising and inert atmospheres and reports the formation of Cr(IV) oxide during the decomposition process in both atmospheres.

A reaction pathway, equations 3.2.14 - 3.2.17, is therefore tentively proposed for the pyrolysis of $NH_4Fe(CrO_4)_2$ at fast heating rates. The identification of the phases $NH_3.FeCr_2O_{7.5}$ and $FeCr_2O_{5.5}$ was not established conclusively owing to the difficulty in separating the reaction stages. It is possible that the steps displayed in the thermogram are the result of overlapping reactions. The weight losses quoted are those found to best fit the percentage loss of each step with a possible chemical formulation for the residue(s) at each inflexion point for the thermogram.

TABLE 3.14

Proposed reaction pathway of $NH_4Fe(CrO_4)_2$ at a heating rate 50^oC/min in air or nitrogen

Decomposition steps	Wt loss % obs	calc
$NH_4Fe(CrO_4)_2 \longrightarrow NH_3.FeCr_2O_{7.5}+\frac{1}{2}H_2O$	2.44	2.62 (3.2.14)
$NH_3.FeCr_2O_{7.5} \longrightarrow FeCr_2O_{5.5}+\frac{1}{2}N_2+\frac{1}{4}O_2+\frac{3}{2}H_2O$	16.80	16.44 (3.2.15)
$FeCr_2O_{5.5} \longrightarrow \frac{1}{2}Fe_2O_3+Cr_2O_3+\frac{1}{2}O_2$	8.35	6.45 (3.2.16)
$NH_4Fe(CrO_4)_2 \longrightarrow \frac{1}{2}Fe_2O_3+Cr_2O_3+\frac{1}{2}N_2+\frac{3}{4}O_2+2H_2O$	21.10	21.42 (3.2.17)

The discrepancy in the observed and calculated losses shown in Table 3.14 may be explained on the basis that the reaction 3.2.15 was assumed to occur without the formation of any chromium oxidation state other than (IV), e.g. $FeCr_2O_6$, or Cr(V). Decomposition of Cr(IV) oxide to Cr(III) oxide was reported by Mahieu et at[69] to occur at 420^oC, which was within the region of an endotherm in the DTA of $NH_4Fe(CrO_4)_2$ (Figure 3.23) at 419^oC (Table 3.13), corresponding to the proposed decomposition of the intermediate $FeCr_2O_{5.5}$ (reaction 3.2.16) to chromium(III) oxide, thus supporting the reaction process set out in Table 3.14.

3.2.3.3 CONCLUSION

The mode of pyrolysis of $NH_4Fe(CrO_4)_2.2H_2O$ appeared to be dependent on reaction conditions and was complex, due in part to the oxidation of ammonium cation to nitrogen. Intermediate states proposed are α-$NH_4Fe(CrO_4)_2$, the complexes $FeCr_2O_6$, $NH_3.FeCr_2O_{7.5}$ and $FeCr_2O_{5.5}$. The latter two complexes are proposed to form at high heating rates.

3.2.4 $MFe(CrO_4)_2$ M = Rb, Cs, Tl

3.2.4.1 ROOM TEMPERATURE MÖSSBAUER PARAMETERS FOR THE CHROMATES $MFe(CrO_4)_2$ M = Rb, Cs, Tl

Parameters for the Mössbauer spectra at room temperature of the chromates $MFe(CrO_4)_2$ (M = Rb, Cs, Tl) are shown in Table 3.15. The isomer shifts of about 0.40 mms^{-1} were consistent with those reported for the chromates $MFe(CrO_4)_2.nH_2O$ (see sections 3.2.1.1 - 3.2.3.1).

TABLE 3.15

Mössbauer parameters for the chromates $MFe(CrO_4)_2$ (M = Rb,Cs,Tl) at 25°C

	- Mössbauer parameters/mms^{-1} -			
Compound	δ	Eq	Γ	χ^2
α-$TlFe(CrO_4)_2$	0.398(2)	0.118(7)	0.305(2)	0.99
β-$TlFe(CrO_4)_2$	0.400(2)	0.192(1)	0.310(2)	0.97
β-$RbFe(CrO_4)_2$	0.391(3)	0.109(3)	0.268(1)	0.91
$CsFe(CrO_4)_2$	0.399(1)	0.094(1)	0.252(2)	0.77

The difference in the quadrupole splittings for the α- and β-phases of $TlFe(CrO_4)_2$ can be attributed to greater distortion of the iron octahedra in the β-phase due to nearest-neighbour effects. This is discussed in section 3.4. The substitution of Cs^+ ions for Rb^+ ions between the chains of polyhedra[15] in $MFe(CrO_4)_2$ chromates gave a slightly lower Eq.

3.2.4.2 THERMAL DECOMPOSITION OF THE SERIES $MFe(CrO_4)_2$ M = Rb, Cs or Tl

Figures 3.26 - 3.28 show representative thermograms for the series $MFe(CrO_4)_2$, where M = Rb, Cs or Tl.

XRD patterns confirmed the presence of $M_2Cr_2O_7$ (M = Rb, Cs, Tl), Fe_2O_3 and Cr_2O_3 in the final reaction products[33]. The proposed reaction stoichiometries as shown in Table 3.16, reactions 3.2.18 and 3.2.19 are similar to those reported by Popel[23]. Thallium iron(III) chromate did not show oxidation of Tl(I) to Tl(III).

TABLE 3.16

Reaction stoichiometries for the thermal decomposition of $MFe(CrO_4)_2$ (M = Rb, Cs or Tl) at heating rate 10^oC/min

Decomposition steps	Wt loss % obs	Wt loss % calc
$RbFe(CrO_4)_2 \rightarrow \frac{1}{2}Rb_2Cr_2O_7+\frac{1}{2}Fe_2O_3+\frac{1}{2}Cr_2O_3+\frac{3}{4}O_2$	6.97±0.15	6.45 (3.2.18)
$CsFe(CrO_4)_2 \rightarrow \frac{1}{2}Cs_2Cr_2O_7+\frac{1}{2}Fe_2O_3+\frac{1}{2}Cr_2O_3+\frac{3}{4}O_2$	6.07±0.20	5.70 (3.2.19)
$TlFe(CrO_4)_2 \rightarrow \frac{1}{2}Tl_2Cr_2O_7+\frac{1}{2}Fe_2O_3+\frac{1}{2}Cr_2O_3+\frac{3}{4}O_2$	4.87±0.10	4.88 (3.2.20)

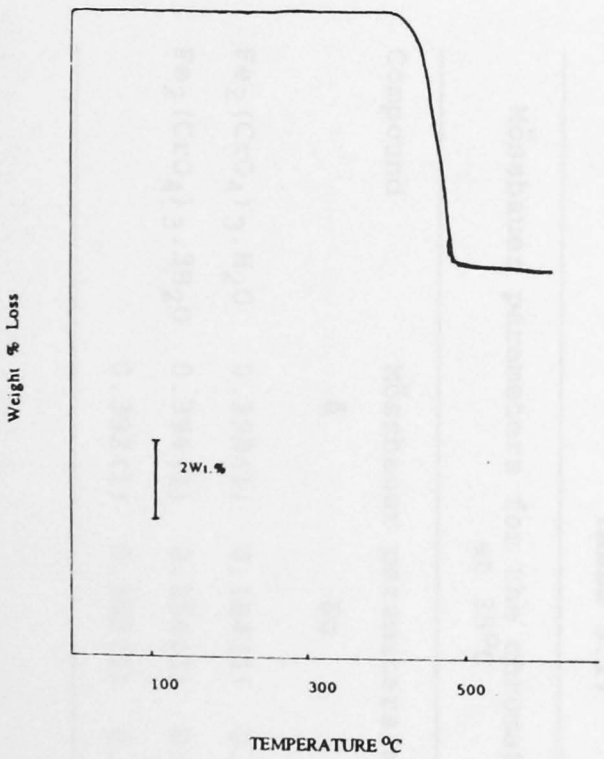

Fig 3.26 Representative thermogram for $RbFe(CrO_4)_2$ heated at 10°C/min

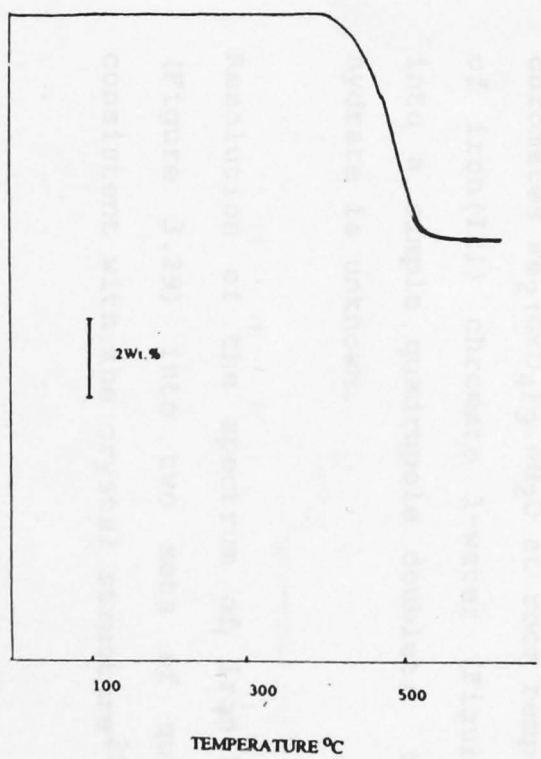

Fig 3.27 Representative thermogram for $CsFe(CrO_4)_2$ heated at 10°C/min

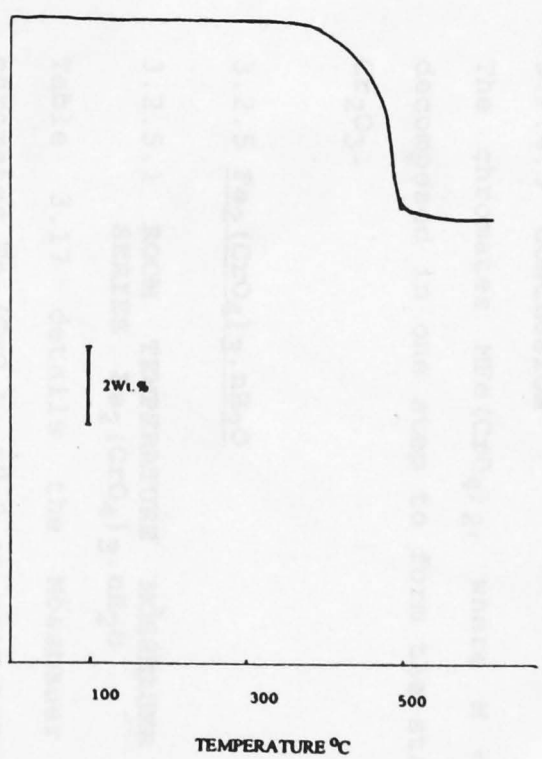

Fig 3.28 Representative thermogram for $TlFe(CrO_4)_2$ heated at 10°C/min

3.2.4.3 CONCLUSION

The chromates $MFe(CrO_4)_2$, where M = Rb, Cs or Tl, each decomposed in one step to form the stable $M_2Cr_2O_7$, Fe_2O_3 and Cr_2O_3.

3.2.5 $\underline{Fe_2(CrO_4)_3.nH_2O}$

3.2.5.1 ROOM TEMPERATURE MÖSSBAUER PARAMETERS FOR THE SERIES $Fe_2(CrO_4)_3.nH_2O$

Table 3.17 details the Mössbauer parameters for the chromates $Fe_2(CrO_4)_3.nH_2O$ at room temperature. The spectrum of iron(III) chromate 1-water (Figure 3.29) was resolved into a simple quadrupole doublet; the structure of this hydrate is unknown.

Resolution of the spectrum of iron(III) chromate 3-water (Figure 3.29) into two sets of quadrupole doublets is consistent with the crystal structure[20] which

TABLE 3.17

Mössbauer parameters for the chromates $Fe_2(CrO_4)_3.nH_2O$ at 25°C

Compound	Mössbauer parameters/mms^{-1}			Peak area ratio	
	δ	Eq	Γ	A_1/A_2	χ^2
$Fe_2(CrO_4)_3.H_2O$	0.399(1)	0.184(1)	0.342(3)	-	1.46
$Fe_2(CrO_4)_3.3H_2O$	0.394(1)	0.154(1)	0.296(3)	1.10	1.55
	0.392(1)	0.352(1)	0.336(2)		

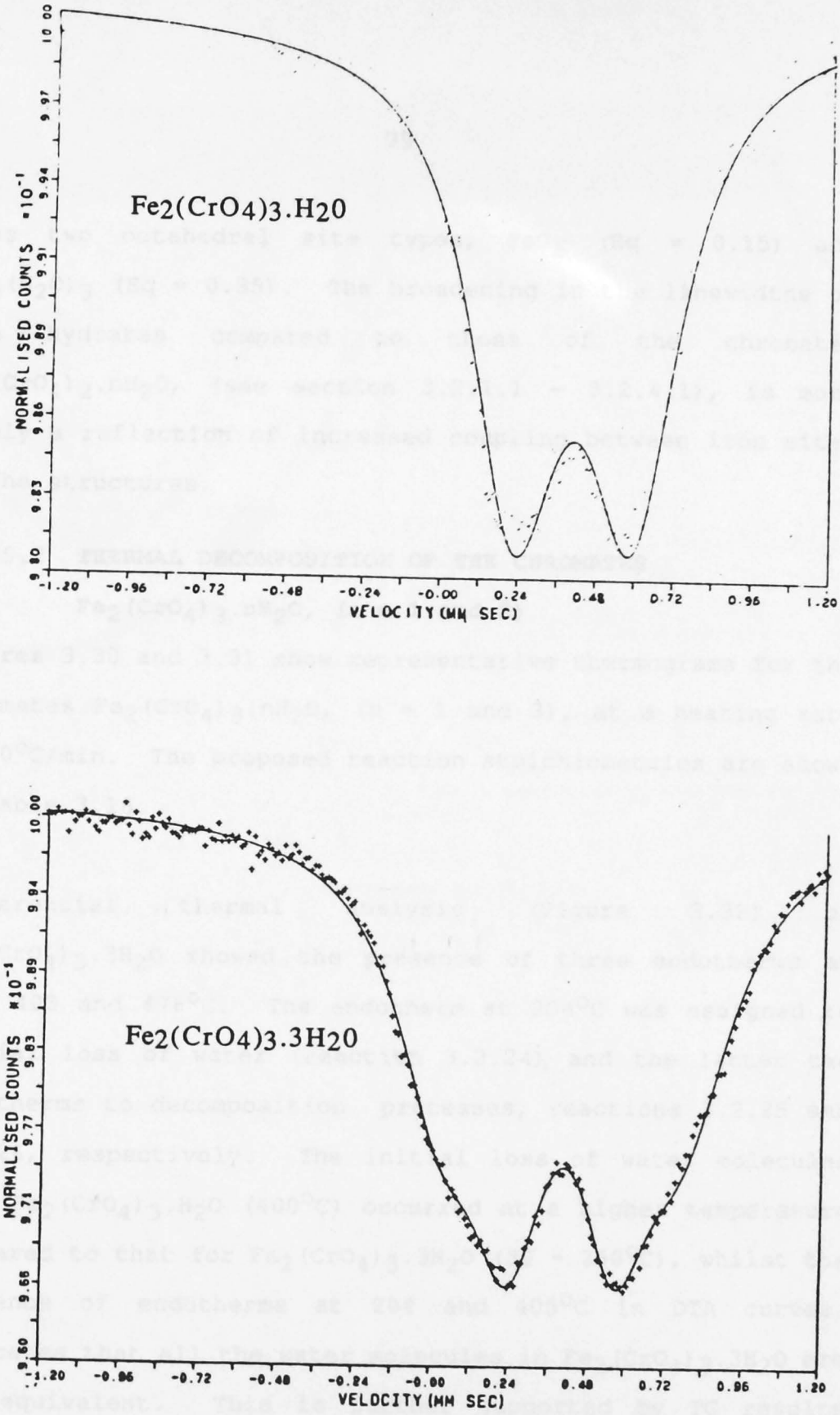

Fig 3.29 Mössbauer spectra of the series $Fe_2(CrO_4)_3.nH_2O$ at 25oC

shows two octahedral site types, FeO_6 (Eq = 0.15) and $FeO_3(H_2O)_3$ (Eq = 0.35). The broadening in the linewidths of both hydrates compared to those of the chromates $MFe(CrO_4)_2.nH_2O$, (see section 3.2.1.1 - 3.2.4.1), is most likely a reflection of increased coupling between iron sites in the structures.

3.2.5.2 THERMAL DECOMPOSITION OF THE CHROMATES $Fe_2(CrO_4)_3.nH_2O$, (n = 1 and 3)

Figures 3.30 and 3.31 show representative thermograms for the chromates $Fe_2(CrO_4)_3.nH_2O$, (n = 1 and 3), at a heating rate of 10°C/min. The proposed reaction stoichiometries are shown in Table 3.18.

Differential thermal analysis (Figure 3.32) of $Fe_2(CrO_4)_3.3H_2O$ showed the presence of three endotherms at 204, 405 and 476°C. The endotherm at 204°C was assigned to partial loss of water (reaction 3.2.24), and the latter two endotherms to decomposition processes, reactions 3.2.25 and 3.2.26, respectively. The initial loss of water molecules from $Fe_2(CrO_4)_3.H_2O$ (400°C) occurred at a higher temperature compared to that for $Fe_2(CrO_4)_3.3H_2O$ (30 - 280°C), whilst the presence of endotherms at 204 and 405°C in DTA curves, indicates that all the water molecules in $Fe_2(CrO_4)_3.3H_2O$ are not equivalent. This is further supported by TG results (Table 3.18) and Mössbauer spectroscopy.

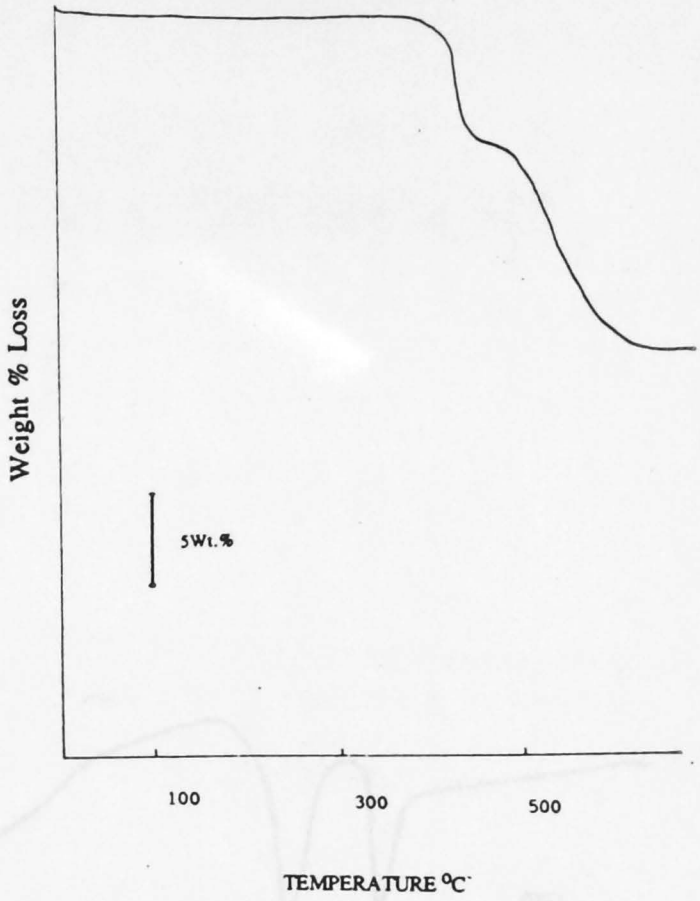

Fig 3.30 Representative thermogram for $Fe_2(CrO_4)_3.H_2O$ heated at 10°C/min

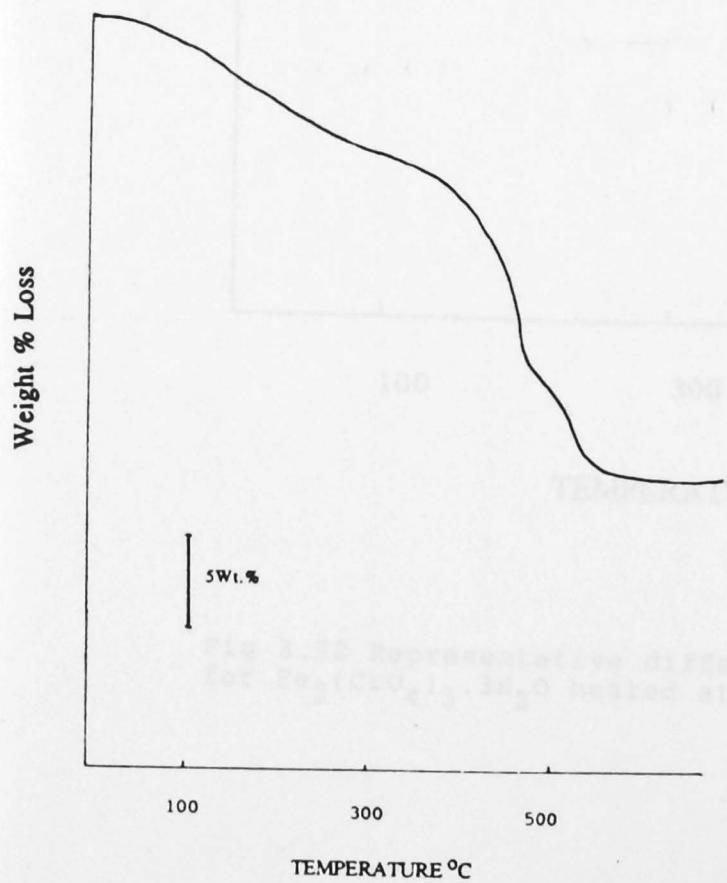

Fig 3.31 Representative thermogram for $Fe_2(CrO_4)_3.3H_2O$ heated at 10°C/min

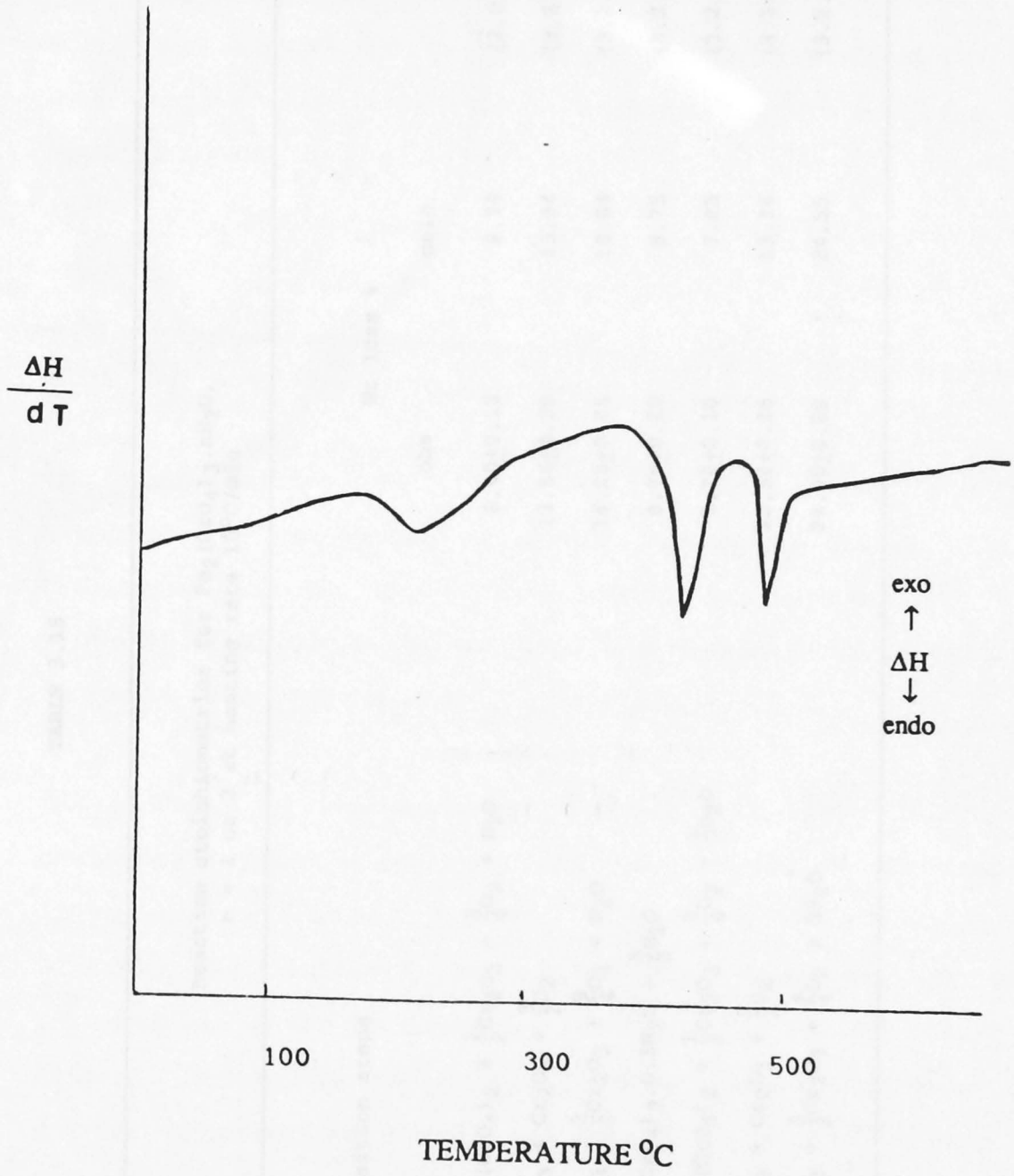

Fig 3.32 Representative differential thermal analysis curve for $Fe_2(CrO_4)_3.3H_2O$ heated at 10°C/min

TABLE 3.18

Reaction stoichiometries for $Fe_2(CrO_4)_3.nH_2O$, n = 1 or 3 at heating rate 10^oC/min

Decomposition steps	Wt loss % obs	Wt loss % calc	
$Fe_2(CrO_4)_3.H_2O \rightarrow Fe_2O(CrO_4)_2 + \frac{1}{2}Cr_2O_3 + \frac{3}{4}O_2 + H_2O$	8.40±0.10	8.79	(3.2.21)
$Fe_2O(CrO_4)_2 \rightarrow Fe_2O_3 + Cr_2O_3 + \frac{3}{2}O_2$	13.56±0.30	13.34	(3.2.22)
$Fe_2(CrO_4)_3.H_2O \rightarrow Fe_2O_3 + \frac{3}{2}Cr_2O_3 + \frac{9}{4}O_2 + H_2O$	18.05±0.25	18.84	(3.2.23)
$Fe_2(CrO_4)_3.3H_2O \rightarrow Fe_2(CrO_4)_3.0.5H_2O + \frac{5}{2}H_2O$	8.76±0.20	8.75	(3.2.24)
$Fe_2(CrO_4)_3.0.5H_2O \rightarrow Fe_2O(CrO_4)_2 + \frac{1}{2}Cr_2O_3 + \frac{3}{4}O_2 + \frac{1}{2}H_2O$	7.20±0.10	7.03	(3.2.25)
$Fe_2O(CrO_4)_2 \rightarrow Fe_2O_3 + Cr_2O_3 + \frac{3}{2}O_2$	12.58±0.25	13.34	(3.2.26)
$Fe_2(CrO_4)_3.3H_2O \rightarrow Fe_2O_3 + \frac{3}{2}Cr_2O_3 + \frac{9}{4}O_2 + 3H_2O$	24.00±0.20	24.55	(3.2.27)

Mössbauer spectra of $Fe_2(CrO_4)_3.3H_2O$ quenched from 400°C were resolved into two sets of quadrupole split doublets of area ratio 1:2.

δ_1	= 0.400 (1) mms^{-1}	δ_2	= 0.376 (2) mms^{-1}
Eq_1	= 0.162 (1) mms^{-1}	Eq_2	= 0.493 (2) mms^{-1}
Γ_1	= 0.263 (3) mms^{-1}	Γ_2	= 0.486 (3) mms^{-1}
A_1/A_2	= 1:2	χ^2	= 0.96

The inner doublet (Eq = 0.16 mms^{-1}) could arise from the presence of iron-oxygen octahedra containing water, whilst the outer doublet (Eq = 0.49 mms^{-1}) was assigned to the presence of $Fe_2O(CrO_4)_2$, owing to the closeness of parameters to those found for $Fe_2O(CrO_4)_2$ (section 3.2.6.2).

XRD patterns of the residues quenched from 380°C for the chromates $Fe_2(CrO_4)_3.nH_2O$ showed the presence of additional lines at d = 5.59(w), 3.86(w), 3.59(w), 3.35(s), 3.29(m), 3.14(m) and 3.04(w), supporting the presence of an intermediate phase as shown in reactions 3.2.21 and 3.2.25. Attempts to isolate $Fe_2O(CrO_4)_2$ in pure form by slow heating of the chromate $Fe_2(CrO_4)_3.H_2O$ at 380°C in air/nitrogen, resulted in a product which showed iron 33.25 $\pm$ 1.20% and chromium 29.80 $\pm$ 0.90%, calculated 32.20 and 28.92%, respectively, for $Fe_2O(CrO_4)_2$. Mössbauer spectra showed peaks due to Fe_2O_3, indicating that the product from 380°C had partially decomposed. XRD patterns of the chromates $Fe_2(CrO_4)_3.nH_2O$, quenched from 550°C, confirmed the presence

of iron(III) and chromium(III) oxides (ASTM powder diffraction file[33]). Finally the overall weight losses for the pyrolyses further supported the reactions 3.2.23 and 3.2.27.

3.2.5.3 **CONCLUSION**

Pyrolysis of the chromates $Fe_2(CrO_4)_3.nH_2O$ proceeded without the formation of $Fe_2(CrO_4)_3$. The new intermediate $Fe_2O(CrO_4)_2$ is postulated from Mössbauer studies to be common to reaction pathways for both n =1 and 3.

3.2.6 **$FeOHCrO_4$, $KFe_3(CrO_4)_2(OH)_6$, $2Fe_2O_3.4CrO_3.H_2O$[+]**

3.2.6.1 **ROOM TEMPERATURE MÖSSBAUER PARAMETERS FOR $FeOHCrO_4$, $KFe_3(CrO_4)_2(OH)_6$, $2Fe_2O_3.4CrO_3.H_2O$**

Table 3.19 gives the Mössbauer parameters for some basic chromates. All spectra (Figures 3.33 and 3.34) were simple quadrupole doublets with isomer shifts similar to those reported for the iron(III) chromates, section 3.2.2.1 - 3.2.5.1.

[+]The mixed oxide representation is used for the compound $2Fe_2O_3.4CrO_3.H_2O$ throughout the text, in keeping with the notation of Briggs[7], because of its nature.

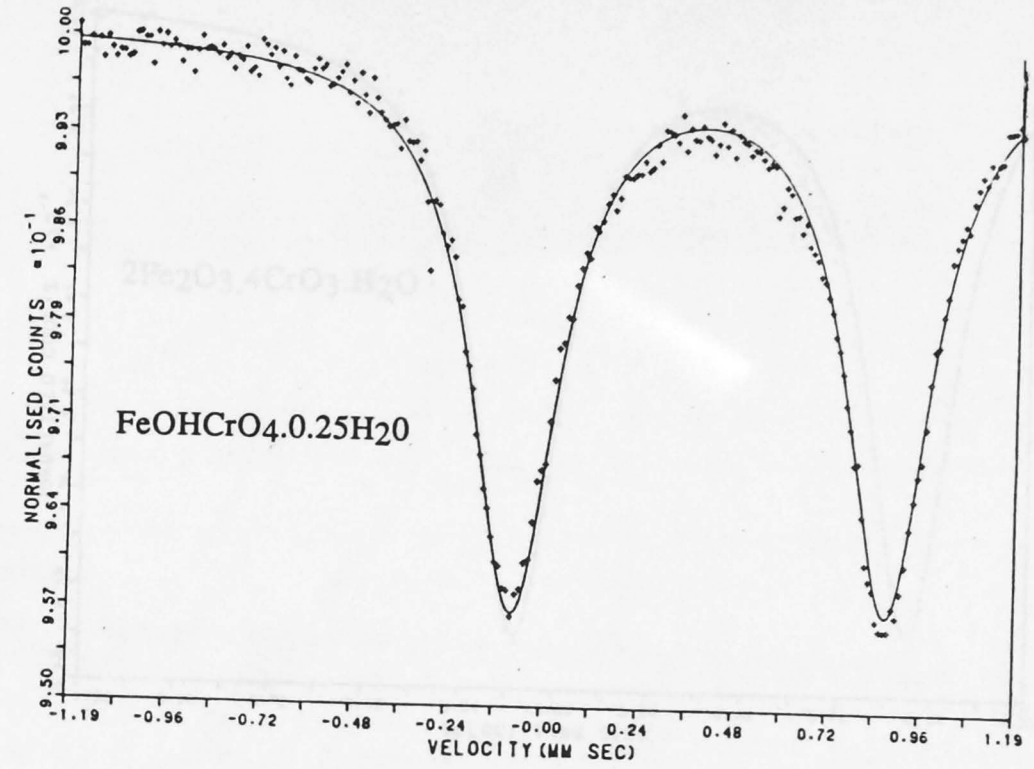

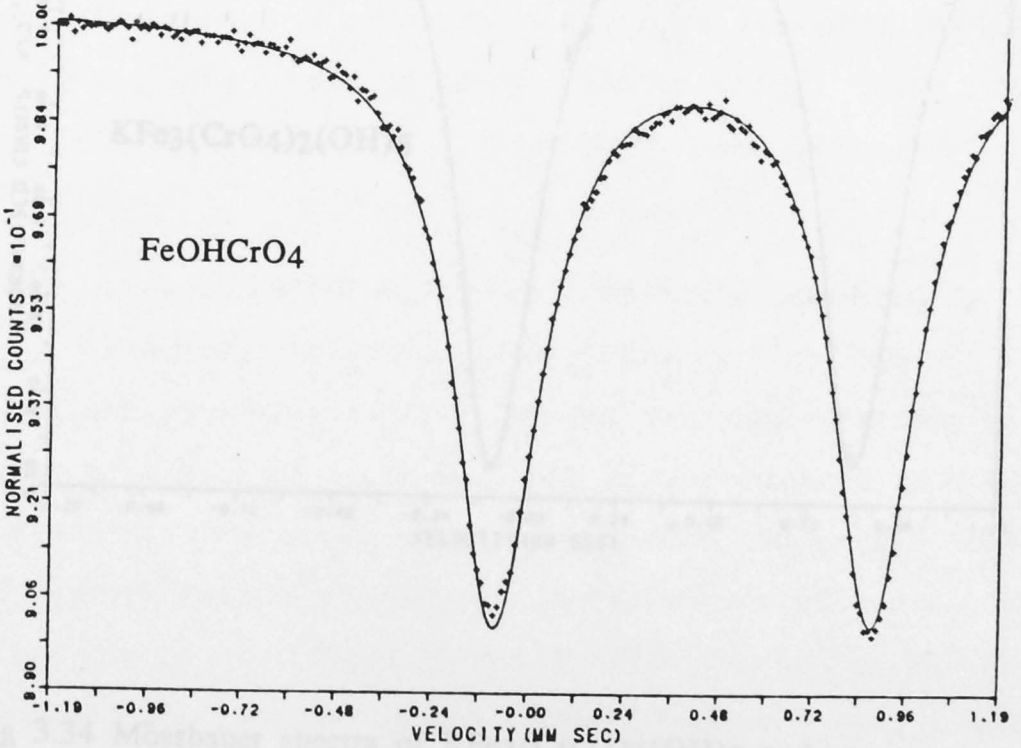

Fig 3.33 Mössbauer spectra of the series $FeOHCrO_4.nH_2O$ at 25°C

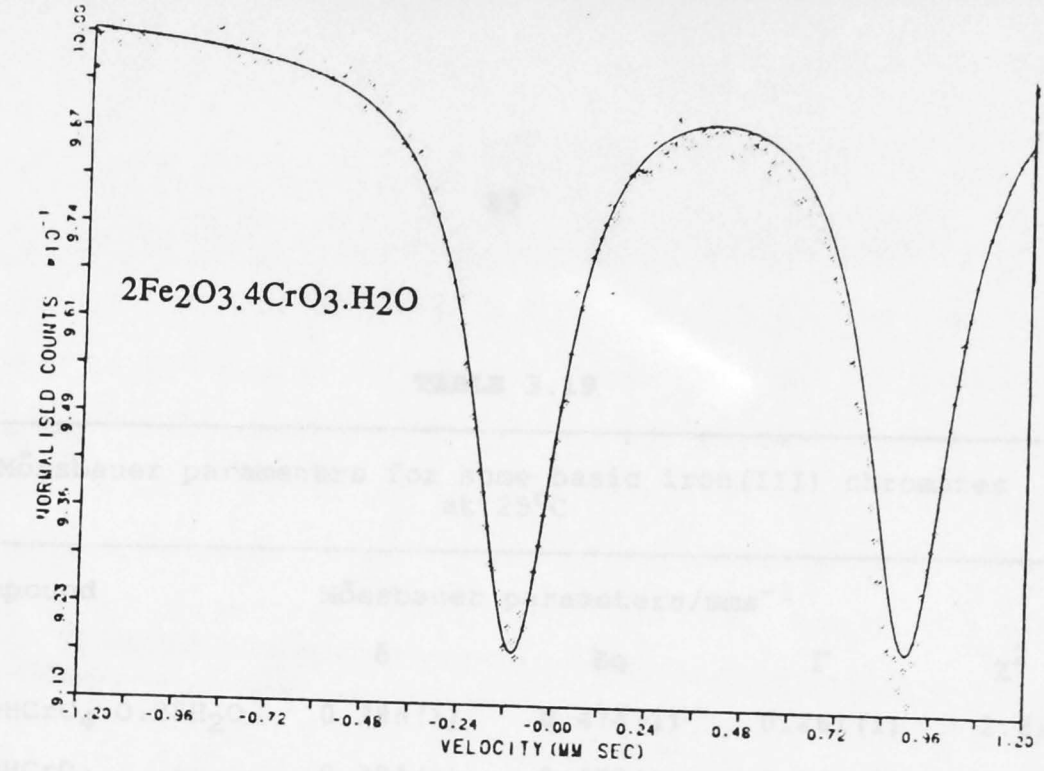

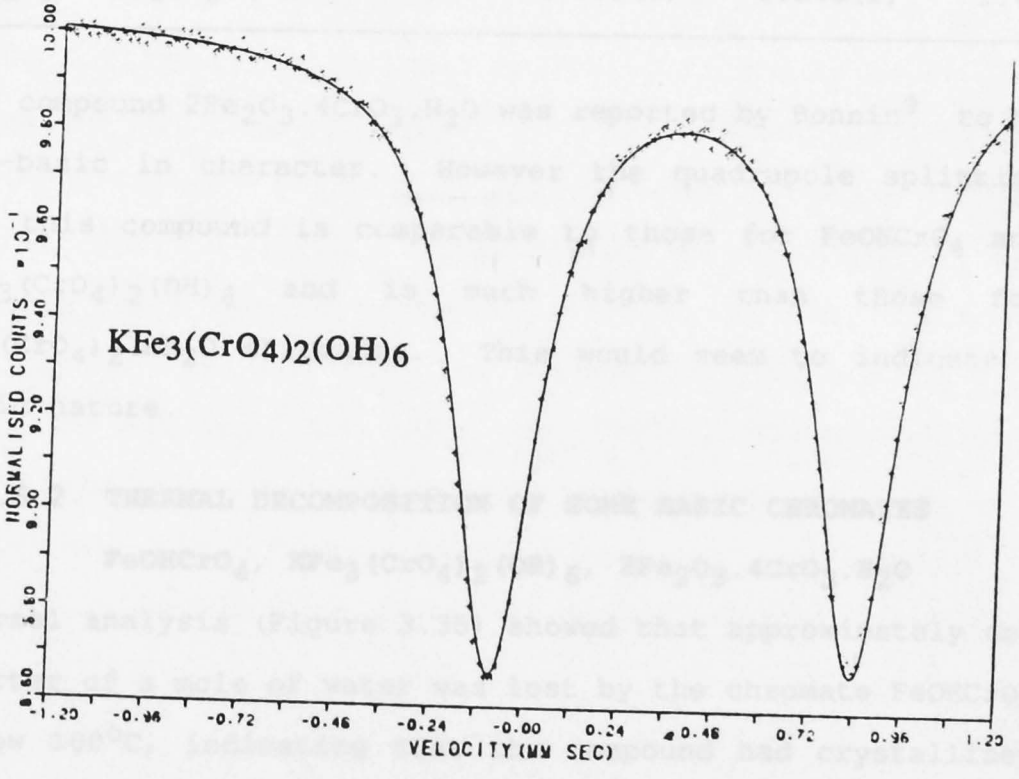

Fig 3.34 Mössbauer spectra of $KFe_3(CrO_4)_2(OH)_6$ and $2Fe_2O_3.4CrO_3.H_2O$ at 25°C

TABLE 3.19

Mössbauer parameters for some basic iron(III) chromates at 25°C

Compound	Mössbauer parameters/mms^{-1}			
	δ	Eq	Γ	χ^2
$FeOHCrO_4$ $0.25H_2O$	0.386(1)	0.474(1)	0.261(1)	2.21
$FeOHCrO_4$	0.384(1)	0.472(1)	0.264(1)	1.97
$KFe_3(CrO_4)_2(OH)_6$	0.366(1)	0.458(1)	0.260(2)	1.99
$2Fe_2O_3.4CrO_3.H_2O$	0.386(1)	0.499(1)	0.266(2)	1.63

The compound $2Fe_2O_3.4CrO_3.H_2O$ was reported by Bonnin[9] to be non-basic in character. However the quadrupole splitting for this compound is comparable to those for $FeOHCrO_4$ and $KFe_3(CrO_4)_2(OH)_6$ and is much higher than those for $MFe(CrO_4)_2.nH_2O$ chromates. This would seem to indicate a basic nature.

3.2.6.2 THERMAL DECOMPOSITION OF SOME BASIC CHROMATES $FeOHCrO_4$, $KFe_3(CrO_4)_2(OH)_6$, $2Fe_2O_3.4CrO_3.H_2O$

Thermal analysis (Figure 3.35) showed that approximately one quarter of a mole of water was lost by the chromate $FeOHCrO_4$ below 100°C, indicating that the compound had crystallised as a hydrate $FeOHCrO_4.0.25H_2O$. The formation of a hydrated species can be contrasted with the behaviour of the sulfate analogue[65,73], which forms the 2-water salt when precipitated from aqueous solution or on standing in air saturated with water.

Mössbauer spectra (Figure 3.33), Table 3.19, of samples heated to 200°C were similiar to those obtained for unheated samples. This result would support the conclusion that the water is most likely present as water of crystallization. Anhydrous $FeOHCrO_4$ left to stand in air saturated with water failed to reabsorb water; TG results supported this finding.

The pyrolysis processes (Table 3.20) for the basic chromates involved at least two stages, as evidenced by the inflexion points in the thermograms (Figures 3.35 - 3.37) at about 440°C. Differential thermal analysis (Figure 3.38) for the chromates $FeOHCrO_4$ and $2Fe_2O_3.4CrO_3.H_2O$ showed the presence of endotherms at (447, 523°C) and (420, 490°C), respectively. Attempts to separate the reactions by slow heating rates were unsuccessful, most likely due to partial overlap of the decomposition processes. XRD patterns of residues quenched from 440°C for $FeOHCrO_4$, $KFe_3(CrO_4)_2(OH)_6$ and $2Fe_2O_3.4CrO_3.H_2O$ showed the presence of new lines at d = 3.56(s), 3.31(s) and 3.06(m), supporting the formation of the same intermediate phase(s), e.g. $Fe_2O(CrO_4)_2$, in each case.

Decomposition of the chromate $2Fe_2O_3.4CrO_3.H_2O$ can be contrasted with that of the mineral Hisinginite - $mFe_2O_3.nSiO_2pH_2O$[74], and its aluminium analogue $mAl_2O_3.nSiO_2.pH_2O$[75]. Both minerals lose water below 150°C,

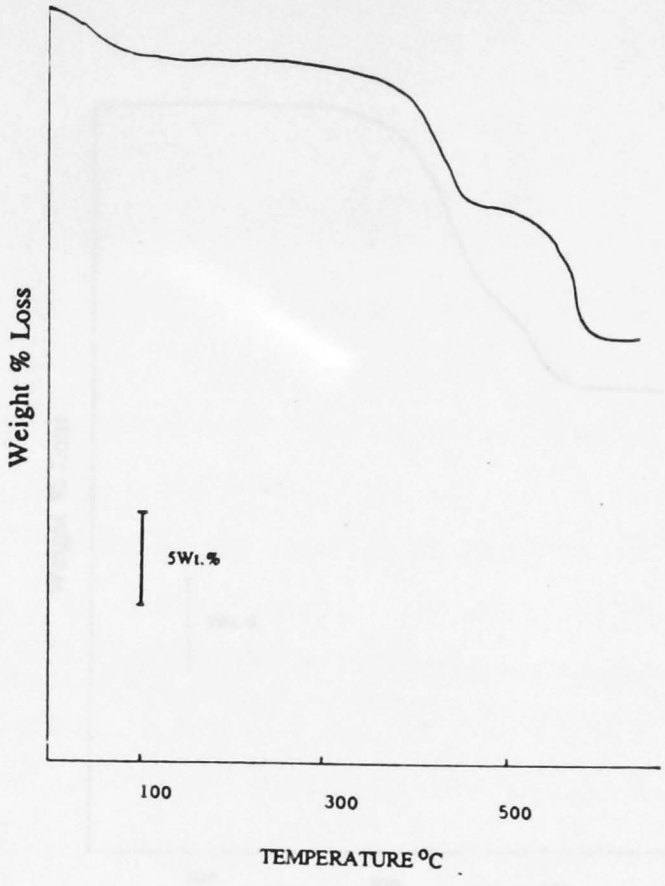

Fig 3.35 Representative thermogram for $FeOHCrO_4$ heated at 10°C/min

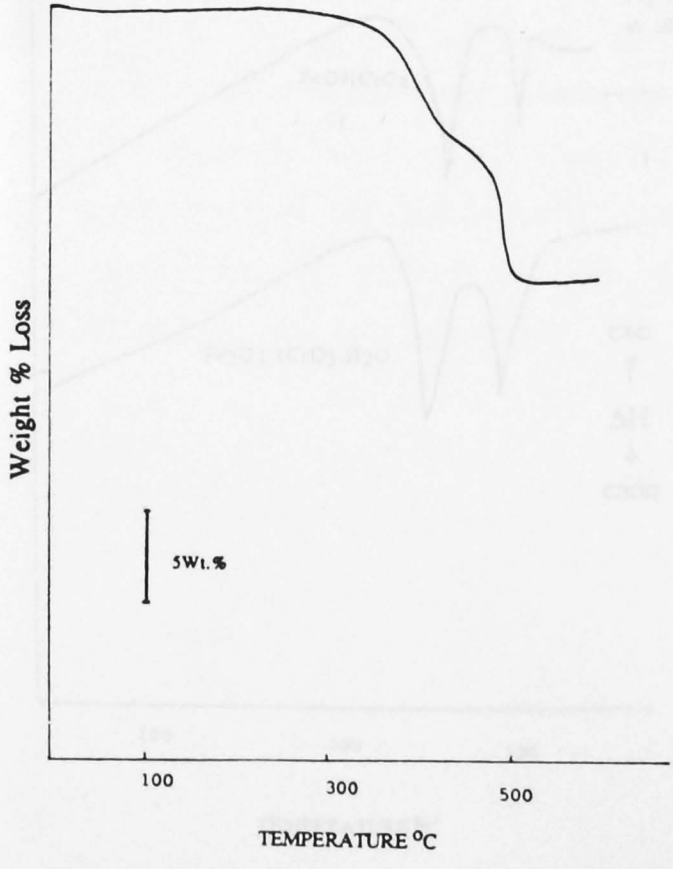

Fig 3.36 Representative thermogram for $KFe_3(CrO_4)_2(OH)_6$ heated at 10°C/min

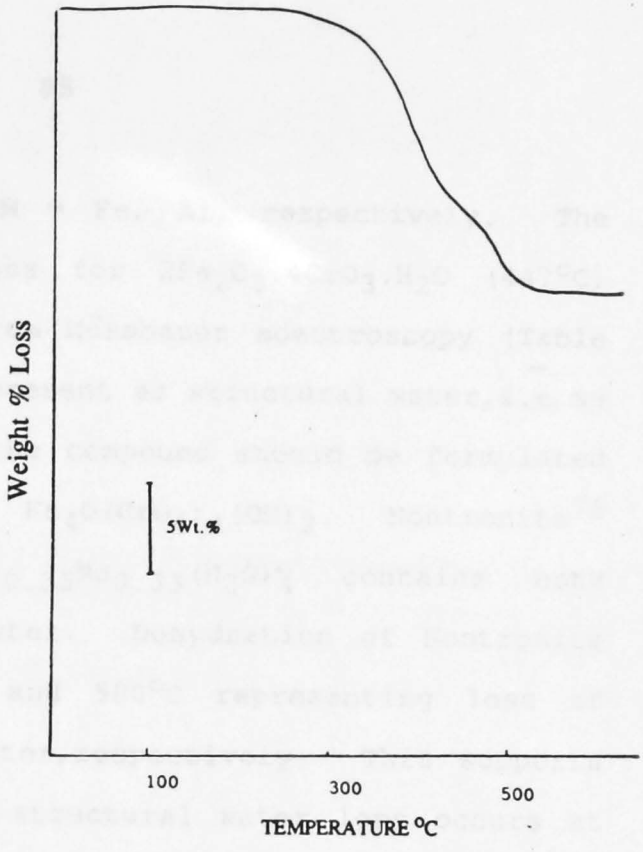

Fig 3.37 Representative thermogram for $2Fe_2O_3.4CrO_3.H_2O$ heated at 10°C/min

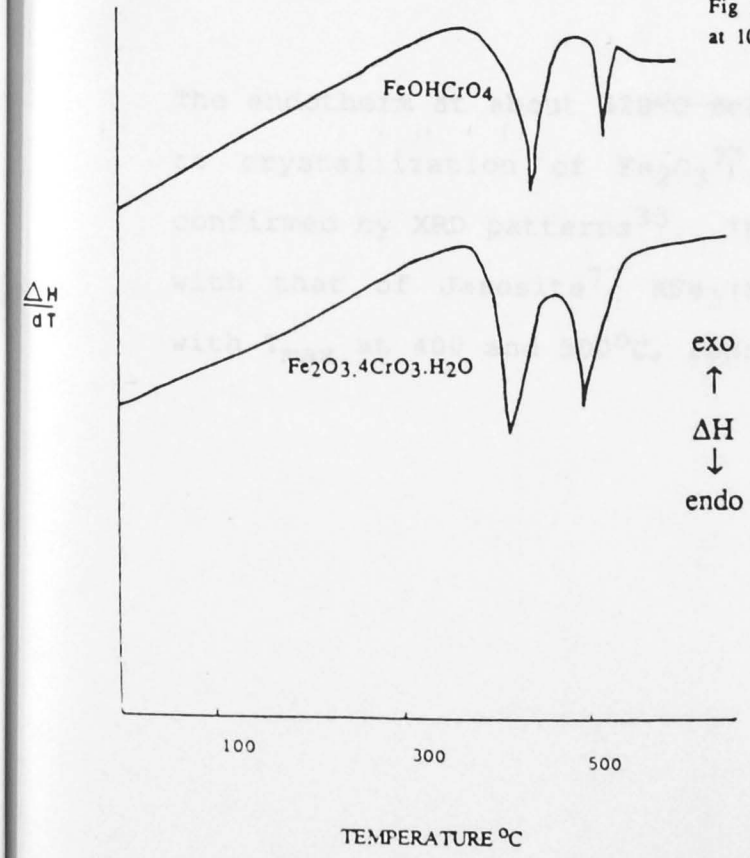

Fig 3.38 Representative differential thermal analysis curves for $FeOHCrO_4$ and $Fe_2O_3.4CrO_3.H_2O$ heated at 10°C /min

T_{max} = 120[74], 140[75] for M = Fe, Al, respectively. The higher T_{max} for water loss for $2Fe_2O_3.4CrO_3.H_2O$ (447°C) supports the conclusion from Mössbauer spectroscopy (Table 3.19) that the water is present as structural water, i.e. as bound molecules, or that the compound should be formulated as the oxo hydroxide $Fe_4O(CrO_4)_4(OH)_2$. Nontronite[76] $Fe_2^{3+}[(OH)_2Al_{0.35}Si_{0.67}O_{10}]_{0.35}Na_{0.33}(H_2O)_4$ contains both adsorbed and structural water. Dehydration of Nontronite occurs with T_{max} at 150 and 500°C representing loss of adsorbed and structural water, respectively. This supports the view that, in general, structural water loss occurs at much higher temperatures.

The endotherm at about 520°C for the basic chromates is due to crystallization of Fe_2O_3[77], the presence of which was confirmed by XRD patterns[33]. This behaviour can be compared with that of Jarosite[77] $KFe_3(SO_4)_2(OH)_6$, which decomposes with T_{max} at 400 and 500°C, representing dehydration to

TABLE 3.20

Reaction stoichiometries for some basic iron(III) chromates at a heating rate of 10°C/min

Decomposition steps	Wt loss % obs	Wt loss % calc	
$2FeOHCrO_4 \rightarrow Fe_2O(CrO_4)_2+H_2O$	5.40±0.30	4.75	(3.2.28)
$Fe_2O(CrO_4)_2 \rightarrow Fe_2O_3+Cr_2O_3+\frac{3}{2}O_2$	12.30±0.20	13.34	(3.2.29)
$2FeOHCrO_4.0.25H_2O \rightarrow Fe_2O_3+Cr_2O_3+\frac{3}{2}O_2+\frac{3}{2}H_2O$	17.69±0.25	19.37	(3.2.30)
$2KFe_3(CrO_4)_2(OH)_6 \rightarrow K_2Cr_2O_7+Fe_2O(CrO_4)_2+2Fe_2O_3+6H_2O$	10.11±0.70	9.81	(3.2.31)
$Fe_2O(CrO_4)_2 \rightarrow Fe_2O_3+Cr_2O_3+\frac{3}{2}O_2$	13.81±0.10	13.34	(3.2.32)
$2KFe_3(CrO_4)_2(OH)_6 \rightarrow K_2Cr_2O_7+3Fe_2O_3+Cr_2O_3+\frac{3}{2}O_2+6H_2O$	14.42±0.30	14.20	(3.2.33)
$2Fe_2O_3.4CrO_3.H_2O \rightarrow Fe_3Cr_{3.5}O_{15}+\frac{1}{2}Fe_2O_3+\frac{1}{4}Cr_2O_3+\frac{3}{8}O_2+H_2O$	4.47±0.20	4.06	(3.2.34)
$Fe_3Cr_{3.5}O_{15} \rightarrow \frac{3}{2}Fe_2O_3+\frac{7}{4}Cr_2O_3+\frac{21}{8}O_2$	14.07±0.20	14.23	(3.2.35)
$2Fe_2O_3.4CrO_3.H_2O \rightarrow 2Fe_2O_3+2Cr_2O_3+3O_2+H_2O$	15.67±0.20	15.44	(3.2.36)

$K_2SO_4.Fe_2(SO_4)_3$ and subsequent formation of Fe_2O_3. This may indicate that the structural features present in both sulfates and chromates[24] are reflected in their decomposition pathways.

Mössbauer spectra of residues from $FeOHCrO_4$ quenched from 400°C (Figure 3.39) were resolved into two sets of quadrupole split doublets, as were spectra of residues from $KFe_3(CrO_4)_2(OH)_6$, Table 3.21.

The presence of two quadrupole doublets in the spectra of $FeOHCrO_4$ quenched from 400°C could indicate the presence of $Fe_2(CrO_4)_3$, in addition to $Fe_2O(CrO_4)_2$.

The observed quadrupole splittings 0.10 - 0.19 mms^{-1} for FeO_6 octahedra in the chromates $MFe(CrO_4)_2$ (sections 3.2.1.2 - 3.2.4.2) lend support also to the postulated presence of $Fe_2(CrO_4)_3$, as it would be expected to contain FeO_6 octahedra. Swamy et al[29] have concluded, on the basis of XRD and DTA studies, that $FeOHSO_4$ (isostructural with $FeOHCrO_4$) decomposes directly to the oxosulfate species $Fe_2O(SO_4)_2$, indirectly supporting reaction 3.2.28. It is conceivable that a similar mechanism for the decomposition of $FeOHCrO_4$ is occurring with the pathway dependent on reaction conditions.

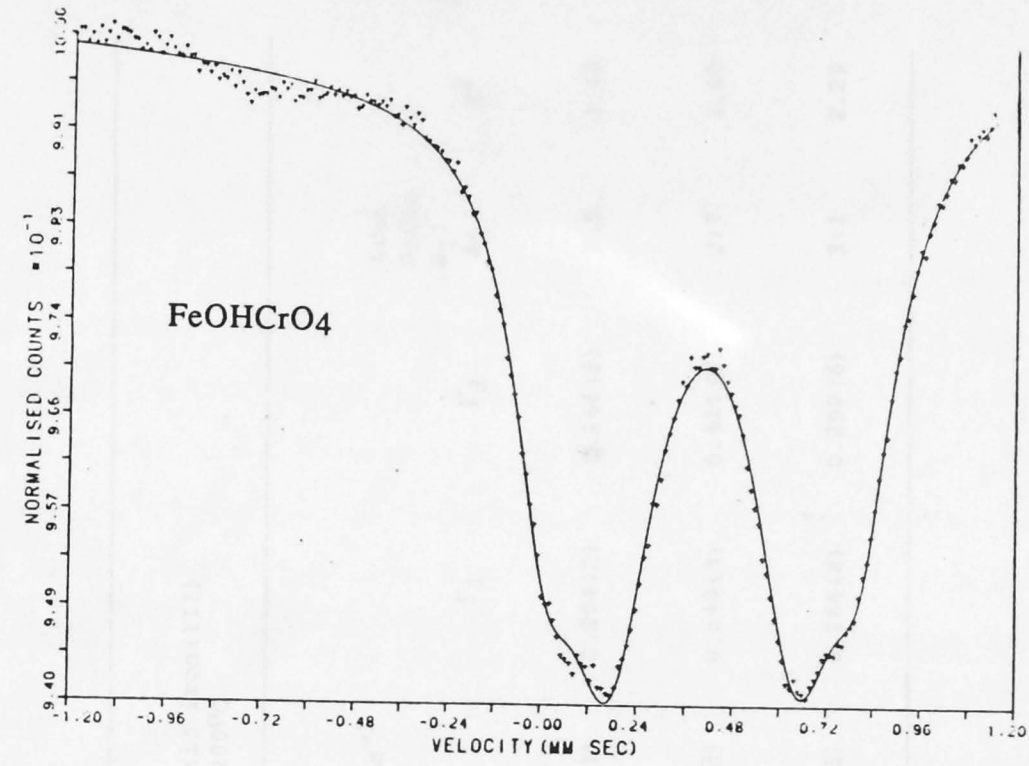

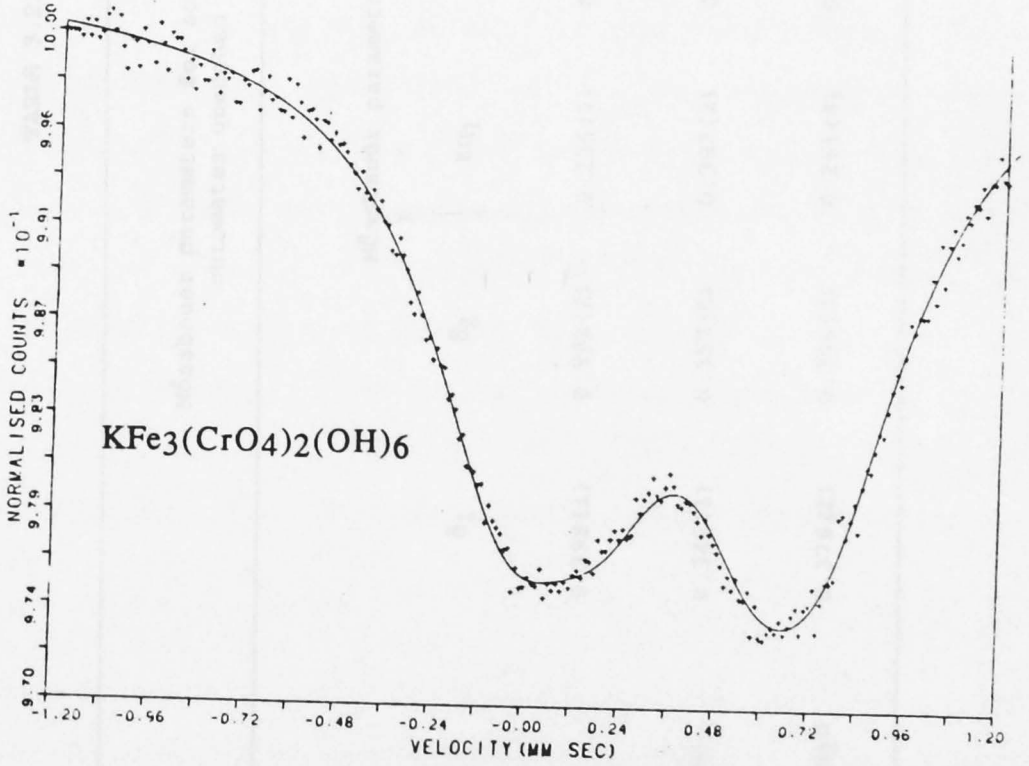

Fig 3.39 Room temperature Mössbauer spectra of $FeOHCrO_4$ and $KFe_3(CrO_4)_2(OH)_6$ quenched from 400^oC

TABLE 3.21

Mössbauer parameters for some basic iron(III) chromates quenched from 400°C

Compound	Mössbauer parameters/mms^{-1}							
	δ_1	δ_2	Eq_1	Eq_2	Γ_1	Γ_2	Area Ratio A_1/A_2	χ^2
$FeOHCrO_4$	0.398(1)	0.398(2)	0.235(1)	0.398(1)	0.284(1)	0.266(2)	2:5	1.62
$KFe_3(CrO_4)_2(OH)_6$	0.342(1)	0.357(5)	0.392(2)	0.342(2)	0.549(3)	0.411(3)	2:7	1.80
$2Fe_2O_3.4CrO_3.H_2O$	0.376(2)	0.396(3)	0.261(4)	0.401(3)	0.266(2)	0.299(6)	3:1	2.29

Spectra of $KFe_3(CrO_4)_2(OH)_6$ residues quenched from 400°C were also interpreted in terms of $Fe_2O(CrO_4)_2$ formation. The asymmetry in the spectrum, Fig 3.39, could be due to either absorber thickness or partial orientation (texture) of the powder. As Figure 3.35 indicates, reaction 3.2.28 occurred over the temperature range 300 - 400°C for the decomposition of $FeOHCrO_4$, whilst the first stage (Figure 3.36) in the decomposition of $KFe_3(CrO_4)_2(OH)_6$ occurred in the range 300 - 460°C to form $Fe_2O(CrO_4)_2$, reaction 3.2.31. The doublet in the spectrum of $KFe_3(CrO_4)_2(OH)_6$ quenched from 400°C, δ_2 = 0.36 mms^{-1} and Eq_2 = 0.34 mms^{-1} shows good agreement with that reported by Kundig et al[78] for amorphous (super paramagnetic) Fe_2O_3 (δ= 0.30-0.38 mms^{-1} and Eq = 0.42-0.98 mms^{-1}), dependent on particle size, giving further support for reaction 3.2.31. Filtration of an aqueous extract of the quenched residue, followed by slow evaporation of the filtrate, yielded orange crystals, which were identified as $K_2Cr_2O_7$ by means of their XRD powder pattern, thereby supporting all the decomposition products as proposed by 3.2.31.

Mössbauer spectra of $2Fe_2O_3.4CrO_3.H_2O$, on quenching from 400°C, (Table 3.21), were also resolved into two sets of quadrupole doublets with parameters similar to those found for $FeOHCrO_4$ quenched from 400°C. XRD patterns, after quenching from 550°C, confirmed the presence of iron(III) and chromium(III) oxides[33].

3.2.6.3 **CONCLUSION**

Decomposition of basic iron(III) chromates was proposed, for all compounds studied, to proceed through the new intermediate $Fe_2O(CrO_4)_2$. Assignment of $Fe_2O(CrO_4)_2$ to the decomposition pathway of $2Fe_2O_3.4CrO_3.H_2O$ was on a tentative basis through the use of Mössbauer spectroscopy.

3.2.7 **MAGNETIC MEASUREMENTS**

Measurements of magnetic susceptibilities in the temperature range 4.2 - 300K, at a field strength of 10 K Gauss, were attempted in order to provide data which could complement existing Mössbauer data for the iron(III) chromates (Appendix II).

However, due to breakdowns and non-availability of instruments, results were processed only for the series $KFe(CrO_4)_2.nH_2O$ n = 0, 1 and 2. Plots of magnetic susceptibility versus temperature, and of magnetic moment versus temperature for the compounds are shown in Figures 3.40 - 3.42.

The susceptibility plot for $KFe(CrO_4)_2$ exhibited a maximum at 48 K, most likely the antiferromagnetic ordering temperature. The small increase in the susceptibility for $KFe(CrO_4)_2$ at low temperatures is probably due to the presence of a paramagnetic phase, possibly residual hydrate.

Plots of X_m^{-1} versus temperature for the series obeyed the Curie-Weiss law

$$X_m = x_o + \frac{C}{T - \theta_w}$$

over the temperature ranges 300 - 5 K for n = 2 or 1 and 300 - 100 K for n = 0 (Figures 3.43, 3.44). The Weiss temperatures (θ_w) were negative, -10 $\pm$ 2K for n = 2, -40 $\pm$ 5 K for n = 1 and -120 $\pm$ 20 K for n = 0, indicating antiferromagnetic coupling. Crystallographic studies[17] indicate that the successive removal of water for the series $KFe(CrO_4)_2.nH_2O$ results in increased crosslinking between the chains of polyhedra in the structure, which possibly facilitates exchange interactions. The antiferromagnetic coupling strength increased with the removal of water. The effective magnetic moments, incorporating θ_w, gave u_β values of 5.68, 5.54 and 4.91 for n = 2, 1 or 0, respectively, showing the iron to be in the S = 5/2 state, as indicated by the isomer shift in Mössbauer spectra.

3.3 CONCLUSIONS ON THERMAL ANALYSIS OF IRON CHROMATES

The ease of dehydration for the chromates $MFe(CrO_4)_2.2H_2O$ was found to be in the order NH_4 > Na > K, whilst the stability (based on T_i) of the anhydrous chromates $MFe(CrO_4)_2$ was found to be in the order Rb > Cs $\tilde{\sim}$ Tl > K > Na > NH_4. The stability of the anhydrous alkali metal iron(III) chromates, as judged by T_i, does not appear to be dependent on the size of the monovalent cation but rather on the formation of $M_2Cr_2O_7$ or M_2CrO_4 as the stable species.

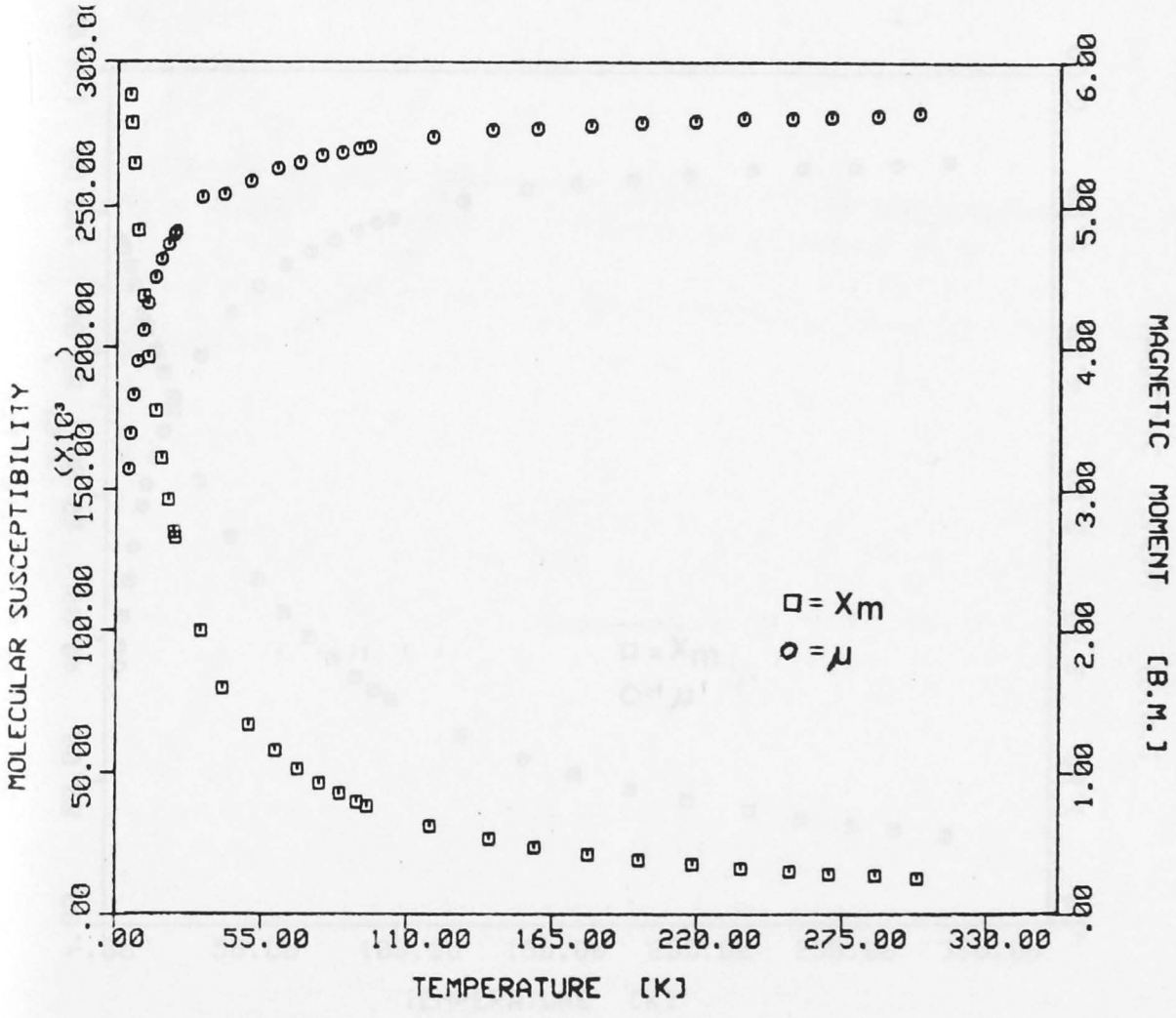

Fig 3.40 Magnetic susceptibility and magnetic moment curves for $KFe(CrO_4)2.2H_2O$

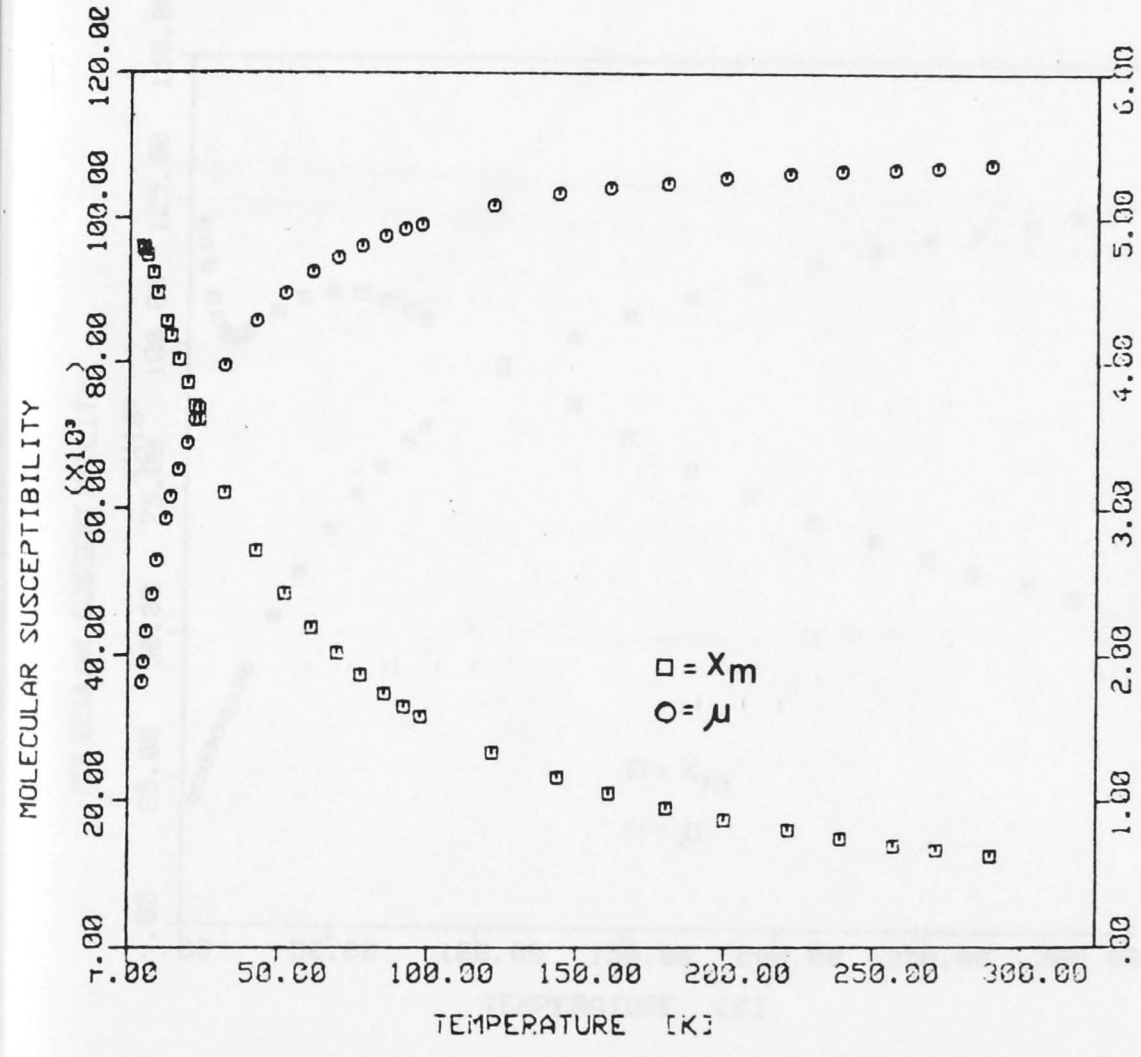

Fig 3.41 Magnetic susceptibility and magnetic moment curves for $KFe(CrO_4)_2.H_2O$

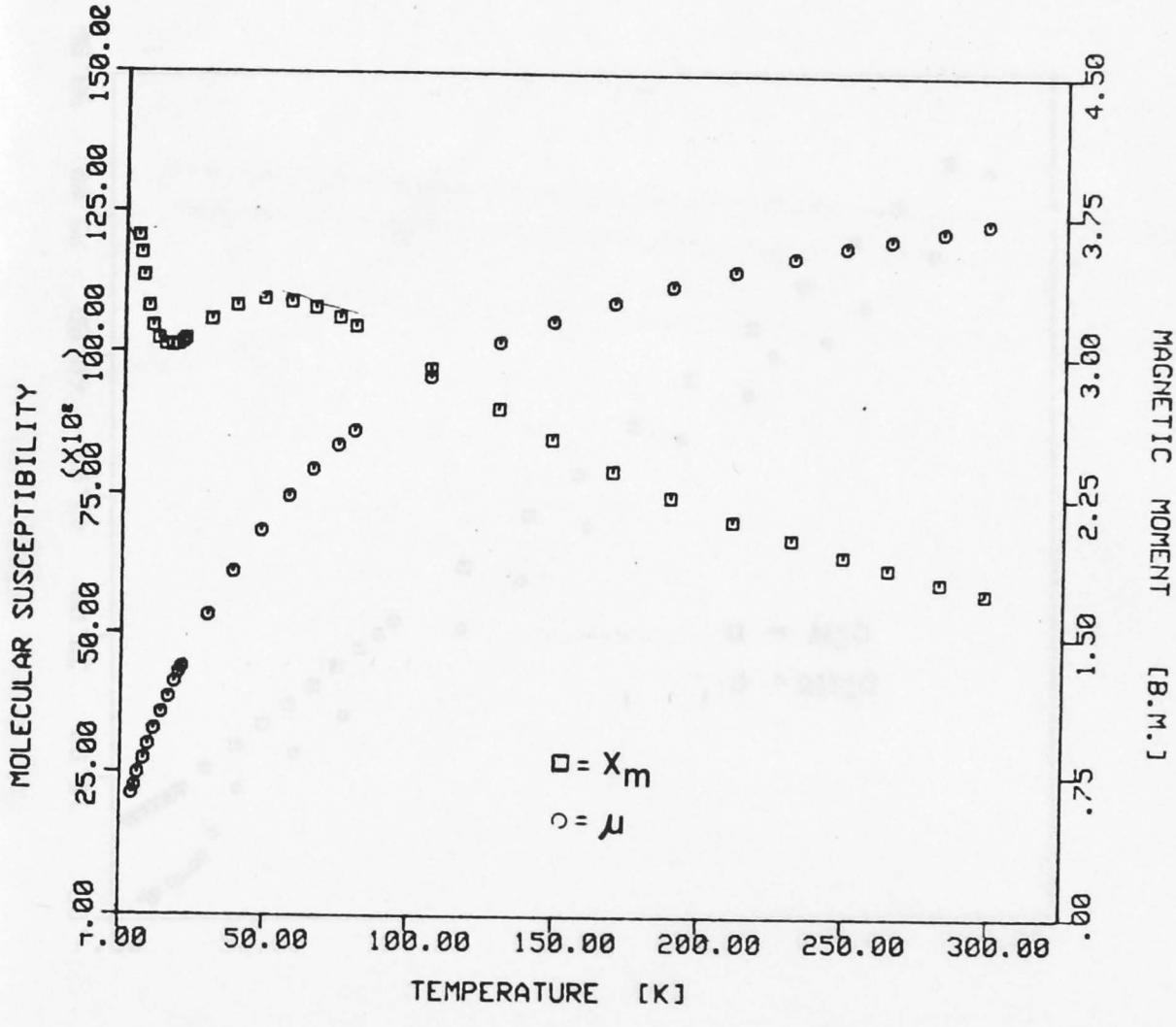

Fig 3.42 Magnetic susceptibility and magnetic moment curves for $KFe(CrO_4)_2$.

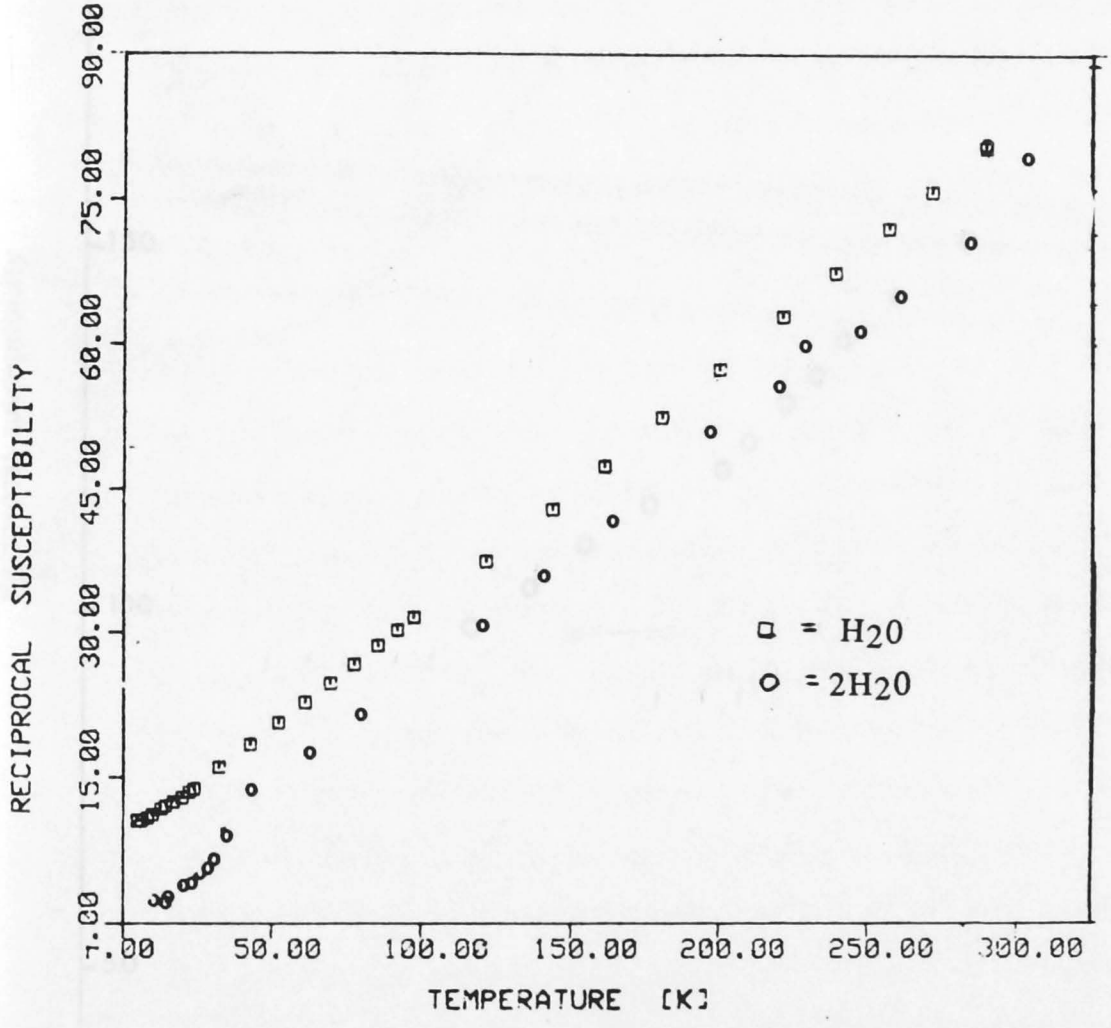

Fig 3.43 Reciprocal magnetic susceptibility plots for $KFe(CrO_4)_2.nH_2O$ n=1 and 2

Fig 3.44 Reciprocal magnetic susceptibility plot for $KFe(CrO_4)_2$.

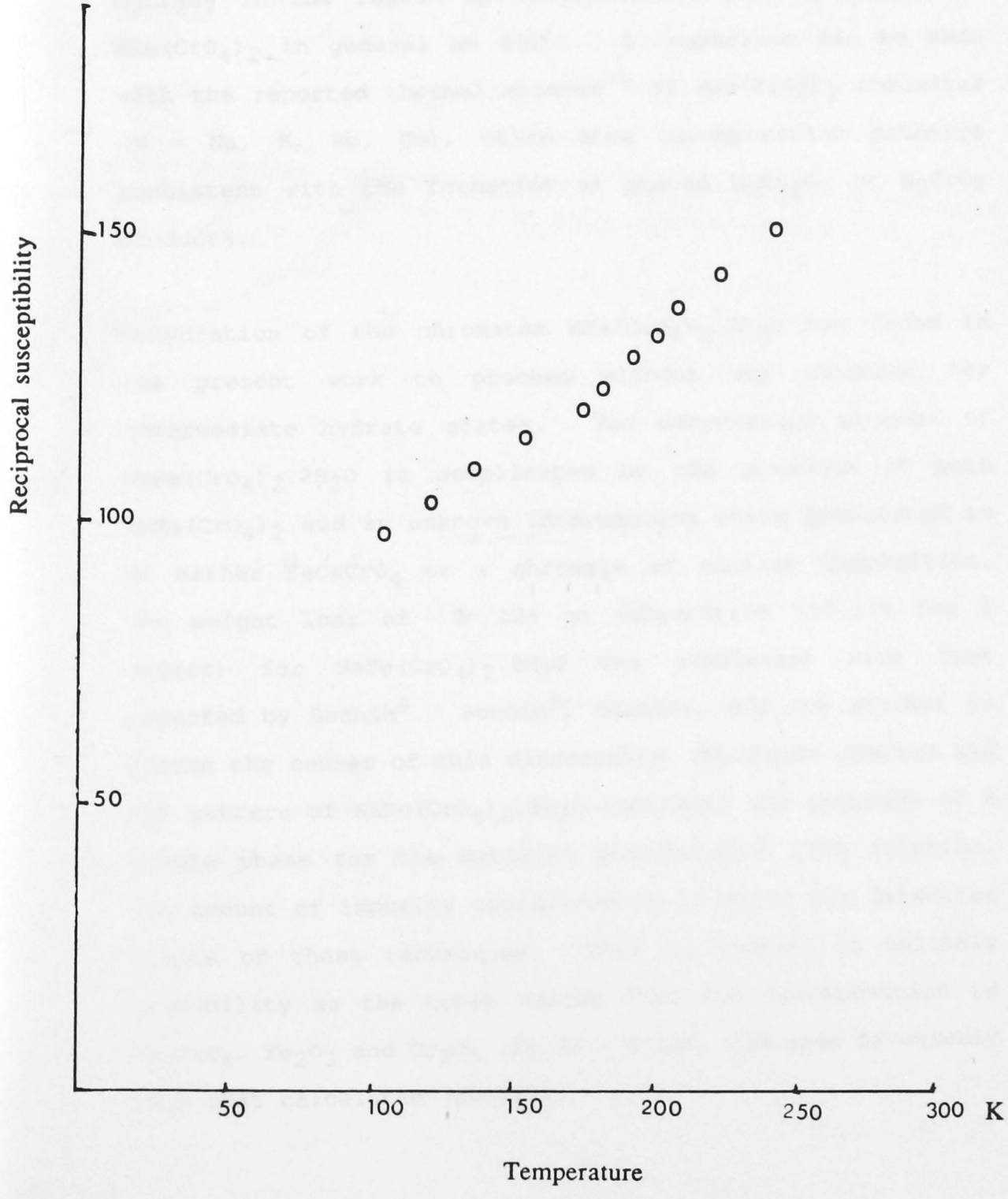

This is clearly evident in the case of the chromates $MFe(CrO_4)_2$ (M = NH_4, Na), the cations of which form unstable $M_2Cr_2O_7$ in the region of decomposition for the chromates $MFe(CrO_4)_2$, in general at 400°C. A comparison can be made with the reported thermal studies[79] of $MSc(CrO_4)_2$ chromates (M = Na, K, Rb, Cs), which show decomposition pathways consistent with the formation of stable $M_2Cr_2O_7$ or M_2CrO_4 products.

Dehydration of the chromates $MFe(CrO_4)_2.2H_2O$ was found in the present work to proceed without any evidence for intermediate hydrate states. The dehydration process of $NaFe(CrO_4)_2.2H_2O$ is complicated by the presence of both, $NaFe(CrO_4)_2$ and an unknown intermediate phase, postulated to be either $FeOHCrO_4$ or a chromate of similar composition. The weight loss of ~ 12% on dehydration (10.31% for 2 waters) for $NaFe(CrO_4)_2.2H_2O$ was consistent with that reported by Bonnin[9]. Bonnin[9], however, did not attempt to pursue the causes of this discrepancy. Mössbauer spectra and XRD pattern of $NaFe(CrO_4)_2.2H_2O$ indicated the presence of a single phase for the material precipitated from solution, the amount of impurity could, however, be below the detection limits of these techniques. This is, however, an unlikely possibility as the total weight loss for decomposition to Na_2CrO_4, Fe_2O_3 and Cr_2O_3 (20.30 $\pm$ 0.12%) compared favourably with that calculated (20.62%).

Therefore the presence of an intermediate phase formed during dehydration of $NaFe(CrO_4)_2.2H_2O$ is considered to be the cause of the additional weight loss. This postulate is further supported by Mössbauer spectra of the dehydration residues which showed the resolution of two quadrupole doublets, with parameters for both doublets consistent with those for previously reported iron chromates, indicating that the confidence in the fitting process is high.

However, the identity of this intermediate phase in the dehydration of $NaFe(CrO_4)_2.2H_2O$ still remains to be determined.

Ammonium iron chromate decomposed with the formation of an intermediate phase - of possible composition $FeCr_2O_6$. Mössbauer studies confirmed that the intermediate contains iron(III). Further characterisation of this product is required, particularly as it was found to be amorphous to X-rays. Popel and Boldog[68] also reported the formation of iron/chromium oxide solid solutions during decomposition of the basic salt $(NH_4)_3(H_2O)_2Fe_8(OH)_{17}(CrO_4)_6$.

Decomposition of the chromates $MFe(CrO_4)_2$, M = Rb, Cs, proceeded in a single step to the respective dichromate, and a mixture of iron(III) and chromium(III) oxides. The results confirmed crystallographic studies[14,15], that these chromates are not precipitated as hydrates. This leads to

the conclusion, that, the thermal analysis data for these chromates reported previously[23], differ from those obtained in the present study.

Thermogravimetry of $Fe_2(CrO_4)_3.nH_2O$ (n = 1, 3) and basic iron(III) chromates showed a number of features common to both groups of compounds (Table 3.22). The intermediate $Fe_2O(CrO_4)_2$ was found to be common to the decomposition pathways of all the compounds studied. The presence of a common intermediate is clearly reflected in the DTA profiles (Figures 3.32 and 3.38). Considering the structural relationships which exist between iron sulfates and their chromate analogues[24], the use of thermal analysis as a structural probe deserves serious consideration.

TABLE 3.22

Proposed intermediates in the pyrolysis of some normal and basic chromates

Compound	Products
$FeOHCrO_4$	$Fe_2O(CrO_4)_2$, $Fe_2(CrO_4)_3$
$Fe_2(CrO_4)_3.H_2O$	$FeOHCrO_4$, $Fe_2O(CrO_4)_2$
$Fe(CrO_4)_3.3H_2O$	$Fe_2O(CrO_4)_2$

Whilst no plateau corresponding to the formation of $Fe_2(CrO_4)_3$ in the thermograms was observed, Mössbauer spectra for samples of $FeOHCrO_4$ quenched from 400°C (Figure 3.39) strongly suggested the presence of a phase such as $Fe_2(Cro_4)_3$. This gives further indirect support to the proposals of Swarmi et al[28-30], that the pyrolysis of iron(III) hydroxy sulfate, $FeOHSO_4$, proceeds via the formation of either iron(III) oxosulfate or iron(III) sulfate.

To exemplify the potential of using thermal analysis in conjunction with structural information, the chromate $2Fe_2O_3.4CrO_3.H_2O$ of unspecified structural formula was examined.

Bonnin[9] has proposed that this chromate is non-basic; however, no supporting thermal or structural evidence was given. The similarity of DTA curves for this compound to those for $FeOHCrO_4$ indicates that the bonding in both structures may be similar. Furthermore, the Mössbauer parameters for $2Fe_2O_3.4CrO_3.H_2O$ are similar to those reported for basic iron(III) chromates, indicating that the environment around each iron is similar. Therefore a better

representation for this compound, based on thermal and Mössbauer evidence, is $Fe_4O(CrO_4)_4(OH)_2$, in which hydroxyl groups rather than water molecules are incorporated in the structure.

The structure[20] of $Fe_2(CrO_4)_3.3H_2O$ contains two inequivalent iron oxygen polyhedra. Mössbauer spectra confirmed this by being resolvable into two quadrupole doublets. Thermal analysis, however, showed that water was lost in the sequence $3H_2O \rightarrow 1/2\ H_2O$. This seems to indicate that the water environments are more complex than crystallographic studies present them to be.

The process of following the thermolysis of compounds by methods other than thermal analysis e.g. Mössbauer spectroscopy, has shown them to be helpful in confirming reaction sequences. Techniques such as Mössbauer spectroscopy are non-destructive and therefore can be used to investigate features in the thermal curves. For example, the endotherm at 500°C present in the DTA curves of basic and normal iron(III) chromates was postulated to indicate the presence of a common intermediate. XRD patterns of the residues were difficult to index due to poor crystallinity. Mössbauer spectroscopy, however, readily resolved the intermediate phase and indicated that the parameters derived from spectral fitting for each residue were comparable.

3.4 CONCLUSIONS FROM MÖSSBAUER SPECTROSCOPY OF IRON CHROMATES

The room temperature parameters for the Mössbauer spectra of some iron(III) chromates (see Section 3.2) are shown in Table 3.23.

All spectra, with the exception of that of $Fe_2(CrO_4)_3.3H_2O$, were simple quadrupole doublets with isomer shifts of about 0.40 mms^{-1}, as expected for high spin iron(III) in octahedral sites [40,41]. The relatively narrow linewidths (Γ) 0.25 - 0.30 mms^{-1}, compared to 0.22 - 0.25 mms^{-1} for natural α-iron foil [34] (figure 2.2), indicated that relaxation effects were not significant for iron(III) chromates.

There appear to be some useful correlations between structure and the Mössbauer quadrupole splittings, which are dependent upon the distortion from cubic symmetry (Eq = 0, for cubic symmetry), the field gradient induced by other cations where present, and on the effective charges on the oxygen atoms in the iron octahedra.

TABLE 3.23

Mössbauer parameters for some iron(III) chromates at room temperature

Example	Site type	Mössbauer parameters/mms^{-1} δ	Eq	Γ	χ^2
$NaFe(CrO_4)_2.2H_2O$	$Fe(OH_2)_2O_4$	0.411(2)	0.356(2)	0.309(7)	1.20
$KFe(CrO_4)_2.2H_2O$	$Fe(OH_2)_2O_4$	0.401(1)	0.341(3)	0.269(3)	1.80
$NH_4Fe(CrO_4)_2.2H_2O$	$Fe(OH_2)_2O_4$	0.428(2)	0.510(2)	0.279(2)	1.10
$NaFe(CrO_4)_2$	FeO_6	0.393(4)	0.152(4)	0.227(1)	1.12
$KFe(CrO_4)_2$	FeO_6	0.412(7)	0.111(1)	0.227(1)	0.99
α-$NH_4Fe(CrO_4)_2$	FeO_6	0.403(1)	0.104	0.259(1)	1.15
α-$TlFe(CrO_2)_4$	FeO_6	0.398(2)	0.118(7)	0.305(1)	1.22
β-$NH_4Fe(CrO_4)_2$	FeO_6(net)	0.407(5)	0.431(2)	0.391(7)	1.15
β-$TlFe(CrO_4)_2$	FeO_6(net)	0.400(2)	0.192(1)	0.310(2)	1.16
β-$RbFe(CrO_4)_2$	FeO_6(net)	0.391(3)	0.109(3)	0.268(1)	0.97
$CsFe(CrO_4)_2$	FeO_6	0.399(1)	0.094(1)	0.252(2)	0.92
$FeOHCrO_4.0.25H_2O$		0.386(1)	0.474(1)	0.261(1)	2.21
$FeOHCrO_4$	$Fe(OH)_2O_4$	0.384(1)	0.472(1)	0.264(1)	1.97
$2Fe_2O_3.4CrO_3.H_2O$		0.386(1)	0.499(1)	0.266(1)	1.63
$KFe_3(CrO_4)_2(OH)_6$	$Fe(OH)_2O_4$	0.366(1)	0.458(1)	0.260(1)	1.99
$Fe_2(CrO_4)_3.H_2O$		0.399(1)	0.184(1)	0.342(3)	1.86
α-$Fe_2(CrO_4)_3.3H_2O$[+]	FeO_6	0.394(1)	0.154(2)	0.296(3)	1.54
	$FeO_3(H_2O)_3$	0.392(1)	0.352(1)	0.336(2)	

[+] contains two iron sites.

Baur[80] has described an empirical method to equate individual bond length d(A-X) with the electrostatic bond strength p_x received by the anion, where X=anion and A=cation, as follows:

$$d(A-X) = (\langle d(A-X) \rangle + b \ \Delta p_x) \ \text{Å}$$

where $\langle d(A-X) \rangle$ and b are empirically derived constants for given pairs of A and X in a given coordination, and Δp_x is the difference between the individual p_x and the mean p_x for the co-ordination polyhedron.

Baur[80] applied the model to silicates, whereby he correctly predicted that as the M-O-M bond angle decreases, causing the bridging oxygen atoms to lose their facility for π-bonding with M cations, bridging oxygen bonds become weaker and longer, whereas non-bridging M-O bonds become stronger.

Consistent with the approach of Baur[80] the observed quadrupole splittings for the hydrated iron(III) chromates were found to be greater than those for the corresponding anhydrous salts, where the Fe-O bonds have been found to be more uniform[13-15,17].

For example, in $NaFe(CrO_4)_2.2H_2O$ the sodium ion is coordinated by eight oxygens,[11] compared to ten for potassium in the corresponding compound[12] and the range of Fe-O bond distances is smaller than that for $KFe(CrO_4)_2.2H_2O$. On the

basis of Baur's criteria[80] and the smaller range of Fe-O bond distances, the distortion in the sodium salt would be expected to be less, whereas on the basis of the Mössbauer spectra the reverse was the case (Table 3.23). Therefore, it can be proposed that since the splittings for both the hydrated and anhydrous sodium salts are greater than those for the respective potassium compounds, the effective field gradient (e.f.g.) generated by the sodium ion is of greater magnitude than that of the potassium ion.

In the case of $NH_4Fe(CrO_4)_2.2H_2O$, the observed Eq splitting is 0.51 mms^{-1}, considerably greater than that for the chromates $MFe(CrO_4)_2.2H_2O$ (M = Na, K). The observed higher Eq is postulated to be due to the hydrogen bonding between the ammonium ions and oxygen atoms of the iron octahedra [67], resulting in a larger departure from octahedral symmetry relative to the other hydrates.

Enwiga et al[81] have reported that, for the series $MFeCl_3.2H_2O$ (M = Rb, Cs), which contain iron octahedra, hydrogen bonding between chains of octahedra is important in determining the magnitude of the quadrupole splittings, whereas the magnitude of Eq showed only a small variation with alkali metal cation size. The much higher Eq value for $NH_4Fe(CrO_4)_2.2H_2O$, in part due to hydrogen bonding, relative to that for the anhydrous $MFe(CrO_4)_2$ (M = NH_4, Na, K, Rb,

Cs, Table 3.22) is in agreement with infrared[67] and XRD powder studies[9], showing that the water molecules are incorporated in octahedral sites of type $FeO_4(H_2O)_2$ in a manner similar to those present in $MFe(CrO_4)_2.2H_2O$ (M = Na, K).

Differences in the Eq parameters for the chromates $MFe(CrO_4)_2$ (M = Na, K) could be due to differences in the size of the alkali metal cation. However, the magnitude of the splittings compared to those for the chromates $MFe(CrO_4)_2$ (M = Rb or Cs), see Table 3.23, which also do not have edge sharing[14,15], suggests that the alkali metal ion size is of little importance. In view of this, the comparable quadrupole splitting for $NaFe(CrO_4)_2$, (0.15 mms^{-1}) with those of $KFe(CrO_4)_2$ (0.11 mms^{-1}) and α-$NH_4Fe(CrO_4)_2$ (0.104mms^{-1}) lends support to the proposal based on infrared spectroscopy, that $NaFe(CrO_4)_2$ is isostructural with the potassium and ammonium salts, which are in turn isostructural with KCr_3O_8[63].

It follows, therefore, that Mössbauer spectroscopy can be used to distinguish between iron sites which contain octahedra of the types $FeO_{6-x}(H_2O)_x$ and FeO_6 using quadrupole splittings for the analysis of iron(III) chromates. The magnitude of Eq showed only a small variation with alkali cation size and the presence of line broadening was not apparent or significant.

Comparison of the Mössbauer parameters for the α- and β-forms of $NH_4Fe(CrO_4)_2$ shows a very large difference in quadrupole splitting (Table 3.23). On the basis of the range of Fe-O bond distances and bond angles for the two phases (Table 3.24)[13,19], one would expect the Eq of β-$NH_4Fe(CrO_4)_2$ to be lower. However this was not found to be the case. It is proposed, therefore, that the relative quadrupole splittings for α- and β-$NH_4Fe(CrO_4)_2$ can be explained on the basis of the effects of nearest neighbours. The surrounding chromate tetrahedra which contribute oxygen atoms to complete the iron octahedral sites are themselves distorted in both α- and β-$NH_4Fe(CrO_4)_2$[13,19]. The β-form contains two types of crystallographically distinct chromate tetrahedra[19], one of which is involved in the bonding between columns of FeO_6 octahedra, in which the Cr-O bond lengths (1.60 - 1.78Å) and O-Cr-O bond angles (99.85-114.15°) show a wide range of variation compared to those for the second type of chromate tetrahedra[13]. It is proposed, therefore, that, whilst both α- and β-$NH_4Fe(CrO_4)_2$ contain slightly distorted FeO_6 octahedra which are corner-shared, it is the origin of the oxygen atoms, which comprise the octahedron, which is important in determining the

magnitude of Eq for these compounds. Support for the postulate can be found in the case of β-$RbFe(CrO_4)_2$ which is isostructural with β-$NH_4Fe(CrO_4)_2$. As in the case of α-$NH_4Fe(CrO_4)_2$, all octahedra in β-$RbFe(CrO_4)_2$ are corner shared.[14] The good agreement between the values of the quadrupole splittings (Table 3.23) for α-$NH_4Fe(CrO_4)_2$ and β-$RbFe(CrO_4)_2$ would indicate that the FeO_6 octahedra in these compounds are distorted in much the same manner. The distortion of the CrO_4 tetrahedra is also similiar in the two compounds and both distortions are significantly less than in β-$NH_4Fe(CrO_4)_2$. Examination of the structure of β-$RbFe(CrO_4)_2$ [14] reveals that the Cr-O bond lengths and O-Cr-O bond angles are in the ranges 107.5^{o} - 112.2^{o} and 1.58 - 1.66Å, respectively, indicating less variation than those in β-$NH_4Fe(CrO_4)_2$, and comparable to those in α-$NH_4Fe(CrO_4)_2$.

The relationship between the crystallographic data concerning distortions in structures and the results obtained from Mössbauer spectroscopy show, therefore, that the latter can be used to give qualitative information on the effect of nearest neighbour environments.

TABLE 3.24

Bond length and Bond angles for $NH_4Fe(CrO_4)_2$ alpha[13] and beta[19] phases (taken from references 13 and 19).

(a) α-$NH_4Fe(CrO_4)_2$

Fe(1)–O(5)	2.00 (3)	Fe(1)–O(10)	1.98 (3)	Cr(1)–O(3')	1.54 (4)	Cr(1)–O(11)	1.65 (3)
Fe(1)–O(7')	2.05 (3)	Fe(1)–O(15')	2.02 (3)	Cr(1)–O(5)	1.71 (3)	Cr(1)–O(12')	1.67 (3)
Fe(1)–O(9')	1.97 (3)	Fe(1)–O(16')	2.04 (2)				
O(5)–Fe(1)–O(7')	176.9 (1.2)			O(3')–Cr(1)–O(5)	110.9 (1.5)		
O(5)–Fe(1)–O(9')	93.6 (1.1)			O(3')–Cr(1)–O(11)	110.7 (1.5)		
O(5)–Fe(1)–O(10)	91.2 (1.1)			O(3')–Cr(1)–O(12')	108.1 (1.5)		
O(5)–Fe(1)–O(15')	88.0 (1.1)			O(5)–Cr(1)–O(11)	109.0 (1.5)		
O(5)–Fe(1)–O(16')	94.7 (1.0)			O(5)–Cr(1)–O(12')	104.8 (1.5)		
O(7')–Fe(1)–O(9')	85.6 (1.1)			O(11)–Cr(1)–O(12')	113.1 (1.5)		
O(7')–Fe(1)–O(10)	91.8 (1.1)						
O(7')–Fe(1)–O(15')	89.1 (1.1)			Cr(2)–O(4)	1.58 (4)	Cr(2)–O(9)	1.69 (3)
O(7')–Fe(1)–O(16')	86.5 (1.0)			Cr(2)–O(6)	1.57 (3)	Cr(2)–O(10)	1.73 (3)
O(9')–Fe(1)–O(10)	90.1 (1.1)						
O(9')–Fe(1)–O(15')	92.4 (1.1)			O(4)–Cr(2)–O(6)	110.4 (1.5)		
O(9')–Fe(1)–O(16')	168.9 (1.0)			O(4)–Cr(2)–O(9)	106.8 (1.5)		
O(10)–Fe(1)–O(15')	177.4 (1.2)			O(4)–Cr(2)–O(10)	107.9 (1.5)		
O(10)–Fe(1)–O(16')	82.4 (1.0)			O(6)–Cr(2)–O(9)	113.1 (1.5)		
O(15')–Fe(1)–O(16')	95.2 (1.0)			O(6)–Cr(2)–O(10)	111.5 (1.5)		
				O(9)–Cr(2)–O(10)	107.5 (1.5)		
Fe(2)–O(6)	2.06 (3)	Fe(2)–O(12)	1.99 (3)	Cr(3)–O(1')	1.61 (4)	Cr(3)–O(13')	1.64 (2)
Fe(2)–O(8)	1.94 (3)	Fe(2)–O(13)	2.00 (2)	Cr(3)–O(7)	1.67 (3)	Cr(3)–O(14)	1.65 (3)
Fe(2)–O(11)	2.00 (3)	Fe(2)–O(14)	2.01 (3)				
O(6)–Fe(2)–O(8)	173.0 (1.2)			O(1')–Cr(3)–O(7)	102.0 (1.5)		
O(6)–Fe(2)–O(11)	88.8 (1.1)			O(1')–Cr(3)–O(13')	104.7 (1.4)		
O(6)–Fe(2)–O(12)	93.6 (1.1)			O(1')–Cr(3)–O(14)	109.4 (1.5)		
O(6)–Fe(2)–O(13)	86.6 (1.0)			O(7)–Cr(3)–O(13')	111.1 (1.4)		
O(6)–Fe(2)–O(14)	82.9 (1.1)			O(7)–Cr(3)–O(14)	110.0 (1.5)		
O(8)–Fe(2)–O(11)	94.8 (1.1)			O(13')–Cr(3)–O(14)	118.2 (1.4)		
O(8)–Fe(2)–O(12)	92.4 (1.1)						
O(8)–Fe(2)–O(13)	87.5 (1.0)			Cr(4)–O(2)	1.59 (4)	Cr(4)–O(15)	1.66 (3)
O(8)–Fe(2)–O(14)	93.1 (1.1)			Cr(4)–O(8)	1.70 (3)	Cr(4)–O(16)	1.68 (2)
O(11)–Fe(2)–O(12)	88.5 (1.1)						
O(11)–Fe(2)–O(13)	88.7 (1.0)			O(2)–Cr(4)–O(8)	108.6 (1.5)		
O(11)–Fe(2)–O(14)	171.0 (1.1)			O(2)–Cr(4)–O(15)	110.6 (1.5)		
O(12)–Fe(2)–O(13)	177.1 (1.0)			O(2)–Cr(4)–O(16)	115.8 (1.4)		
O(12)–Fe(2)–O(14)	95.6 (1.1)			O(8)–Cr(4)–O(15)	109.4 (1.5)		
O(13)–Fe(2)–O(14)	87.3 (1.0)			O(8)–Cr(4)–O(16)	107.7 (1.4)		
				O(15)–Cr(15)–O(16)	103.6 (1.4)		
NH_4(1)–O(3")	3.25 (6)	NH_4(1)–O(12")	3.34 (6)	NH_4(2)–O(2")	2.81 (6)	NH_4(2)–O(1)	3.37 (6)
NH_4(1)–O(2')	3.48 (6)	NH_4(1)–O(4)	3.07 (6)	NH_4(2)–O(3")	3.19 (6)	NH_4(2)–O(14)	3.05 (6)
NH_4(1)–O(15")	3.22 (6)	NH_4(1)–O(4')	3.46 (6)	NH_4(2)–O(3")	3.53 (6)	NH_4(2)–O(7)	3.08 (6)
NH_4(1)–O(8')	2.98 (6)	NH_4(1)–O(1')	2.79 (6)	NH_4(2)–O(12")	3.17 (6)	NH_4(2)–O(7")	2.98 (6)
NH_4(1)–O(8")	3.25 (6)	NH_4(1)–O(9)	3.15 (6)	NH_4(2)–O(11')	2.98 (6)	NH_4(2)–O(9")	3.23 (6)
NH_4(1)–O(11')	3.48 (6)	NH_4(1)–O(10')	2.89 (6)	NH_4(2)–O(4)	3.29 (6)	NH_4(2)–O(10")	3.35 (6)

TABLE 3.24 cont.

(b) β-$NH_4Fe(CrO_4)_2$

	Fe—O(3)	2.007 Å		NH_4–O′(1)	2.751 Å
	Fe—O(4)	1.991	2	NH_4–O′(6)	3.033
2	Fe—O(5)	1.966		NH_4–O″(2)	3.071
2	Fe—O′(6)	1.955	2	NH_4–O″(4)	3.113
	Cr(1)–O′(2)	1.533	2	NH_4–O(1)	3.184
	Cr(1)–O′(4)	1.738	2	NH_4–O′(5)	3.203
2	Cr(1)–O(5)	1.665		NH_4–O‴(2)	3.638
	Cr(2)–O(1)	1.607		*etc.*	*etc.*
	Cr(2)–O′(3)	1.615			
2	Cr(2)–O′(6)	1.785			
	O(3)–Fe–O(4)	179°40′		O′(2)–Cr(1)–O′(4)	107°36′
	O(3)–Fe–O(5)	90 51		O′(2)–Cr(1)–O(5)	109 00
	O(3)–Fe–O′(6)	95 37		O′(4)–Cr(1)–O(5)	110 55
	O(4)–Fe–O(5)	88 54		O(5)–Cr(1)–O(5)	109 35
	O(4)–Fe–O′(6)	84 37		O(1)–Cr(2)–O′(3)	111 10
	O(5)–Fe–O′(6)	90 27		O(1)–Cr(2)–O′(6)	108 37
	O(5)–Fe–O(5)	89 14		O′(3)–Cr(2)–O′(6)	114 05
	O′(6)–Fe–O′(6)	89 17		O′(6)–Cr(2)–O′(6)	99 47

All iron sites in $KFe_3(CrO_4)_2(OH)_6$ [66] were equivalent as evidenced by the spectrum being resolved into a single quadrupole doublet (Figure 3.34). This is consistent with the results of crystallographic studies[20]. Replacement of water molecules by hydroxyl ions, as in the case of the basic chromates, introduces a greater negative charge on some of the oxygen atoms which comprise the iron octahedra. This replacement by hydroxyl ions also introduces a somewhat greater distortion in the structure, which is reflected in

the larger Eq splittings (Table 3.23) for the basic chromates relative to those for the hydrated iron(III) chromates. Comparison of the Mössbauer spectra of the basic chromates with those of the basic sulfates (Table 3.25) leads to a number of conclusions.

The structures of the basic chromates and sulfates, $FeOHXO_4$, and $MFe_3(XO_4)_2(OH)_6$ are very similar, being composed of $Fe(OH)_2O_4$ octahedra linked by trans hydroxy bridges into chains, which are joined by XO_4 tetrahedra into sheets[9,65]. The quadrupole splittings for the hydroxy sulfates (Table 3.25) are large for high spin iron(III) and in general greater than those for the corresponding chromates. Of the various factors that can contribute to asymmetry of the electric field gradient around the iron, physical distortion of the octahedron does not appear to be a significant factor in this instance. Assuming this to be correct, it can be postulated that the factor determining the magnitude of the Eq spittings is the partial charges on the oxygen atoms. On the basis of simple electronegativity considerations,the oxygen atoms of the sulfate ion may be expected to carry a lower negative partial charge than those of the chromate anion, hence the greater Eq splittings of the sulfates.

The α-form of $Fe_2(CrO_4)_3.3H_2O$, in which there are sheets of FeO_6 octahedra linked by chains of $FeO_3(H_2O)_3$ octahedra[20], has two distinct iron sites. Within the

sheets the octahedra share an edge, the remaining positions being occupied by chromate oxygen atoms. Consistent with this structure, the Mössbauer spectrum of the compound was

TABLE 3.25

Mössbauer parameters of some iron sulfates

Example	Site Type	Mössbauer parameters/mms^{-1} δ	Eq	Γ
$FeOHSO_4$[74]	$Fe(OH)_2O_4$	0.44	1.45	-
$MFe_3(SO_4)_2(OH)_6$[82,83] ($M = NH_4$, K)	$Fe(OH)_2O_4$	0.45	1-1.15	-
$FeOHSO_4(OH_2)_2$[73]	$Fe(OH_2)(OH)_2$	0.42	0.97	-
$Fe_2(SO_4)_3$[41]	FeO_6	0.49	0.30	-
		0.49	0.15	
$KFe(SO_4)_2$*	FeO_6	0.473(1)	0.154(2)	0.254(1)

* this work

resolved into two doublets (Figure 3.29) which have approximately equal areas and isomer shifts (0.39 mms^{-1}). Comparison of the listed Eq splittings, 0.15 and 0.35 mms^{-1}, respectively, with others listed in Table 3.23 suggests that the outer doublet arises from the octahedra containing water and the inner doublet from FeO_6 octahedral sites. The slightly larger quadrupole splittings relative to those for each octahedral site type for the chromates in Table 3.23

may reflect the sharing of a common edge. Pauling[85] has pointed out that edges shared between polyhedra tend to be shorter than unshared ones. The bond angles corresponding to shortened edges are therefore smaller than in an ideal polyhedron. Cardile and Johnston[86] have reported the Mössbauer spectra of Fe^{3+} containing calcium nontronites, in which there are two $FeO_4(OH)_2$ octahedral sites. The spectra of the Nontronites were resolved into two sets of quadrupole doublets of equal isomer shift (0.38 mms^{-1}) and differing Eq splittings 0.25 and 0.66 mms^{-1}, thus supporting the ability of Mössbauer spectroscopy to distinguish iron sites of slightly differing environments.

For structures in which the iron octahedra share corners (e.g. $KFe(CrO_4)_2$)[17] or edges (e.g. $Fe_2(CrO_4)_3.3H_2O$)[20] some spin interaction is expected. Iron (111) compounds relax via spin-spin relaxation. The rate of interaction is strongly concentration dependent and decreases as the distance between neighbouring ions decreases. Fast rates of spin-spin relaxation result in sharp linewidths. Although hydroxyl groups are less effective than oxobridges in facilitating this interaction, Powers et al[24] observed magnetic moments at room temperature for iron of about 3.5 BM for the basic sulfates and chromates and for some compounds of the Jarosite type. The Mössbauer linewidths (Table 3.23) for the chromates containing shared corners or edges of polyhedra were found to be greater than for those in which

direct bridging is absent, but the extent of the broadening was not large.

Sherman[87] has applied the results of self consistent field (SCF) and molecular orbital (MO) calculations to Fe-O and Fe-OH bonding based on data obtained from Mössbauer and magnetic measurements for hydroxyl bearing Fe^{3+} oxides and silicates. Sherman reported that the Fe^{3+}-OH^- bond was more ionic in character than the Fe^{3+}-O^{2-} bond. In the present studies the quadrupole splittings due to $Fe(OH)_2O_4$ octahedra were greater than those for either $Fe(OH_2)_2O_4$ or FeO_6, which is consistent with the conclusion by Sherman for ionicity of Fe^{3+}-OH^- bonds[87].

The greater ionicity of the Fe^{3+}-OH^- bond compared to the Fe^{3+}-O^{2-} bond leads to the conclusion that the Fe^{3+} hyperfine (HHF) field would be expected to be greater for Fe-OH containing compounds, than for compounds in which Fe is bonded to O^{2-} only. Sherman[87] has reviewed the literature on magnetic hyperfine fields (HHF) for Fe^{3+} minerals and observed that in practice the opposite is found i.e. the HHF of Fe-O bonded sites is greater than that of Fe-OH sites. Sherman[87] accounted for the observed paradox in this ordering of HHF's by examining MO calculations for FeO_6^{9-} and $Fe(OH)_2O_4^{7-}$ clusters, and suggesting that the

replacement of O^{2-} ligands by OH^- groups results in an increase in interaction between Fe^{3+} and remaining O^{2-} ligands. This was thought to lead to a decrease in the effective spin of the iron atoms, hence the observed decrease in the magnetic hyperfine field.

The measurement of low temperature Mőssbauer spectra was limited by funding constraints, but chromates containing $Fe(OH_2)_2O_4$, $Fe(OH)_2O_4$ and FeO_6 sites were studied and their magnetic hyperfine fields measured in the solid state Physics Department at ANU by Dr Geoff Whittle (Table 3.26). $NaFe(CrO_4)_2.2H_2O$ was found to be non-magnetic at 4.2 K, and a doublet spectrum resulted. The non-magnetic behaviour may arise from the fast relaxation rates of the occupied spin level, so that the average value of the magnetic field at the iron nucleus during measurement is zero[88]. Spectra of $FeOHCrO_4$ and $KFe(CrO_4)_2$, representing $Fe(OH)_2O_4$ and FeO_6 octahedral sites, respectively, were resolved into six line spectra at 4.2 K, indicating magnetic ordering. The lower HHF for Fe^{3+}-OH^- bonded sites ($FeOHCrO_4$) was consistent with the proposal by Sherman[87] that Fe^{3+}-O^{2-} bonds show greater covalency than the more ionic Fe^{3+}-OH^- bond. Further deductions are difficult to draw owing to lack of experimental data.

TABLE 3.26

Hyperfine Fields for Some Iron (111) Chromates

Compound	Iron site	δ (mms^{-1})	HHF (K Gauss)
$NaFe(CrO_4)_2.2H_2O$	$FeO_4(H_2O)_2$	0.625(13)	-
$KFe(CrO_4)_2$	FeO_6	0.664(30)	426
$FeOHCrO_4$	$FeO_4(OH)_2$	0.525(20)	411

CHAPTER FOUR

MELT-SOLUTE REACTIONS

4.1 INTRODUCTION

It is evident from the literature on iron chromates[9-22], that basic iron chromates are present as minor components when aqueous methods of preparation are employed, under certain reaction conditions. Their occurrence may be a result of hydrolytic equilibria.

For example, Popel and Boldog[22] examined aqueous mixtures of the system $Fe(NO_3)_3$-M_2CrO_4-H_2O, (M = NH_4, Na, K), heated at unspecified temperatures for periods of 3 to 20 days, and reported the isolation and chemical characterisation of a range of double chromates e.g. $NH_4Fe(CrO_4)_2$, and amorphous basic iron chromates (not containing M^+ cation), e.g. $Fe_2(OH)_4CrO_4.3H_2O$. The basic chromates were formed only in dilute solutions, (e.g. concentration of M_2CrO_4 < 0.025M).

The aim of the present investigation, therefore, was to determine whether the dissolution of dichromate ion, $Cr_2O_7^{2-}$, into a melt of an iron salt hydrate, e.g. $Fe(NO_3)_3.9H_2O$ (m.p., 47°C) [88], would result in the formation of a chemically identifiable iron chromate. A concentrated aqueous solution of $Fe(NO_3)_3.9H_2O$ was used as a source of iron, for the preparation of iron chromates in the Fe_2O_3-Cr_2O_3-H_2O system [9].

Chromium sources used for such preparations have typically involved CrO_3 and/or $M_2Cr_2O_7$. To avoid the precipitation of basic chromates as observed by Popel and Boldog[22] when using M_2CrO_4, the chromium source was chosen as $M_2Cr_2O_7$.

An advantage of using an hydrated salt melt is, therefore, the possibility of bringing together the reactants in a concentration range not available through reactions in aqueous media, thereby favouring Fe^{3+}/CrO_4^{2-} bond formation. For example, a solution of 1g of $K_2Cr_2O_7$ in 1g of $Fe(NO_3)_3.9H_2O$ in a melt can be obtained, while the solubility of $K_2Cr_2O_7$ is 0.5g in 1g of aqueous solution at 100°C. From this data it can be deduced that the reactants can be brought together at a higher concentration in the melt. From investigations of hydrated nitrate melts over the temperature range 12-92°C, Gupta et al[89] established that a $Fe(NO_3)_3.9H_2O$ melt is stable when heated at 67°C for up to 6 hours. Studies involving molten salts as both solvent and reactant, in particular nitrates, have been reviewed by Kerridge[89a].

In the present study the reactions of NH_4, Li, Na, K, Rb and Cs dichromates with molten iron(III) nitrate 9-water are reported and discussed.

4.2 RESULTS AND DISCUSSION OF MELT-SOLUTE REACTIONS

4.2.1 AQUEOUS EXTRACTION OF DICHROMATE-MELT MIXTURES

On the addition of $M_2Cr_2O_7$ (M = NH_4, Li, Na, K, Rb, Cs) to a $Fe(NO_3)_3.9H_2O$ melt at 65°C, the colour changed from brown to orange. After completion of the reaction period (1-2 hours) each melt was extracted with distilled water and the insoluble residue (if any) separated by filtration and analysed.

Chemical analyses of the products showed lack of agreement in the iron and chromium contents with those of the respective $MFe(CrO_4)_2.2H_2O$ or $MFe(CrO_4)_2$ for M = NH_4 or K (Table 4.1). For $M_2Cr_2O_7$ (M = Li, Na) reactions, the chemical analyses could be best fitted to new chromates $M_2Fe_3(OH)_5(CrO_4)_3.3H_2O$ (M = Li, Na). XRD powder patterns of the residues were recorded and the patterns indexed, in an attempt to positively identify the phase(s) present (Table 4.2). Comparison of the observed patterns with those calculated by a Rietveld program[34] are shown in Figures 4.1 - 4.4 for M = NH_4, K, Rb, Cs.

TABLE 4.1

Analyses for water insoluble products isolated from the system $M_2Cr_2O_7$-$Fe(NO_3)_3.9H_2O$ (1:1 mole ratio) heated at 65°C for 1 hour.

	Analyses			
$M_2Cr_2O_7$	Fe	Cr	M^+	Yield† (mg)
NH_4	19.37±0.25 (18.26)*	28.01±0.18 (34.00)	3.83±0.10 (3.58)	20
°Li	25.20±0.28 (25.10)	24.40±0.25 (24.40)	2.21±0.10 (2.10)	30
°Na	24.05±0.16 (23.82)	22.75±0.25 (22.30)	6.65±0.10 (6.56)	35
xK	15.76±0.26 (15.39)	21.87±0.15 (28.65)	-	100
Rb	13.95±0.36 (14.96)	26.84±0.15 (27.80)	-	50
Cs	13.66±0.27 (13.27)	25.15±0.28 (24.72)	-	25

analyses are the average of at least two determinations

* parentheses indicate calculated percentages for

$MFe(CrO_4)_2$

X $MFe(CrO_4)_2.2H_2O$

o $M_2Fe_3(OH)_5(CrO_4)_3.3H_2O$

performed by microanalytical unit, A.N.U. Canberra;

†yield based on 1 gram of $Fe(NO_3)_3.9H_2O$

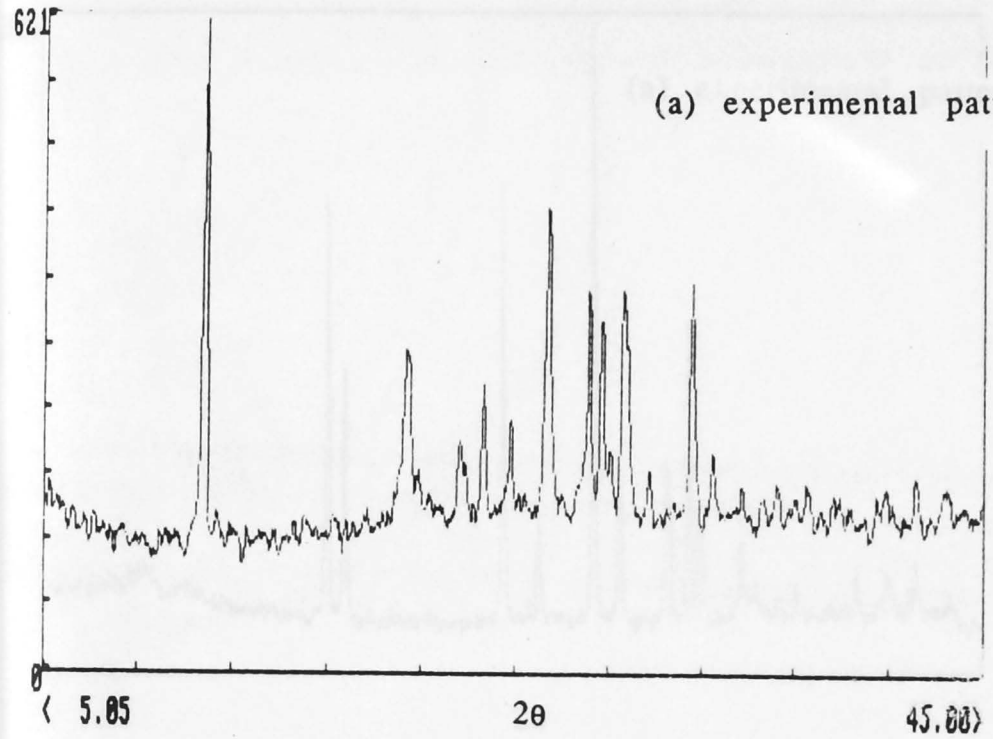

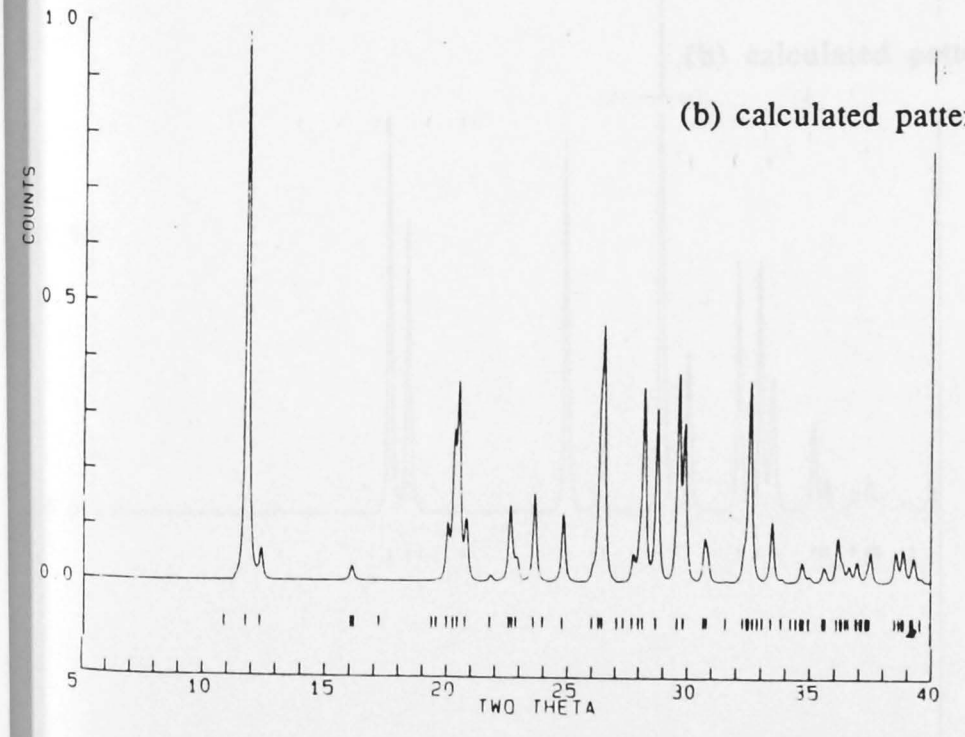

(b) calculated pattern for α- $NH_4Fe(CrO_4)_2$

Fig 4.1 XRD powder pattern of the product isolated from 1:1 mole mixtures of $(NH_4)_2Cr_2O_7$-$Fe(NO_3)_3 9H_2O$ at 65°C

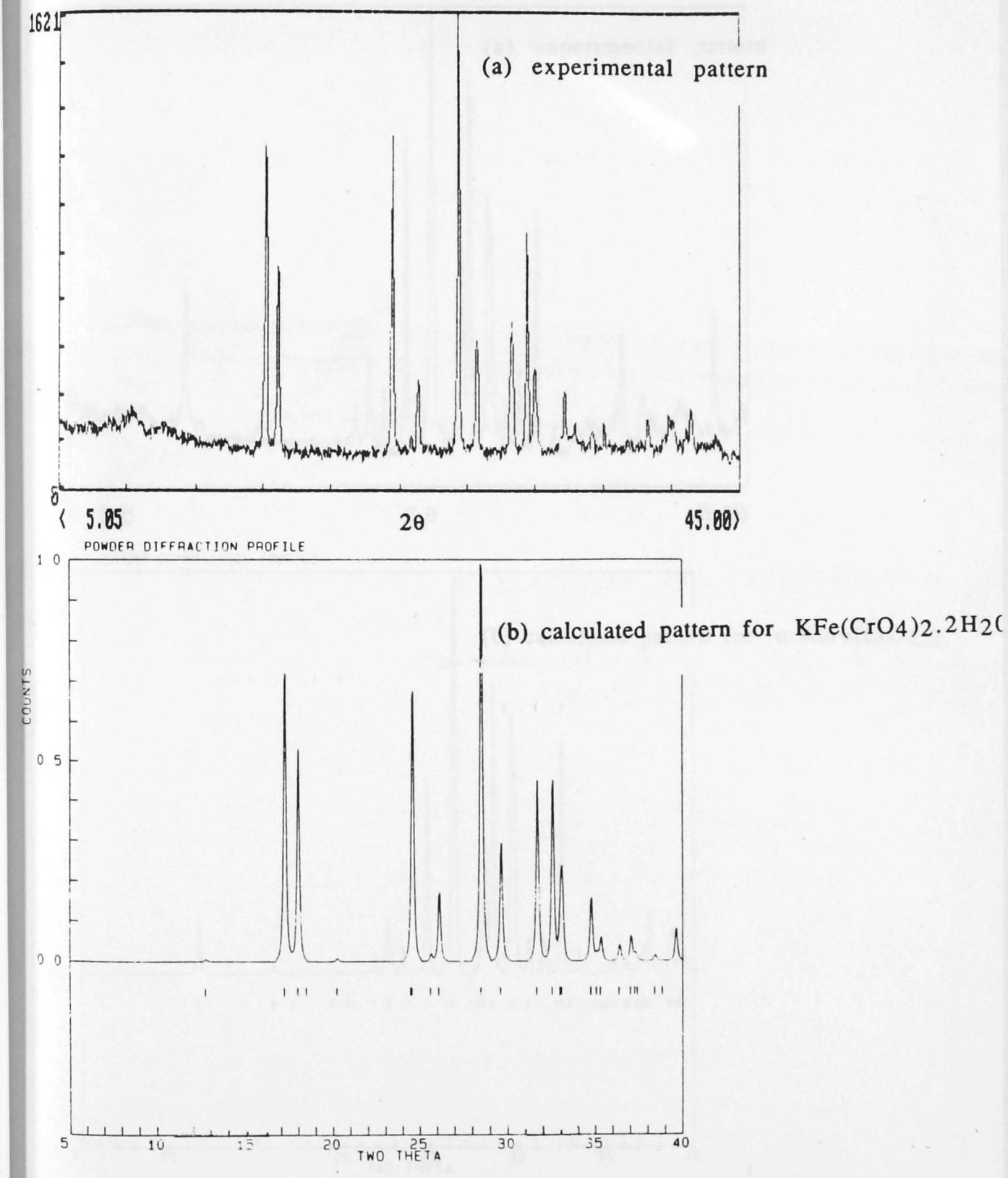

Fig 4.2 XRD powder pattern of the product isolated from 1:1 mole mixtures of $K_2Cr_2O_7$-$Fe(NO_3)_3 9H_2O$ at 65°C

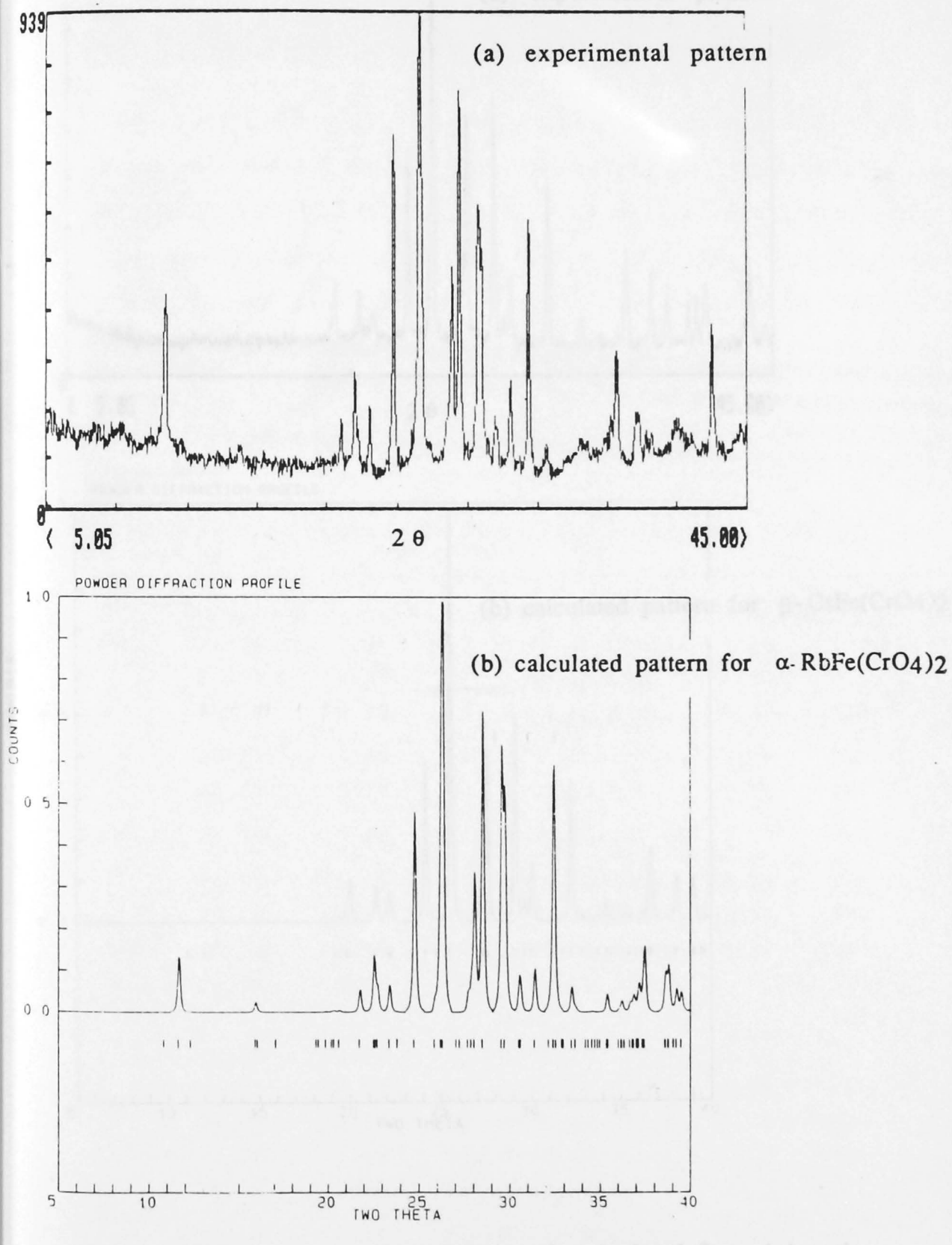

Fig 4.3 XRD powder pattern of the product isolated from 1:1 mole mixtures of $Rb_2Cr_2O_7$-$Fe(NO_3)_3 9H_2O$ at 65°C

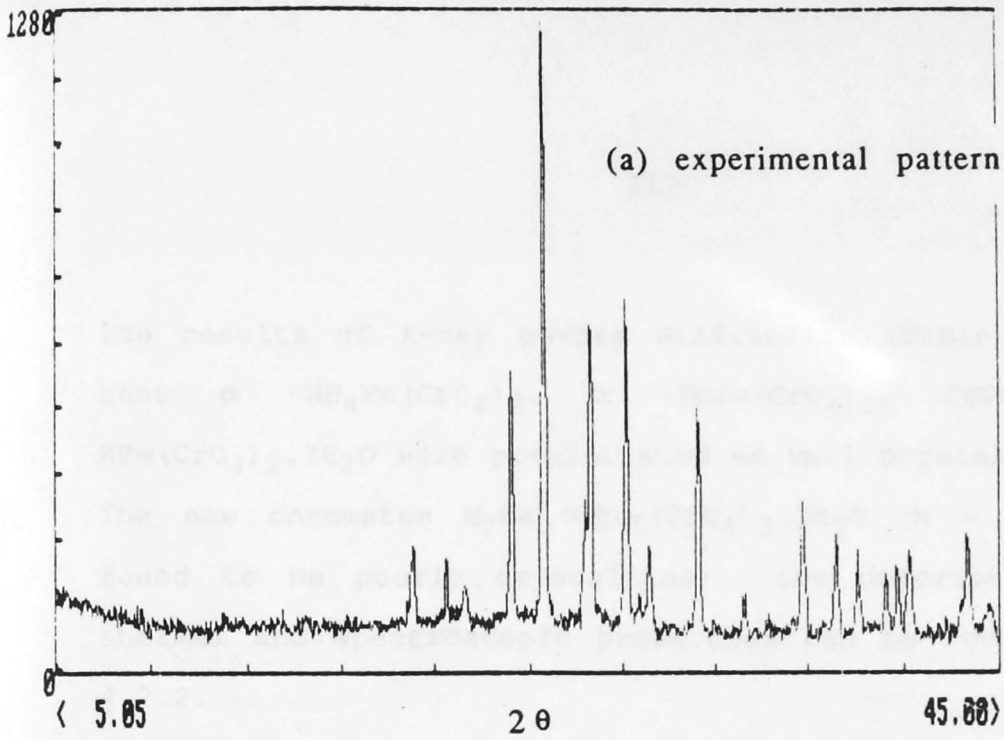

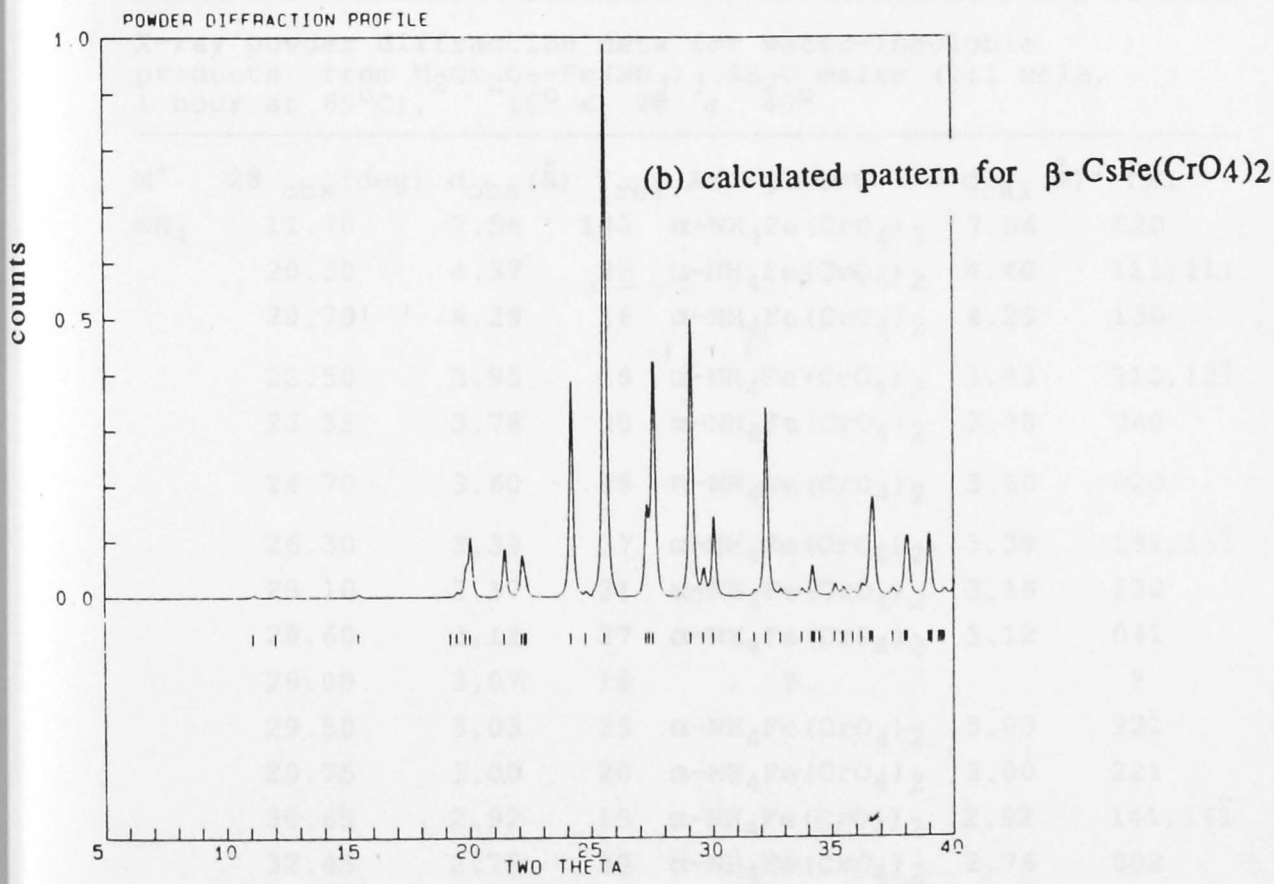

Fig 4.4 XRD powder pattern of the product isolated from 1:1 mole mixtures of $Cs_2Cr_2O_7$-$Fe(NO_3)_3.9H_2O$ at 65°C

The results of X-ray powder diffraction (Table 4.2) showed that α -$NH_4Fe(CrO_4)_2$, α -$RbFe(CrO_4)_2$, $CsFe(CrO_4)_2$ and $KFe(CrO_4)_2.2H_2O$ were precipitated as well crystallised phases. The new chromates $M_2Fe_3(OH)_5(CrO_4)_3.3H_2O$ (M = Li, Na) were found to be poorly crystalline; the description of their thermal and spectroscopic properties can be found in section 4.2.2.

TABLE 4.2

X-ray powder diffraction data for water-insoluble products from $M_2Cr_2O_7$-$Fe(NO_3)_3.9H_2O$ melts (1:1 mole, 1 hour at 65°C), $10^o \leqslant 2\theta \leqslant 40^o$

M^+	$2\theta_{obs}$(deg)	d_{obs}(Å)	I_{rel}	Assignment	d_{cal}(Å)*	hkl
NH_4	11.70	7.56	100	α-$NH_4Fe(CrO_4)_2$	7.56	020
	20.30	4.37	23	α-$NH_4Fe(CrO_4)_2$	4.40	111,111
	20.70	4.29	16	α-$NH_4Fe(CrO_4)_2$	4.29	130
	22.50	3.95	18	α-$NH_4Fe(CrO_4)_2$	3.93	210,12$\bar{1}$
	23.55	3.78	30	α-$NH_4Fe(CrO_4)_2$	3.78	040
	24.70	3.60	18	α-$NH_4Fe(CrO_4)_2$	3.60	020
	26.30	3.39	37	α-$NH_4Fe(CrO_4)_2$	3.38	131,13$\bar{1}$
	28.10	3.17	31	α-$NH_4Fe(CrO_4)_2$	3.18	230
	28.60	3.12	27	α-$NH_4Fe(CrO_4)_2$	3.12	041
	29.00	3.07	16	?		?
	29.50	3.03	25	α-$NH_4Fe(CrO_4)_2$	3.03	22$\bar{1}$
	29.75	3.00	20	α-$NH_4Fe(CrO_4)_2$	3.00	221
	30.65	2.92	13	α-$NH_4Fe(CrO_4)_2$	2.92	141,14$\bar{1}$
	32.45	2.76	30	α-$NH_4Fe(CrO_4)_2$	2.76	002
	33.35	2.68	15	α-$NH_4Fe(CrO_4)_2$	2.68	310
	35.60	2.52	15	α-$NH_4Fe(CrO_4)_2$	2.55	151,15$\bar{1}$
	36.15	2.48	15	α-$NH_4Fe(CrO_4)_2$	2.48	24$\bar{1}$,12$\bar{2}$
	37.25	2.40	15	α-$NH_4Fe(CrO_4)_2$	2.41	330

TABLE 4.2 CONT.

M^+	$2\theta_{obs}$(deg)	d_{obs}(Å)	I_{rel}	Assignment	d_{cal}(Å)	* hkl
K	17.20	5.15	71	$KFe(CrO_4)_2.2H_2O$	5.16	$20\bar{1}$
	17.95	4.94	42	$KFe(CrO_4)_2.2H_2O$	4.95	$20\bar{2}$
	24.55	3.63	72	$KFe(CrO_4)_2.2H_2O$	3.64	110
	26.10	3.41	16	$KFe(CrO_4)_2.2H_2O$	3.41	$20\bar{3}$
	28.50	3.13	100	$KFe(CrO_4)_2.2H_2O$	3.13	111
	29.60	3.02	24	$KFe(CrO_4)_2.2H_2O$	3.01	$31\bar{2}$
	31.65	2.82	29	$KFe(CrO_4)_2.2H_2O$	2.82	$31\bar{3}$
	32.55	2.75	49	$KFe(CrO_4)_2.2H_2O$	2.75	020
	33.00	2.71	18	$KFe(CrO_4)_2.2H_2O$	2.70	$40\bar{3}$
	34.75	2.58	12	$KFe(CrO_4)_2.2H_2O$	2.58	$40\bar{2}$
	35.35	2.54	5	$KFe(CrO_4)_2.2H_2O$	2.57	$11\bar{3}$
	39.60	2.28	6	$KFe(CrO_4)_2.2H_2O$	2.27	112
Na	24.30	3.66	30	?	-	-
	26.27	3.39	100	?	-	-
	26.91	3.31	5	?	-	-
Li	24.44	3.64	5	?	-	-
	26.27	3.39	25	?	-	-
	26.75	3.33	100	?	-	-
Rb	11.70	7.56	25	α-$RbFe(CrO_4)_2$	7.60	020
	21.80	4.08	11	α-$RbFe(CrO_4)_2$	4.08	200
	22.60	3.93	18	α-$RbFe(CrO_4)_2$	3.94	$210, 12\bar{1}$
	23.40	3.80	13	α-$RbFe(CrO_4)_2$	3.80	040
	24.75	3.60	50	α-$RbFe(CrO_4)_2$	3.60	220
	26.25	3.39	100	α-$RbFe(CrO_4)_2$	3.40	$13\bar{1}, 131$
	28.05	3.18	36	α-$RbFe(CrO_4)_2$	3.18	230
	28.50	3.13	68	α-$RbFe(CrO_4)_2$	3.13	041
	29.55	3.02	57	α-$RbFe(CrO_4)_2$	3.02	$22\bar{1}$

TABLE 4.2 CONT.

M^+	$2\theta_{obs}$(deg)	d_{obs}(Å)	Irel	Assignment	d_{cal}(Å)*	hkl
Rb	30.55	2.93	16	α-$RbFe(CrO_4)_2$	2.93	$14\bar{1}$
	31.35	2.85	20	α-$RbFe(CrO_4)_2$	2.85	150
	32.40	2.76	54	α-$RbFe(CrO_4)_2$	2.76	002
	33.45	2.68	12	α-$RbFe(CrO_4)_2$	2.68	310
	35.35	2.54	12	α-$RbFe(CrO_4)_2$	2.54	$15\bar{1}$
	37.45	2.40	25	α-$RbFe(CrO_4)_2$	2.40	330
	38.65	2.33	17	α-$RbFe(CrO_4)_2$	2.33	$32\bar{1}$,$13\bar{2}$
Cs	20.00	4.44	16	$CsFe(CrO_4)_2$	4.43	111
	21.44	4.14	12	$CsFe(CrO_4)_2$	4.14	002
	22.18	4.01	10	$CsFe(CrO_4)_2$	3.99	211,400
	24.20	3.68	42	$CsFe(CrO_4)_2$	3.68	202
	25.60	3.48	100	$CsFe(CrO_4)_2$	3.49	311
	27.60	3.26	20	$CsFe(CrO_4)_2$	3.26	112
	29.10	3.23	46	$CsFe(CrO_4)_2$	3.24	410
	29.10	3.07	48	$CsFe(CrO_4)_2$	3.07	212
	29.66	3.01	8	$CsFe(CrO_4)_2$	3.01	411
	30.12	2.97	12	$CsFe(CrO_4)_2$	2.98	501
	32.18	2.78	34	$CsFe(CrO_4)_2$	2.78	020
	34.16	2.62	6	$CsFe(CrO_4)_2$	2.63	021,203
	36.70	2.45	14	$CsFe(CrO_4)_2$	2.46	320
	38.12	2.36	14	$CsFe(CrO_4)_2$	2.37	213,321
	38.98	2.31	12	$CsFe(CrO_4)_2$	2.31	022

*d_{calc} derived from crystal data[9-21] of the respective chromates.

Precipitation of the α-phases for $NH_4Fe(CrO_4)_2$ and $RbFe(CrO_4)_2$ from $Fe(NO_3)_3.9H_2O$ melt at 65°C (Fig. 4.1 and 4.3) is therefore of interest, as both α - and β - forms for each chromate have been isolated from aqueous reaction media[13,14,19].

The α -$NH_4Fe(CrO_4)_2$ phase is usually prepared[19] at reaction temperatures below 50°C, to avoid precipitation of β -$NH_4Fe(CrO_4)_2$ from the aqueous mixture. The preparative procedure for α-$RbFe(CrO_4)_2$ is unknown, but β-$RbFe(CrO_4)_2$ requires elevated temperatures (140°C) under sealed reaction conditions[14] for its formation. Thus, the use of a low melting salt e.g. $Fe(NO_3)_3.9H_2O$ as solvent, should favour the deposition of the pure crystalline α-form for the anhydrous chromates M = NH_4, Rb, whilst also extending the temperature region from which α -$NH_4Fe(CrO_4)_2$ can be isolated. The use of a melt as solvent therefore provides a convenient means for the preparation of what are difficult materials to prepare. Further to this, this synthetic procedure reduces considerably the reaction period required for the preparation of the chromates - from several days to an hour or less.

The powder pattern for α-$RbFe(CrO_4)_2$ was initially indexed using the unit cell parameters of α-$NH_4Fe(CrO_4)_2$, which were then adjusted to achieve a better fit of experimental

and calculated d-values. The final unit cell parameters used to calculate the diffraction pattern listed in Table 4.2 are: a = 8.18, b = 15.23, c = 5.53Å, β= 90.4°. The atomic coordinates used to calculate the powder pattern shown in Fig 4.3(b) were the same as for α-$NH_4Fe(CrO_4)_2$. The powder patterns for Figures 4.1 - 4.4 were recorded on a Philips PW1050 powder diffractometer fitted with a stepping motor and Sietronics SIE112 automation software.

4.2.2 CHARACTERISATION OF THE NEW CHROMATES $M_2Fe_3(OH)_5(CrO_4)_3.3H_2O$ (M = Li, Na)

(a) Thermal analysis

The thermograms for both $Li_2Fe_3(OH)_5(CrO_4)_3.3H_2O$ (Fig. 4.5) and $Na_2Fe_3(OH)_5(CrO_4)_3.3H_2O$ (Fig. 4.6) showed at least two stages (Table 4.3). X-ray powder diffraction patterns of the residues quenched from 550°C gave d spacings at 3.64 (30), 2.66 (100) and 2.48 (80), consistent with those in the literature for Fe_2O_3 and Cr_2O_3[34]. The results of DTA are tabulated in Table 4.4. Endotherms at 240° and 259°C were attributed to the loss of water, whilst endotherms at about 430°C were proposed to represent the simultaneous dehydration/decomposition processes of reactions 4.2.2 and 4.2.5. The endotherm at about 500°C appears to be a characteristic feature of basic chromate decompositions (Section 3.2.6.2), and is thought to represent the decomposition of an oxochromato phase, e.g. $Fe_2O(CrO_4)_2$, to a mixture of iron(III) and chromium(III) oxides.

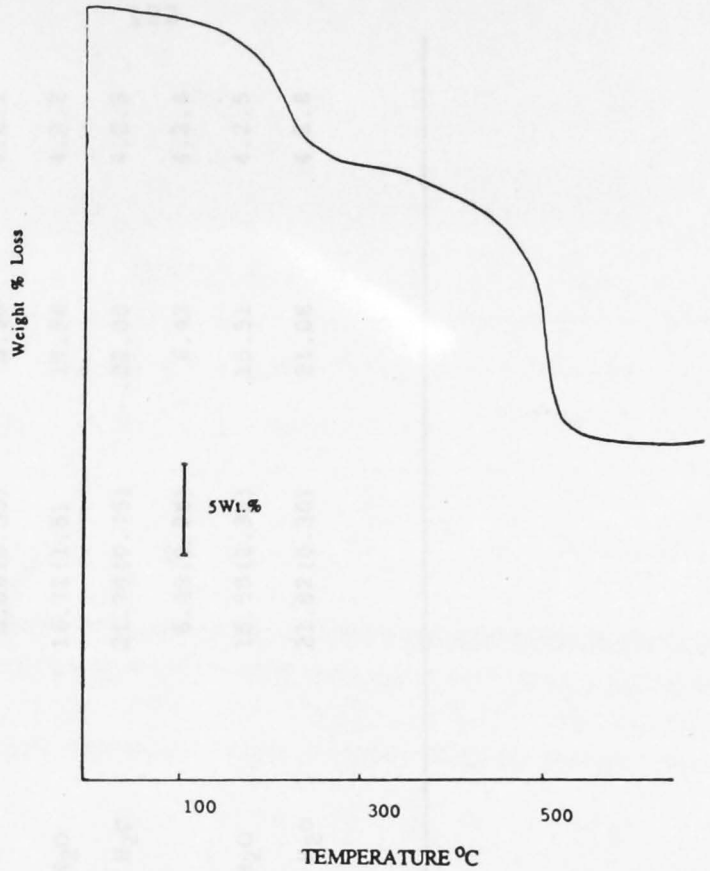

Fig 4.5 Representative thermogram for $Li_2Fe_3(OH)_5(.CrO_4)_3.3H_2O$ heated at 10°C/min

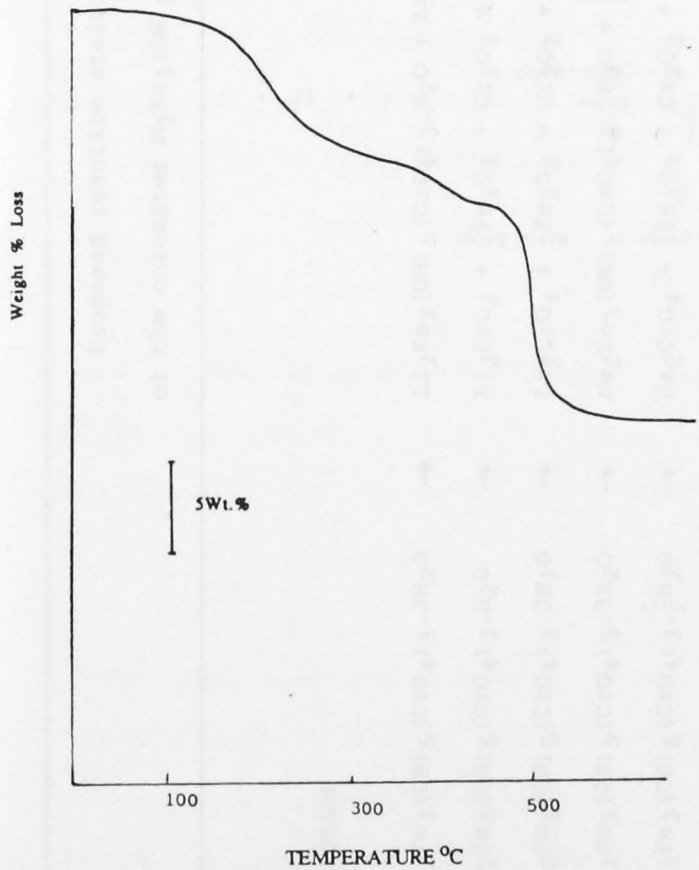

Fig 4.6 Representative thermogram for $Na_2Fe_3(OH)_5(CrO_4)_3.3H_2O$ heated at 10°C/min

TABLE 4.3

Proposed reaction stoichiometries for the thermal decomposition of the chromates $M_2Fe_3(OH)_5(CrO_4)_3.3H_2O$ at a heating rate of 10°C/min

Reaction			% Weight Loss found	% Weight Loss calculated	Equation
$Li_2Fe_3(OH)_5(CrO_4)_3.3H_2O$	→	$Li_2Fe_3(OH)_5(CrO_4)_3.H_2O + 2H_2O$	5.88(0.35)	5.38	4.2.1
$Li_2Fe_3(OH)_5(CrO_4)_3.H_2O$	→	$Li_2CrO_4 + \frac{3}{2}Fe_2O_3 + Cr_2O_3 + \frac{3}{2}O_2 + \frac{7}{2}H_2O$	16.72(1.5)	17.56	4.2.2
$Li_2Fe_3(OH)_5(CrO_4)_3.3H_2O$	→	$Li_2CrO_4 + \frac{3}{2}Fe_2O_3 + Cr_2O_3 + \frac{3}{2}O_2 + \frac{11}{2}H_2O$	21.70(0.75)	22.00	4.2.3
$Na_2Fe_3(OH)_5(CrO_4)_3.3H_2O$	→	$Na_2Fe_3(OH)_5(CrO_4)_3.\frac{1}{2}H_2O + \frac{5}{2}H_2O$	6.42(0.25)	6.42	4.2.4
$Na_2Fe_3(OH)_5(CrO_4)_3.\frac{1}{2}H_2O$	→	$Na_2CrO_4 + \frac{3}{2}Fe_2O_3 + Cr_2O_3 + \frac{3}{2}O_2 + 3H_2O$	15.50(0.30)	15.51	4.2.5
$Na_2Fe_3(OH)_5(CrO_4)_3.3H_2O$	→	$Na_2CrO_4 + \frac{3}{2}Fe_2O_3 + Cr_2O_3 + \frac{3}{2}O_2 + \frac{11}{2}H_2O$	21.82(0.30)	21.06	4.2.6

TABLE 4.4

Differential thermal analysis of the chromates $M_2Fe_3(OH)_5(CrO_4)_3.3H_2O$ at a heating rate of 10°C/min

Compound	*T_i	T_{max}	T_f	ΔH	Reaction
$Li_2Fe_3(OH)_5(CrO_4)_3.3H_2O$	120	240	270	endo	$-H_2O$
	275	420	490	endo	$-H_2O, -O_2$
	490	502	505	endo	$-O_2$
$Na_2Fe_3(OH)_5(CrO_4)_3.3H_2O$	115	259	275	endo	$-H_2O$
	277	439	485	endo	$-H_2O, -O_2$
	492	505	508	endo	$-O_2$

* T_i = initial departure of curve from baseline

T_{max} = maximum departure from baseline

T_f = return to baseline

(b) **Infrared spectroscopy**

Infrared spectra (Fig 4.7) of the Li and Na iron chromates exhibited free OH stretching and M-OH bending vibrations at around 3650 and 1000cm^{-1} (Table 4.5).

The broad absorption maxima (Fig. 4.7) at around 3400cm^{-1} and sharp peaks at about 1600cm^{-1} were assigned to the stretching and bending modes of coordinated water[90]. The position and shape of bands at about 2900cm^{-1} are consistent with those reported[90] for long range OH...O hydrogen bond

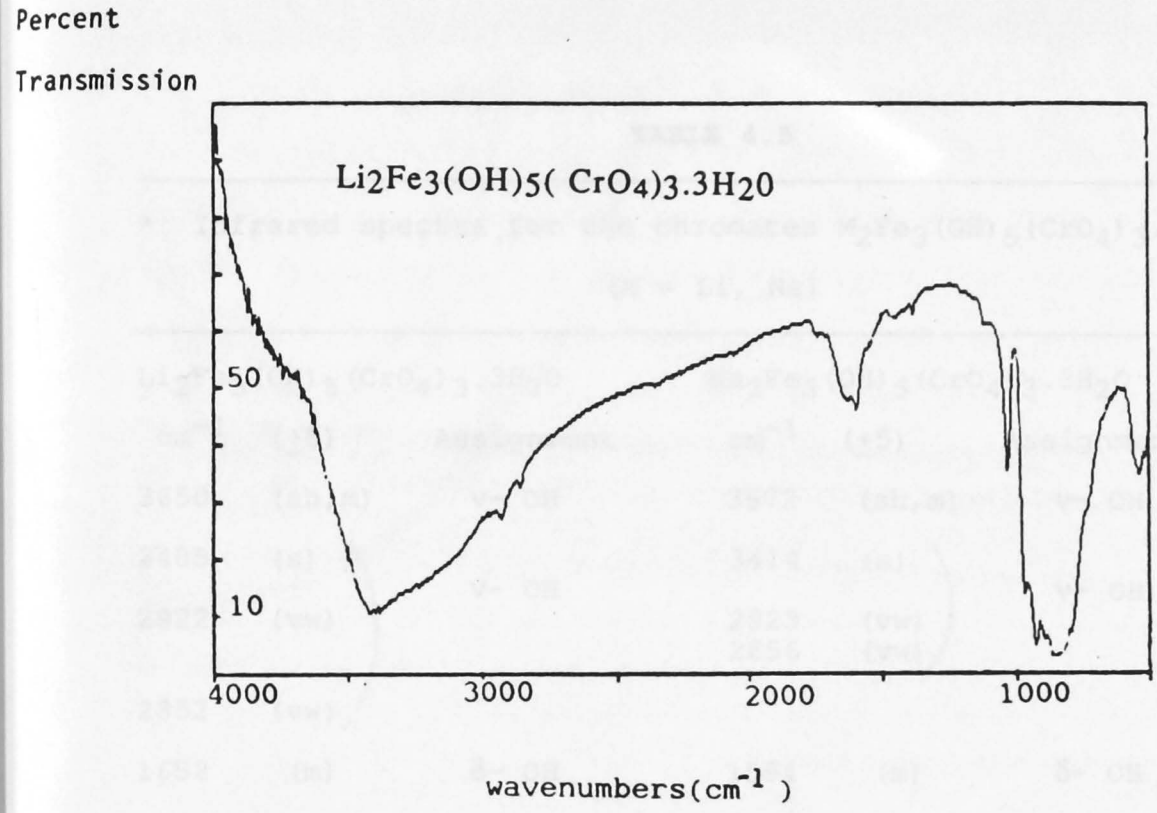

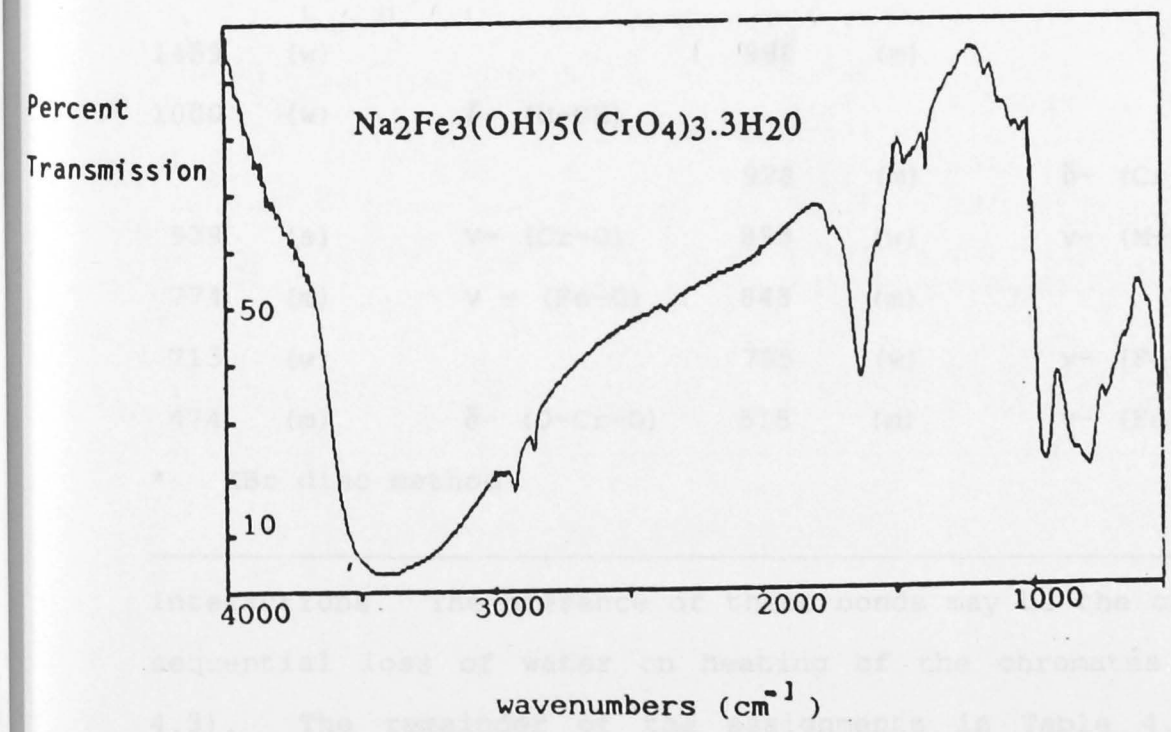

Fig 4.7 Infrared spectra for the chromates $M_2Fe_3(OH)_5(CrO_4)_3.3H_2O$ M=Li,Na

TABLE 4.5

* Infrared spectra for the chromates $M_2Fe_3(OH)_5(CrO_4)_3.3H_2O$ (M = Li, Na)

$Li_2Fe_3(OH)_5(CrO_4)_3.3H_2O$			$Na_2Fe_3(OH)_5(CrO_4)_3.3H_2O$		
cm^{-1}	(±5)	Assignment	cm^{-1}	(±5)	Assignment
3650	(sh,m)	ν- OH	3672	(sh,m)	ν- OH
3405	(s)	ν- OH	3414	(s)	ν- OH
2922	(vw)		2923	(vw)	
2852	(vw)		2856	(vw)	
1652	(m)	δ- OH	1594	(m)	δ- OH
			1030	(s)	δ- (M-OH)
1459	(w)		968	(m)	
1000	(w)	δ- (M-OH)			
			928	(m)	δ- (Cr-O)
939	(s)	ν- (Cr-O)	893	(w)	ν- (M-O)
774	(m)	ν - (Fe-O)	848	(m)	
713	(w)		795	(w)	ν- (Fe-O)
474	(m)	δ- (O-Cr-O)	515	(m)	ν- (Fe-O)

* KBr disc method

interactions. The presence of these bonds may be the cause of sequential loss of water on heating of the chromates (Table 4.3). The remainder of the assignments in Table 4.5, are based on those reported by Cudennec et al[21] for the basic chromate $KFe_3(OH)_6(CrO_4)_2$.

(c) **Room Temperature Mössbauer Spectroscopy**

The correlations, developed in Section 3.4, between the quadrupole splitting value and structure were used as an aid in the characterisation of these poorly crystalline chromates. Table 4.6 lists the room temperature Mössbauer parameters for the fitting of each spectrum to two or three sets of quadrupole split doublets (Fig. 4.8).

TABLE 4.6

Mössbauer parameters for chromates $M_2Fe_3(OH)_5(CrO_4)_3.3H_2O$

			Mössbauer parameters/mms^{-1}		
	$^+$Fit	χ^2	δ	Eq	Γ^*
$Li_2Fe_3(OH)_5(CrO_4)_3.3H_2O$	2T2	2.51	0.392(2)	0.151(2)	0.251(3)
			0.392(2)	0.365(8)	0.371(6)
	2T3	0.92	0.392(2)	0.159(2)	0.291(2)
			0.392(2)	0.331(5)	0.280(4)
			0.392(2)	0.452(5)	0.226(1)
$Na_2Fe_3(OH)_5(CrO_4)_3.3H_2O$	2T2	2.45	0.392(2)	0.161(3)	0.273(2)
			0.392(2)	0.388(9)	0.345(9)
	2T3	0.95	0.391(1)	0.176(2)	0.316(6)
			0.391(1)	0.351(2)	0.278(6)
			0.389(1)	0.462(2)	0.274(4)

* = linewidth at half peak height

$^+$2T2 = fitted to two sets of quadrupole split doublets

2T3 = fitted to three sets of quadrupole split doublets

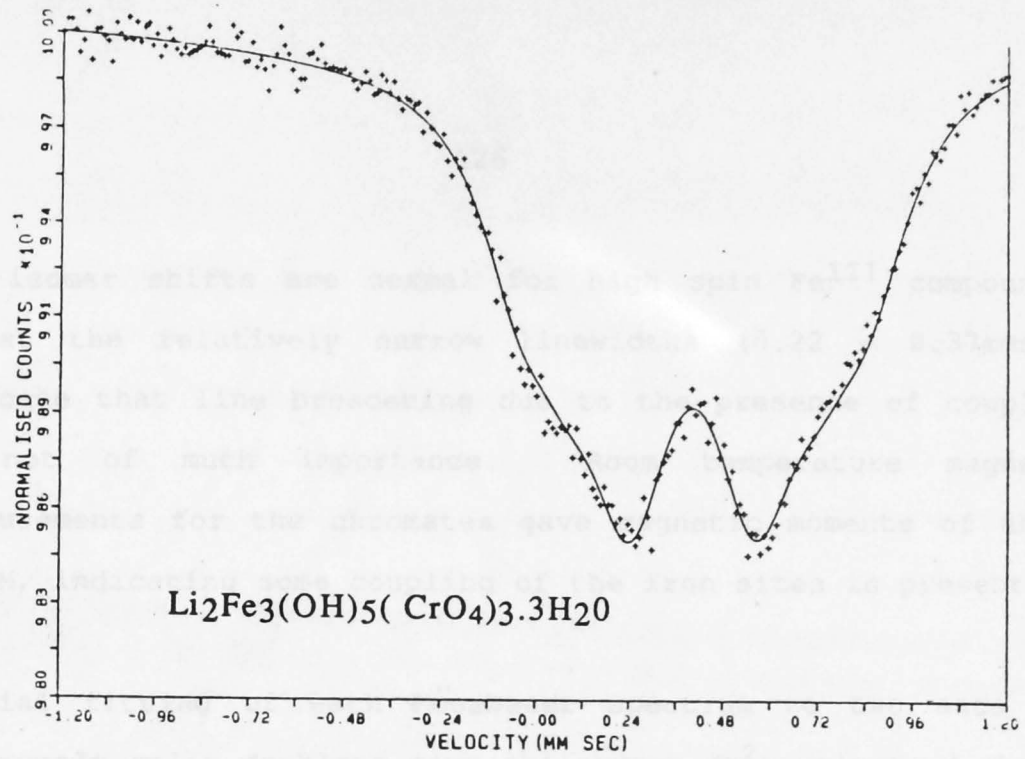

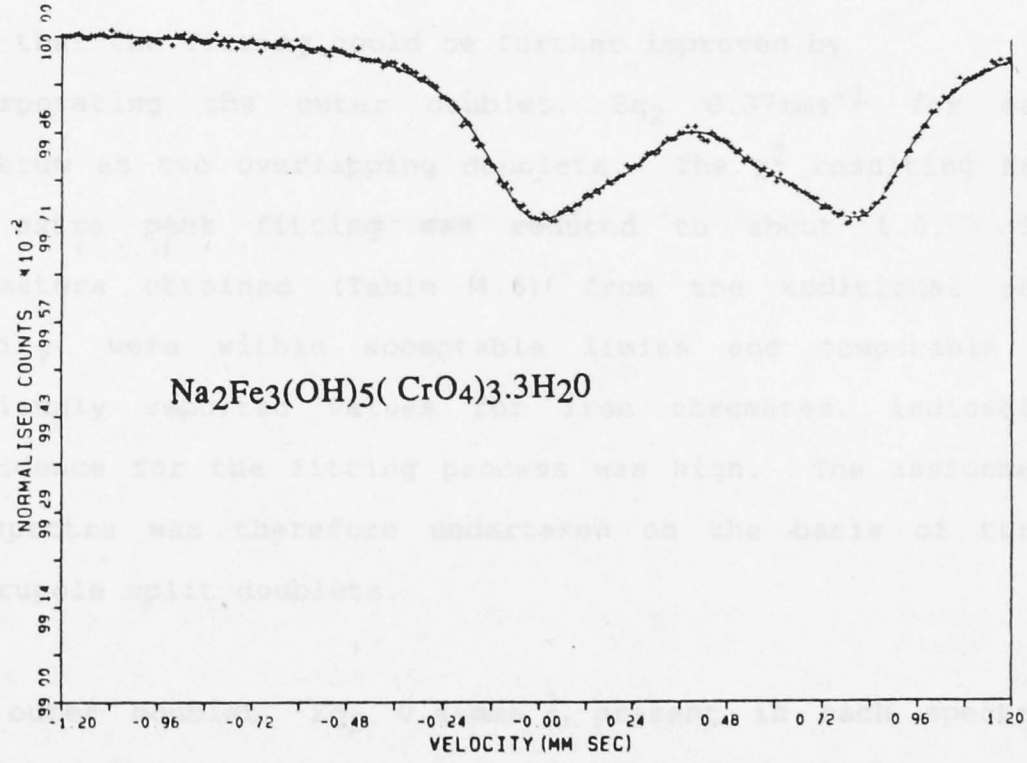

Fig 4.8 Room temperature Mössbauer spectra for the chromates $M_2Fe_3(OH)_5(.CrO_4)_3.3H_2O$ M=Li,Na

The isomer shifts are normal for high spin Fe^{III} compounds, whilst the relatively narrow linewidths (0.22 - 0.37mms^{-1}) indicate that line broadening due to the presence of coupling is not of much importance. Room temperature magnetic measurements for the chromates gave magnetic moments of about 3.4BM, indicating some coupling of the iron sites is present.

Initial fitting of each Mössbauer spectrum to two sets of quadrupole split doublets gave chi-square (χ^2) values of about 2.5, indicating only a fair fit (Table 4.6). It was therefore felt that the fitting could be further improved by incorporating the outer doublet, Eq_2 0.37mms^{-1} for each spectrum as two overlapping doublets. The χ^2 resulting from the extra peak fitting was reduced to about 1.0. The parameters obtained (Table 4.6) from the additional peak fitting were within acceptable limits and comparable to previously reported values for iron chromates, indicating confidence for the fitting process was high. The assignment of spectra was therefore undertaken on the basis of three quadrupole split doublets.

The outer doublet, Eq_2 0.46mms^{-1}, present in each spectrum (Table 4.6) was assigned to the presence of iron-oxygen polyhedra containing hydroxyl ions - $Fe(OH)_xO_{6-x}$. This assignment was based on the previously reported trend, Section 3.4, that the replacement of oxygen atoms by either hydroxyl or water groups leads to an increase in the

magnitude of the quadrupole splitting relative to that due to 'pure' iron-oxygen polyhedra (Eq 0.10mms^{-1}). By analogous argument, the two inner doublets for each chromate, Eq = 0.16 and 0.33mms^{-1}, were assigned to $Fe(OH_2)_x O_{6-x}$ polyhedra. The conclusion that there was more than one environment involving water molecules in the chromates $M_2Fe_3(OH)_5(CrO_4)_3.3H_2O$ (M = Li, Na) agreed with the conclusions from both infrared spectroscopy (Table 4.5) and thermal analysis (Table 4.3).

4.2.3 THERMOGRAVIMETRY OF DICHROMATE-MELT REACTIONS (1:1 MOLE)

4.2.3.1 THE REACTION BETWEEN AMMONIUM DICHROMATE AND IRON(III) NITRATE 9-WATER

The thermogram for the product resulting from a 1:1 mixture of $(NH_4)_2Cr_2O_7$ and $Fe(NO_3)_3.9H_2O$ was comprised of at least two steps between 25 to 500°C (Fig. 4.9). The XRD trace recorded after the first stage (Table 4.7) exhibited peaks due to α-$NH_4Fe(CrO_4)_2$, NH_4NO_3 and a small amount of $(NH_4)_2Cr_2O_7$. No peaks due to iron(III) nitrate were apparent. A plateau was observed in the thermogram from 300 - 320°C, which was followed by a slow weight loss to 500°C. The XRD trace recorded after this stage showed the presence of Fe_2O_3 and Cr_2O_3. The absence of $NH_4Fe(CrO_4)_2$ and NH_4NO_3 can be explained on the basis of two decomposition

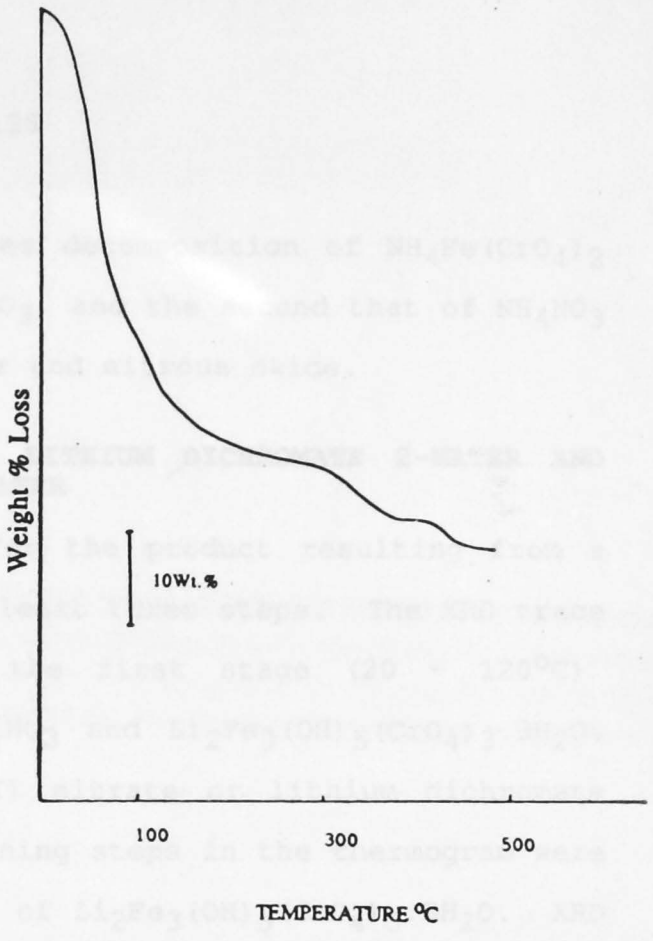

Fig 4.9 Representative thermogram for the system $(NH_4)_2Cr_2O_7$-$Fe(NO_3)_3.9H_2O$
(1:1 mole ratio)

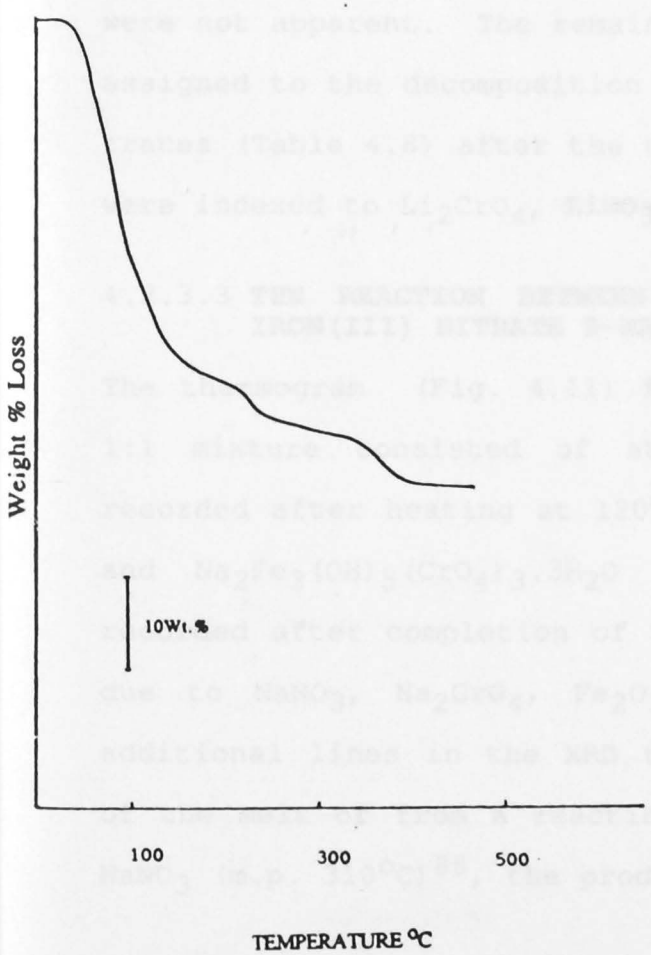

Fig 4.10 Representative thermogram for the system $Li_2Cr_2O_7$-$Fe(NO_3)_3.9H_2O$
(1:1 mole ratio)

reactions. The first involves decomposition of $NH_4Fe(CrO_4)_2$ to a mixture of Fe_2O_3 and Cr_2O_3, and the second that of NH_4NO_3 to a mixture of ammonia, water and nitrous oxide.

4.2.3.2 THE REACTION BETWEEN LITHIUM DICHROMATE 2-WATER AND IRON(III) NITRATE 9-WATER

The thermogram (Fig. 4.10) for the product resulting from a 1:1 mixture consisted of at least three steps. The XRD trace (Table 4.8) recorded after the first stage (20 - 120°C) indicated the presence of $LiNO_3$ and $Li_2Fe_3(OH)_5(CrO_4)_3.3H_2O$. Peaks due to either iron(III) nitrate or lithium dichromate were not apparent. The remaining steps in the thermogram were assigned to the decomposition of $Li_2Fe_3(OH)_5(CrO_4)_3.3H_2O$. XRD traces (Table 4.8) after the completion of the heating process were indexed to Li_2CrO_4, $LiNO_3$, Fe_2O_3 and Cr_2O_3.

4.2.3.3 THE REACTION BETWEEN SODIUM DICHROMATE 2-WATER AND IRON(III) NITRATE 9-WATER

The thermogram (Fig. 4.11) for the product resulting from a 1:1 mixture consisted of at least two steps. XRD traces recorded after heating at 120°C showed the presence of $NaNO_3$ and $Na_2Fe_3(OH)_5(CrO_4)_3.3H_2O$ (Table 4.9). The XRD trace recorded after completion of the heating process showed lines due to $NaNO_3$, Na_2CrO_4, Fe_2O_3 and Cr_2O_3. The presence of additional lines in the XRD traces may arise from hydrolysis of the melt or from a reaction of the reaction products with $NaNO_3$ (m.p. 310°C)[88], the products of which are unknown.

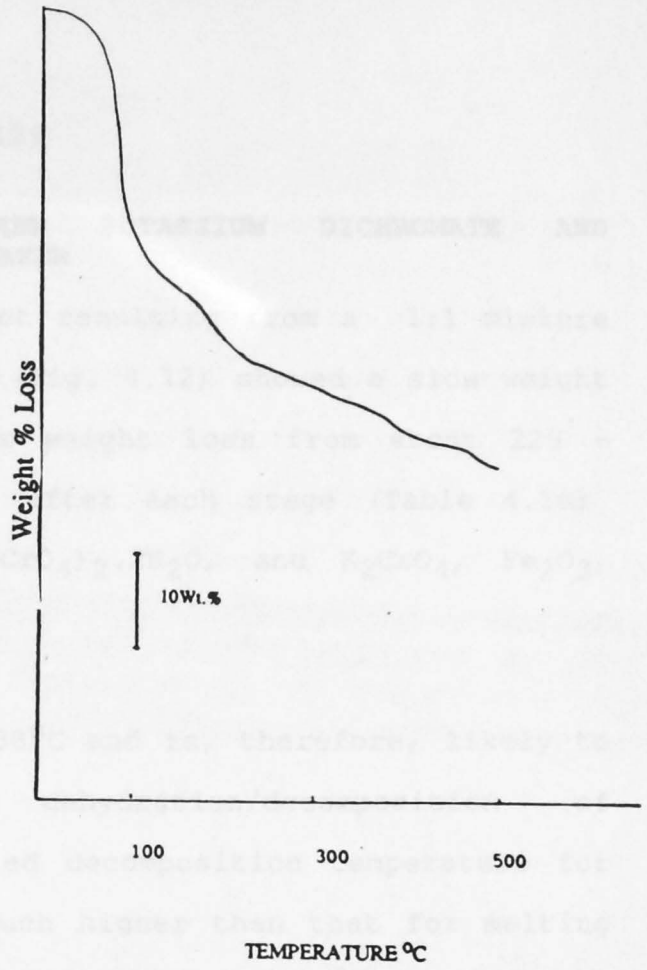

Fig 4.11 Representative thermogram for the system $Na_2Cr_2O_7$-$Fe(NO_3)_3.9H_2O$
(1:1 mole ratio)

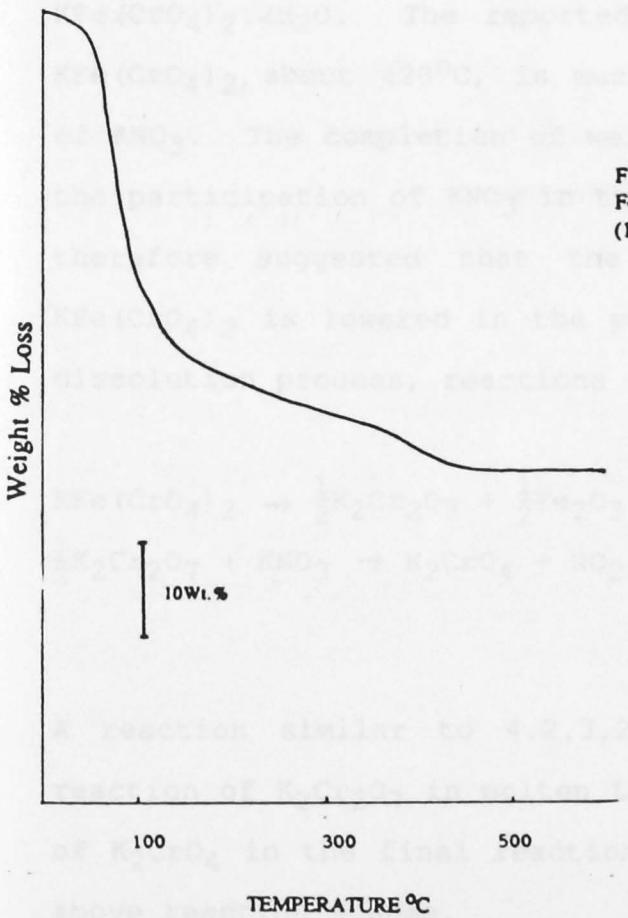

Fig 4.12 Representative thermogram for the system $K_2Cr_2O_7$-$Fe(NO_3)_3.9H_2O$
(1:1 mole ratio)

4.2.3.4 THE REACTION BETWEEN POTASSIUM DICHROMATE AND IRON(III) NITRATE 9-WATER

The thermogram for the product resulting from a 1:1 mixture of $K_2Cr_2O_7$ and $Fe(NO_3)_3.9H_2O$ (Fig. 4.12) showed a slow weight loss to 120°C and a further weight loss from about 220 - 400°C. XRD traces recorded after each stage (Table 4.10) were indexed to KNO_3, $KFe(CrO_4)_2.2H_2O$, and K_2CrO_4, Fe_2O_3, Cr_2O_3, respectively.

Potassium nitrate melts at 338°C and is, therefore, likely to be involved in the dehydration/decomposition of $KFe(CrO_4)_2.2H_2O$. The reported decomposition temperature for $KFe(CrO_4)_2$, about 420°C, is much higher than that for melting of KNO_3. The completion of weight loss by 400°C may support the participation of KNO_3 in the decomposition process. It is therefore suggested that the decomposition temperature of $KFe(CrO_4)_2$ is lowered in the presence of KNO_3, due to a melt dissolution process, reactions 4.2.3.1 and 4.2.3.2.

$$KFe(CrO_4)_2 \rightarrow \tfrac{1}{2}K_2Cr_2O_7 + \tfrac{1}{2}Fe_2O_3 + \tfrac{1}{2}Cr_2O_3 + \tfrac{3}{4}O_2 \qquad (4.2.3.1)$$

$$\tfrac{1}{2}K_2Cr_2O_7 + KNO_3 \rightarrow K_2CrO_4 + NO_2 + \tfrac{1}{4}O_2 \qquad (4.2.3.2)$$

A reaction similar to 4.2.3.2 has been reported[91] for the reaction of $K_2Cr_2O_7$ in molten Li/KNO_3 eutectic . The presence of K_2CrO_4 in the final reaction products further supports the above reaction scheme.

4.2.3.5 THE REACTION BETWEEN RUBIDIUM DICHROMATE AND IRON(III) NITRATE 9-WATER

The thermogram (Fig. 4.13) for the product resulting from a 1:1 mixture of $Rb_2Cr_2O_7$ and $Fe(NO_3)_3.9H_2O$ showed a gradual weight loss to 370°C. XRD traces recorded (Table 4.11) for samples quenched from 120°C showed the presence of $RbNO_3$ and α-$RbFe(CrO_4)_2$. The cessation of the weight loss at about 370°C was significant, as $RbFe(CrO_4)_2$ decomposes (see Section 3.2.4.2), in the temperature region 450 - 530°C, to $Rb_2Cr_2O_7$, Fe_2O_3 and Cr_2O_3. Rubidium nitrate melts at 305°C[88] and a reaction process similar to that postulated in section 4.2.3.4 is proposed.

$$RbFe(CrO_4)_2 \rightarrow \tfrac{1}{2}Rb_2Cr_2O_7 + \tfrac{1}{2}Fe_2O_3 + \tfrac{1}{2}Cr_2O_3 + \tfrac{3}{4}O_2 \qquad (4.2.3.3)$$

$$\tfrac{1}{2}Rb_2Cr_2O_7 + RbNO_3 \rightarrow Rb_2CrO_4 + NO_2 + \tfrac{1}{4}O_2 \qquad (4.2.3.4)$$

Rubidium chromate, and iron(III) and chromium(III) oxides were identified from the XRD traces (Table 4.11) of residues recorded after the cessation of the weight loss. The presence of a small amount of unassigned material from the XRD trace of the residues may indicate that additional melt processes with $RbNO_3$ are occurring, the reaction mechanisms of which are unknown.

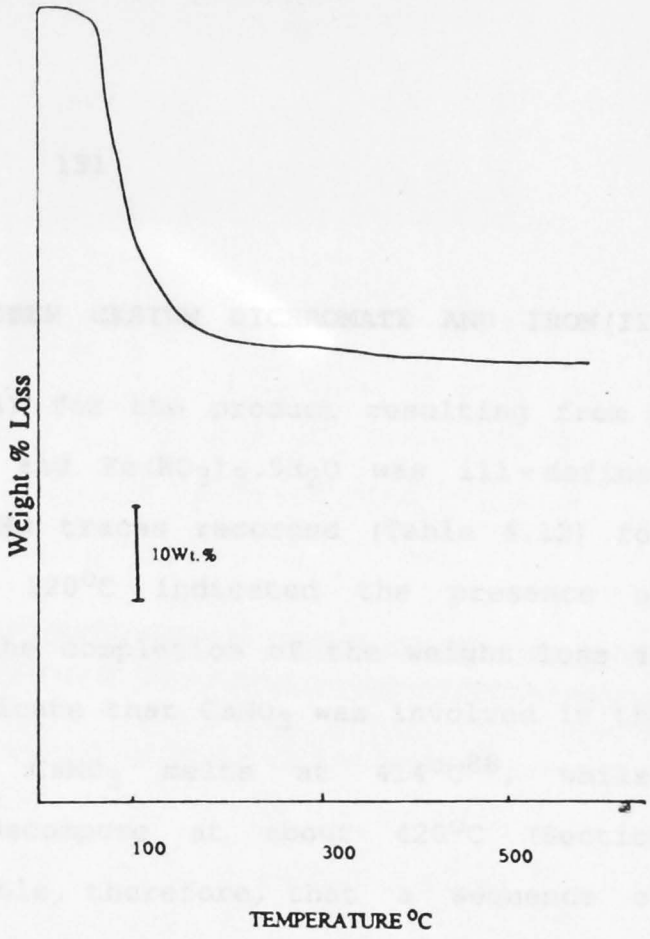

Fig 4.13 Representative thermogram for the system $Rb_2Cr_2O_7$-$Fe(NO_3)_3.9H_2O$
(1:1 mole ratio)

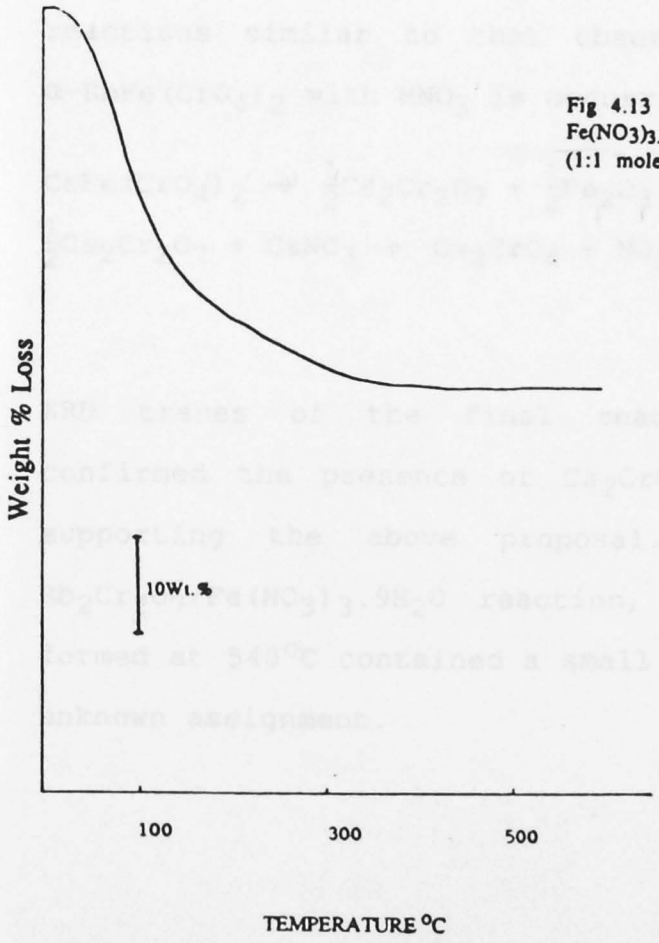

Fig 4.14 Representative thermogram for the system $Cs_2Cr_2O_7$-$Fe(NO_3)_3.9H_2O$
(1:1 ratio)

4.2.3.6 THE REACTION BETWEEN CESIUM DICHROMATE AND IRON(III) NITRATE 9-WATER

The thermogram (Fig. 4.14) for the product resulting from a 1:1 mixture of $Cs_2Cr_2O_7$ and $Fe(NO_3)_3.9H_2O$ was ill-defined between 20 and 340°C. XRD traces recorded (Table 4.12) for samples quenched from 120°C indicated the presence of $CsFe(CrO_4)_2$ and $CsNO_3$. The completion of the weight loss at 340°C was thought to indicate that $CsNO_3$ was involved in the decomposition process. $CsNO_3$ melts at 414°C[88], whilst $CsFe(CrO_4)_2$ begins to decompose at about 420°C (Section 3.2.4.2). It is probable, therefore, that a sequence of reactions similar to that observed for $KFe(CrO_4)_2.2H_2O$ and α-$RbFe(CrO_4)_2$ with MNO_3 is occurring.

$$CsFe(CrO_4)_2 \rightarrow \tfrac{1}{2}Cs_2Cr_2O_7 + \tfrac{1}{2}Fe_2O_3 + \tfrac{1}{2}Cr_2O_3 + \tfrac{3}{4}O_2 \qquad (4.2.3.5)$$

$$\tfrac{1}{2}Cs_2Cr_2O_7 + CsNO_3 \rightarrow Cs_2CrO_4 + NO_2 + \tfrac{1}{4}O_2 \qquad (4.2.3.6)$$

XRD traces of the final reaction products (Table 4.12) confirmed the presence of Cs_2CrO_4, Fe_2O_3 and Cr_2O_3, thereby supporting the above proposal. As was found for the $Rb_2Cr_2O_7/Fe(NO_3)_3.9H_2O$ reaction, the XRD traces of products formed at 540°C contained a small number of additional lines of unknown assignment.

TABLE 4.7

X-ray powder diffraction data for $(NH_4)_2Cr_2O_7$-$Fe(NO_3)_3.9H_2O$ (1:1 mole) melt products (unwashed) quenched from 120°C and 540°C, in the range $10^o \leq 2\theta \leq 40^o$.

Temperature	$2\theta_{obs}$ (deg)	d_{obs} (Å)	Irel	Assignment	d_{calc}
120°C	11.70	7.56	100	α-$NH_4Fe(CrO_4)_2$	7.57
	12.20	7.25	35	?	
	23.26	3.82	10	α-$NH_4Fe(CrO_4)_2$	3.78
	23.70	3.75	25		
	24.36	3.65	5	α-$NH_4Fe(CrO_4)_2$	3.60
	26.03	3.42	20	NH_4NO_3	3.40
				α-$NH_4Fe(CrO_4)_2$	3.43
	27.42	3.25	20	NH_4NO_3	3.25
	27.86	3.20	20	NH_4NO_3	3.22
	29.26	3.05	20	?	3.03
	31.94	2.80	5	α-$NH_4Fe(CrO_4)_2$	2.76
	36.64	2.45	5	NH_4NO_3	2.47
	37.44	2.40	35	α-$NH_4Fe(CrO_4)_2$	2.40
	40.04	2.25	10	NH_4NO_3	2.29
				α-$NH_4Fe(CrO_4)_2$	2.21
540°C	23.71	3.75	100	Fe_2O_3/Cr_2O_3	3.63
	32.53	2.75	30	Fe_2O_3/Cr_2O_3	2.66
	35.90	2.50	65	Fe_2O_3/Cr_2O_3	2.48

TABLE 4.8

X-ray powder diffraction data for $Li_2Cr_2O_7.2H_2O$-$Fe(NO_3)_3.9H_2O$ (1:1 mole) melt products (unwashed) quenched from 120°C and 540°C, in the range $10° \leq 2\theta \leq 40°$

Temperature	$2\theta_{obs}$ (deg)	d_{obs} (Å)	I_{rel}	Assignment	d_{calc}
120°C	23.39	3.60	30	$Li_2Fe_3(OH)_5(CrO_4)_3.3H_2O$	3.64
	25.80	3.45	100	$Li_2Fe_3(OH)_5(CrO_4)_3.3H_2O$	3.39
	27.00	3.30	80	$Li_2Fe_3(OH)_5(CrO_4)_3.3H_2O$	3.33
	30.58	2.82	20	$LiNO_3$	2.79
	33.80	2.65	10	$LiNO_3$	2.54
540°C	20.08	4.42	15	Li_2CrO_4	4.39
	21.65	4.10	40	Li_2CrO_4	4.10
	25.06	3.55	20	Li_2CrO_4	3.50
	25.80	3.45	5	?	
	27.86	3.20	35	Li_2CrO_4	3.22
	29.06	3.07	10	?	
	30.07	2.97	100	?	
	30.80	2.90	65	Li_2CrO_4	2.85
	31.36	2.85	45	$LiNO_3$	2.82
	32.53	2.65	30	Fe_2O_3/Cr_2O_3	2.66
	34.19	2.62	10	Li_2CrO_4	2.64
	35.16	2.55	100	Fe_2O_3/Cr_2O_3	2.51

TABLE 4.9

X-ray powder diffraction data for $Na_2Cr_2O_7.2H_2O$ - $Fe(NO_3)_3.9H_2O$ (1:1 mole) melt products (unwashed) quenched from 120° and 540°C, in the range $10° \leq 2\theta \leq 40°$

Temperature	$2\theta_{obs}$ (deg)	d_{obs} (Å)	I_{rel}	Assignment	d_{calc}
120°C	22.50	3.95	45	$NaNO_3$	3.89
	23.26	3.82	35	?	
	24.36	3.65	10	$Na_2Fe_3(OH)_5(CrO_4)_3.3H_2O$	3.66
	24.42	3.50	70	?	
	26.18	3.40	30	$Na_2Fe_3(OH)_5(CrO_4)_3.3H_2O$	3.39
	27.00	3.30	75	$Na_2Fe_3(OH)_5(CrO_4)_3.3H_2O$	3.31
	29.36	3.05	100	$NaNO_3$	3.03
	31.70	2.82	50	$NaNO_3$	2.81
	33.80	2.65	45	$NaNO_3$	2.53
	37.12	2.42	45	$NaNO_3$	2.31
540°C	20.02	4.32	20	?	
	21.66	4.10	20	Na_2CrO_4	
	22.66	3.92	15	Na_2CrO_4	3.89
	22.78	3.90	20	$NaNO_3$(?)	
	23.71	3.75	20	Fe_2O_3/Cr_2O_3	3.63
	24.57	3.62	20	Na_2CrO_4	3.57
	25.80	3.45	15	?	
	27.00	3.30	20	?	
	28.78	3.10	60	$NaNO_3$	3.03
	30.59	2.92	20	Na_2CrO_4	2.90
	31.94	2.80	30	$NaNO_3$	2.81
	33.40	2.68	100	Fe_2O_3/Cr_2O_3	2.66
	36.64	2.45	35	Fe_2O_3/Cr_2O_3	2.48

TABLE 4.10

X-ray powder diffraction data for $K_2Cr_2O_7$-$Fe(NO_3)_3.9H_2O$ (1:1 mole) melt products (unwashed), quenched from 120°C and 540°C, in the range $10^o \leq 2\theta \leq 40^o$

Temperature	$2\theta_{obs}$ (deg)	d_{obs} (Å)	I_{rel}	Assignment	d_{calc}
120°C	17.31	5.12	65	$KFe(CrO_4)_2.2H_2O$	5.16
	17.90	4.95	30	$KFe(CrO_4)_2.2H_2O$	4.95
	21.87	4.06	20	?	
	23.39	3.80	15	KNO_3	3.78
	26.34	3.38	35	$KFe(CrO_4)_2.2H_2O$	3.41
	28.76	3.10	100	$KNO_3/KFe(CrO_4)_2.2H_2O$	3.10,3.07
	29.74	3.00	25	$KNO_3/KFe(CrO_4)_2.2H_2O$	3.03,3.01
	31.71	2.83	30	$KNO_3/KFe(CrO_4)_2.2H_2O$	2.82,2.77
	33.18	2.70	35	$KNO_3/KFe(CrO_4)_2.2H_2O$	2.70,2.66
	34.46	2.60	20	$KNO_3/KFe(CrO_4)_2.2H_2O$	2.64
	35.60	2.52	20	$KFe(CrO_4)_2.2H_2O$	2.58
540°C	21.13	4.20	25	K_2CrO_4	4.29
	23.08	3.85	30	K_2CrO_4	3.83
	24.36	3.65	10	Fe_2O_3/Cr_2O_3	3.63
	24.72	3.60	30	K_2CrO_4	3.59
	27.42	3.25	100	K_2CrO_4	3.21
	29.26	3.05	30	K_2CrO_4	3.08
	33.52	2.67	45	Fe_2O_3/Cr_2O_3	2.66
	35.16	2.55	25	Fe_2O_3/CrO_2O_3	2.55

TABLE 4.11

X-ray powder diffraction data for $Rb_2Cr_2O_7$-$Fe(NO_3)_2.9H_2O$ (1:1) mole) melt products (unwashed) quenched from 120° and 540°C, in the range $10° \leqslant 2\theta \leqslant 40°$

Temperature	$2\theta_{obs}$ (deg)	d_{obs} (Å)	I_{rel}	Assignment	d_{calc}
120°C	24.30	3.66	100	$RbNO_3$	3.67
	24.99	3.56	10	α-$RbFe(CrO_4)_2$	3.60
	26.03	3.42	15	α-$RbFe(CrO_4)_2$	3.40
	26.83	3.32	65	?	
	28.22	3.16	75	α-$RbFe(CrO_4)_2$	3.18
	29.26	3.05	60	$RbNO_3$	3.03
	29.86	2.99	65	α-$RbFe(CrO_4)_2$	3.02
	30.26	2.95	15	?	
	32.78	2.73	10	α-$RbFe(CrO_4)_2$	2.76
	33.52	2.66	55	α-$RbFe(CrO_4)_2$	2.68
	36.04	2.49	45	α-$RbFe(CrO_4)_2$	2.53
	37.44	2.40	30	α-$RbFe(CrO_4)_2$	2.42
540°C	20.64	4.30		$RbNO_3$	4.28
	23.89	3.80		?	
	23.70	3.75		Rb_2CrO_4	3.74
	24.92	3.57		Fe_2O_3/Cr_2O_3	3.66
	26.59	3.35		Rb_2CrO_4	3.34
	27.86	3.20		Rb_2CrO_4	3.26
	28.59	3.12		Rb_2CrO_4	3.08
	29.74	3.00		Rb_2CrO_4	3.03
	34.46	2.60		Fe_2O_3/Cr_2O_3	2.66
	38.26	2.35		Rb_2CrO_4	2.36

TABLE 4.12

X-ray powder diffraction data for $Cs_2Cr_2O_7$-$Fe(NO_3)_3.9H_2O$ (1:1 mole) melt products (unwashed) quenched from 120° and 540°C, in the range $10° \leq 2\theta \leq 40°$

Temperature	$2\theta_{obs}$ (deg)	d_{obs} (Å)	I_{rel}	Assignment	d_{calc}
120°C	21.92	4.05	40	$CsFe(CrO_4)_2$	4.14
	23.70	3.75	55	$CsFe(CrO_4)_2$	3.68
	25.42	3.50	100	$CsFe(CrO_4)_2$	3.49
	27.68	3.22	45	$CsFe(CrO_4)_2/CsNO_3$	3.24,3.18
	28.78	3.10	80	$CsFe(CrO_4)_2$	3.07
	29.26	3.05	75	$CsFe(CrO_4)_2$	3.01
	32.52	2.75	80	$CsFe(CrO_4)_2$	2.78
	37.12	2.42	30	$CsFe(CrO_4)_2$	2.46
540°C	20.89	4.25	20	Cs_2CrO_4	4.21
	22.78	3.90	100	Cs_2CrO_4	3.94
	24.37	3.65	15	Fe_2O_3/Cr_2O_3	3.63
	25.06	3.55	30	Cs_2CrO_4	3.50
	27.86	3.20	50	Cs_2CrO_4	3.21
	28.58	3.12	25	Cs_2CrO_4	3.15
	29.26	3.05	15	?	
	30.80	2.90	15	?	
	34.46	2.60	15	Fe_2O_3/Cr_2O_3	2.66
	35.60	2.52	15	Fe_2O_3/Cr_2O_3	2.51
	37.44	2.40	35	Cs_2CrO_4	2.44
	38.78	2.32	40	Cs_2CrO_4	2.33

4.3 CONCLUSIONS FROM MELT-SOLUTE REACTIONS

The reactions of metal dichromates (M = NH_4, Li, Na, K, Rb, Cs) with iron(III) nitrate 9-water at 65°C, resulted in the formation of a range of iron(III) chromates. The chromates identified in the reaction products were α-$NH_4Fe(CrO_4)_2$, α-$RbFe(CrO_4)_2$, $CsFe(CrO_4)_2$, $KFe(CrO_4)_2.2H_2O$ and $M_2Fe_3(OH)_5(CrO_4)_3.3H_2O$ (M = Li, Na). Chemical analysis of the NH_4^+ and K^+ salts indicated the co-precipitation of some contaminants, however, the XRD traces of all chromates were `clean'. The results of the work confirmed that non-aqueous methods, e.g. $Fe(NO_3)_3.9H_2O$ melt, can provide a synthetic route to the preparation of well crystallised iron(III) chromates. In those reactions where small amounts of impurities were found, it is thought that these may arise from the hydrolysis of the melt.

Table 4.13 schematically describes the reaction pathway and products for each metal dichromate reaction with molten $Fe(NO_3)_3.9H_2O$ over the temperature range 65 - 500°C. In all reactions, with the exception of that involving $(NH_4)_2Cr_2O_7$, the final reaction products were the respective alkali chromate, and iron(III) and chromium(III) oxides.

Acid-base reactions[91] between $Cr_2O_7^{2-}$ and NO_3^-, such as

$$Cr_2O_7^{2-} + NO_3^- \longrightarrow 2CrO_4^{2-} + NO_2^+$$

are postulated to explain the absence of both MNO_3 and $M_2Cr_2O_7$, and the presence of M_2CrO_4 for those reactions (M = K, Rb, Cs) where the iron chromate formed in the initial stages of the reaction is known to undergo a decomposition step to dichromate, e.g. $KFe(CrO_4)_2.2H_2O$.

The use of low melting salt hydrates, e.g. $Fe(NO_3)_3.9H_2O$, therefore offers an attractive synthetic route to the preparation of iron chromates. This greatly simplifies the preparative procedures with a reduction in preparation time, whilst also showing some selective synthesis, i.e. formation of α-phases for M = NH_4, Rb.

TABLE 4.13

Summary of Proposed Reaction Steps during the Heating of 1:1 Mixtures of Alkali Metal Dichromates and Iron(III) Nitrate 9-water to 540°†

$K_2Cr_2O_7 + Fe(NO_3)_3\ 9H_20$	$\rightarrow KFe(CrO_4)_2\ 2H_20 + KNO_3$	$\rightarrow K_2Cr_2O_7 + KNO_3 + Fe_2O_3 + Cr_2O_3 + O_2$	$\rightarrow K_2CrO_4 + NO_2 + O_2$
$(NH_4)_2Cr_2O_7 + Fe(NO_3)_3\ 9H_2O$	$\rightarrow \alpha\text{-}NH_4Fe(CrO_4)_2 + NH_4NO_3$	$\rightarrow Fe_2O_3 + Cr_2O_3 + NH_3 + H_2O + N_2O$	
$M_2Cr_2O_7 + Fe(NO_3)_3\ 9H2O$ where M=Li, Na	$\rightarrow M_2Fe_3(OH)_5(CrO_4)_3\ 3H_2O + MNO_3$	$\rightarrow M_2Fe_3(OH)_5(CrO_4)_3\ nH_2O$[a]	$\rightarrow M_2CrO_4 + Fe_2O_3 + Cr_2O_3 + O_2$ (↘ / ↗ $Fe_2O(CrO_4)_2$?)
$M_2Cr_2O_7 + Fe(NO_3)_3\ 9H2O$ where M=Rb,Cs	$\rightarrow MFe(CrO_4)_2$[b] $+ MNO_3$	$\rightarrow M_2Cr_2O_7 + MNO_3 + Fe_2O_3 + Cr_2O_3 + O_2$	$\rightarrow M_2CrO_4 + NO_2 + O_2$

† Details of individual reactions given in section 4.2

[a] For M=Li, n=1; M=Na, n=½

[b] α-form of $RbFe(CrO_4)_2$

CHAPTER FIVE

SUMMARY

5.1 SUMMARY

A series of iron(III) chromates were studied using thermal analysis methods in conjunction with Mössbauer spectroscopy. The results provide structural information on the chromates which complement the results of existing crystallographic studies. The use of other techniques together with thermogravimetry, eg. Mössbauer spectroscopy, for the study of a decomposition pathway confirmed in some cases the presence of an intermediate phase(s) and, sometimes, provided evidence for the identification of the intermediate.

Previously reported[9,23] decomposition pathways for iron(III) chromates contain numerous uncertainties. Some of these uncertainties relate to whether intermediate crystalline hydrates were formed during dehydration of the chromates, $MFe(CrO_4)_2.2H_2O$ (M = Na, K) [23], and to the degree of hydration of the chromates $MFe(CrO_4)_2$ (M = Rb, Cs) [23]. In addition, the decomposition of $NH_4Fe(CrO_4)_2$, $FeOHCrO_4$, $KFe_3(CrO_4)_2(OH)_6$, $Fe_2(CrO_4)_3.H_2O$ and $Fe_2(CrO_4)_3.3H_2O$ had either not been reported or had been incompletely described. However, in this study, the formation of intermediate crystalline hydrates in the decomposition of $MFe(CrO_4)_2.2H_2O$ (M = NH_4, Na, K) chromates was not observed, nor was water found to be present in $MFe(CrO_4)_2$ (M = Rb, Cs) chromates. The formation of an intermediate phase, possibly a basic chromate, during the dehydration of $NaFe(CrO_4)_2.2H_2O$ was detected by Mössbauer spectroscopy. This phase was amorphous and therefore could

not be detected by X-ray powder diffraction. The identification of the intermediate was further complicated by its formation being dependent on reaction conditions.

A dependence of decomposition pathway on reaction conditions was also found for $NH_4Fe(CrO_4)_2$. Decomposition of this salt is also complicated by the oxidisability of the cation and reducibility of the anion. Electron spin resonance techniques could possibly aid in clarification of the oxidation changes taking place during the thermal decomposition of this salt, e.g. Cr (VI) to Cr (V). It is proposed that, the intermediate isolated from the decomposition of $NH_4Fe(CrO_4)_2$ at about 270°C is $FeCr_2O_6$, but further characterisation is required. Hydrothermal synthesis may provide a means of obtaining a crystalline sample of this compound suitable for structural analysis.

One reason for the study of the thermal decomposition pathways of basic iron chromates was that it might also shed light on the mode of decomposition of iron sulfates. Iron(III) sulfates are isostructural with the chromates, and oxosulfate phases had been postulated, but as yet not established conclusively to be present during decomposition[25-30]. In the decomposition of all the basic chromates studied, an intermediate phase $Fe_2O(CrO_4)_2$ was isolated. Its formation was first indicated by a weight loss on thermal decomposition, and it was identified by Mössbauer spectroscopy. The formation of $Fe_2O(CrO_4)_2$

indirectly supports the conclusions drawn by Swamy et al[30] from a review of the literature on iron sulfates, that any oxosulfato phase present during their decomposition was most likely to be $Fe_2O(SO_4)_2$.

The absence of $Fe_2(CrO_4)_3$ during the dehydration of $Fe_2(CrO_4)_3.3H_2O$ conflicted with the report of Bonnin[9], who observed a plateau corresponding to the anhydrate in his thermogram. Chemical analysis of a residue, isolated at 380°C from the thermal decomposition of $Fe_2(CrO_4)_3.3H_2O$, agreed with values calculated for the compound $Fe_2O(CrO_4)_2$. This feature of the thermogram was not reported by Bonnin[9]. The Mössbauer spectrum of the sample showed parameters which were consistent with those for $Fe_2O(CrO_4)_2$, identified as a product during the decomposition of $FeOHCrO_4$. The findings in the present study are based on chemical, thermogravimetric and spectroscopic evidence, and highlight the variation which can arise from the description of decomposition pathways, which are based solely on weight loss.

Investigations into the use of a molten salt as a reaction medium for the preparation of iron chromates proved successful. The chromates $KFe(CrO_4)_2.2H_2O$, α-$NH_4Fe(CrO_4)_2$, α-$RbFe(CrO_4)_2$, $CsFe(CrO_4)_2$ and the novel chromates $M_2Fe_3(OH)_5(CrO_4)_3.3H_2O$ were prepared using molten $Fe(NO_3)_3.9H_2O$. It was further observed that in this melt there was a tendency for hydrolysis to occur. Provided this problem can be overcome the technique offers

significant advantages over the aqueous methods, through the reduction in preparation time from days to hours.

The agreement in conclusions drawn from the use of Mössbauer spectroscopy with those derived from X-ray powder diffraction and infrared spectroscopy for compounds whose structures are unknown, e.g. $NaFe(CrO_4)_2$, would suggest that the application of the technique was successful. To extend and develop the correlations deduced thus far, the study of the effect of variation in temperature on quadrupole splitting, combined with a study of the single crystals for each chromate could be useful. The use of a single crystal would lead to the deduction of the sign and asymmetry factor of the field gradient at the nucleus; for example, single crystals of sodium nitroprusside have been used for this purpose[92].

The magnetic behaviour of the iron chromates had been intended to be examined. However, due to problems associated with access to instrumentation at another institution, only cursory observations could be made. There is, therefore, still a requirement for magnetic data to complement the existing Mössbauer studies. Some low temperature Mössbauer measurements were also recorded. The chromate, $NaFe(CrO_4)_2.2H_2O$, was found to be non-magnetic at 4.2K and spectra for both $FeOHCrO_4$ and $KFe(CrO_4)_2$ were resolved into sextets at 4.2K, indicating magnetic ordering. Sherman[87] predicted on the basis of SCF-MO calculations for iron

sulfates and silicates that the ionicity of a Fe^{3+}-OH^{-} bond is greater than that of a Fe^{3+}-O^{2-} bond. The result of this is a lower effective spin of the iron atoms associated with a Fe^{3+}-O^{2-} bond, and an observed decrease in the magnetic hyperfine field. The lower value for the hyperfine field (411 K Gauss) for $FeOHCrO_4$ compared to that of $KFe(CrO_4)_2$ (426 K Gauss) was consistent with Sherman's postulate. A similar series of calculations and experiments for other iron chromates would therefore be of fundamental interest.

APPENDIX I

PREPARATION OF COMPOUNDS

AMMONIUM IRON(III) CHROMATE 2-WATER[9] $NH_4Fe(CrO_4)_2.2H_2O$

An aqueous solution (50 cm^3) containing ammonium dichromate (8.8 g), ammonium chromate (0.5 g) and iron(III) nitrate 9-water (14.9 g) was placed in a 100 cm^3 flask and left to stand at 0°C for 20 h. The red product was collected by decantation, washed with cold water and dried in air. Yield 0.5 g.

XRD pattern of the compound was as follows:

d (obs)	Intensity	d(lit)[9]	d (obs)	Intensity	d(lit)[9]
7.10	vs	7.07	3.11	vw	
4.97	m	4.97	3.06	m	3.05
3.70	m	3.66	2.88	w	2.84
3.52	w	3.53	2.71	s	2.73
3.32	s	3.44	2.65	w	2.61
3.13	w	3.18	2.45	w	2.45
			2.37	w	2.31

d (obs) = observed d spacing (Å)

d (lit) = reported d spacing (Å)

vs = very strong, s = strong, m = medium, w = weak

SODIUM IRON(III) CHROMATE 2-WATER[9] $NaFe(CrO_4)_2.2H_2O$

Solutions of sodium dichromate 2-water (14.9g in $10cm^3$ of water) and iron(III) chloride (1.6g in $10cm^3$ of water) were mixed, filtered and the filtrate left to stand at 0^oC for 24 h. The resulting orange-yellow precipitate was collected by filtration, washed with 60 cm^3 of acetone and dried at 60^oC for 4 h. Yield 0.4 g.

Chemical analyses of the product showed Fe, 14.75 $\pm$ 0.26; Cr, 29.55 $\pm$ 0.20%, requires Fe, 14.99; Cr, 29.98%.

XRD pattern of the compound was as follows:

d (obs)	Intensity	d(lit)[9]	d (obs)	Intensity	d(lit)[9]
4.98	m	5.04	2.64	m	2.65
4.82	w	4.88	2.50	m	2.51
3.53	s	3.55	2.41	w	2.44
3.35	w	3.35	2.40	w	2.40
3.01	m	3.03			
2.95	m	2.96			
2.76	m	2.71			
2.69	m	2.66			

POTASSIUM IRON(III) CHROMATE 2-WATER[9] $KFe(CrO_4)_2.2H_2O$

Two solutions (20 cm^3) containing iron(III) nitrate 9-water (3.2 g) and potassium chromate (6.2 g), respectively, were mixed and heated on a water bath for 0.5 h. The orange precipitate was collected by filtration, washed with water (50 cm^3) and acetone (10 cm^3) and dried over concentrated sulfuric acid. Yield 0.3 g.

Chemical analyses showed Fe, 15.51 $\pm$ 0.22; Cr, 28.02 $\pm$ 0.25; H_2O, 10.15 $\pm$ 0.20, requires Fe, 15.39; Cr, 28.65; H_2O, 9.90%.

XRD pattern of the compound was as follows:

d (obs)	Intensity	d(lit)[9]	d (obs)	Intensity	d(lit)[9]
5.14	m	5.17	2.81	m	2.83
4.90	m	4.95	2.75	m	2.75
3.61	s	3.63	2.61	w	2.71
3.42)	w	3.42	2.58	w	2.58
3.39)	m		2.27	w	2.28
3.12	vs	3.13	2.20	w	2.19
2.99	w	3.02	2.14	w	2.14

POTASSIUM IRON(II) CHROMATE 1-WATER[9] $KFe(CrO_4)_2.H_2O$

Hot aqueous solutions of potassium dichromate (9.7g in $10cm^3$) and iron(III) nitrate 9-water (10.2g in $10cm^3$) were separately pipetted into a glass ampoule, which was sealed under atmospheric pressure. The tube was then heated for 48 h at 150°C, the red-orange contents cooled, removed and filtered, washed with water (30 cm^3) and acetone (10 cm^3) and dried in air. Yield 0.2 g.

Chemical analyses of the product showed Fe, 16.40 ± 0.12; Cr, 29.98 ± 0.25%; requires Fe, 16.33; Cr, 30.23%.

XRD pattern was as follows:

d (obs)	Intensity	d(lit)[9]	d (obs)	Intensity	d(lit)[9]
7.62	w	7.56	3.11	s	3.10
6.46	m	6.46	3.06	w	3.05
4.62	s	4.59	3.02	w	3.02
4.31	m	4.30	2.81	w	2.80
3.83	m	3.83	2.80	w	2.78
3.63	w	3.62	2.74	w	2.74
3.40	m	3.38	2.67	m	2.67

THALLIUM IRON(III) CHROMATE 1-WATER[9] $TlFe(CrO_4)_2.H_2O$

An aqueous solution (100 cm^3) of chromium trioxide (2.0 g), iron(III) nitrate 9-water (3.4 g) and thallium(I) nitrate (4.0 g) was placed in a glass ampoule which was sealed under atmospheric pressure and heated for five days at 120°C to produce a red powder which was filtered, and washed with acetone (30 cm^3) and left to dry in air. Yield 0.2 g.

XRD pattern of the compound was as follows:

d (obs)	Intensity	d(lit)[9]	d (obs)	Intensity	d(lit)[9]
7.62	w	7.58	3.06	s	3.06
4.74	m	4.71	2.84	w	2.84
4.64	s	4.57	2.80	w	2.80
4.22	m	4.19	2.75	m	2.75
3.80	w	3.78	2.67	m	2.67
3.53	m	3.63	2.65	m	2.64
3.40	w	3.39	2.58	w	2.58
3.14	m	3.13			

α-AMMONIUM IRON(III) CHROMATE[9] $NH_4Fe(CrO_4)_2$

A solution (10 cm^3) containing iron(III) chloride (3.2 g) was filtered directly into a solution of ammonium dichromate (5.0g in 8cm^3 of water) heated on a water bath. The mixture was heated at 40°C for 0.75 h, then cooled to room temperature. The solid which formed was filtered, washed with water (50 cm^3) and acetone (10 cm^3) and dried over concentrated sulfuric acid. Yield 1.0 g.

XRD pattern of the compound was as follows:

d (obs)	Intensity	d(lit)[9]	d (obs)	Intensity	d(lit)[9]
7.55	vs	7.56	3.12	m	3.11
4.40	m	4.47	3.02)	m	3.01
3.95	w	3.94	3.00)	m	
3.78	w	3.77	2.76	w	2.76
3.60	w	3.60	2.69	w	2.68
3.38	m	3.38	2.44	w	2.40
3.18	m	3.17			

α-THALLIUM IRON(III) CHROMATE[9] $TlFe(CrO_4)_2$

The compound was prepared by dehydration of thallium iron(III) chromate 1-water at 240°C for 6 h in air.

XRD pattern of the compound was as follows:

d (obs)	Intensity	d(lit)[9]
4.62	m	4.64
4.32	m	4.30
3.95	m	3.93
3.90	s	3.86
3.06	s	3.05
2.90	m	2.89
2.75	m	2.75
2.55	m	2.54

β -THALLIUM IRON(III) CHROMATE[9] $TlFe(CrO_4)_2$

The compound was prepared by heating the α-form at 330°C for 12 h in air.

XRD pattern of the compound was as follows:

d (obs)	Intensity	d(lit)[9]	d (obs)	Intensity	d(lit)[9]
7.31	w	7.27	3.33	s	3.32
4.57	w	4.57	3.03	vs	3.06
4.35	m	4.35	2.85	m	2.84
4.23	w	4.20	2.75	m	2.76
4.06	w	4.13	2.73	m	2.73
3.90	w	3.88	2.63	w	2.67
3.60	m	3.60			

β -RUBIDIUM IRON(III) CHROMATE[14] $RbFe(CrO_4)_2$

Iron(III) chromate 1-water (4.8g) prepared as described on p158, rubidium dichromate (3.0g), chromium trioxide (2.5g) and water (7.2g) were sealed in a glass ampoule at atmospheric pressure and heated for eight (8) days at 160°C. A small quantity of crystals were removed from the cooled ampoule, washed with acetone by decantation and dried over sulfuric acid. Yield 50 mg.

XRD pattern of the compound was as follows:

d (obs)	Intensity	d(lit)[x]	d (obs)	Intensity	d(lit)[x]
			2.79	w)	2.74
5.18	w	5.13	2.75	m)	
		(4.42			
4.39	w	(4.38	2.62	m	2.62
4.14	w	4.17	2.47	w	2.46
3.69	w	3.63			
3.46	w	3.41			
3.22	m	3.24			
3.06	w	3.09			
2.86	m	2.90			

x calculated from crystal data reported in ref.(14).

CESIUM IRON(III) CHROMATE[15] $CsFe(CrO_4)_2$

Iron(III) chromate 1-water (4.8 g) prepared as described on p158, cesium dichromate (4.8 g), chromium trioxide (2.5 g) and water (7.2 g) were sealed in a glass ampoule at atmospheric pressure and heated for eight (8) days at 130°C. A small quantity of crystals were removed from the cooled ampoule, washed with acetone by decantation and dried over sulfuric acid. Yield 80 mg.

Chemical analyses showed Fe, 13.88 ± 0.15; Cr, 25.02 ± 0.17%, requires Fe, 13.27 and Cr, 24.72%.

XRD pattern of the compound was as follows:

d (obs)	Intensity	d(lit)*	d (obs)	Intensity	d(lit)*
7.95	s	7.96	3.26	m	3.26,3.23
7.39	m	7.36	3.04	w	3.07
5.50	vw	5.72	3.01	w	3.01
4.58	m	4.56	2.85	m)	2.78
4.42	w	4.43	2.75	m)	
4.13	w	4.14	2.72	m	2.73
3.99	m	4.01	2.61	m	2.62
3.68	m	3.68			
3.51	m	3.48			

* Calculated from the crystal data reported in reference (14). The observed intensity of d = 7.95, 7.39, 4.13, 3.01 and 2.61 lines may be affected by preferred orientation. Chemical analyses, however, were consistent with $CsFe(CrO_4)_2$.

IRON(III) CHROMATE 1 WATER[9] $Fe_2(CrO_4)_3.H_2O$

Iron(III) hydroxy chromate (1.9 g) and water (1.3 g) were placed in a glass ampoule, which was sealed and heated for ten (10) days at 160°C. The contents of the ampoule were allowed to cool to room temperature, and the dark platelets filtered and washed with acetone (10 cm^3) and dried in air. Yield 0.1 g.

XRD pattern of the compound was as follows:

d (obs)	Intensity	d(lit)[9]
10.86	m	10.82
5.62	m	5.69
3.83	w	3.83
3.59	vs	3.61
3.52	w	3.55
3.44	w	3.46
3.33	w	3.31
2.86	w	2.87

IRON(III) CHROMATE 3-WATER $Fe_2(CrO_4)_3.3H_2O$

A procedure for the preparation of $Fe_2(CrO_4)_3.3H_2O$ differing from the literature method[22] was employed for larger amounts of material. Iron(III) nitrate 9-water (0.01 mol) and magnesium chromate 7-water (0.01 mol) were mixed and placed in an oven at 65°C for 1 h. The resultant melt was cooled, water was added and the black insoluble product removed by filtration, washed with water and dried in air. Yield 0.5 g.

Chemical analyses of the product showed; Fe, 21.86 ± 0.15; Cr, 29.94 ± 0.22; H_2O, 10.61 ± 0.15; requires Fe, 21.74; Cr, 30.36 and H_2O, 10.51%.

XRD pattern of the compound was as follows:

d (obs)	Intensity	d(lit)[9]	d (obs)	Intensity	d(lit)[9]
8.52	m	8.53	2.96	w	2.96
4.89	w	4.89	2.82	w	2.82
4.34	m	4.32	2.76	w	2.76
4.15	w	4.15	2.66	m	2.67
3.89	vs	3.89	2.58	w	2.59
3.77	m	3.78	2.46	w	2.49
3.63	m	3.63			
3.52	w	3.53			
3.31	s	3.32			

IRON(III) HYDROXY CHROMATE[9] $FeOHCrO_4$

Sodium dichromate 2-water (2.1 g), sodium chromate (2.4 g) and iron(III) nitrate 9-water (6.1 g) were added to water (10 cm^3). The mixture was stirred and the solution pipetted into a glass ampoule, which was sealed at atmospheric pressure and heated for 48 h at 110°C. After cooling the ampoule was opened and the solid product filtered and washed with acetone (50 cm^3), then dried in air. Yield 1.0 g.

XRD pattern of the compound was as follows:

d (obs)	Intensity	d(lit)[9]
4.92	m	4.89
3.59	m	3.64
3.22	vs	3.33
3.12	ms	3.17
2.61	s	2.65
2.27	m	2.28
2.13	wm	2.13

POTASSIUM IRON(III) HYDROXY CHROMATE[9] $KFe_3(CrO_4)_2(OH)_6$

Equimolar solutions (1M) of potassium dichromate (50 cm^3) and iron(III) nitrate 9-water (50 cm^3) were pipetted into a glass ampoule, which was sealed at atmospheric pressure and heated for 24 h at 180°C. After cooling the product was precipitated from solution by the addition of absolute alcohol, washed with cold water (50 cm^3) and allowed to dry in air. Yield 1.5 g.

XRD pattern of the compound was as follows:

d (obs)	Intensity	d(lit)[9]
6.02	m	6.04
5.10	m	5.18
3.67	w	3.71
3.14	s	3.16
3.10	vs	3.12
2.99	w	3.02
2.57	w	2.58

BASIC IRON(III) CHROMATE[7] $2Fe_2O_3.4CrO_3.H_2O$

Aqueous solutions containing iron(III) chloride (4.9g in 12cm^3) and sodium chromate (1.6g in 30cm^3) were mixed and heated on a water bath for 1 h during which a brown precipitate formed. The precipitate was filtered, dried at 70^{o}C for 2 h and a weighed amount (1.8 g) placed in a glass ampoule containing chromium trioxide (2.0 g) and water (0.2 g). The ampoule was sealed and heated at 200^{o}C for 4 h. The black material deposited in the ampoule was removed on cooling, filtered, washed with acetone (30 cm^3) and dried in air. Yield 1.0 g.

XRD pattern of the compound was as follows:

d (obs)	Intensity
4.82	w
3.58	m
3.27	vs
3.16	m
2.63	w
2.30	w

POTASSIUM IRON(III) SULFATE $KFe(SO_4)_2$[93]

A suspension of iron(III) oxide (2.9 g) in a solution of potassium sulfate (2.9g in 100cm^3 of water) was heated to 60°C and maintained at this temperature whilst concentrated sulfuric acid (29.10 cm^3) was added to the mixture slowly. The resulting grey solution was evaporated to near dryness. The grey paste remaining after evaporation was transferred to a muffle furnace and heated to constant weight at 300°C (about 48 h). The product was then powdered and washed with warm water (100 cm^3) and dried over sulfuric acid. Yield 3.0 g.

XRD pattern of the compound was as follows:

d (obs)	Intensity	d(lit)[93]	d (obs)	Intensity	d(lit)[93]
7.92	m	7.58	3.04	w	3.01
4.00	m	3.94	2.96	s	3.01
3.82	m	3.78	2.82	m	2.88
3.60	m	3.54	2.64	w	2.65
3.34	w	3.33	2.35	w	2.43
3.22	w	3.18			

APPENDIX II

MAGNETIC SUSCEPTIBILITY TABLES FOR CHROMATES

$KFe(CrO_4)_2.nH_2O$ n = 0, 1 and 2

Magnetic susceptibility for $KFe(CrO_4)_2.2H_2O$ from 4.2 - 300K at field strength 10K Gauss

Temp (K)	$X_g(\times 10^6)$	$X_m \times 10^6$	$\frac{1}{X_m}$	μ_{eff} (BM)
5.14	768.11	278859.30	3.59	3.39
6.30	730.47	265201.79	3.77	3.66
7.88	664.76	241353.14	4.14	3.90
9.74	600.47	218024.59	4.59	4.12
11.80	541.24	196537.44	5.09	4.31
14.21	488.46	177373.40	5.64	4.49
16.60	442.97	160865.37	6.22	4.62
19.09	402.78	146280.45	6.84	4.73
21.79	366.79	133221.71	7.51	4.82
21.40	371.22	134830.20	7.42	4.80
32.07	275.30	100020.90	10.00	5.06
40.35	219.99	79947.13	12.51	5.08
49.86	184.52	67076.79	14.91	5.17
59.79	158.88	57769.15	17.31	5.26
68.24	141.74	51549.22	19.40	5.30
76.52	128.39	46705.47	21.41	5.35
84.23	117.70	42825.71	23.35	5.37
90.89	110.06	40053.84	24.97	5.40
94.71	106.01	38582.55	25.92	5.41
119.05	86.76	31599.23	31.65	5.49
141.12	74.25	27057.29	36.96	5.53
158.67	66.42	24217.75	41.29	5.54
178.58	59.32	21641.61	46.21	5.56
197.91	53.89	19669.72	50.84	5.58
218.44	48.98	17886.23	55.91	5.59
237.13	45.36	16574.69	60.33	5.61
255.03	42.26	15450.94	64.72	5.61
269.84	40.01	14630.85	68.35	5.62
287.83	37.67	13783.92	72.55	5.63
303.36	35.94	13155.28	76.02	5.65

ligand correction = -113×10^{-6}
Molecular weight = 362.9

Magnetic susceptibility for $KFe(CrO_4)_2.H_2O$ from 4.2 - 300K at field strength 10K Gauss

Temp (K)	$X_g(\times 10^6)$	$X_m \times 10^6$	$\frac{1}{x_m}$	μ_{eff} (BM)
4.25	277.81	95915.12	10.43	1.81
4.97	277.17	95696.50	10.45	1.95
6.14	274.37	94730.68	10.56	2.16
7.88	267.67	92420.95	10.82	2.41
9.74	259.70	89671.61	11.15	2.64
12.49	248.18	85697.62	11.67	2.93
14.17	241.91	83533.64	11.97	3.08
16.67	232.82	80401.00	12.44	3.27
19.27	223.54	77198.33	12.95	3.45
22.00	214.46	74067.59	13.50	3.61
23.63	209.01	72188.00	13.85	3.69
31.91	179.84	62127.00	16.10	3.98
42.46	156.90	54215.00	18.45	4.29
51.77	140.10	48420.00	20.65	4.48
61.12	91.65	43899.00	22.78	4.63
69.34	116.87	40408.00	24.75	4.73
77.44	108.18	37411.00	26.73	4.81
85.25	100.84	34880.00	28.67	4.88
92.03	95.30	32969.00	30.33	4.93
97.51	91.15	31538.03	31.71	4.96
121.49	77.03	26666.36	37.50	5.09
143.37	67.21	23281.03	42.95	5.17
160.77	60.86	21091.50	47.41	5.21
180.67	54.91	19038.25	52.53	5.24
199.89	50.18	17407.58	57.45	5.28
221.67	45.88	15923.12	62.80	5.31
239.15	42.72	14833.33	67.42	5.33
256.95	39.97	13884.07	72.02	5.34
271.57	37.97	13197.45	75.77	5.35
289.48	35.87	12471.55	80.18	5.37

Ligand correction = -100×10^{-6}
Molecular weight = 344.9

Magnetic susceptibility for $KFe(CrO_4)_2$ from 4.2 - 300K at field strength 10K Gauss

Temp (K)	$X_g(\times 10^6)$	$X_m \times 10^6$	$\frac{1}{X_m}$	μ_{eff} (BM)
4.24	36.61	12056.18	82.94	0.64
4.80	35.70	11758.57	85.04	0.67
6.02	34.44	11348.31	88.12	0.74
7.75	32.80	10809.41	92.51	0.82
9.59	31.67	10440.25	95.78	0.89
11.56	31.03	10233.21	97.72	0.97
14.02	30.69	10122.08	98.79	1.07
16.31	30.60	10090.88	99.10	1.15
18.67	30.73	10132.74	98.69	1.23
21.18	31.00	10222.56	97.82	1.32
20.20	30.85	10173.08	98.30	1.28
30.18	32.05	10565.08	94.65	1.60
38.57	32.88	10836.81	92.28	1.83
48.16	33.20	10941.85	91.39	2.05
57.61	33.11	10912.17	91.64	2.24
66.07	32.74	10791.14	92.67	2.39
74.39	32.22	10620.64	94.16	2.51
79.98	31.77	10472.87	95.48	2.59
106.03	29.47	9721.72	102.86	2.87
129.60	27.32	9018.41	110.88	3.06
148.12	25.71	8492.45	117.75	3.17
168.95	24.06	7953.93	125.72	3.28
189.01	22.68	7501.27	133.31	3.37
210.70	21.66	7070.46	141.43	3.45
230.79	20.36	6744.83	148.26	3.53
249.04	19.45	6445.55	155.15	3.58
264.33	18.74	6215.07	160.90	3.62
282.63	17.97	5962.97	167.70	3.67
298.22	17.40	5774.74.	173.17	3.71

Ligand correction = -87×10^{-6}

Molecular weight = 326.95

APPENDIX III PUBLICATIONS

1. Mineely, P.J. and Scott D.L.,"The Characterisation of Some Iron Chromates", Aust. J. Chem., 1987,40,387.

2. Mineely, P.J.,"Thermal Decomposition of Some Iron(III) Chromates", Aust. J. Chem., 1988,41, 263.

3. Mineely, P.J.,"Characterisation of Some New Chromates $M_2Fe_3(OH)_5(CrO_4)_3.3H_2O$ (M = Li, Na)", Thermochimica Acta, 1989,137,197.

Aust. J. Chem., 1987, **40**, 387–93

The Characterization of Some Iron Chromates

Aust. J. Chem., 1987, **40**, 387–93

The Characterization of Some Iron Chromates

Patrick J. Mineely[A,B] *and Dereham L. Scott*[A]

[A] Department of Chemistry, Faculty of Science, Australian National University, P.O. Box 4, Canberra, A.C.T. 2601.
[B] Author to whom correspondence should be addressed.

Abstract

As the first step in a systematic review of a range of iron(III) chromates, the Mössbauer chemical shifts, quadrupole splittings and linewidths have been measured for a number of compounds. These parameters have been correlated with available structural information and the correlations have been applied to compounds with unknown structures and to the thermal decomposition products of the double chromates $MFe(CrO_4)_2.nH_2O$ with M = Na, K, Rb, Cs, NH_4. Decomposition of the ammonium salt follows a different pathway, with the new mixed-valence compound, $FeCr_2O_6$, as an apparent intermediate.

Introduction

The literature records a considerable number and variety of iron chromates, but it is only since Bonnin's review[1] in 1970 that some of these have been structurally characterized through diffraction and spectroscopic studies. Some of these compounds are not easy to make, the preparations being complicated by hydrolytic and polymerization equilibria; careful control of conditions, and patience, are required to form products of definite, reproducible composition. Crystals suitable for diffraction analysis have not yet been grown for some compounds and tentative structural assignments for these have been based on less-than-conclusive infrared data.[2] The compound $NH_4Fe(CrO_4)_2.2H_2O$, which is potentially of some interest, is efflorescent.

In an attempt to clarify the position, we have begun a systematic review of the spectroscopic and magnetic properties and thermal decomposition patterns of these compounds. In particular, we have been using Mössbauer spectroscopy, both as a structural probe for the parent compounds and as a tool for characterizing their thermal decomposition products. This paper reports the room-temperature Mössbauer parameters for a range of compounds, and the extent to which these can be correlated with structure, and the thermal decomposition behaviour for some double chromates. Where possible, we have explored similarities between these chromates and the analogous sulfates. A subsequent paper will deal with infrared and Raman spectra, low-temperature Mössbauer spectroscopic and magnetic results and further thermal behaviour.

[1] Bonnin, A., Ph.D. Thesis, Rennes, 1970.
[2] Mellier, A., and Gravereau, P., *Spectrochim. Acta, Part A*, 1973, **29**, 2043.

0004-9425/87/020387$02.00

The following groups of compounds have been examined: (A) the normal chromates, $Fe_2(CrO_4)_3.nH_2O$ (n = 1, 3);[3] (B) the basic chromate $FeOHCrO_4$;[4] (C) the double chromates, $MFe(CrO_4)_2.nH_2O$, with M = alkali metals, NH_4 and Tl and n = 0, 1 and 2,[1,5–10] (D) the complex double chromate analogues of jarosite, $KFe_3(CrO_4)_2(OH)_6$.[4]

As far as they are known, the structures may be visualized as consisting of $[FeO_6]$ octahedra linked by $[CrO_4]$ tetrahedra to give chains, sheets and three-dimensional nets. Oxygen atoms from H_2O, OH^- and CrO_4^{2-} make up the coordination octahedra around iron(III), and dehydration results in further crosslinking as chromate oxygens fill the vacated sites. For example, in the series $KFe(CrO_4)_2.nH_2O$,[11] the sequence for n = 2 to 0 is of simple chains of $[Fe_2(CrO_4)_2.2H_2O]^-$ units, double chains of $[Fe_2(CrO_4)_4.2H_2O]^{2-}$ units and sheets of $KFe(CrO_4)_2$. In some cases, the $[FeO_6]$ octahedra share corners and edges. Several compounds have been shown to be dimorphic and some structural relationships with analogous sulfates and chromium chromates have been identified.[10]

Apart from structural characterization, little work has been done on these compounds. Popel[12] has reported an incomplete study of the thermal decomposition of the chromates $MFe(CrO_4)_2.2H_2O$ (M = Na K) and $MFe(CrO_4)_2$ (M = Rb, Cs), with the end products around 400°C being the alkali metal chromate or dichromate and the mixed oxide $(Fe,Cr)_2O_3$. We have confirmed the principal stages of the sequences reported by Popel,[12] but like Popel we also noted some extraneous features of the thermograms, in particular those for the sodium salt. After a careful study of this salt, we now believe that these features arise from the presence of basic chromates,[13] which are probable contaminants in the sodium case and are not exhibited by the pure compound. The problems associated with interpretation of thermal decomposition data are typified by the conflicting claims in the many papers on the hydrated iron sulfates. Swarmy *et al.*[14] have recently reviewed about thirty papers on the thermal decomposition of iron(II) sulfate hydrates in an attempt to resolve the discrepancies.

We have extended these studies to observations on the thermal decomposition behaviour of the ammonium salt, which is potentially complicated by three factors—the volatility of ammonia, the oxidizability of the ammonium cation and the existence of two known forms of the anhydrous salt (α,[6] with a sheet structure, and the three-dimensional β.[5] A further complication is the great ease of dehydration, it being necessary to ensure that contamination by the anhydrous salt is minimal. The stability of the dihydrates appears to be critically dependent upon the extent of hydrogen bonding between the chains. This in turn depends upon the size of the univalent cation and even for the potassium salt the hydrogen bonds are quite

[3] Bonnin, A., *C. R. Acad. Sci., Ser. C*, 1970, **271**, 639.
[4] Bonnin, A., and Lecerf, A., *C. R. Acad. Sci., Ser. C*, 1966, **262**, 1782.
[5] Gravereau, P., and Gaboriaud, F., *Acta Crystallogr., Sect. B*, 1972, **28**, 2329.
[6] Gravereau, P., Hardy, A., and Bonnin, A., *Acta Crystallogr., Sect. B*, 1977, **33**, 1362.
[7] Hardy, A., and Gravereau, P., *C. R. Acad. Sci., Ser. C*, 1970, **271**, 1304.
[8] Hardy, A., and Gravereau, P., *Acta Crystallogr., Sect. B*, 1972, **28**, 2333.
[9] Bonnin, A., Hardy, A., and Garnier, E., *C. R. Acad. Sci., Ser. C*, 1973, **276**, 138.
[10] Bonnin, A., Diaz-Caceres, J., Gravereau, P., and Hardy, A., *C. R. Acad. Sci., Ser. C*, 1974, **279**, 939.
[11] Gravereau, P., and Hardy, A., *Bull. Soc. Fr. Mineral. Crystallogr.*, 1976, **99**, 206.
[12] Popel, P. P., *Russ. J. Inorg. Chem.*, 1982, **27**, 81.
[13] Popel, P. P., and Boldog, I. I., *Russ. J. Inorg. Chem.*, 1979, **24**, 1828.
[14] Swarmy, M. S. R., Prasada, T. P., and Scant, B. R. J., *J. Therm. Anal.*, 1979, **15**, 307.

long at 295 pm.[2] The non-existence of the hydrated rubidium and caesium salts is presumably due to the inhibition of effective hydrogen bonding by these larger cations and it would seem that the effective size of the ammonium ion here is such as to place the dihydrate on the borderline of stability. Indeed, both forms of the anhydrous salt may be crystallized from aqueous solution.[5,6]

The pyrolysis of ammonium dichromate under controlled conditions has attracted a considerable amount of attention. In a comprehensive study, Mahieu *et al.*[15] report a sequence of steps in which the chromium is progressively reduced from the VI state through V and IV to Cr_2O_3, with part of the ammonia being oxidized to dinitrogen. On the other hand, a more recent study failed to confirm this, finding CrO as the only intermediate for the decomposition in air, with direct decomposition to Cr_2O_3, and dinitrogen in inert atmospheres and under vacuum.[16] If the very considerable differences between the various proposed pyrolysis schemes are real, then the pathway must be critically dependent on the conditions.

Experimental

Materials

Compounds were prepared according to methods in the literature cited above and characterized by analysis and, where possible, by X-ray powder diffraction. Where they were available, atomic-coordinate data were converted into powder diffraction lines by means of a Rietveld program.[17]

Physical Measurements

Thermogravimetric analysis was performed on a Stanton Redcroft TG750/770 thermal analysis unit in air and nitrogen atmospheres. Differential thermal analysis was carried out on a Rigaku–Denki modular thermoflex thermal analyser under air. X-ray powder patterns were recorded on a Philips PW1050 diffractometer, with a wide-angle goniometer, under Cu Kα radiation. Mössbauer spectra were obtained from a conventional constant-acceleration system,[18] by using a 50–60 mCi ^{57}Co source in a rhodium matrix. Samples containing about 2 mg cm^{-2} of iron were prepared by compressing powdered material with benzophenone matrix and, on the basis of the linewidths obtained, showed no significant thickness effects. The spectrometer was calibrated with natural α-iron foil and isomer shifts are reported relative to the centroid of this spectrum.[19] Spectra were collected by a PDP 10/11 computer and fitted by a pseudo-Lorentzian program using an iterative, non-linear least-squares method, on the basis of the χ^2 values, consistency of parameters and convergence of the fitting process.[20]

Results and Discussion

The Thermal Decomposition of $NH_4Fe(CrO_4)_2.2H_2O$

The dihydrate loses both water molecules in a single step below 85°C and at room temperature under vacuum. Comparison of the powder pattern of the anhydrous compound with those generated from published atomic-coordinate data indicates that the anhydrous product is the α-form and annealing of this product at 135°C for 4 hours failed to produce any of the β-form.

[15] Mahieu, B., Apers, D. J., and Capron, P. C., *J. Inorg. Nucl. Chem.*, 1971, **33**, 2857.
[16] Shmerkovich-Galev, G. I., *Zh. Vses. Khim. Ova*, 1977, **22**, 463 (*Chem. Abstr.*, 1977, **87**, 210454y).
[17] Wiles, D. B., and Young, R. A., *J. Appl. Crystallogr.*, 1981, **14**, 149.
[18] Window, B., Dickson, B. L., Routcliffe, P., and Srivastava, K. K. P., *J. Phys. E*, 1974, **7**, 916.
[19] Violet, C. E., and Pipkorn, D. W., *J. Appl. Phys.*, 1971, **42**, 4339.
[20] Price, D., *Aust. J. Phys.*, 1981, **34**, 51.

Pyrolysis of the anhydrous salt involves two well resolved stages, with an endotherm at 336°C and an exotherm at 457°C in the differential thermal analysis curve. The weight loss at the first stage was 16·34±0·67%, compared with a calculated value of 16·34% for the loss of (1N, 4H and 2O) per mole of the anhydrous salt. Pressure measurements showed the loss of 0·5 moles of permanent gas. These observations are consistent with the equation as shown below:

$$NH_4Fe(CrO_4)_2 \rightarrow FeCr_2O_6 + \tfrac{1}{2}N_2 + 2H_2O \quad (1)$$

According to this scheme, half the Cr^{VI} is reduced in oxidation of ammonia to Cr^{III}, generating the proposed new mixed-valence compound $FeCr_2O_6$ (analysis 22·57±0·3% Fe, 38·25±0·5% Cr; calculated 21·83 and 40·75%). The product is amorphous to X-rays and we are currently trying to synthesize this compound for further characterization.

The second stage of the decomposition to mixed oxides, equation (2):

$$FeCr_2O_6 \rightarrow \tfrac{1}{2}(Fe, Cr)_2O_3 + \tfrac{3}{2}O_2 + \tfrac{1}{2}Cr_2O_3 \quad (2)$$

occurred over the range 400–475°C, with a total weight loss of 25·33±0·65%, calculated 24·27% for reactions (1+2).

Mössbauer Spectra

The parameters of the Mössbauer spectra of some iron chromates recorded in Table 1 clearly show some correlation with known structural types. All spectra listed were simple quadrupole doublets, with isomer shifts around 0·40 mm s^{-1} as expected for high-spin iron(III) in $[FeO_6]$ octahedra. There appear to be useful correlations between structure and the Mössbauer quadrupole splittings, which are dependent upon the distortion from cubic symmetry, the field gradient induced by other cations where present and on the effective charges on the oxygen atoms in the $[FeO_6]$ octahedra.

The potassium and sodium salts, $MFe(CrO_4)_2.2H_2O$, are reported to be similar in structure, with $[FeO_6]$ octahedra linked by $[CrO_4]$ tetrahedra in simple chains, although they belong to different space groups and the ammonium analogue is inferred from infrared spectra to be isostructural with the potassium salt.[2] The anhydrous potassium and sodium salts are believed to have the same structure,[11] while the anhydrous ammonium compound adopts both sheet and three-dimensional forms.

As is consistent with Baur's approach top bond lengths and distortions in coordination polyhedra in ionic structures,[2,21] the $Fe–OH_2$ bond in the hydrates is appreciably longer than the Fe–$[OCrO_3]$ bond, and the observed splittings are greater than in the anhydrous salts, where the Fe–O bond lengths are more uniform.

In the sodium dihydrate, the sodium ion is coordinated by eight oxygens, compared with ten for potassium in the analogous compound. On the basis of both the smaller range in the Fe–O distances and Baur's criterion, the distortion in the sodium salt would be expected to be smaller, whereas the reverse is observed. We conclude, since the splittings for both the hydrated and anhydrous salts are greater than those for the potassium compounds, that the effective field gradient generated by the sodium ion is greater (see above). The larger splitting for the ammonium dihydrate may

[21] Baur, W. H., *Am. Crystallogr. Trans.*, 1970, **6**, 129.

conceivably arise from possible hydrogen bonding between the ammonium ion and the octahedra.[2]

The parameters for the two salts $NaFe(CrO_4)_2$ and $NH_4Fe(CrO_4)_2.2H_2O$, for which single-crystal X-ray data are not available, are not then inconsistent with the inferred structures. The small differences between the parameters for the anhydrous potassium and sodium salts may be ascribed to the difference in size of the alkali metal cation and indeed the splitting does decrease further with the rubidium and caesium analogues (0·10 and 0·09 mm s^{-1}) although, since these latter have slightly different structures, the trend cannot be considered to be definitely established.

Table 1. Mössbauer parameters for some iron chromates, grouped according to type of octahedral iron site

(δ, isomer shift; ΔE, quadrupole splitting; Γ, linewidth at half peak height)

Site type	Example	Mössbauer parameters/mm s^{-1}		
		δ	ΔE	Γ
$FeO_4(OH_2)_2$	$NaFe(CrO_4)_2.2H_2O$	0·41	0·36	0·31
	$KFe(CrO_4)_2.2H_2O$	0·40	0·34	0·26
	$NH_4Fe(CrO_4).2H_2O$	0·43	0·51	0·36
$FeO_4(OH)_2$	$FeOHCrO_4$	0·39	0·47	0·26
	$KFe_3(CrO_4)_2(OH)_6$	0·37	0·46	0·26
FeO_6 (sheet)	$NaFe(CrO_4)_2$	0·39	0·15	0·23
	$KFe(CrO_4)_2$	0·41	0·11	0·25
	α-$NH_4Fe(CrO_4)_2$	0·40	0·10	0·26
FeO_6(3D net)	β-$NH_4Fe(CrO_4)_2$	0·40	0·43	0·39

The anhydrous compounds of potassium and ammonium (α-form), with known sheet structures, have similar parameters and the splittings are consistent with more symmetrical iron environments. Since the bond lengths and angles in the $[FeO_6]$ octahedra of the two forms of the anhydrous ammonium salt are very similar, the splitting for the three-dimensional β-form—comparable to those for the hydrated and basic compounds—appears to be surprisingly large. However, it has been suggested[5] that the presence of chromates tetrahedra between the chains of octahedra results in an added 'tension' in the structure. The 'tension' may manifest itself in the larger quadrupole splitting for the β-form. As a consequence, the environment about the iron is less symmetric. The Mössbauer parameters for synthetic yavapaiite, $KFe(SO_4)_2$, are very similar to those for the isostructural chromate.[4] Parameters for other natural and synthetic sulfates are not yet available.

As expected from the greater negative charge on oxygen, replacement of water molecules by hydroxyl ions in the iron octahedra for the basic salts introduces a somewhat greater distortion, reflected by the greater splittings. All iron sites in $KFe_3(CrO_4)_2(OH)_6$, isostructural with alunite $KAl_3(SO_4)_2(OH)_6$ and jarosite $KFe_3(SO_4)_2(OH)_6$,[22] are crystallographically equivalent. The $[Fe(OH)_4O_2]$ octahedra share four vertices, linked through the hydroxyl groups and are grouped in threes, surrounding a common $[CrO_4]$ tetrahedron. The structures of the basic chromates and sulfates, $FeOH(XO_4)$, are very similar to one another with $[Fe(OH)_2O_4]$ octahedra linked by *trans*-hydroxy bridges into chains, which are joined by $[XO_4]$ tetrahedra

[22] Cudennec, Y., Riou, A., Bonnin, A., and Caillet, P., *Rev. Chim. Miner.*, 1980, **17**, 158.

into sheets.[23] The quadrupole splittings for the hydroxy sulfates are very large for high-spin iron(III)[24] (Table 2, which also records further literature data[25–27]) and are much larger than those for the related chromates, but the values for the two series are much closer when the iron is coordinated only by oxygens from $[XO_4]$ tetrahedra.

Table 2. Mössbauer parameters of some iron sulfates

Site type	Example	Mössbauer parameters/mm s^{-1} δ	ΔE
$FeO_4(OH)_2$	$FeOHSO_4$ [24]	0·44	1·45
	$KFe_3(SO_4)_2(OH)_6$ [25]	0·45	1·00–1·15
$Fe(OH)_2O_2(OH_2)_2$	$FeOHSO_4(OH_2)_2$ [24]	0·42	0·97
FeO_6	$Fe_2(SO_4)_3$ [26,27]	0·49	0·30
		0·49	0·15
	$KFe(SO_4)_2$ (this work)	0·47	0·15

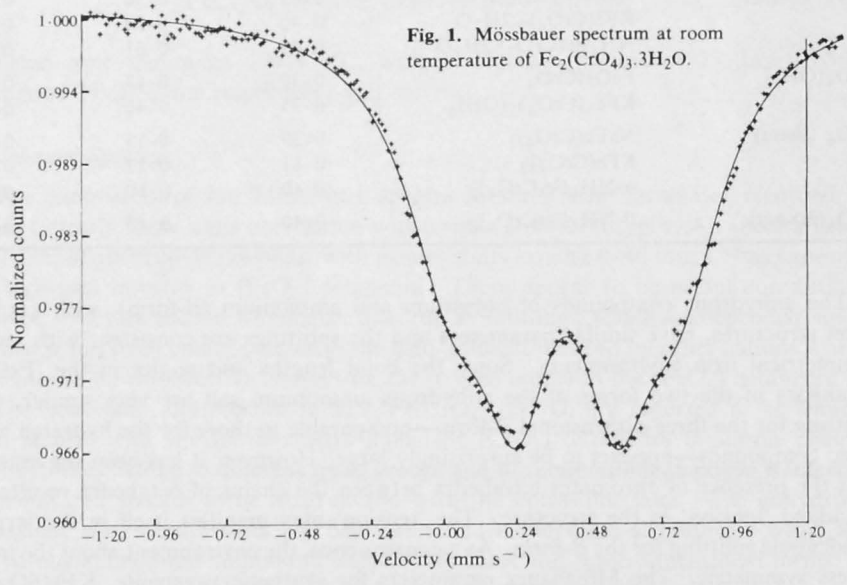

Fig. 1. Mössbauer spectrum at room temperature of $Fe_2(CrO_4)_3.3H_2O$.

Of the various factors that contribute to asymmetry of the electric field around the iron, physical distortion of the octahedron as measured by the range of Fe–O distances and bond angles does not appear to be significant. Neither do the univalent cations play a significant role; Hrynkiewicz *et al.*[25] report for a series of jarosites quadrupole splittings increasing from 1·00 to 1·15 mm s^{-1} as the Pauling radii of

[23] Powers, D. A., Rossman, G. R., Schugar, H. J., and Gray, H. B., *J. Solid State Chem.*, 1975, **13**, 1.

[24] Morais, P. C., and Neto, K. S., *Polyhedron*, 1983, **2**, 875.

[25] Hrynkiewicz, A. Z., Kubisz, J., and Kulgawcuk, D. S., *Inorg. Nucl. Chem. Lett.*, 1965, **27**, 2513.

[26] Long, G. J., Longworth, G., Battle, P., Cheetham, A. K., Thundathil, R. V., and Beveridge, D., *Inorg. Chem.*, 1979, **18**, 624.

[27] Riou, A., and Bonnin, A., *Acta Crystallogr., Sect. B*, 1978, **34**, 706.

the univalent cations range from 95 to 145 pm. This leaves, as the determining factor, the effective charges on the coordinated oxygens and leads to the conclusion that the sulfate oxygen atoms carry a significantly lower negative charge than those in the chromate anion, as expected on a simple electronegativity argument.

The α-form of $Fe_2(CrO_4)_2.3H_2O$ has two distinct iron sites, with sheets containing $[FeO_6]$ octahedra linked by chains of $[FeO_3(H_2O)_3]$ octahedra. Within the sheets, the octahedra are paired, with a common edge, the remaining positions being occupied by chromate oxygens in the usual way. Consistent with this structure, the Mössbauer spectrum (Fig. 1) resolves into two doublets with equal areas and the same shift (0·39 mm s^{-1}). Comparison of the two splittings of 0·16 and 0·37 mm s^{-1} with the calibration data of Table 1 suggests that the outer doublet arises from the octahedra containing water. The linewidths are 0·29 and 0·37 mm s^{-1}; the sharing of edges by the pairs of $[FeO_6]$ octahedra does not produce the significant broadening that might have been expected from the possibility of increased coupling.

For those structures in which the iron octahedra share corners or edges some spin interaction is to be expected. Although hydroxyl bridges are less effective than oxo bridges in facilitating this interaction, Powers *et al.*[23] observed room-temperature iron moments of around 3·5 BM for the basic sulfate and chromate, and for some compounds of the jarosite type. The Mössbauer linewidths for these chromates are certainly greater than those for compounds in which direct bridging is absent but the extent of broadening is not great.

In conclusion, the correlations between structure and quadrupole splitting so far available appear to have some value for the characterization of both the chromates and sulfates and they are currently being applied to studies of some other compounds to be reported at a later date.

Acknowledgments

For their assistance and the use of their apparatus, we gratefully acknowledge Dr A. Stewart and Dr G. Whittle, Department of Solid State Physics, the Australian National University (Mössbauer spectroscopy) and Dr J. O. Hill, Chemistry Department, La Trobe University (differential thermal analysis). We thank also Dr M. Sterns of this Department for her help with crystallographic interpretation and application of the Rietveld program. P.J.M. acknowledges the support of a Commonwealth Postgraduate Research Scholarship.

Manuscript received 14 March 1986

Aust. J. Chem., 1988, **41**, 263–8

Thermal Decomposition of Some Iron(III) Chromates

Aust. J. Chem., 1988, **41**, 263–8

Thermal Decomposition of Some Iron(III) Chromates

Patrick J. Mineely

Department of Chemistry, Faculty of Science, Australian National University, P.O. Box 4, Canberra, A.C.T. 2601.
Present address: Department of Chemistry, Monash University, Clayton, Vic. 3168.

Abstract

The thermal decomposition of the chromates $FeOHCrO_4$, $KFe_3(CrO_4)_2(OH)_6$, $Fe_2(CrO_4)_3.H_2O$ and $Fe_2(CrO_4)_3.3H_2O$ have been studied by thermal analysis and Mössbauer spectroscopy. The possible presence of $Fe_2O(CrO_4)_2$ as a second phase formed during the decomposition is discussed. Final products in all reactions were oxides of iron(III) and chromium(III). In addition $K_2Cr_2O_7$ was present in the reaction products for $KFe_3(CrO_4)_2(OH)_6$.

Introduction

Most studies to date on the chemistry of iron(III) chromates have focused on aspects of preparation[1,2] and structure determination.[1,3–13] Considering the structural relationships which exist between the chromates and iron(III) sulfates[1,14] and the numerous studies[15–20] into the decomposition of iron sulfates, the little work[1,21–22] on the decomposition of iron(III) chromates is surprising. Iron(III) chromate, $Fe_2(CrO_4)_3$, has been proposed[1] as an intermediate during the dehydration of $Fe_2(CrO_4)_3.3H_2O$. Whilst the loss of water for the chromate $Fe_2(CrO_4)_3.H_2O$ is reported[1] to be accompanied by the simultaneous loss of oxygen, identification of the product(s) formed was not attempted.

[1] Bonnin, A., Ph.D. Thesis, Rennes, 1970.
[2] Popel, P. P., and Boldog, I. I., *Russ. J. Inorg. Chem.*, 1979, **24**, 1828.
[3] Mellier, A., and Gravereau, P., *Spectrochim. Acta, Part A*, 1973, **29**, 2043.
[4] Bonnin, A., *C. R. Acad. Sci., Ser. C*, 1970, **271**, 639.
[5] Bonnin, A., and Lecerf, A., *C. R. Acad. Sci., Ser. C*, 1966, **262**, 1782.
[6] Gaboriaud, F., and Hardy, A., *Acta Crystallogr., Sect. B*, 1972, **28**, 2329.
[7] Gravereau, P., Hardy, A., and Bonnin, A., *Acta Crystallogr., Sect. B*, 1977, **33**, 1362.
[8] Hardy, A., and Gravereau, P., *C. R. Acad. Sci., Ser. C*, 1970, **271**, 1304.
[9] Hardy, A., and Gravereau, P., *Acta Crystallogr., Sect. B*, 1972, **28**, 2333.
[10] Bonnin, A., Hardy, A., and Garnier, E., *C. R. Acad. Sci., Ser. C*, 1973, **276**, 138.
[11] Bonnin, A., Diaz-Caceres, J., Gravereau, P., and Hardy, A., *C. R. Acad. Sci., Ser. C*, 1974, **279**, 939.
[12] Gravereau, P., and Hardy, A., *Bull. Soc. Fr. Mineral. Crystallogr.*, 1976, **99**, 206.
[13] Riou, A., and Bonnin, A., *Acta Crystallogr., Sect. B*, 1978, **34**, 706.
[14] Powers, D. A., Rossman, G. R. Schugar, H. J., and Gray, H. B., *J. Solid State Chem.*, 1975, **13**, 1.
[15] Bristotti, A., Kunrath, J. I., Viccaro, P. J., and Bergter, L., *J. Inorg. Nucl. Chem.*, 1975, **37**, 1149.
[16] Swamy, M. S. R., Prasad, T. P., and Sant, B. R., *J. Therm. Anal.*, 1979, **15**, 307.

References 17–21 *on page* 264

0004-9425/88/020263$03.00

In this report the findings on the decomposition of some basic and normal iron(III) chromates are presented, to establish the temperatures of decomposition and the presence, if any, of intermediates, by a combination of thermal analysis and Mössbauer spectroscopy. In a previous communication,[22] Mössbauer spectroscopy was shown to be a useful tool for the characterization of iron(III) chromates.

Experimental

Materials

Compounds were prepared according to methods in the literature[1,5] and characterized by elemental analysis (Fe, Cr). X-Ray powder diffraction patterns of the compounds were also compared with those available in the literature.[1,5]

Physical Measurements

Atomic absorption spectroscopy was performed on a Varian Techtron 1200 spectrophotometer, an air–acetylene flame being used. Thermogravimetric analysis was performed on a Stanton Redcroft TG 750 thermal analysis unit in air and nitrogen atmospheres. Differential thermal analysis was carried out on a Rigaku–Denki modular thermoflex thermal analyser under air. X-Ray powder patterns of samples mounted on slides were recorded on a Philips PW 1050 diffractometer, with a wide-angle goniometer, Cu Kα radiation being used. Mössbauer spectra were obtained from a conventional constant-acceleration system,[23] a 50–60 mCi ^{57}Co source in a rhodium matrix being used. Samples containing 2–5 mg cm^{-2} of iron were prepared by compressing powdered material with benzophenone matrix and, on the basis of linewidth obtained, showed no significant thickness effects. The spectrometer was calibrated with natural α-iron foil and isomer shifts are reported relative to the centroid of this spectrum.[24] Spectra were collected by a PDP 10/11 computer and fitted to a pseudo-Lorenztian equation by using an iterative, non-linear least-squares method, on the basis of the chi-squared values, consistency of parameters and convergence of the fitting process.[25]

Results and Discussion

The weight loss data are presented in Table 1. X-Ray powder diffraction patterns of samples quenched under a stream of argon from 550°C for each chromate confirmed the presence of iron(III) and chromium(III) oxides. In addition $K_2Cr_2O_7$ was confirmed in residues from $KFe_3(CrO_4)_2(OH)_6$.

Thermogravimetry and differential thermal analysis (d.t.a.) curves indicate that the decomposition of the basic chromates occurs in at least two stages, as shown by the inflexion (i.e. change in direction) in the thermograms at 440°C and the presence of endotherms (Fig. 1) at 447, 523°C and 430, 500°C for $FeOHCrO_4$ and $KFe_3(CrO_4)_2(OH)_6$ respectively. The endotherms at 430 and 447°C were

[17] Swamy, M. S. R., and Prasad, T. P., *J. Therm. Anal.*, 1979, **16**, 471.
[18] Swamy, M. S. R., and Prasad, T. P., *J. Therm. Anal.*, 1980, **19**, 297.
[19] Margulis, E. V., Shokarev, M. M., Savchenko, L. A., Kopylov, N. I., and Beisekeeva, L. I., *Russ. J. Inorg. Chem.*, 1971, **16**, 392.
[20] Warner, N. A., and Ingraham, I. R., *Can. J. Chem. Eng.*, 1962, **40**, 263.
[21] Popel, P. P., *Russ. J. Inorg. Chem.*, 1982, **27**, 81.
[22] Mineely, P. J., and Scott, D. L., *Aust. J. Chem.*, 1987, **40**, 387.
[23] Window, B., Dickson, B. L., Routcliffe, P., and Srivastava, K. K. P., *J. Phys. E*, 1974, **7**, 916.
[24] Violet, C. E., and Pipkorn, D. W., *J. Appl. Phys.*, 1971, **42**, 4339.
[25] Price, D., *Aust. J. Phys.*, 1981, **34**, 51.

Table 1. Proposed reaction stoichiometrics for some basic and normal iron(III) chromates at heating rate 10°C/min in air or nitrogen

Decomposition steps at various temperature ranges (°C)	Wt loss (%) Obs.	Calc.	Equation
$2FeOHCrO_4 \xrightarrow{320-440} Fe_2O(CrO_4)_2 + H_2O$	5·40±0·30	4·75	(1)
$Fe_2O(CrO_4)_2 \xrightarrow{440-520} Fe_2O_3 + Cr_2O_3 + \frac{3}{2}O_2$	12·30±0·20	13·34	(2)
$2FeOHCrO_4 \longrightarrow Fe_2O_3 + Cr_2O_3 + \frac{3}{2}O_2 + H_2O$	17·69±0·25	17·47	(3)
$2KFe_3(CrO_4)_2(OH)_6 \xrightarrow{310-425} K_2Cr_2O_7 + Fe_2O(CrO_4)_2 + 2Fe_2O_3 + 6H_2O$	10·11±0·70	9·81	(4)
$Fe_2O(CrO_4)_2 \xrightarrow{425-515} Fe_2O_3 + Cr_2O_3 + \frac{3}{2}O_2$	13·81±0·10	13·34	(5)
$2KFe_3(CrO_4)_2(OH)_6 \longrightarrow K_2Cr_2O_7 + 3Fe_2O_3 + Cr_2O_3 + \frac{3}{2}O_2 + 6H_2O$	14·42±0·40	14·20	(6)
$Fe_2(CrO_4)_3.H_2O \xrightarrow{400-500} Fe_2O(CrO_4)_2 + \frac{1}{2}Cr_2O_3 + \frac{3}{4}O_2 + H_2O$	8·40±0·10	8·79	(7)
$Fe_2O(CrO_4)_2 \xrightarrow{500-520} Fe_2O_3 + Cr_2O_3 + \frac{3}{2}O_2$	13·56±0·30	13·34	(8)
$Fe_2(CrO_4)_3.H_2O \longrightarrow Fe_2O_3 + \frac{3}{2}Cr_2O_3 + \frac{9}{4}O_2 + H_2O$	18·05±0·25	18·84	(9)
$Fe_2(CrO_4)_3.3H_2O \xrightarrow{40-270} Fe_2(CrO_4)_3.0·5H_2O + \frac{5}{2}H_2O$	8·76±0·20	8·75	(10)
$Fe_2(CrO_4)_3.0·5H_2O \xrightarrow{275-400} Fe_2O(CrO_4)_2 + \frac{1}{2}Cr_2O_3 + \frac{3}{4}O_2 + \frac{1}{2}H_2O$	7·20±0·15	7·03	(11)
$Fe_2O(CrO_4)_2 \xrightarrow{400-510} Fe_2O_3 + Cr_2O_3 + \frac{3}{2}O_2$	12·58±0·25	13·34	(12)
$Fe_2(CrO_4)_3.3H_2O \longrightarrow Fe_2O_3 + \frac{3}{2}Cr_2O_3 + \frac{9}{4}O_2 + 3H_2O$	24·00±0·20	24·55	(13)

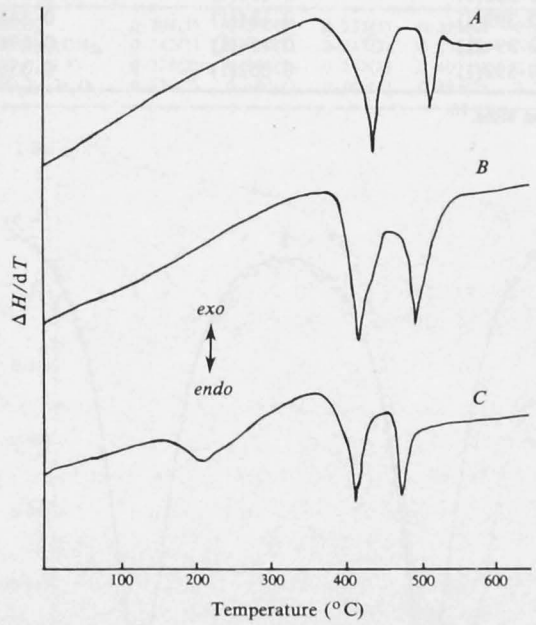

Fig. 1. Differential thermal analysis curves of basic and normal iron(III) chromates at a heating rate 10°C/min. *A*, $FeOHCrO_4$; *B*, $KFe_3(CrO_4)_2(OH)_6$; *C*, $Fe_2(CrO_4)_3.3H_2O$.

assigned to the formation of the oxochromate species–$Fe_2O(CrO_4)_2$ [equations (1) and (4), Table 1]. Attempts to separate the reaction steps by slow heating (2°C/min) were unsuccessful. This was supported by the discrepancy between the observed and calculated weight losses (Table 1), most likely due to partial overlap of the decomposition processes. X-Ray diffraction patterns of quenched residues from

440°C for $FeOHCrO_4$ and $KFe_3(CrO_4)_2(OH)_6$ showed the presence of several new lines at $d = 3{\cdot}56$(s), $3{\cdot}31$(m) and $3{\cdot}06$(m). The presence of these lines in the X-ray diffraction patterns tends to support the results of d.t.a., t.g. and Mössbauer spectroscopy (Table 3, Fig. 3) for the existence of a second phase during the decomposition of basic chromates.

For the normal chromates $Fe_2(CrO_4)_3.nH_2O$ ($n = 1$ or 3), no plateau corresponding to the formation of $Fe_2(CrO_4)_3$ was observed in the thermogram, contrary to the report of Bonnin.[1] D.t.a. curves of the chromates $Fe_2(CrO_4)_3.nH_2O$ indicated the presence of endotherms at 204, 405, 476°C for $n = 3$, and 420, 485°C for $n = 1$. The endotherm at 204°C was assigned to a dehydration process [equation (10)], whilst the endotherms at 405 and 420°C to oxochromate and chromium(III) oxide formation [equations (7), (11)]. The analogous sulfate compound, $Fe_2O(SO_4)_2$, has been the subject of much discussion. Margulis *et al.*[19] and Warner and Ingraham[20] conclude on the basis of weight loss studies, the absence of oxosulfate species, e.g. $Fe_2O(SO_4)_2$, during the decomposition of iron(III) sulfate hydrate and iron(III) hydroxy sulfate. However, Bristotti *et al.*[15] and Swamy *et al.*[16–18] concluded, on the basis of Mössbauer

Table 2. Mössbauer parameters (mm s^{-1}) for some basic and normal iron(III) chromates

Iron chromate	Isomer shift (δ)	Quadrupole splitting (ΔE)	Linewidth (Γ)[B]
$FeOHCrO_4$	0·384(1)	0·472(1)	0·264(1)
$KFe_3(CrO_4)_2(OH)_6$	0·366(1)	0·458(1)	0·266(2)
$Fe_2(CrO_4)_3.H_2O$	0·399(2)	0·184(1)	0·342(3)
$Fe_2(CrO_4)_3.3H_2O$[A]	0·394(1)	0·154(1)	0·296(3)
	0·392(1)	0·352(1)	0·336(2)

[A] Contains two crystallographic iron sites.[13]
[B] Linewidth at half peak height.

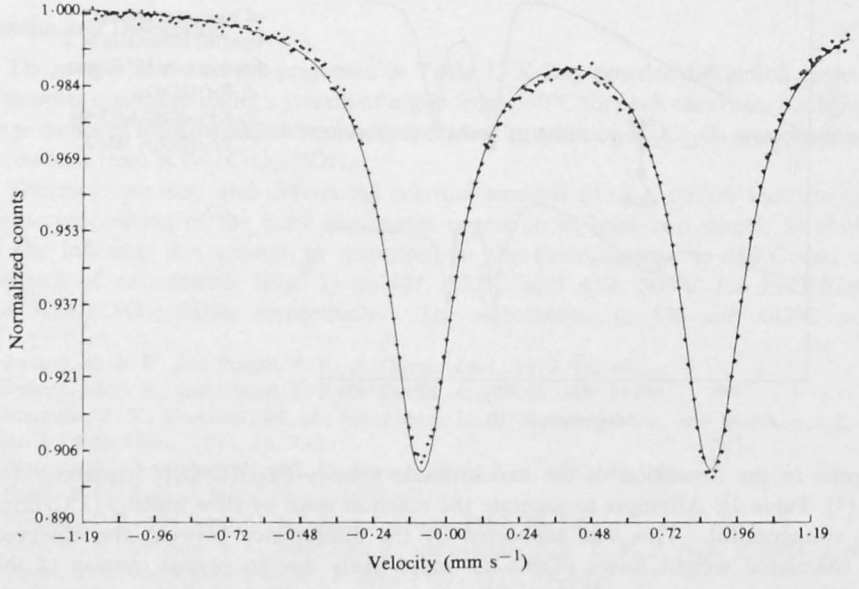

Fig. 2. Room temperature Mössbauer spectrum of iron(III) hydroxy chromate, $FeOHCrO_4$.

and X-ray diffraction results respectively, the existence of $Fe_2O(SO_4)_2$ [equation (14)] during the decomposition of iron(III) hydroxy sulfate

$$2FeOHSO_4 \rightarrow Fe_2O(SO_4)_2 + H_2O \quad (14)$$

Room Temperature Mössbauer Spectra for the Chromates

The room temperature Mössbauer parameters for the chromates are shown in Table 2. A representative spectrum for the chromates is shown in Fig. 2. All spectra of the parent compounds with the exception of $Fe_2(CrO_4)_3.3H_2O$ were simple quadrupole split doublets consistent with crystallographic studies.[1,12,13]

Room Temperature Mössbauer Spectra for the Chromates Quenched from 400°C

Spectra of all residues on quenching from 400°C (Table 3) were clearly resolved into two sets of quadrupole split doublets, indicating the presence of a second phase as supported by weight loss (Table 1) and d.t.a. results. A representative spectrum, for $FeOHCrO_4$, is shown in Fig. 3. The doublet in all spectra (Table 3),

Table 3. Mössbauer parameters (mm s^{-1}) for some basic and normal iron(III) chromates quenched from 400°C

Iron chromate	Isomer shift δ_1	δ_2	Quadrupole splitting ΔE_1	ΔE_2	Linewidth Γ_1	Γ_2	Peak area ratio A_1/A_2	χ^2
$FeOHCrO_4$	0·398(1)	0·398(2)	0·235(1)	0·398(1)	0·284(1)	0·206(2)	2 : 8	1·62
$KFe_3(CrO_4)_2(OH)_6$	0·342(1)	0·357(5)	0·342(2)	0·392(2)	0·411(3)	0·549(3)	2 : 7	1·80
$Fe_2(CrO_4)_3.H_2O$	0·376(2)	0·380(2)	0·252(1)	0·401(3)	0·301(3)	0·299(1)	1 : 3	1·59
$Fe_2(CrO_4)_3.3H_2O$	0·376(2)	0·400(1)	0·162(1)	0·393(2)	0·263(3)	0·486(3)	1 : 2	0·96

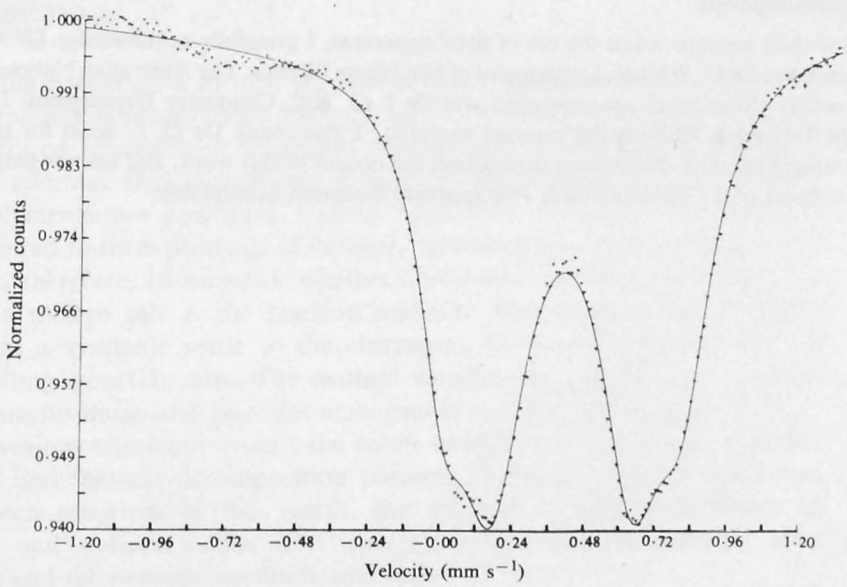

Fig. 3. Room temperature Mössbauer spectrum of iron(III) hydroxy chromate, $FeOHCrO_4$, residues on quenching from 400°C.

$\delta \approx 0{\cdot}39$ mm s^{-1} and $\Delta E \approx 0{\cdot}39$ mm s^{-1}, was assigned to the presence of the secondary phase $Fe_2O(CrO_4)_2$ (Table 1). Bristotti *et al.*[15] have reported the spectrum of the analogous $Fe_2O(SO_4)_2$, $\delta = 0{\cdot}47$ mm s^{-1} and $\Delta E = 0{\cdot}43$ mm s^{-1}. The variation in parameters for the respective oxochromato and sulfato species can be attributed to differences in the effective charges on the coordinated oxygens, as the sulfate oxygens carry a lower negative charge than those for the chromate anion, as expected on a simple electronegativity argument.

For the chromate $KFe_3(CrO_4)_2(OH)_6$ the inner doublet ($\delta \approx 0{\cdot}34$ mm s^{-1}, $\Delta E \approx 0{\cdot}34$ mm s^{-1}) was assigned to amorphous α-Fe_2O_3 [equation (4)]. The room temperature spectrum of amorphous Fe_2O_3 (<18 nm) is a simple quadrupole split doublet[26] ($\delta = 0{\cdot}32$ mm s^{-1}, $\Delta E = 0{\cdot}38$ mm s^{-1}). The inner doublet present in the spectrum for $FeOHCrO_4$ ($\delta = 0{\cdot}40$ mm s^{-1}, $\delta \approx 0{\cdot}23$ mm s^{-1}) may be due to residual $FeOHCrO_4$. Swamy and Prasad[17] report that for iron(III) hydroxy sulfate, $FeOHSO_4$, isostructural with $FeOHCrO_4$,[14] the decomposition pathway may be dependent on reaction conditions (rate of heating—dynamic or isothermal), as equation (14) can also proceed with the formation of $Fe_2(SO_4)_3$ which, once formed, decomposes, immediately to $Fe_2O(SO_4)_2$. However, no 'd' spacings for $Fe_2(CrO_4)_3$ were observed in X-ray powder diffraction patterns.

The inner doublets for the chromates $Fe_2(CrO_4)_3 \cdot nH_2O$ (Table 3) were assigned to residual hydrate on the basis of weight loss studies which indicated that water was still present at 400°C.

In conclusion, thermal analysis and Mössbauer spectroscopy indicates the existence of a second phase during the decomposition of basic and normal iron(III) chromates; this is postulated to be $Fe_2O(CrO_4)_2$, by analogy with the sulfate system.

Acknowledgments

For their assistance and the use of their apparatus, I gratefully acknowledge Dr A. Stewart and Dr G. Whittle, Department of Solid State Physics, The Australian National University (Mössbauer spectroscopy) and Dr J. O. Hill, Chemistry Department, La Trobe University (differential thermal analysis). I also thank Dr D. L. Scott for his encouragement and discussions throughout the course of this work, and acknowledge the support of a Commonwealth Postgraduate Research Scholarship.

[26] Kündig, W., Bömmel, H., Constabaris, G., and Lindquist, R. H., *Phys. Rev.*, 1966, **142**, 327.

Thermochimica Acta, 137 (1989) 197–204
Elsevier Science Publishers B.V., Amsterdam – Printed in The Netherlands

CHARACTERISATION OF SOME NEW CHROMATES $M_2Fe_3(OH)_5(CrO_4)_3 \cdot 3H_2O$ (M = Li, Na) *

PATRICK J. MINEELY

Department of Physical Chemistry, Monash University, Clayton, Vic. 3168 (Australia)

(Received 28 January 1988)

ABSTRACT

The chromates $M_2Fe_3(OH)_5(CrO_4)_3 \cdot 3H_2O$ were prepared as amorphous red–brown powders from mixtures of $Fe(NO_3)_3 \cdot 9H_2O$ and $M_2Cr_2O_7$ (M = Na, Li) fused at 65 °C. Decomposition of the chromates occurred over the range 110–530 °C to yield the respective alkali chromate and a mixture of iron(III) and chromium(III) oxides. Infrared spectroscopy of the chromates showed the presence of coordinated water and long range OH · · · O interactions, whilst Mössbauer spectra indicate the presence of more than one iron site.

INTRODUCTION

For the preparation of iron chromates from aqueous solution, high iron and chromium concentrations are required [1–3]. This necessitates the use of concentrated solutions of chromium trioxide and iron(III) nitrate or chloride. In addition, they are not easy to make, being complicated by hydrolytic and polymerization equilibria. Careful control of conditions and patience are required to form products of definite, reproducible compositions. It is of interest, therefore, to establish whether chromates can be prepared by the use of a molten salt as the reaction medium. This method is particularly suited to a synthetic route to the chromates, in view of the existence of low-melting iron(III) salts. The method satisfies the requirement for high iron concentrations and provides manageable reaction conditions.

In previous communications, the room temperature Mössbauer parameters [4] and thermal decomposition patterns [5] for a range of chromates have been reported. In this report, the reactions of the dichromates of lithium and sodium metals with iron(III) nitrate hydrate melt [6] were studied and the reaction products analysed.

* This work was undertaken at the Department of Chemistry, Faculty of Science, Australian National University, Canberra, A.C.T. 2601.

0040-6031/89/$03.50

EXPERIMENTAL

Analytical

The chemical constituents of the basic chromates were determined by conventional chemical means: lithium, sodium, iron and chromium by atomic absorption spectroscopy, and water by measuring the weight loss on dehydration.

Instrumentation

Mössbauer, X-ray powder diffraction, thermogravimetry, differential thermal analysis, magnetic measurements and atomic absorption spectrometry were all performed as described previously [4]. Infrared spectra were measured on a Perkin-Elmer 1800 Fourier Transform Infrared Spectrophotometer using the KBR disc method. Mössbauer spectra were collected by a PDP 10/11 computer and fitted by a pseudo-Lorenztian program using an iterative, non-linear least-squares method, on the basis of the chi-square (χ^2) values, consistency of parameters and convergence of the fitting process [7].

Materials

B.D.H. $Li_2Cr_2O_7 \cdot 2H_2O$ (96%), May and Baker $Na_2Cr_2O_7 \cdot 2H_2O$ (98%), and AJAX $Fe(NO_3)_3 \cdot 9H_2O$ (AR) were all used as supplied.

Preparation of $Na_2Fe_3(OH)_5(CrO_4)_3 \cdot 3H_2O$

An excess of $Fe(NO_3)_3 \cdot 9H_2O$ (1.0 g, 2.60 mmol) was placed into a silica crucible to which was added sodium dichromate (0.74 g, 2.47 mmol). The contents were mixed thoroughly and heated in an oven at 65 °C for 2 h. The crucible contents were then placed in water, and a red-brown insoluble powder filtered off, washed with water (20 ml) and then acetone (20 ml). Yield 50 mg. Found (wt.%): Na, 6.65; Fe, 24.05; Cr, 22.75; H_2O, 14.63. $Na_2Fe_3(OH)_5(CrO_4)_3 \cdot 3H_2O$ requires (wt.%) Na, 6.56; Fe, 23.82; Cr, 22.30; H_2O, 14.13. The room temperature magnetic moment measured was $\mu_{eff} = 3.4$ BM.

Preparation of $Li_2Fe_3(OH)_5(CrO_4)_3 \cdot 3H_2O$

This was prepared similarly to the corresponding sodium salt, $Li_2Cr_2O_7 \cdot 2H_2O$ (0.65 g, 2.44 mmol), $Fe(NO_3)_3 \cdot 9H_2O$ (1.0 g, 2.60 mmol). Yield of red powder 35 mg. Found (wt.%): Li, 2.21; Fe, 25.50; Cr, 24.40; H_2O, 14.61. $Li_2Fe_3(OH)_5(CrO_4)_3 \cdot 3H_2O$ requires (wt.%) Li, 2.10.; Fe, 25.10; Cr, 24.40; H_2O, 14.81. Magnetic moment, $\mu_{eff} = 3.3$ BM.

RESULTS AND DISCUSSION

Thermal analysis

Weight loss (TG) and differential thermal analysis (DTA) results are shown in Tables 1 and 2 respectively. The chromates decomposed in several stages. The final weight losses were in close agreement with those calculated of 22.00% and 21.06% for the lithium and sodium complexes, respectively (eqns. (3) and (6) in Table 1). X-ray powder diffraction (XRD) patterns of the chromate residues quenched from 550 °C, showed the presence of the respective alkali metal chromate, and a mixture of iron(III) and chromium(III) oxides, further supporting eqns. (3) and (6). Decomposition of the chromates $M_2Fe_3(OH)_5(CrO_4)_3 \cdot 3H_2O$ confirms the general trend as proposed by Golub and Popel [8], that coordinated water is lost prior to dehydroxylation in basic chromate hydrates. The instability of the anhydrous salts $M_2Fe_3(OH)_5(CrO_4)_3$, as judged by the absence of a plateau in the TG corresponding to their formation, appears not to be dependent on the size of the monovalent cation, but rather on whether the cations form stable $M_2Cr_2O_7$ or M_2CrO_4 species. This point is clearly demonstrated for the chromates $MFe(CrO_4)_2$ ($M = NH_4$, Na, K, Rb, Cs). The cations of the ammonium and sodium salts form unstable dichromates in the region of decomposition (400 °C) [4,9], whilst the potassium, rubidium and cesium salts all form stable dichromates and decompose at much higher temperatures (500 °C) [9].

The presence of endotherms at about 500 °C (Table 2) is a characteristic feature of basic iron chromate decomposition [5]. The intermediate phase $Fe_2O(CrO_4)_2$ has been observed during the decomposition of all basic iron chromates reported thus far in the literature [5]. The occurrence of an endotherm within this temperature region is thought, therefore, to be associated with the formation of the unstable oxochromato species $Fe_2O(CrO_4)_2$. The remaining endotherms (Table 2) were assigned to dehydration processes.

X-ray powder diffraction.

The red-brown powders deposited from the melt were amorphous to X-rays. Investigations are at present underway to procure suitable crystalline material for structural analysis.

Infrared spectroscopy

The chromates exhibit free OH stretching and M–OH bending vibrations at around 3650 and 1000 cm^{-1}, respectively (Table 3). Broad absorption maxima (Fig. 1) at around 3400 cm^{-1} and sharp peaks at about 1600 cm^{-1} are assigned to the stretching and bending modes of coordinated water [10].

TABLE 1

Proposed reaction stoichiometries for the thermal decomposition of the chromates $M_2Fe_3(OH)_5(CrO_4)_3 \cdot 3H_2O$ at a heating rate of 10 °C min^{-1}

Reaction	Weight loss (%)		Equation
	Found	Calculated	
110–290			
$Li_2Fe_3(OH)_5(CrO_4)_3 \cdot 3H_2O \rightarrow Li_2Fe_3(OH)_5(CrO_4)_3 \cdot H_2O + 2H_2O$	5.88(0.35)	5.38	(1)
295–595			
$Li_2Fe_3(OH)_5(CrO_4)_3 \cdot H_2O \rightarrow Li_2CrO_4 + 3/2\ Fe_2O_3 + Cr_2O_3 + 3/2\ O_2 + 7/2\ H_2O$	16.72(1.5)	17.56	(2)
$Li_2Fe_3(OH)_5(CrO_4)_3 \cdot 3H_2O \rightarrow Li_2CrO_4 + 3/2\ Fe_2O_3 + Cr_2O_3 + 3/2\ O_2 + 11/2\ H_2O$	21.70(0.75)	22.00	(3)
108–240			
$Na_2Fe_3(OH)_5(CrO_4)_3 \cdot 3H_2O \rightarrow Na_2Fe_3(OH)_5(CrO_4)_3 \cdot 1/2\ H_2O + 5/2\ H_2O$	6.42(0.25)	6.42	(4)
245–530			
$Na_2Fe_3(OH)_5(CrO_4)_3 \cdot 1/2\ H_2O \rightarrow Na_2CrO_4 + 3/2\ Fe_2O_3 + Cr_2O_3 + 3/2\ O_2 + 3H_2O$	22.41(0.30)	21.98	(5)
$Na_2Fe_3(OH)_5(CrO_4)_3 \cdot 3H_2O \rightarrow Na_2CrO_4 + 3/2\ Fe_2O_3 + Cr_2O_3 + 3/2\ O_2 + 11/2\ H_2O$	21.82(0.30)	21.06	(6)

TABLE 2

Differential thermal analysis of the chromates $M_2Fe_3(OH)_5(CrO_4)_3 \cdot 3H_2O$ at a heating rate of 10 °C min^{-1}

Compound	T_i [a]	T_{max} [b]	T_f [c]	ΔH	Reaction
$Li_2Fe_3(OH)_5(CrO_4)_3 \cdot 3H_2O$	120	240	270	Endo	$-H_2O$
	275	420	490	Endo	$-H_2O$, $-O_2$
	490	502	505	Endo	$-O_2$
$Na_2Fe_3(OH)_5(CrO_4)_3 \cdot 3H_2O$	115	259	275	Endo	$-H_2O$
	277	439	485	Endo	$-H_2O$, $-O_2$
	492	505	508	Endo	$-O_2$

[a] T_i, initial departure of curve from baseline.
[b] T_{max}, maximum departure from baseline.
[c] T_f, return to baseline.

The position and shape of bands at 2900 cm^{-1} are consistent with long range OH · · · O hydrogen bond interactions [11,12]. Their presence explains the sequential loss of water (eqns. (1) and (4), Table 1) for the chromates, owing to some water molecules being more strongly coordinated to the iron atoms. The remainder of the assignments in Table 3 are based on those reported by Cudennec et al. for the basic chromate $KFe_3(OH)_6(CrO_4)_2$ [13].

Room temperature Mössbauer

Table 4 lists the Mössbauer parameters for the chromates. The isomer shifts δ are normal for high spin Fe(III) compounds. Their relatively narrow

TABLE 3

Infrared band positions for the chromates (KBr disc)

Compound			
$Li_2Fe_3(OH)_5(CrO_4)_3 \cdot 3H_2O$		$Na_2Fe_3(OH)_5(CrO_4)_3 \cdot 3H_2O$	
ν (± 5 cm^{-1})	Assignment	ν (± 5 cm^{-1})	Assignment
3650 (sh, m)	ν(M–OH)	3672 (sh, m)	ν(M–OH)
3405 (s)	ν(OH)	3414 (s)	ν(OH)
2922 (vw)		2923 (vw)	
2852 (vw)		2856 (vw)	
		1594 (m)	δ(OH)
1652 (m)	δOH	1030 (s)	δ(M–OH)
1459 (w)		968 (m)	
1000 (w)	δ(M–OH)	928 (m)	δ(Cr–O)
939 (s)	ν(Cr–O)	893 (w)	ν(M–O)
774 (m)	ν(Fe–O)	848 (m)	
713 (w)		795 (w)	ν(Fe–O)
474 (m)	δ(O–Cr–O)	515 (m)	ν(FeO)

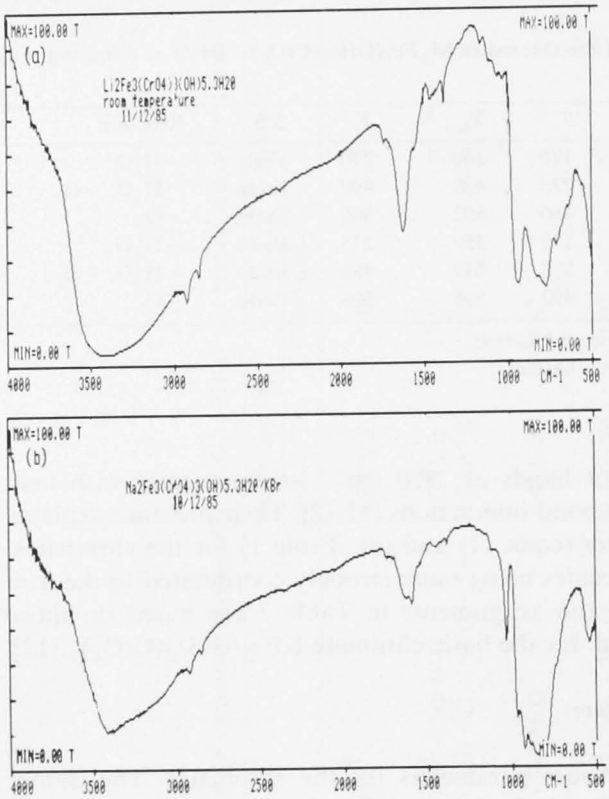

Fig. 1. Infrared spectra of chromates (a) $Na_2Fe_3(OH)_5(CrO_4)_3 \cdot 3H_2O$; (b) $Li_2Fe_3(OH)_5(CrO_4)_3 \cdot 3H_2O$.

TABLE 4

Mössbauer parameters for chromates $M_2Fe_3(OH)_5(CrO_4)_3 \cdot 3H_2O$

Example	Fit [a]	Chi-squared χ^2	Mössbauer parameters (mm s^{-1})		
			δ	ΔE	Γ [b]
$Li_2Fe_3(OH)_5(CrO_4)_3 \cdot 3H_2O$	2T2	2.51	0.392(2)	0.151(2)	0.251(3)
			0.392(2)	0.365(8)	0.371(6)
	2T3 [c]	0.92	0.392(2)	0.159(2)	0.291(2)
			0.392(2)	0.331(5)	0.280(4)
			0.392(2)	0.452(5)	0.226(1)
$Na_2Fe_3(OH)_5(CrO_4)_3 \cdot 3H_2O$	2T2	2.45	0.392(2)	0.161(3)	0.273(2)
			0.392(2)	0.388(9)	0.345(9)
	2T3	0.95	0.391(1)	0.176(2)	0.316(6)
			0.391(1)	0.351(2)	0.278(6)
			0.389(1)	0.462(2)	0.274(4)

[a] 2T2, fitted to two sets of quadrupole split doublets.
[b] Γ, linewidth at half peak height.
[c] 2T3, fitted to three sets of quadrupole split doublets.

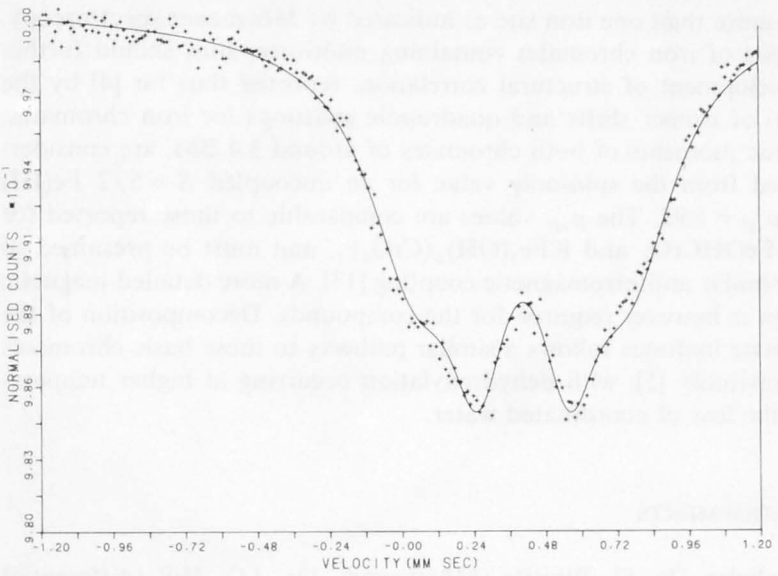

Fig. 2. Representative Mössbauer spectrum of the basic chromates $Li_2Fe_3(OH)_5(CrO_4)_3 \cdot 3H_2O$.

line widths (0.22–0.31 mm s^{-1}), indicate that line broadening due to the presence of coupling is not of much importance. Initial fitting of each spectrum (Figure 2) to two sets of quadrupole split doublets (ΔE) gave χ^2 values of about 2.5—a fair fit. It was felt that the fits could be improved by incorporating the outer doublet ($\Delta E \simeq 0.37$ mm s^{-1}) as two overlapping doublets. On doing so the χ^2 values were reduced to about 1.0, an excellent fit, and the parameters obtained were within acceptable limits. Assignment of spectra are shown in Table 4. The outer doublet ($\Delta E \simeq 0.46$ mm s^{-1}) was assigned to the presence of iron–oxygen polyhedra containing hydroxyl ions, $Fe(OH)_xO_{6-x}$, based on the reported trend [4] that the replacement of oxygen atoms by hydroxyl or water groups results in an increase in ΔE. The order of increase in quadrupole splitting on incorporation is $OH^- > H_2O > O^{2-}$. The measured ΔE of this doublet is consistent with those reported for $Fe(OH)_xO_{6-x}$ containing chromates [4,5] of between 0.46 and 0.49 mm s^{-1}. A similar argument sees the two inner doublets, ΔE 0.16 and 0.33 mm s^{-1}, being assigned to $Fe(OH_2)_xO_{6-x}$ polyhedra. The presence of more than one water environment is consistent with the infrared spectra (Fig. 1) which show the presence of coordinated water of varying strengths.

CONCLUSION

Synthetic routes to iron chromates using low melting iron(III) salt hydrates, has the potential for the preparation of a range of new chromates,

containing more than one iron site as indicated by Mössbauer spectroscopy. The synthesis of iron chromates containing multi-iron sites should further aid the development of structural correlation, reported thus far [4] by the compilation of isomer shifts and quadrupole splittings for iron chromates. The magnetic moments of both chromates of around 3.4 BM, are considerably reduced from the spin-only value for an uncoupled $S = 5/2$ Fe(III) state (viz. $\mu_{eff} = 5.92$. The μ_{eff} values are comparable to those reported for chromates $FeOHCrO_4$ and $KFe_3(OH)_6(CrO_4)_2$, and must be presumed to arise from similar antiferromagnetic coupling [13]. A more detailed magnetic investigation is however required for the compounds. Decomposition of the basic chromate hydrates follows a similar pathway to those basic chromates reported previously [5], with dehydroxylation occurring at higher temperatures than the loss of coordinated water.

ACKNOWLEDGEMENTS

I acknowledge Dr. G. Whittle (Mössbauer), Dr. J.O. Hill (differential thermal analysis) and Mr. D. Bogsanyi (infrared) for the use of their apparatus and technical advice, and also the support of a Commonwealth Postgraduate Research Award.

REFERENCES

1 A. Bonnin, Ph.D. Thesis, Rennes, 1970.
2 A. Bonnin, C.R. Acad. Sci., Ser. C., 271 (1970) 639.
3 A. Bonin and A. Lecerf, C.R. Acad. Sci., Ser. C., 262 (1966) 1782.
4 P.J. Mineely and D.L. Scott, Aust. J. Chem., 40 (1987) 387.
5 P.J. Mineely, Aust. J. Chem., 41 (1988) 263.
6 R.C. Weast (Ed.), Handbook of Chemistry and Physics, CRC Press, Florida, 1984, p. B104.
7 D. Price, Aust. J. Phys., 34 (1981) 51.
8 A.A. Golub and P.P. Popel, Ukr. Khim. Zh., 43 (1977) 353.
9 P.P. Popel, Russ. J. Inorg. Chem., 27 (1982) 81.
10 K. Nakamato, Infrared and Raman Spectra of Inorganic and Coordination Compounds, Wiley, New York, 1978.
11 R.E. Rundle and M.J. Parasol, Chem. Phys., 20 (1952) 1487.
12 K. Nakamoto, M. Margashes and R.E. Rundle, J. Am. Chem. Soc., 77 (1955) 6486.
13 Y. Cudennec, A. Riou and P. Caillet, Rev. Chim. Miner., 17 (1980) 158.

REFERENCES

1. Averbukh, T. D. and Pavlov, P. G., eds., 'The Technology of Chromium Compounds', IZD. (Khimya: Leningrad 1967).

2. Krause, A. and Kotouski, S., Przem. Chem., 1961, 40, 631.

3. Elliot, H. and Storer, N., Proc. Am. Acad., 1861, 5, 192.

4. Kletzinsky, A., Dinglers Polyt J., 1873, 83, 207.

5. Hensgen, C., Ber., 1879, 12, 1656.

6. Weinland, R. and Mergenthaler, E., Ber. 1924, 133, 1386.

7. Briggs, S. H. C., J. Chem. Soc., 1929, 242.

8. Husain, S. and Partington, J. R., Chem. News, 1926, 133, 1386.

9. Bonnin, A., Ph.D. thesis, Rennes, 1970.

10. Bonnin, A. and Lecerf, A., C. R. Acad. Sci., Ser. C., 1966, 262, 1782.

11. Hardy, A. and Gravereau, P., C. R. Acad. Sci., Ser. C., 1970, 271, 1306.

12. Gravereau, P. and Hardy, A., Acta Crystallogr., Sect. B., 1972, 28, 2333.

13. Hardy, A. and Gaboriaud, F., Acta Crystallogr., Sect. B., 1972, 28, 2329.

14. Bonnin, A., Hardy, A. and Garnier, E., C. R. Acad. Sci., Ser. C., 1973, 276, 1381.

15. Bonnin, A., Diaz-Caceres, J., Gravereau, P. and Hardy, A., C. R. Acad. Sci., Ser. C., 1974, 279, 939.

16. Debelle, V., Gravereau, P. and Hardy, A., Acta Crystallogr., Sect. B., 1974, 30, 2185.

17. Gravereau, P. and Hardy, A., Bull. Soc. Fr. Mineral. Crystallogr., 1976, 99, 206.

18. Gerault, Y. and Bonnin, A., Bull. Soc. Fr. Mineral. Crystallogr., 1976, 99, 197.

19. Gravereau, P., Hardy, A. and Bonnin, A., Acta Crystallogr., Sect. B., 1977, 33, 1362.

20. Riou, A., and Bonnin, A., Acta Crystallogr., Sect. B., 1978, 34, 706

21 Cudennec, Y., Riou, A., Bonnin, A. and Caillet, P., Rev. Chim. Miner.,1980, 17, 158.

22. Popel, P. P. and Boldog, I. I., Russ. J. Inorg. Chem., 1979, 24, 1828.

23. Popel, P. P., Russ. J. Inorg. Chem., 1982, 27, 81.

24. Powers, D. A., Rossman, G. R., Schugar, H. S. and Gray, H. B., J. Solid State Chem., 1975, 13, 1.

25. Margulis, E. V., Shokarev, M. M., Savchenko, L. A., Kopylov, N. I. and Beisekeeva, L. I., Russ. J. Inorg. Chem., 1971, 16, 392.

26. Warner, N. A. and Ingraham, T. R., Can. J. Chem. Eng., 1962, 40, 263.

27. Bristotti, A., Kunrath, K. J. I., Viccaro, P. J. and Bergter, L., J. Inorg. Nucl. Chem., 1975, 37, 1149.

28. Swami, M. S. R., Prasad, T. P. and Scant, B. R., J. Therm. Anal., 1979, 15, 307.

29. Swami, M. S. R., Prasad, T. P. and Scant, B. R., J. Therm. Anal., 1979, 16, 471.

30. Swami, M. S. R., and Prasad, T. P., J. Therm. Anal., 1980, 19, 297.

31. Bonnin, A., C. R. Acad. Sci., Ser. C., 1970, 271, 639.

32. Lombardi, G, ed., 'ICTA- For Better Thermal Analysis', (2nd Edition, Rome, 1980).

33. Wiles, D. B. and Young, R. A., J. Appl. Cryst., 1981, 14, 149.

34. Smith, J.V., ed., ' ASTM Powder Diffraction File', (Baltimore:1963).

35. Window, B., Dickson, B. L., Routcliffe, P and Srivasta, K. P. P., J. Phys., Part E, 1974, 7, 916.

36. Violet, C. E. and Pipkorn, D. W., J. Appl. Phys., 1971, 42, 4339.

37. Price, D. C., Aust. J. Phys., 1981, 34, 51.

38. Takashima, Y. and Ohaski, S., Bull. Chem. Soc. Japan., 1965, 38, 1684.

39. Saegusa, N., Ph.D. thesis, Canberra, 1978.

40. Bancroft, G. M., Maddock, A. G. and Burns, R. G., Geoch. Cosmoch. Acta., 1965, 18, 249.

41. Haven, Y. and Noftle, R.E., J. Chem Phys., 1977, 67, 2825.

42. Mossbauer, R. L., Ann. Rev. Nucl. Sci., 1962, 12, 123.

43. Boyle, A.J.F. and Hall, H. E., Rept. Prog. Phys., 1962, 25, 441.

44. Herber, R. H., Prog. Inorg. Chem., 1967, 8, 1.

45. Newkirk, A.E., Anal. Chem., 1958, 30, 982.

46. Le Chatelier., J. Phys., 1887, 6, 23.

47. Paulik, F., Paulik, J . and Erdey, L., Acta. Chim. Acad. Sci. Hung., 1961, 26, 143.

48. Vallet, P. and Richter, A., Bull. Soc. Chim. France., 1953, 198.

49. Arens, P. L. ed. 'A Study of Differential Thermal Analysis of Clays and Clay Minerals' (The Hague, 1951).

50. Kissinger, H. E., J. Res. Natl. Bur. Std., 1956, 57, 217.

51. Stone, R. L., Anal. Chem., 1960, 32, 1582.

52. Bancroft, G. M., ed., 'Mőssbauer Spectroscopy' (Wiley: New York 1963).

53. Blume, M., Phys. Rev. Lett., 1965, 14, 96.

54. Bancroft, G. M., Burns, R. G. and Maddock, A. G., Am. Mineral., 1967, 52, 1009.

55. Pollack, H., De Coster, M. and Amelinckxs, S., Proc. Second Int. Conference on Mössbauer Effect, Saclay, France. Sept 13-15, 1961.

56. Schwartz, L., Inst. J. Nondest. Testing, 1970, 1, 357.

57. Housely, R. M., Grant, R. W., Blander, M , Abdel-Gawad, M. and Muir, A. H., Geoch.Cosmoch. Acta, Suppl., 1, 1970, 34, 2251.

58. Housely, R. M., Grant, R. W., Blander, M , Abdel-Gawad, M. and Muir, A. H., 'Proceedings of the Second Lunar Science Conference', Vol. 3, 2125 . (MIT Press: 1971).

59. Gakiel, U. and Malamund, M., Am. Mineral., 1969, 54, 259.

60. Bancroft, G. M., Burns, R. G. and Stone, R. L., Geoch Cosmoch. Acta.,1968, 32, 547.

61. Sato, N., Sano, H., Tominga, T and Ambe, F., Bull. Chem. Soc. Japan., 1965, 38, 681.

62. Duncan, J. F., Mackenzie, K .J. D. and Stewart, D. J., Symp. Faraday Soc., 1967, 1, 103.

63. Wilhelmi, K. A., Acta. Chem. Scand., 1965, 19, 165.

64. Kokkoras, P. A., Mineral. Petrog. Mitt., 1965, 16, 45.

65. Johansson, G., Acta. Chem. Scand., 1962, 16, 1234.

66. Wang,R., Bradley,W.F and Steinfink,H., Acta Crystallogr.,1965,18,249.

67. Mellier., A. and Gravereau, P., Spectrochim. Acta, Part A, 1973, 29, 2043.

68. Popel,P. P. and Boldog,I.I., Visn. Kiiv. Univ., Khim.,1981,22,8.

69. Mahieu, B., Apers, D. J. and Capron, P. C., J. Inorg. Nucl. Chem., 1971, 33, 2851.

70. Shmerkovich-Galev, G.I., Zh. Vses. Khim., 1977, 22, 463.

71. Schwartz, H., Z. Anorg. Chem., 1963, 322, 1.

72. Schwartz, H., Z. Anorg. Chem., 1963, 322, 129.

73. Morais, P. C. and Neto, S. K., Polyhedron , 1983, 2, 875.

74. Sudo, T., Clay Minerals Bull., 1954, 2, 96.

75. Sudo, T. and Nakamura, T., Am. Miner., 1953, 37, 618.

76. Mackenzie, R. C. ed., 'The Differential Thermal Investigation of Clays', (Mineralogical Society: London 1957).

77. Caillere, S. and Hein, S., Bull. Soc. Fr. Mineral. Crist., 1954, 77, 479.

78. Kundig, W., Bommel, H., Constabaris, G. and Lindquist, R. H., Phys. Rev., 1966, 142, 327.

79. Komissarova,V.M.,Shatskii,V.M and Anashina,N.P., Russ.J.Inorg.Chem.,1970,15,1678.

80. Baur, W. H., Amer. Crystallogr. Trans., 1970, 6, 129.

81. Enwiga, B. Y., Silver, J. and Morrison, I. E. G., Inorg. Chim. Acta , 1984, 86, 113.

82. Hrynkiewcz, A. Z., Kubisz, J. and Kulgawczuk, D. S., J. Inorg. Nucl. Chem., 1965, 27, 2513.

83. Takano, M., Shinjo, T., Kiyama, M. and Takada, T., J. Phys. Soc. Japan , 1968, 25, 902.

84. Brophy, G. P., Scott, E. S. and Snellgrove, R. A., Amer. Miner., 1962, 47, 112.

85. Pauling,L., J. Am. Chem. Soc., 1929,51,1010.

86. Cadile,C.M and Johnston,J.M., Clay Miner.,1985,33,295.

87. Sherman, D. M., Phys. Chem. of Minerals , 1985, 12, 311.

88. Aylward, G.H. and Findlay, T. J., ed., 'SI Chemical Data', (Wiley : Hong Kong 1977)

89. Gupta, S., Sharma, R. C. and Gaur, H. C., J. Chem. Eng. Data ,1981, 26, 187.

89a. Kerridge, D. H., 'Chemistry of Molten Nitrates and Nitrites', Int. Rev. Sci., Inorg. Chem., Series One, 1972, 2, 29.

90. Nakamoto, K., Margoshes, M. and Rundle, R. E., J. Am. Chem. Soc., 1955, 77, 6486.

91. Brough, B. J., Kerridge, D. H. and Tariq, S. A., Inorg. Chim. Acta , 1967, 1, 267.

92. Danon, J., ed., 'Lectures on the Mössbauer Effect', (Gordon and Breach: New York 1968).

93. Corey, R.C. and Sidhu, S. S., J. Am. Chem. Soc., 1945, 67, 1490.